

# 2026 The 15th ACOMFR



The 15th Asian Congress of  
Oral and Maxillo-Facial Radiology  
in conjunction with  
The 58th Annual Scientific Meeting of KAOMFR

**April 30(Thu) - May 2(Sat), 2026**  
ST Center, Seoul, Korea

## ABSTRACT BOOK

***Imaging Science:  
Leading the Innovation in Dentistry***



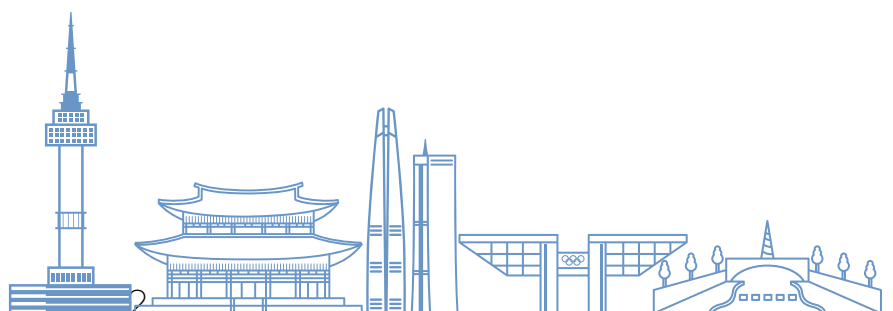
대한영상  
치의학회

KOREAN ACADEMY OF  
ORAL AND MAXILLOFACIAL  
RADIOLOGY



# Contents

Organizing Committee .....	03
Program at a Glance .....	05
Invited Session .....	08
Quiz .....	29
Oral Presentation .....	32
e-Poster .....	60
Author Index .....	140





# Organizing Committee

## Consultant

---

**Tae-Won Park**  
Seoul National University

**Kwang-Joon Koh**  
Jeonbuk National University

**Soon-Chul Choi**  
Seoul National University

**Byung-Cheol Kang**  
Chonnam National University

**Eun-Kyung Kim**  
Dankook University

**Karp-Shik Choi**  
Kyungpook National University

**Eui-Hwan Hwang**  
Kyung Hee University

## Advisor

---

**Byung-Do Lee**  
Wonkwang University

**Bong-Hae Cho**  
Pusan National University

**Yun-Hoa Jung**  
Pusan National University

**Won-Jeong Han**  
Dankook University

**Suk-Ja Yoon**  
Chonnam National University

**Won-Jin Yi**  
Seoul National University

**Chang-Hyeon An**  
Kyungpook National University

**Sang-Sun Han**  
Yonsei University

## President of KAOMFR

---

**Hang-Moon Choi**  
Kangwon National University

## Vice President of KAOMFR

---

**Jin-Soo Kim**  
Chosun University

**Seungmok Na**  
Manan Dental Clinic

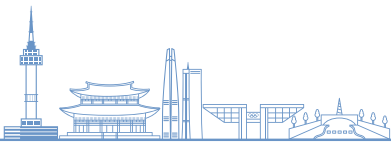
## Honorary President

---

**Jae-Duk Kim**  
Chosun University

**Chang-Seo Park**  
Yonsei University

**Sam-Sun Lee**  
Seoul National University



# Organizing Committee

## President & Chair of Organizing Committee

---

### **In-Woo Park**

Kangwon National University

## Vice President

---

### **Min-Suk Heo**

Seoul National University

## General Affairs Committee

---

Director

### **Kyoung-A Kim**

Jeonbuk National University

Associate Director

### **Chena Lee**

Yonsei University

Member

### **Chang-Ki Min**

Jeonbuk National University

Member

### **Ah-Young Kwon**

Dankook University

## Scientific Committee

---

Director

### **Kyung-Hoe Huh**

Seoul National University

Associate Director

### **Jo-Eun Kim**

Seoul National University

Member

### **Jin-Woo Han**

Kangwon National University

Member

### **Ju-Hee Kang**

Seoul National University

## Finance & Exhibition Committee

---

Director

### **Kug Jin Jeon**

Yonsei University

Associate Director

### **Gyu-Dong Jo**

Yonsei University

Member

### **Yoon-Joo Choi**

Yonsei University

## Social Program Committee

---

Director

### **Jin-Woo Choi**

Dankook University

Associate Director

### **Hak-Sun Kim**

Kyung Hee University

Member

### **Jae-Seo Lee**

Chonnam National University

## Registration Committee

---

Director

### **Wan Lee**

Wonkwang University

Associate Director

### **Han-Gyeol Yeom**

Wonkwang University

Member

### **Gyu-Tae Kim**

Kyung Hee University

Member

### **Yo-Seob Seo**

Chosun University

## Publicity Committee

---

Director

### **Seo-Young An**

Kyungpook National University

Associate Director

### **Young-Eun Kwon**

Kyungpook National University

Member

### **Jae-Joon Hwang**

Pusan National University

Member

### **Kyoung-Soo Kim**

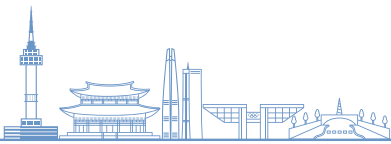
Kangwon National University



# Program at a Glance

## DAY 1. April 30 (Thu)

	Room A	Room B	Room C	
09:00	<b>Opening Ceremony</b> (09:00-09:30)	<b>e-Poster Display</b>		
09:30				
10:00	<b>Invited Session 1</b> Expanding roles of imaging science in modern dentistry (09:30-10:50)			
10:30				
11:00	<b>Break</b> (10:50-11:10)			
11:30	<b>Invited Session 2</b> Advanced imaging approaches beyond conventional radiography (11:10-12:30)			
12:00				
12:30	<b>Lunch</b> (12:30-13:30)			
13:00				
13:30	<b>Invited Session 3A</b> Principles and clinical applications of multimodality imaging (13:30-14:50)			<b>Oral Presentation 1</b> (13:30-14:30)
14:00				
14:30	<b>Break</b> (14:50-15:10)			
15:00				
15:30	<b>Quiz 1</b> Horse VS Zebra (15:10-16:10)			<b>Oral Presentation 2</b> (15:10-17:00)
16:00				
16:30	<b>Invited Session 3B</b> Principles and clinical applications of multimodality imaging (16:10-17:30)			
17:00				
17:30				
18:00	<b>Welcome Party</b> @Anais & Iris Hall, 12F (18:00-)			



# Program at a Glance

## DAY 2. May 1 (Fri)

	Room A	Room B	Room C
09:00			
09:30	<b>Invited Session 4A</b> Clinical decision-making and precision diagnosis using advanced imaging (09:00-10:50)	<b>e-Poster Display</b>	<b>Oral Presentation 3</b> (09:30-10:30)
10:00			
10:30			
11:00	<b>Break</b> (10:50-11:10)		<b>Oral Presentation 4</b> (11:10-11:40)
11:30	<b>Invited Session 4B</b> Clinical decision-making and precision diagnosis using advanced imaging (11:10-12:30)		
12:00			
12:30		<b>Lunch</b> (12:30-13:30)	
13:00			
13:30	<b>Invited Session 5A</b> Advances in imaging science and their impact on predictive dentistry (13:30-14:50)	<b>Oral Presentation 5</b> (13:30-14:50)	
14:00			
14:30			
15:00	<b>Break</b> (14:50-15:10)	<b>Oral Presentation 6</b> (15:10-16:20)	
15:30	<b>Quiz 2</b> Horse VS Zebra (15:10-16:10)		
16:00			
16:30	<b>Invited Session 5B</b> Advances in imaging science and their impact on predictive dentistry (16:10-16:50)		
17:00		<b>General Assembly</b> "2026 Prize for the Best Article" (16:50-17:30)	
17:30			
18:00	<b>Gala Dinner</b> @Anais Hall, 12F (18:00-)		

## Program at a Glance

### DAY 3. May 2 (Sat)

	Room A	Room B
09:00 –	<p><b>Invited Session 6A</b> Artificial intelligence in dentomaxillofacial radiology: Current applications and future perspectives (09:00-10:50)</p>	<p><b>e-Poster Display</b></p>
09:30 –		
10:00 –		
10:30 –		
11:00 –	<p><b>Break (10:50-11:10)</b></p>	
11:30 –	<p><b>Invited Session 6B</b> Artificial intelligence in dentomaxillofacial radiology: Current applications and future perspectives (11:10-11:50)</p>	
12:00 –	<p><b>Closing Ceremony</b> (11:50-12:30)</p>	
12:30 –		

### Day 0. April 29 (Wed)

- 13:30–19:00 Pre-Congress Tour & Welcome Reception
- Tour Location: Bukchon Hanok Village (Located near Anguk Station, Subway Line 3)
- Welcome Reception: Eobumong Insadong Branch



# Invited Session



**Invited Session 1**

Expanding roles of imaging science in modern dentistry

April 30 (Thu), 09:30-10:50

Room A

IS1-1



## Is it feasible to incorporate panoramic radiography into the national health and nutrition examination survey?: A pilot study

**Hang-Moon Choi**<sup>1\*</sup>, Kyoung-A Kim<sup>2</sup>, Jo-Eun Kim<sup>3</sup>, Jin-Woo Choi<sup>4</sup>, Sang-Sun Han<sup>5</sup>,  
Jae-In Ryu<sup>6</sup>

<sup>1</sup>Department of Oral and Maxillofacial Radiology, Kangwon National University, South Korea

<sup>2</sup>Department of Oral and Maxillofacial Radiology, Jeonbuk National University, South Korea

<sup>3</sup>Department of Oral and Maxillofacial Radiology, Seoul National University, South Korea

<sup>4</sup>Department of Oral and Maxillofacial Radiology, Dankook University, South Korea

<sup>5</sup>Department of Oral and Maxillofacial Radiology, Yonsei University, South Korea

<sup>6</sup>Department of Preventive and Social Dentistry, Kyung Hee University, South Korea

The Korea National Health and Nutrition Examination Survey (KNHANES) is a national surveillance system that has been assessing the health and nutritional status of Koreans since 1998, based on the National Health Promotion Act.

The oral examination of KNHANES is used as key statistical data for the establishment and evaluation of national oral health policies. Dental caries and periodontal diseases are conditions that are prone to inter-investigator variability due to differing judgment criteria. Therefore, training and systematic quality management of investigators are essential to ensure the reliability and objectivity of the examination.

Panoramic radiographic imaging was added to improve reliability and objectivity. A vehicle equipped with a panoramic X-ray machine was developed to travel nationwide for imaging. To improve the quality of imaging, operators received theoretical and practical imaging training. An interpretation guideline was developed. Five oral and maxillofacial radiologists interpreted the images according to the guidelines. Two radiologists interpreted each image, and in cases of disagreement, a decision was made through discussion.

The oral examination involved visual inspections for identifying dental caries, restoration, prosthesis, as well as periodontal probing for measuring periodontal pockets. In panoramic radiographs, dental caries, alveolar bone loss and calculus were assessed.

When panoramic radiographs were added to the oral examination, the prevalence of proximal caries and calculus increased due to its superior detection ability for interproximal decay and interproximal calculus. There was a low correlation between periodontal pockets and alveolar bone loss. Although the sample size was small and not representative, utilizing panoramic radiographs seems to aid in accurately determining the prevalence of dental caries and calculus. Since the degree of alveolar bone loss does not accurately reflect the current state of periodontal disease, it could be used as an indicator of accumulated periodontal disease outcomes in the health and nutrition survey.

**IS1-2**

## Reimagining oral radiology in Indonesia – A journey toward precision dentistry

**Isti Rahayu Suryani***Dentomaxillofacial Radiology Department, Faculty of Dentistry, Universitas Gadjah Mada, Indonesia*

Indonesia's oral radiology landscape stands at a transformative crossroads, where technological innovation meets persistent challenges in accessibility, infrastructure, and standardization. This presentation chronicles the nation's evolving journey toward precision dentistry, examining both obstacles and opportunities in advancing diagnostic imaging across the archipelago's diverse healthcare ecosystem.

Despite growing adoption of Cone Beam Computed Tomography (CBCT) in urban centers, significant disparities persist in equipment availability, radiological expertise, and standardized imaging protocols across Indonesia's 34 provinces. Training gaps in advanced imaging interpretation and limited integration of digital workflows impede optimal patient care, particularly in underserved regions. These challenges mirror broader Southeast Asian patterns, where resource constraints and educational infrastructure limitations affect diagnostic quality and treatment planning precision.

Artificial intelligence presents unprecedented opportunities to democratize expertise and enhance diagnostic accuracy. Recent advances in deep learning algorithms demonstrate remarkable performance in automated detection of dental pathologies, implant planning, and anatomical landmarking from CBCT datasets, achieving diagnostic accuracy exceeding 90% in multiple clinical applications. Integration of AI-assisted CBCT analysis with digital treatment planning workflows enables true precision dentistry—personalized, predictable, and minimally invasive interventions guided by three-dimensional anatomical intelligence.

This presentation proposes a collaborative framework for advancing oral radiology in resource-variable settings, emphasizing telemedicine-enabled expert consultation networks, AI-augmented diagnostic support systems, and regional training partnerships.

**Invited Session 2**

April 30 (Thu), 11:10-12:30

Advanced imaging approaches beyond conventional radiography

Room A

IS2-1

**Maxillofacial radiology and 3D printing in medicine & dentistry****Zainul Ahmad Rajion***International Islamic University Malaysia (IIUM), Malaysia*

Imaging is a keystone in understanding and delivery of craniofacial health care. Recent developments in imaging have brought forth many diverse technologies and approaches. Following the invention of the first computed tomography (CT) scanner in the early 1970s, many innovations in three-dimensional (3D) diagnostic imaging technology have occurred, leading to a wide range of applications in medicine, dentistry and in addition to craniofacial clinical practice and research.

Advances in craniofacial medical imaging, provide superior and more detailed information compared with conventional plain (2D) radiography. Current state-of-the-art multidetector CT (MDCT), also known as medical CT, has an important role in diagnosis and management of craniofacial injuries and pathology. In recent years, 3D printing (additive manufacturing) have provided new possibilities to visualize complex radiological data through the generation of 3D reconstruction physical models that can be used to assist with diagnosis, surgical planning, prosthesis design, and patient communication. It also allowed the design of custom-made implants based on computer-aided design and manufacturing (CAD/CAM). The production of implant commences by capturing a 3D craniofacial data from craniofacial medical imaging CT scan. The virtual 3D model of the implant is then constructed via CAD software before transforming into a real model through 3D printing.

IS2-2



## **Image fusion - A new diagnostic approach to TMJ related abnormalities**

**Gang Li**

*Department of oral and maxillofacial Radiology, Peking University School and Hospital of Stomatology, Beijing, China*

Image fusion is a technique that can be used to merge characteristics of images from different modalities so that certain features can be enhanced, which is not visible in either of the single data alone. Temporomandibular joint (TMJ) is the most delicate and intricate joint structure in the human body, and may be malfunctioned by several categories of diseases. Application of fused images by cone beam CT/CT and MRI gives an intuitive observation of condyle, TMJ disc and related structure changes. This helps in diagnosis of TMJ related abnormalities.

## Invited Session 3A

Principles and clinical applications of multimodality imaging

April 30 (Thu), 13:30-14:50  
Room A

IS3A-1



### Principles and artifacts of CT image reconstruction

**Yoshinori Arai**

*Department of Oral and Maxillofacial Radiology, Nihon University, School of Dentistry, Japan*

This presentation offers a clear and comprehensive overview of the principles underlying CT image reconstruction and common artifacts. It also addresses core concepts such as filtered backprojection and methods for reducing metal artifacts.

The presentation utilizes a CT simulator developed with Visual Studio 2022 (Microsoft, USA), which illustrates object rotation and provides real-time sinogram visualization, like a movie. The simulator models beam hardening and radial metal artifacts, and demonstrates techniques for reducing metal artifacts.

The simulated object includes a dental arch with zero to three metal crowns, enabling variable artifact intensity and reduction parameters. Beam hardening, resulting from sensor saturation, can be identified in the sinogram, while radial metal artifacts arise from sampling instabilities at metal boundaries—also observable within the sinogram. By understanding the origins of these artifacts, we gain insight into effective artifact reduction strategies.

This CT simulator facilitates understanding of the image reconstruction process and provides valuable support for mastering artifact mitigation principles.

The presentation explains the fundamentals of CT image reconstruction and artifact formation, with an emphasis on filtered backprojection and metal artifact reduction.

## IS3A-2

**Intraoral ultrasonography**

**Tanaka Ray**<sup>1\*</sup>, Hayashi, Takafumi<sup>2</sup>, Nalley, Andrew<sup>1</sup>, Hung, Kuo Feng<sup>1</sup>, Kan, Yee Ting Alice<sup>3</sup>, Kobayashi, Taichi<sup>2</sup>, Cardinal, Dayan Roxas Clarence<sup>1</sup>, Fok, Rachel Melissa<sup>3</sup>, Bornstein, Michael M<sup>4</sup>, Yeung, Wai Kan Andy<sup>1</sup>

<sup>1</sup>Applied Oral Sciences & Community Dental Care, The Faculty of Dentistry, The University of Hong Kong, Hong Kong SAR, China

<sup>2</sup>Division of Oral and Maxillofacial Radiology, Faculty of Dentistry and Niigata University Graduate School of Medicine, Dentistry and Health Sciences, Niigata University, Japan

<sup>3</sup>Periodontology & Implant Dentistry, The Faculty of Dentistry, The University of Hong Kong, Hong Kong SAR, China

<sup>4</sup>Department of Oral Health & Medicine, University Center for Dental Medicine Basel UZB, University of Basel, Basel, Switzerland

Have you ever called out loudly toward the mountains? “Echo” might have responded to you using the same words you said. Today, I would like to discuss another kind of “echo” — those captured in ultrasound diagnostic imaging — with a particular focus on intraoral ultrasonography in dentistry.

Intraoral ultrasonography has long been used to detect and diagnose soft-tissue lesions in areas such as the tongue and oral mucosa. More recently, however, it has gained attention as a promising non-invasive imaging modality capable of detailed evaluation of the teeth and the periodontal tissues. As the technology continues to advance, it holds significant potential to transform periodontal diagnostics and improve patient care through precise, non-invasive, real-time imaging.

This lecture will begin with a comprehensive overview of the principles, strengths, and limitations of ultrasound diagnostics, highlighting representative clinical applications of both extraoral and intraoral ultrasound techniques currently used in dentistry.

Next, focusing specifically on intraoral ultrasonography for periodontal tissues, I will introduce ongoing research aimed at validating its clinical utility. These efforts include confirming periodontal tissue anatomy and assessing the accuracy and reproducibility of measurements such as alveolar bone levels and soft-tissue morphology. Within this section, special emphasis will be placed on our own research, which involves classifying furcation involvement and assessing peri-implant osseous defects using ultrasonography. Our studies demonstrate that this modality can successfully visualize complex periodontal structures and potentially support more accurate diagnosis and treatment planning.

Finally, I will discuss future directions: the innovative coupling materials to enhance image quality and patient comfort, as well as the refinement of transducer designs to improve accessibility and usability within the oral cavity. These advancements highlight an exciting future in which ultrasonography plays a greater role in diagnostic imaging of the oral cavity without the risk of ionizing radiation.

**Invited Session 3B**

Principles and clinical applications of multimodality imaging

April 30 (Thu), 16:10-17:30

Room A

**IS3B-1****Basic principles of MRI and its application in the oral region****Shumei Murakami***Executive Assistant to the President**Department of Oral and Maxillofacial Radiology, Graduate School of Dentistry**The University of Osaka*

The first half of this lecture will explain the principles of MRI.

First, I will explain the behavior of protons in MRI, focusing on the Larmor precession and frequency, NMR phenomena, and the two relaxation processes. This section requires an understanding of energy transfer and phase convergence and divergence.

Next, I will define the T1 and T2 relaxation times and present the T1 and T2 relaxation times of normal oral tissues.

Next, I will introduce the five steps of MRI imaging and explain signal acquisition methods, including SE, GRE, and FSE sequences. To explain the FSE sequence, I will also briefly explain k-space. Here, I will explain how contrast is created by combining TR and TE. Larmor frequency is useful for deciding a tomographic plane.

Next, the characteristics of MRI are compared with CT. This comparison will help guide strategies for selecting imaging modalities in general clinical practice.

In the second half of this lecture, I will discuss the application of MRI to the oral region.

I will summarize key points and introduce relevant case studies. I will present cases of cysts, benign tumors, malignant tumors, inflammation, and temporomandibular joint disorders.

In the oral region, magnetic susceptibility artifacts from prosthetics and orthodontic appliances are often problematic. This presentation will discuss the latest findings regarding the impact of these artifacts on diagnostic imaging. It will also discuss the forces and torques exerted on prosthetic and orthodontic appliances, both inside and outside the MRI scanner.

Finally, I will introduce the latest MRI techniques for imaging teeth and bones, as well as dynamic swallowing and temporomandibular joint movement.

IS3B-2



## PET-CT(Fusion Imaging): The paradigm shift in oncological protocols

**Sunali Khanna**

*Department of Oral Medicine & Radiology, Nair Hospital Dental College, India*

Head and neck cancers, particularly oral cavity malignancies, present unique diagnostic and therapeutic challenges due to their complex anatomy, variable patterns of spread, and the need to balance oncologic control with functional preservation. Positron Emission Tomography–Computed Tomography (PET-CT) fusion imaging has emerged as a pivotal modality in the oncologic imaging of oral cancer, integrating metabolic information with high-resolution anatomic detail to enhance clinical decision-making across the disease continuum.

PET-CT, most commonly using 18F-fluorodeoxyglucose (FDG), enables sensitive detection of primary tumors, regional nodal metastases, and distant disease, often surpassing conventional imaging in identifying occult lesions. Fusion imaging improves tumor delineation in anatomically complex regions, aids in accurate staging, and refines risk stratification, directly influencing treatment planning. In oral cancer, PET-CT plays a critical role in assessing depth of invasion, nodal burden, and extracapsular spread, which are key prognostic indicators. Furthermore, PET-CT has demonstrated significant value in radiation therapy planning by enabling biologically guided target volume definition, potentially reducing treatment-related morbidity.

Beyond initial staging, PET-CT is increasingly integral to response assessment and post-treatment surveillance, allowing early differentiation between residual or recurrent disease and post-therapeutic changes. Emerging applications, including quantitative metabolic parameters, radiomics, and integration with artificial intelligence, hold promise for personalized oncologic imaging and outcome prediction.

This keynote will highlight the current evidence, clinical impact, limitations, and future directions of PET-CT fusion imaging in oral cancer, emphasizing its role in multidisciplinary care and precision oncology. As imaging continues to evolve from purely diagnostic to decisional and prognostic, PET-CT stands at the forefront of transforming head and neck cancer management.

## Invited Session 4A

Clinical decision-making and precision diagnosis using advanced imaging

May 1 (Fri), 09:00-10:50

Room A

IS4A-1



### From images to pathology: A precision medicine approach to periapical lesions

**Wen-Chen Wang**<sup>1,2</sup>

<sup>1</sup>*School of Dentistry, Oral and Maxillofacial Image Center, Kaohsiung Medical University, Taiwan*

<sup>2</sup>*Department of Dentistry, Division of Oral Pathology and Oral & Maxillofacial Radiology, Kaohsiung Medical University, Taiwan*

Periapical lesions can arise from a variety of causes. Beyond traditional imaging tools, the introduction of cone-beam computed tomography (CBCT) has greatly improved lesion visualization. Yet, despite extensive radiographic speculation, only histopathology can provide a definitive diagnosis.

The Department of Oral Pathology and Maxillofacial Imaging at Kaohsiung Medical University Hospital, Taiwan, is among the few clinical departments worldwide that integrate oral pathology and oral radiology. In this session, we will share selected periapical cases from our combined oral pathology and imaging databases—tracing the diagnostic journey from grayscale radiographic findings to the final colorful histopathological confirmation.

By reviewing these cases, we aim to enrich diagnostic experience, promote the use of appropriate diagnostic tools, and encourage analytical thinking among clinicians. Ultimately, this integration enhances the diagnosis and management of periapical and periodontal lesions, advancing the goal of precision dentistry.

**IS4A-2**

## **2 Radiologic insights: Bridging everyday cases and exceptional findings**

**Onanong Silkosessak***Department of Radiology, Faculty of Dentistry, Chulalongkorn University, Thailand*

Radiographic interpretation is more than simply reading images—it is a discipline that demands both technical knowledge and clinical experience. While conventional radiography remains the cornerstone of diagnostic imaging, the integration of advanced modalities such as CT, MRI, US and digital enhancements has expanded both the complexity and the potential of interpretation. Under the theme “*Radiologic Insights: Bridging Everyday Cases and Exceptional Findings*”, This session will highlight the interplay between traditional techniques and modern innovations, underscoring how experience shapes the ability to discern subtle findings, avoid common pitfalls and translate images into meaningful clinical decisions. Participants will be guided through illustrative cases that demonstrate the necessity of practice, exposure and critical thinking in mastering radiographic interpretation. More than a passive lecture, this will be an interactive opportunity to strengthen interpretive skills and appreciate the evolving role of imaging in patient care. You are warmly invited to join the session, engage with the discussion and enhance your expertise through shared learning.

**Invited Session 4A**

Clinical decision-making and precision diagnosis using advanced imaging

May 1 (Fri), 09:00-10:50

Room A

IS4A-3

**CBCT in endodontic retreatment: A tool for precision in calcified and complex root canal cases****Ming-Gen Tu**<sup>1,2</sup><sup>1</sup>*School of Dentistry, China Medical University, Taiwan*<sup>2</sup>*Department of Endodontics, China Medical University Hospital, Taiwan*

Treating calcified canals presents a significant challenge in endodontics due to the difficulty in locating and negotiating the canals, the increased risk of instrument separation, and the potential for inadequate cleaning and shaping. Radiographic imaging plays a crucial role in the diagnosis, assessment, and treatment planning of these complex cases. Periapical radiographs offer initial insights into the presence and extent of canal calcification. However, cone-beam computed tomography (CBCT) provides a more detailed, three-dimensional evaluation of the root canal anatomy. Unlike conventional periapical radiography, CBCT eliminates superimposition of surrounding structures, offering clinically relevant information through axial, sagittal, and coronal slices. CBCT imaging significantly enhances diagnostic accuracy and guides more effective treatment strategies, particularly in complex cases such as calcified canals, retreatment procedures, and internal or external root resorption. In this presentation, we will share a series of successfully managed cases involving these conditions, where the use of CBCT imaging contributed to improved outcomes. The detailed anatomical information obtained through CBCT led to more precise treatment planning and more predictable clinical results. While CBCT may not be necessary for every root canal treatment, it is increasingly considered a valuable tool and potentially the standard of care for managing challenging endodontic cases.

**IS4B-1****Radiographic diagnosis of root fracture****Masahiro Iikubo***Department of Dental Informatics and Radiology, Tohoku University Graduate School of Dentistry, Japan*

Root fractures of human permanent teeth are usually caused by high-impact force such as trauma or excessive occlusal forces. Accurate diagnosis of tooth root fracture is essential to assess the prognosis and determine appropriate treatment for the tooth. Intraoral radiography has been commonly used for diagnosing root fractures. However, root fractures are difficult to detect on intraoral radiographs during an initial examination immediately after fracture. Recently, dental cone beam CT (dental CT), with its wide adoption, has been used to detect root fractures that cannot be identified with intraoral radiography. However, many studies have reported that artifacts caused by root canal filling materials on dental CT images reduced the diagnostic accuracy for root fractures. In this presentation, I will introduce the research findings regarding the pattern of artifact based on our phantom study and the latest research on the development of the dental CT machine and dental materials to reduce these artifacts. I hope this presentation will be useful for your clinical diagnosis of root fractures and contribute to the advancement of new research.

**Invited Session 4B**

Clinical decision-making and precision diagnosis using advanced imaging

May 1 (Fri), 11:10-12:30

Room A

IS4B-2

**Nasopharynx on cone-beam computed tomography****David MacDonald***Dept: Oral, medical and biological Sciences. University of British Columbia, Canada.*

Nasopharyngeal carcinoma (NPC) is endemic in East Asians, North Africans, their diasporas and the Inuit of Greenland and Canada. Radiologically it is first identified as asymmetry of the *Fossa of Rosenmüller* (FoR) in the nasopharynx. This asymmetry is also readily displayed on the *cone-beam computed tomography* (CBCT), as reflected in the outcomes of recent research, performed in Canada and Korea. This research is based around Takasugi *et al*'s three patterns of FoR observed on *multi-detector CT* (MDCT). These patterns varied in prevalence between the sexes, which in part may explain the higher prevalence of NPC in males. The nasopharynx is prominently displayed on medium-to-large *fields-of-view* (FOV) CBCT, because the pharynx of the vertically-positioned patient displayed on the CBCT hangs more openly than when the patient is lying supine for a MDCT. Although a minority of CBCTs display asymmetry of the FoR that will be easily visible to dentists, it is necessary to avoid undue referral of these cases as many may be false positives and could overwhelm already over-worked specialist services. Therefore, care should also be taken with regards to the clinical history and examination of the neck, especially for lymphadenopathy. Finally, attention needs to be paid to the velopharynx in such medium-to-large FOV CBCTs, which is immediately inferior to the nasopharynx., as this may reveal paragangliomas. These were just recently *all* pronounced malignant by the *World Health Organization* (WHO).

**IS5A-1****Bone quality prediction using diagnostic images****Min-Suk Heo***Department of Oral and Maxillofacial Radiology, School of Dentistry, Seoul National University, Korea*

Bone quality prediction using dental diagnostic images has become an important goal for improving treatment planning, implant stability assessment, and understanding overall bone health. There have been many studies on predicting bone condition by measuring clear and objective features from routine images, instead of relying only on simple visual inspection. These measurements include structural patterns, cortical thickness, radiographic density (or Hounsfield units in CBCT or CT), and texture features such as fractal dimension, which can provide useful clues about both local bone structure and general bone strength. Various methods have been used so far, and each has strengths and weaknesses in accuracy, reproducibility, and sensitivity to imaging conditions. Many reports show that these image-based features can reflect changes in trabecular organization and cortical quality, allowing earlier detection of weak bone and more reliable preoperative assessment. This lecture will review current evidence on predicting bone quality from diagnostic images, compare the advantages and limitations of commonly used approaches, and discuss how these techniques may be applied in clinical practice, along with future directions for more stable and practical prediction.

**Invited Session 5A**

Advances in imaging science and their impact on predictive dentistry

May 1 (Fri), 13:30-14:50  
Room A

IS5A-2

**From image recognition to multimodal understanding:  
Emerging AI trends in oral and maxillofacial radiology****Sang-Sun Han***Department of Oral and Maxillofacial Radiology, Yonsei University College of Dentistry, Republic of Korea  
Institute for Innovation in Digital Healthcare, Yonsei University College of Dentistry, Republic of Korea*

The field of artificial intelligence (AI) in dentistry has been continuously evolving, with a persistent focus on radiographic feature identification and single-modality analysis. These models have demonstrated meaningful analytical capabilities and objectivity at the pixel level in identifying specific findings or anatomical structures, steadily expanding their potential as clinical decision support tools. This ongoing advancement in visual recognition models serves as a fundamental process in validating the practical utility and clinical reliability of AI within Oral and Maxillofacial Radiology (OMFR).

This lecture provides a structured review of imaging-based AI research in OMFR, tracing its development from early machine learning approaches to contemporary deep learning models. Key research themes — including detection, segmentation, and classification across various dental imaging modalities — are examined from the perspective of their clinical relevance and applicability.

As multimodal technologies gain increasing attention in the broader medical AI field, dentistry is seeing growing interest in integrated attempts to combine radiographic information with textual data while maintaining visual analytical precision. This lecture also introduces recent research trends in multimodal approaches, including Large Vision-Language Models (LVLMs).

Through this, attendees will gain an overview of the current trajectory of imaging-based AI research and a preliminary understanding of how multimodal technologies may gradually inform the diagnostic workflows of the next generation of OMFR.

## IS5B-1



## Image modality innovations in oral and maxillofacial imaging: Promises and challenges

**Jie Yang**

*Temple University Kornberg School of Dentistry, USA*

Dental-dedicated MRI (ddMRI) represents one of the leading innovations in oral and maxillofacial radiology and has demonstrated potential for evaluating soft tissues in the oral and maxillofacial region, including pulpal tissues, gingiva and periodontal ligament spaces, the temporomandibular joint (TMJ) disc, and surrounding soft-tissue structures. However, clinical implementation of current ddMRI systems remains challenging. High cost, limited technical accessibility for routine dental practice, and uncertain clinical advantages in endodontic and periodontal applications continue to hinder widespread adoption. Substantial reductions in system size, cost, and image acquisition time are required before ddMRI can be broadly implemented in general dental practice.

Digital sensor technology is widely used in dentistry. With the emergence of artificial intelligence (AI) and machine learning for disease detection, the future of diagnostic imaging is primarily constrained by the physical limitations of X-ray detectors, scintillators, and X-ray source focal spot size. This presentation introduces a newly developed imaging system that integrates a novel intraoral sensor prototype, a crystal-based scintillator, and a microfocus X-ray source. The system operates at a very low tube current (0.3 mA) with a 10–30  $\mu\text{m}$  focal spot and incorporates AI-based image denoising. We demonstrate that integration of a back-illuminated (BI) sensor, a LYSO(Ce) scintillator, and a microfocus X-ray source improves spatial resolution, reduces radiation dose, and enables real-time cinematic imaging. The BI sensor and LYSO(Ce) scintillator facilitate the clinical use of microfocus X-ray sources. Collectively, these technologies have the potential to expand diagnostic capabilities in both dental and medical radiography.

## Invited Session 6A

Artificial intelligence in dentomaxillofacial radiology: Current applications and future perspectives

May 2 (Sat), 09:00-10:50

Room A

IS6A-1



### AI and virtual reality in teaching oral and maxillofacial radiology

**Ingrid Różyło-Kalinowska**

*Department of Dental and Maxillofacial Radiodiagnostics, Medical University of Lublin, Poland*

The aim of the lecture is to examine the expanding role of machine-learning tools and virtual reality in teaching dentomaxillofacial radiology, showing how machine learning based platforms can enhance students' interpretative skills through adaptive case presentation, automated feedback, and dynamic visualization of anatomical structures and pathologies. It also outlines practical approaches to integrating these technologies into curricula, including structured reporting exercises supported by AI and progress-tracking dashboards. Own experiences in teaching dental student will be presented. Key ethical and pedagogical considerations - such as transparency, data protection, and avoiding overreliance on algorithms - are highlighted to guide responsible implementation in radiology education.

**IS6A-2****DMFR in the age of AI – What changes will we have to expect?****Michael M. Bornstein***University of Basel, Switzerland*

Personalized medicine and dentistry refers to the tailoring of diagnostics and therapeutics to individuals based on each patient's biological, social, and behavioral characteristics and needs. While personalized dental medicine is still far from being a reality, advanced artificial intelligence (AI) technologies with improved data analytic approaches are expected to integrate diverse data from the individual, setting, and system levels, which may facilitate a deeper understanding of the interaction of these multi-level data and therefore bring us closer to more personalized, predictive, preventive, and participatory dentistry, also known as P4 dentistry. In the field of dentomaxillofacial imaging, a wide range of AI applications, including several commercially available software options, have been proposed to assist dentists in the diagnosis and treatment planning of various dentomaxillofacial diseases, with performance similar or even superior to that of specialists. The present lecture will discuss and elaborate on the impact of these dental AI applications on treatment decision, clinical and patient-reported outcomes, and cost-effectiveness. Such information should be further investigated to provide patients, providers, and healthcare organizers a clearer picture of the true usefulness of AI in daily dental practice.

*Learning objectives:*

- Know the definition of 4P medicine and dentistry
- Know about history of AI in general, and dental medicine / dento-maxillofacial radiology more specifically
- Know about current use of AI for image diagnosis and treatment planning
- Know about future developments of AI in dental medicine with special focus on LLM / multimodal AI models

**Invited Session 6A**

Artificial intelligence in dentomaxillofacial radiology: Current applications and future perspectives

May 2 (Sat), 09:00-10:50

Room A

**IS6A-3****AI medical devices and AI for everyday use in dentistry****Akitoshi Katsumata***Department of Radiology, Asahi University, Japan*

There are two major categories of artificial intelligence: narrow AI, which is designed for specific functions, and general-purpose AI for everyday use, such as ChatGPT. We have developed a specialized narrow AI system for screening osteoporosis using panoramic X-ray images. This system, called PanoSCOPE, has been approved and implemented as the first medical AI device for dentistry in Japan. At the same time, there is increasing interest in how general-purpose AI can be incorporated into dental practice.

PanoSCOPE is a software-as-a-medical-device that evaluates the mandibular inferior cortex and automatically determines the mandibular cortical index (MCI). It replicates the diagnostic workflow of expert oral and maxillofacial radiologists for visual MCI assessment. The system was trained on expert-annotated image datasets and was validated using images independently evaluated by other experts for MCI classification. The explainable nature of the system—based on predefined regions of interest and explicit diagnostic criteria—played an important role in obtaining regulatory approval. Moreover, combining traditional rule-based processing with AI-driven functions appears necessary for practical clinical devices.

In contrast, general-purpose AI systems, such as ChatGPT, are pretrained on large-scale internet-derived datasets and can be used simply by prompting. Because general-purpose models evolve rapidly, their potential medical applications may outpace traditional research and development cycles. For example, when DICOM files are submitted to ChatGPT, tag information that was unreadable in earlier versions has become interpretable in newer versions. Such systems can also assist with evaluating intraoral photographs and evaluating tongue coating according to the Oral Health Assessment Tool (OHAT) criteria. Furthermore, by providing radiographs with marked target lesions along with clinical symptoms, they can generate structured imaging reports that are clinically convincing.

However, the responses generated by general-purpose AI are not always correct. Medical professionals should therefore use such systems cautiously and avoid placing unwarranted trust in non-validated outputs.

## IS6B-1



## Beyond X-rays: Entering the AI-enhanced dental-dedicated MRI era – What does the future hold for dentistry?

**Kaan Orhan**

*Ankara University, Faculty of Dentistry, Department of Dentomaxillofacial Radiology, Ankara, Türkiye*

Artificial intelligence (AI) in healthcare refers to the use of advanced algorithms and computational models to approximate human cognition in the analysis of complex medical data. Unlike traditional technologies, AI systems have the capacity to acquire information, process large datasets, learn from them, and generate well-defined, clinically meaningful outputs without continuous human intervention. These capabilities—powered primarily by machine learning and deep learning—enable the recognition of intricate patterns and the development of autonomous decision-making logic.

As dentistry transitions **beyond conventional X-ray-based imaging** into the era of **AI-enhanced dental-dedicated MRI (ddMRI)**, the potential impact on diagnostics, treatment planning, and patient safety is transformative. ddMRI offers radiation-free, high-contrast visualization of soft tissues, pulpal structures, TMJ, and peri-implant tissues—domains where traditional imaging is limited. When combined with AI-driven reconstruction, segmentation, image quality enhancement, and automated diagnostic workflows, ddMRI stands poised to redefine the future of dental radiology.

This lecture will (1) explain the fundamental principles of deep learning, (2) discuss the integration of AI with emerging ddMRI technologies, (3) provide key technical requirements for implementing AI and blockchain systems in healthcare, and (4) present examples of successful AI applications in dentistry and dentomaxillofacial radiology, based on our recent clinical and research studies. The session will also explore how blockchain, NFTs, and IoT infrastructures may support secure data management and interoperability in next-generation dental imaging ecosystems.



# Quiz



Q1



## Horses and Zebras in head and neck imaging (I)

**Chena Lee**

*Department of Oral and Maxillofacial Radiology, Yonsei University College of Dentistry, Republic of Korea*

Differentiating among a wide range of oral and maxillofacial lesions can be challenging, particularly when diverse cystic, fibro-osseous, inflammatory, and neoplastic conditions present with overlapping radiographic features. This interactive seminar is designed to support learners in navigating these complexities by guiding them through a stepwise diagnostic reasoning process that incorporates multiple potential lesion categories. Using real clinical cases, participants are first encouraged to consider a broad differential list and then progressively refine it as additional imaging findings and clinical details are introduced. Real-time polling and brief group discussions allow learners to test their diagnostic hypotheses and receive immediate feedback that emphasizes key distinguishing characteristics across lesion groups. By engaging in this iterative process, participants practice recognizing radiographic patterns, evaluating clinical relevance, and weighing competing possibilities—skills essential for effective differential diagnosis. The seminar ultimately aims to help learners approach multifaceted diagnostic scenarios with greater confidence and clarity, promoting a more integrated and clinically grounded understanding of oral and maxillofacial pathology.

Q2



## Horses and Zebras in head and neck imaging (II)

**Jo-Eun Kim**

*Department of Oral and Maxillofacial Radiology, School of Dentistry, Seoul National University, Rep. of Korea*

Diagnosis in imaging is rarely as straightforward as textbooks suggest. In real clinical practice, radiologists integrate subtle imaging clues with clinical findings to construct a differential diagnosis and progressively narrow it toward a final conclusion. Despite this systematic approach, certain entities remain easily confused.

This session focuses on diseases in the head and neck region that are frequently misinterpreted on imaging and explores practical strategies for differential diagnosis. Rather than a one-way lecture, the session is designed as an interactive experience in which participants actively engage through real-time voting and discussion, collectively building and refining differential diagnoses.

Among the many potentially confusing conditions, particular emphasis will be placed on distinguishing inflammatory diseases from malignant tumors, as well as differentiating among various benign tumors. Through shared reasoning and case-based discussion, participants will practice the interpretive process that underlies accurate radiologic diagnosis in complex, real-world settings.



# Oral Presentation



## Oral Presentation 1

April 30 (Thu), 13:30-14:30 | Room C

### OPI-1

## Amelogenesis imperfecta associated with taurodontism as an incidental radiographic finding: A rare case report and recent literature review

**Farah Fadhilah**<sup>1\*</sup>, Barunawaty Yunus<sup>1,2</sup>, Fadhil Ulum<sup>1,2</sup>, Irfan Sugianto<sup>1,2</sup>, Dwi Putri Wulansari<sup>1,2</sup>, Babatunde Olamide Bamgbose<sup>2,3</sup>

<sup>1</sup>Dentomaxillofacial Radiology Specialist Study Program, Faculty of Dentistry Hasanuddin University, Indonesia

<sup>2</sup>Department of Oral and Maxillofacial Radiology, Faculty of Dentistry, Hasanuddin University, Makassar, Indonesia

<sup>3</sup>Department of Oral Diagnostic Sciences, Faculty of Dentistry, Bayero University, Kano, Nigeria

**Introduction:** Amelogenesis imperfecta (AI) is a rare hereditary enamel disorder that affects both primary and permanent dentitions, presenting with variable clinical severity ranging from mild hypomineralization to complete enamel absence.

**Case:** A 17-year-old male presented for a routine panoramic evaluation following extraction of the lower right molar. Clinical examination revealed generalized enamel defects characterized by generalized attrition and yellowish discoloration. The primary dentition exhibited similar abnormalities. Panoramic imaging demonstrated markedly reduced enamel radiopacity, loss of enamel–dentin contrast, and generalized enamel thinning. These clinical and radiographic features are consistent with incidental diagnosis of amelogenesis imperfecta.

**Discussion:** The incidental identification of amelogenesis imperfecta in this patient underscores the essential role of radiographic assessment in detecting enamel defects that may be overlooked clinically, especially in individuals who adapt to long-standing structural abnormalities. A comprehensive literature search across PubMed, ScienceDirect, Wiley Online Library, and PLOS ONE databases yielded only two similar cases of amelogenesis imperfecta with taurodontism underscoring the extreme rarity of our AI presentation. Giv-

en the limited reports in the literature, this finding highlights the importance of comprehensive imaging during routine evaluations, as early recognition facilitates appropriate counseling, preventive strategies, and long-term restorative planning.

### OPI-2

## Mandibular neurofibroma with extensive osseous changes in Neurofibromatosis Type 1: A case report

**Nantawat Joombal**<sup>1\*</sup>, Poramaporn Klanrit<sup>1</sup>, Wariya Panprasit<sup>1</sup>

<sup>1</sup>Department of Oral Diagnosis, Faculty of Dentistry, Khon Kaen University, Thailand

**Introduction:** Neurofibromatosis Type 1 (NF1) is an autosomal dominant genetic disorder. While NF1 frequently affects the skin and nervous system, the localized presentation of neurofibroma within the mandible is exceedingly rare.

**Case:** We present the case of an 18-year-old Thai male with NF1. The patient presented with a large, slowly progressing swelling of the right cheek, and multiple hyperpigmented macules were noted. A panoramic radiograph demonstrated prominent unilateral mandibular hypoplasia and a flattened mandibular angle on the right side. The right mandibular notch appeared markedly deeper than the contralateral side. The right condyle appeared diminished in size and showed elongation of the condylar process. Computed tomography (CT) imaging corroborated these osseous deformities, particularly the elongation of the right condylar process. The right mandibular foramen area showed an expansion at the lingual surface of the right ramus, associated with mild lingual cortical plate expansion and a thinned buccal cortical plate. The associated soft tissue swelling was heterogeneous with areas of hypodensity relative to the adjacent masticatory muscles. This hypodense mass also displayed a multilobulated configuration. Magnetic Resonance Imaging (MRI) displaying the lesion as heterogeneously hyperintense on T2-weighted images and consisting of multiple nodules. An incisional biopsy was performed in the mandibular region, and histopathological examination

confirmed the diagnosis of neurofibroma.

**Discussion:** This case suggests the utility of multi-modal imaging, particularly panoramic radiography, CT, and MRI, for the comprehensive preoperative evaluation of rare mandibular lesions associated with NF1.

### OP1-3

## Diffusion weighted magnetic resonance imaging in diagnosis of vascular anomalies of oral and maxillofacial region: A retrospective study

**Medhana Mangoanker**<sup>1\*</sup>, Manisha Khorate<sup>1</sup>,  
Sonali Parvatkar<sup>1</sup>, Sushmita Wayadande<sup>1</sup>

<sup>1</sup>Department of Oral Medicine & Radiology, Goa Dental College and Hospital, Goa University, India

**Introduction:** Vascular anomalies appear as bluish – red lesion in oral cavity, with incidence of <5%. They have a varied clinical picture which makes the diagnosis uncertain; thus, thorough history of the lesion and clinical examination with appropriate imaging is of great importance. Imaging modalities such as Ultrasound and Magnetic Resonance Imaging (MRI) are considered the gold standard for evaluating internal echotexture, feeding vessels, and flow characteristics in such conditions, further enhancing treatment planning.

Diffusion Weighted Magnetic Resonance Imaging (DW-MRI) is a sequence of MRI and can be used as a non-invasive biomarker, that creates Apparent Diffusion Coefficient maps, that quantify water diffusivity within individual voxels. This quantitative approach facilitates data acquisition while minimizing the risks associated with radiation and contrast agents.

**Objective:** To evaluate the diagnostic accuracy of diffusion weighted magnetic resonance imaging in vascular anomalies in oral and maxillofacial region.

**Materials and Methods:** 10 Patients who reported to the Department of Oral Medicine and Radiology from 2022 to 2024, with DW-MRI as the imaging modality,

were evaluated for diagnostic features of vascular anomalies.

**Results:** The majority of the patients in the study demonstrated the slow-flow, venous malformation. The MRI exhibited low to intermediate signals on T1-weighted imaging (T1WI), signals ranging from low to intermediate-to-high on T2WI. DW-MRI illustrated high signal intensity with facilitated diffusion in the majority of cases. The mean ADC value ranged <math>2 \times 10^{-3}</math> mm<sup>2</sup>/s.

**Conclusions:** DW-MRI is a reliable imaging modality that, along with ADC values provide quantitative information that diagnose vascular anomalies based on their underlying cellularity and microstructural characteristics. Further research with a larger sample size is required to evaluate the combined application of DW-MRI and existing imaging modalities to enhance diagnostic accuracy.

### OP1-4

## CT-based assessment of dento-periodontal and maxillofacial side effects of radiotherapy in ENT cancer patients

**Antohei Cristina**<sup>1\*</sup>, Haba Danisia<sup>2</sup>, Cernei Radu Eduard<sup>2</sup>, Popescu Roxana Mihaela<sup>2</sup>, Dobrovat Bogdan Ionut<sup>2</sup>, Salceanu Mihaela<sup>1</sup>, Concita Corina Alexandra<sup>1</sup>, Hamburda Tudor<sup>1</sup>, Giuroiu Cristian Levente<sup>1</sup>, Gheorghe Angela<sup>3</sup>, Pancu Galina<sup>3</sup>, Nica Irina<sup>3</sup>

<sup>1</sup>ENDONTOLOGY, UMF GR T POPA, Romania

<sup>2</sup>Surgery, UMF GR T POPA, Romania

<sup>3</sup>Cariology, UMF GR T POPA, Romania

**Introduction:** Radiotherapy, with or without chemotherapy, is a cornerstone in the management of head and neck malignancies. Despite its therapeutic benefits, ionizing radiation can induce significant acute and chronic side effects affecting oral, dental, and maxillofacial structures. Computed tomography (CT) plays a key role in the objective evaluation of post-therapeutic changes. This study aimed to compare dento-periodontal and maxillofacial CT findings in ENT cancer patients before radiotherapy and/or chemotherapy.

**Material and Method:** This retrospective study included 35 patients (34 males, 1 female), aged 32–81 years, treated at the Regional Institute of Oncology, Iași, between May 2019 and May 2021. Diagnoses included laryngeal, oropharyngeal, oral cavity, nasopharyngeal, hypopharyngeal, and sinonasal cancers. Pre- and post-radiotherapy and/or chemotherapy CT scans were analyzed for periapical lesions, radiomucositis severity, osteoradionecrosis, and sinus involvement.

**Results:** Post-treatment CT imaging revealed a significantly higher prevalence of periapical pathology, moderate to severe radiomucositis, osteoradionecrosis, and sinus alterations in oncologic patients compared with healthy controls. Findings were more pronounced following combined radio-chemotherapy and correlated with tumor site and radiation field.

**Conclusions:** CT imaging is essential for detecting and monitoring dento-periodontal and maxillofacial side effects of radiotherapy in head and neck cancer patients. Early identification supports multidisciplinary care and may improve long-term outcomes.

#### OPI-5

### Enhancing radiomic feature reproducibility in nasopharyngeal carcinoma MRI: A comparative evaluation of manual and semi-automatic segmentation techniques

**Norasikin Ismail**<sup>1\*</sup>, Muhammad Khalis Abdul Karim<sup>2</sup>, Izdihar Kamal<sup>3</sup>, Mohd Hafiz bin Mohd Zaid<sup>4</sup> and Kasturi Nair Tangaraju<sup>5</sup>

<sup>1-4</sup>Department of Physics, Faculty of Science, Universiti Putra Malaysia, 43400 Serdang, Selangor, Malaysia.

<sup>5</sup>Department of Radiology, Institut Kanser Negara (IKN), Putrajaya 62250, Malaysia

**Introduction:** Radiomics is a non-invasive technique that converts medical images into quantitative biomarkers for cancer diagnosis and prognosis. In nasopharyngeal carcinoma (NPC), MRI-based radiomic features can characterize tumour heterogeneity and predict treatment outcome. However, its reliability highly depends on the accuracy of the segmentation.

Manual segmentation is expert-driven but time-consuming and prone to interobserver variability, whereas algorithms and expert input drive semi-automatic segmentation to enhance consistency and reduce human bias. Thus, this study is to evaluate and compare the reproducibility of radiomic features derived from manual and semi-automatic segmentation of NPC on MRI.

**Materials and Methods:** Thirty (30) contrast-enhanced T1-weighted (CE-T1WI) MRI scans of histologically confirmed NPC were retrospectively analyzed. Tumor regions of interest were segmented manually and semi-automatically using the level-tracing algorithm in 3D Slicer by two radiology observers. A total of 107 radiomic features (first-order, shape, and texture) were extracted with PyRadiomics. Interclass correlation coefficients (ICC) were computed to evaluate inter-observer reproducibility, categorized as poor (< 0.5), moderate (0.5–0.75), good (0.75–0.9), and excellent (> 0.9).

**Results:** Semi-automatic segmentation achieved higher reproducibility (mean ICC = 0.92 ± 0.06) than manual segmentation (mean ICC = 0.80 ± 0.13). Approximately 77% of features from semi-automatic segmentation reached excellent ICC compared to 10% in manual delineation. Notably, shape and texture features showed the most improvement, while first-order features remained relatively consistent across methods.

**Conclusions:** Semi-automatic segmentation substantially improves radiomic feature reproducibility in MRI-based assessment of NPC by reducing observer variability and standardizing feature extraction. This approach strengthens the reliability of radiomics for clinical decision-making and multicenter research standardization.

#### OPI-6

### Tumoral cells highway: An approach to the perineural spread in nasopharyngeal tumors

**Danisia Haba**<sup>1,2\*</sup>, Ilinca Diana Andreea<sup>1,2</sup>, Roxana Popescu<sup>1</sup>, Bogdan Dobrovat<sup>1</sup>, Ana Sirghe<sup>1</sup>, Emilia Marciuc<sup>1</sup>, Daniela Pomohaci<sup>1</sup>, Cristina Antohi<sup>3</sup>

<sup>1</sup>Department of Surgery, UMF Gr.T.Popa Iasi, Romania

<sup>2</sup>Department of Radiology, Medimagis, Romania

<sup>3</sup>Department of Edontology, UMF Gr.T.Popa Iasi, Romania

**Introduction:** Perineural spread (PNS) is an important but underdiagnosed and under detected pathway of extension in nasopharyngeal carcinoma. Tumors may use established anatomical neural corridors – particularly involving the pterygopalatine fossa, vidian nerve and trigeminal branches. This study outlines the CT and MRI key imaging patterns of PNS and their clinical relevance.

**Materials and Methods:** We retrospectively studied and reviewed 30 nasopharyngeal carcinoma cases, diagnosed with PNS in the Emergency Hospital N .Oblu Iasi, Romania, between 2019-2025. CT and MR Imaging was assessed for identifying involvement of major entry zones (vidian canal, foramen rotundum, foramen spinosum), nerve enhancement or widening. Pathways of spread were mapped based on skull-base anatomy.

**Results:** The most common route of PNS originated in the nasopharynx, extended into the pterygopalatine fossa and progresses along the maxillary nerve toward the cavernous sinus. Frequent imaging findings were nerve thickening and contrast enhancement, foraminal enlargement and atrophy of muscles . Early identification using MRI examinations of PNS can alter treatment planning by expanding radiotherapy target volumes.

**Conclusions:** Nasopharyngeal carcinoma can extend through predictable neural “highways” often without associated symptomatology (silent spread). Recognizing the patterns in CT and MRI, especially along the vidian and trigeminal routes is essential for accurate staging and treatment planning.

## Oral Presentation 2

April 30 (Thu), 15:10-17:00 | Room C

### OP2-1

## Evaluation of root canal visibility and traceability at different root levels using various CBCT dose protocols

**Clarence Dayan Roxas Cardinal**<sup>1</sup>, Andrew Nalley<sup>1</sup>, Andy Wai Kan Yeung<sup>1</sup>, Ray Tanaka<sup>1</sup>, Kuo Feng Hung<sup>1</sup>

<sup>1</sup>Oral and Maxillofacial Radiology, Applied Oral Sciences and Community Dental Care, Faculty of Dentistry, The University of Hong Kong, Hong Kong SAR, China

**Introduction:** This study aims to assess root canal visibility and traceability at different root levels in all tooth types, and separately in non-molar and molar teeth, using three CBCT dose protocols.

**Materials and Methods:** Seventy-five teeth in 20 dry mandibles were scanned with CBCT using high-, standard-, and low-dose protocols (1362-305 mGy×cm<sup>2</sup>). Root canal visibility at the coronal, middle, and apical thirds was rated on a 5-point scale and traceability from orifice to apical foramen was assessed as traceable or non-traceable for 225 teeth on 60 scans by a blinded examiner. Pairwise comparisons for visibility and traceability between protocols were performed using Wilcoxon signed-rank or McNemar tests.

**Results:** Across all tooth types, canal visibility decreased from coronal to apical thirds (4.39-3.81 to 2.64-1.84) and from high- to low-dose scans (4.39-2.64 to 3.81-1.84). Traceability reduced with lower dose protocols (97.3% to 86.7%). Non-molars showed higher visibility and traceability across all root levels and dose protocols, with high-dose scans improving visibility at the middle and apical thirds, while in molars both high- and standard-dose scans enhanced visibility at all root levels compared to low-dose scans. In non-molars high-dose scans improved visibility at the middle and apical thirds while in molars both high- and standard-dose scans enhanced visibility at all root levels compared to low-dose scans. Traceability was unaffected by different protocols in non-molars but

was significantly reduced in low-dose scans for molars.

**Conclusions:** Higher CBCT dose protocols significantly improved root canal visibility and traceability, particularly at the apical third. While non-molars maintain high traceability across all protocols, molar teeth show reduced traceability with low-dose scans.

## OP2-2

### Evaluation of the diagnostic value of dental MRI using a dental-dedicated magnetic resonance imaging coil

Hyewon Seo<sup>\*1</sup>, Chena Lee<sup>1,2</sup>

<sup>1</sup>Department of Oral and Maxillofacial Radiology, Yonsei University College of Dentistry, Seoul, Korea

<sup>2</sup>Oral Science Research Center, Yonsei University College of Dentistry, Seoul, Korea

**Introduction:** This prospective study aimed to quantitatively evaluate the image quality of dental magnetic resonance imaging (MRI) obtained using a dental-dedicated coil in comparison with conventional Head&Neck MRI coils. The primary objective was to compare signal-to-noise ratio (SNR) among different coil configurations to assess the potential diagnostic value of a Dental-dedicated coil for dental and maxillofacial imaging.

**Materials and Methods:** Dental and maxillofacial MRI scans were acquired using three different radiofrequency coils: a 21-channel Head&Neck coil, a 16-channel Flexible coil, and an 11-channel Dental-dedicated coil. Quantitative image analysis was conducted by placing standardized regions of interest (ROIs) in the dental region. SNR was calculated as the ratio of mean signal intensity within the ROI to the standard deviation of background noise.

**Results:** The 21-channel Head&Neck coil demonstrated a mean signal intensity of 4,605.60 with a noise standard deviation of 12.71, resulting in an SNR of 362.4. The 16-channel Flexible coil showed a mean signal intensity of 12,293.13 and a noise standard deviation of 10.17, yielding the highest SNR of 1,208.4. The 11-channel Dental-dedicated coil exhibited a

mean signal intensity of 14,870.51 with a noise standard deviation of 17.66, corresponding to an SNR of 841.9. The SNR of the dental-dedicated coil was 69.7% of that achieved by the coil with the highest SNR, while it reached 232.4% of the SNR obtained with the coil with the lowest value.

**Conclusions:** Quantitative analysis revealed that MRI coil configuration has a significant impact on SNR in dental imaging. The dental-dedicated coil provided markedly improved SNR compared with a conventional 21-channel Head&Neck coil, supporting its potential clinical usefulness.

## OP2-3

### Effect of focus adjustment function of panoramic system based on tomosynthesis method on the visibility of maxillary and mandibular incisors

Nur Redannia Redzuan<sup>1\*</sup>, Ikuho Kojima<sup>1</sup>, Mihoko Suzuki<sup>1</sup>, Yusuke Shimada<sup>1</sup>, Masahiro Iikubo<sup>1</sup>

<sup>1</sup>Department of Dental Informatics and Radiology, Tohoku University, Japan

**Introduction:** Recent advances in panoramic X-ray systems with tomosynthesis enable post-acquisition focusing and adjustable imaging planes. This study compared the visibility of maxillary and mandibular incisors using three tomosynthesis panoramic radiograph (TPAN) reconstructions: pre-autofocus (Pre-AF), post-autofocus (Post-AF), and self-adjusted layer (Self-AL).

**Materials and Methods:** This study assessed TPAN images (PanoACT; AXION JAPAN Corp.) of 204 incisors (maxilla: 101; mandible: 103). Two reviewers assessed root morphology (RM), canal morphology (CM), periodontal ligament (PDL), and overall image quality (OvQ) using a 5-point scale (1 = barely visible, 2 = poorly visible, 3 = moderately visible, 4 = well visible, and 5 = excellent visibility), and then classified into a binary classification: good (3-5) and poor (1-2) visibility. Cochran's Q test and ROC curve analysis (AUC) were used for statistics.

**Results:** All reconstruction methods demonstrated high AUC values (0.89–0.98). The mandible generally

showed higher AUCs than the maxilla, except for RM in Self-AL. Using 0.95 as the evaluation cutoff, Pre-AF AUCs in the maxilla were below 0.95 for all items, Post-AF AUCs were above, except for CM, and Self-AL AUCs exceeded 0.95 for RM and PDL. In the mandible, Pre-AF and Post-AF AUCs were above 0.95 for all items, whereas Self-AL AUCs for CM and OvQ were below 0.95. In the binary classification, Post-AF yielded the highest rates of good visibility for the maxilla across all items, followed by Self-AL, with Pre-AF lowest. In the mandible, Post-AF had the highest good visibility rates for all except CM, while Pre-AF had higher percentages than Self-AL in all but RM.

**Conclusions:** Post-AF may appear preferable for routine anterior tooth evaluation in panoramic imaging, offering enhanced anatomical detail without additional adjustment.

#### OP2-4

### Evaluation of imaging protocols for detecting tooth ankylosis using different CBCT devices

Selale Ozel<sup>1</sup>, Taha Emre Kose<sup>2</sup>, **Samed Satir**<sup>3\*</sup>

<sup>1</sup>Department of Oral and Maxillofacial Radiology, Faculty of Dentistry, Altinbas University, Turkiye

<sup>2</sup>Department of Oral and Maxillofacial Radiology, Faculty of Dentistry, Recep Tayyip Erdogan University, Turkiye

<sup>3</sup>Department of Oral and Maxillofacial Radiology, Faculty of Dentistry, Karamanoglu Mehmetbey University, Turkiye

**Introduction:** Tooth ankylosis is the fusion of the cementum or dentin of the tooth root to the surrounding alveolar bone and partial or complete obliteration of the periodontal ligament (PDL) space. In the present study, aim is to compare the diagnostic accuracy of CBCT images acquired with different voxel sizes and imaging protocols, providing further insight into optimal imaging protocols for ankylosis detection.

**Materials and Methods:** 30 extracted teeth included for tooth ankylosis simulation. To simulate the PDL space, the roots were coated with Teflon tape. In the simulated ankylosis group, the Teflon tape was carefully removed in assigned locations. The teeth were then embedded in plaster blocks. The samples imaging were performed in four different imaging pro-

ocols using two CBCT devices (NewTom VGi Evo and KaVo OP 3D Pro). The findings were recorded as “present” or “absent”. Micro-CT imaging (SkyScan 1173) was performed on 20% of the specimens to verify the accuracy of the simulation. Fleiss’ Kappa analysis was used for the overall agreement. Sensitivity, specificity, positive predictive value (PPV), and negative predictive value (NPV) were calculated.

**Results:** The smallest voxel size (0.25 mm) demonstrated the most favorable overall results. Although its Cohen’s Kappa coefficient indicated only slight agreement (0.113), the protocol achieved relatively high sensitivity (71.4%) and acceptable predictive values (PPV: 52.6%, NPV: 60%). The largest voxel size (0.35 mm) showed the weakest performance, with a negative Kappa value (−0.104), the lowest sensitivity (53.8%), and reduced predictive values (PPV: 43.8%, NPV: 45.5%).

**Conclusions:** CBCT imaging demonstrated high sensitivity in detecting ankylosis, but specificity was considerably low. Although a moderate level of agreement was observed among imaging protocols, the diagnostic capacity of 0.30 mm voxel size was markedly more limited compared with smaller voxel sizes.

#### OP2-5

### Quantitative texture analysis of vertical root fracture on panoramic radiograph: A pilot study

**Young-Eun Kwon**<sup>1\*</sup>, Seo-Young An<sup>2</sup>, Sung-min Hwang,<sup>3</sup> Chang-Hyeon An<sup>1</sup>

<sup>1</sup>Department of Oral and Maxillofacial Radiology, School of Dentistry, IHBR, Kyungpook National University, South Korea

<sup>2</sup>Department of Oral and Maxillofacial Radiology, School of Dentistry, IHBR, ITRD, Kyungpook National University, South Korea

<sup>3</sup>Department of periodontology, School of Dentistry, IHBR, Kyungpook National University, South Korea

**Introduction:** Diagnosing vertical root fractures (VRFs) on panoramic radiographs is challenging because fracture lines are often indistinct. This study aimed to quantitatively characterize trabecular bone alterations surrounding VRF roots using texture analysis of panoramic images and to explore indirect imag-

ing patterns that may assist in VRF evaluation.

**Materials and Methods:** In this retrospective single-center study, 38 patients with surgically confirmed VRF were included, comprising 40 fractured roots and 40 matched control roots without clinical or radiographic evidence of fracture. Seven anatomically standardized regions of interest (ROIs) were manually placed around each root. Six texture parameters were extracted, including gray-level co-occurrence matrix (GLCM) features (contrast, ASM, entropy, and IDM), fractal dimension (FD), and lacunarity. Inter-observer agreement was assessed using intraclass correlation coefficients and Bland–Altman analysis. Group differences were analyzed using ROI-level comparisons, relative percentage changes ( $\Delta\%$ ), and correlation analysis among texture features.

**Results:** ROI-averaged analysis showed considerable overlap between groups. However, region-specific evaluation demonstrated consistent directional changes. In the VRF group, GLCM contrast decreased by approximately 11–29% across all ROIs, whereas IDM increased by 14–19% ( $p < 0.001$ ). Lacunarity exhibited localized differences depending on the ROI. Although FD did not show significant absolute differences, correlations involving FD demonstrated moderate shifts ( $\Delta r = 0.20$ – $0.30$ ). Inter-observer reliability ranged from good to excellent.

**Conclusions:** Texture-based analysis of panoramic radiographs revealed spatially organized trabecular alterations around VRF roots, even when fracture lines were not radiographically visible. These findings suggest that quantitative texture features derived from routine panoramic imaging may provide supplementary information for VRF assessment.

## OP2-6

### Impact of field of view size in cone-beam computed tomography on periodontal bone level assessment

**Shun Miwa\***, Takashi Kamio, Taisuke Kawai  
*Department of Oral and Maxillofacial Radiology, School of Life Dentistry at Tokyo, The Nippon Dental University, Japan*

**Introduction:** In dental cone-beam computed tomography (CBCT) imaging, it is generally recommended to select an optimal field-of-view (FOV) for the diagnostic purpose. However, evaluating alveolar bone loss across multiple teeth in periodontitis requires a wide imaging area using a larger FOV. Large FOVs cover wider areas but tend to have lower resolution, whereas small FOVs display high resolution within a limited area. The impact of FOV on image quality has not yet been fully clarified. This study investigated the impact of FOV size on the accuracy of quantitative linear measurements in alveolar bone loss and qualitative clinical staging assessment.

**Materials and Methods:** CBCT images of six human dry skulls were acquired with four FOVs: 40×40 mm (reference standard; voxel size 0.080 mm), 60×60 mm (0.125 mm), 80×80 mm (0.160 mm), and 170×120 mm (0.250 mm). Alveolar bone level (AL) and radiographic bone loss (RBL) were assessed at four sites for each tooth. Differences among the FOVs were analyzed using generalized linear mixed models (GLMM) with the skull defined as a random intercept. RBL severity was classified and evaluated based on degrees of alveolar bone loss.

**Results:** Intra-observer reliability was excellent (ICC > 0.85). GLMM analysis revealed a mean bias of 0.10 mm (95% CI: 0.06–0.14 mm) for AL and 0.71% (95% CI: 0.41–1.01%) for RBL, relative to the reference FOV. Concordance for RBL severity between the reference and larger FOVs was approximately 90%, with discrepancies observed in approximately 10% of sites.

**Conclusions:** The impact of FOV size on linear measurement accuracy appeared minimal. However, clinical staging classification exhibited minor variability. Further study is required to assess the impact of FOV differences on clinical staging of periodontitis.

## OP2-7

## Predicting C-shaped canal morphology using MediXpar texture analysis on panoramic radiographs: A pilot study

**Sultan Uzun**<sup>\*1,4</sup>, Samed Satir<sup>2</sup>, Turgut Felek<sup>4</sup>, Güldane Mağat<sup>4</sup>

<sup>1</sup>Department of Oral and Maxillofacial Radiology, Faculty of Dentistry, Bilecik Şeyh Edebali University, Bilecik, Türkiye

<sup>2</sup>Department of Oral and Maxillofacial Radiology, Faculty of Dentistry, Karamanoğlu Mehmetbey University, Karaman, Türkiye

<sup>3</sup>Department of Information Technologies, Faculty of Engineer, Akdeniz University, Antalya, Türkiye

<sup>4</sup>Department of Oral and Maxillofacial Radiology, Faculty of Dentistry, Necmettin Erbakan University, Konya, Türkiye

**Introduction:** This study aimed to explore the diagnostic potential of panoramic radiographs for identifying C-shaped canal configurations in mandibular first premolars through the MediXpar bioinformatic framework. By quantifying image characteristics such as pixel density and grayscale depth, the research sought to determine whether panoramic images could yield predictive morphological insights comparable to cone-beam computed tomography (CBCT). The ultimate goal was to support more accurate diagnosis and treatment planning while minimizing patient exposure to ionizing radiation.

**Materials and Methods:** Panoramic images were retrospectively analyzed using the MediXpar platform. Quantitative parameters—Xpar, Power Xpar, and Pixel Count—were measured under zoomed and non-zoomed conditions at two-pixel resolutions (1023 × 496 and 1023 × 593). Logistic regression and receiver operating characteristic (ROC) analyses determined each parameter's predictive performance for identifying C-shaped canals, with statistical significance set at  $p < 0.05$ .

**Results:** Dentin-pulp complex volume was significantly greater in C-shaped premolars ( $p = 0.001$ ), while pulp length showed no difference ( $p > 0.05$ ). Digital zoom significantly increased pixel-dependent parameters ( $p \leq 0.01$ ), confirming that resampling enhances matrix density without adding anatomical information. Among all metrics, Power Xpar achieved the highest

diagnostic performance (AUC = 0.917 in zoomed and 0.950 in non-zoomed images), indicating robust discrimination across resolutions.

**Conclusions:** Digital magnification alters image perception without improving diagnostic accuracy. Power Xpar emerged as a resolution-stable descriptor, offering consistent diagnostic reliability independent of zoom level. Zooming enhances visibility but may distort quantitative interpretation. MediXpar-based analysis—particularly through Power Xpar—provides an accessible, reproducible tool for morphometric evaluation in cases where CBCT is unavailable.

## OP2-8

## Comparative radiographic analysis of mandibular third molar impaction pattern and odontectomy difficulty index in Indonesian and Nigerian populations

Irfan Sugianto<sup>1</sup>, **Babatunde Olamide Bamgbose**<sup>1\*,2</sup>, Rezky Amalia<sup>3</sup>, Muhammad Teguh Putra<sup>3</sup>, Bernard Emeka Ogbozor<sup>2,4</sup>

<sup>1</sup>Department of Oral and Maxillofacial Radiology, Faculty of Dentistry, Hasanuddin University, Makassar, Indonesia

<sup>2</sup>Department of Oral Diagnostic Sciences, Faculty of Dentistry, Bayero University, Kano, Nigeria

<sup>3</sup>Dentomaxillofacial Radiology Specialist Study Program, Faculty of Dentistry Hasanuddin University, Indonesia

<sup>4</sup>Department of Dental and Maxillofacial Surgery, University of Nigeria, Enugu campus

**Introduction:** This study explored craniofacial variations between Southeast Asian and West African populations by evaluating the classification patterns and radiographic predictors of surgical difficulty for impacted mandibular third molars using OPG.

**Materials and Methods:** A cross-sectional, retrospective radiographic study based on digital Orthopantomogram (OPG) images from the hospital databases in Indonesia and Nigeria over two years. Participants, aged 17 to 70, had at least one impacted mandibular third molar on OPG. The study included categorical

variables like Angulation of Impaction, Class, and Level of Impaction and Difficulty Index.

**Results:** The Indonesian sample included 1813 participants (64.7% female, 35.3% male), and the Nigerian sample had 1165 participants (49.94% female, 50.04% male).

The overall Odds Ratio (OR) for angulation of impaction was 0.99 (95% CI: [0.27; 3.56]), with substantial variability ( $I^2 = 99.5\%$ ,  $p < 0.001$ ). For Class of impaction, the OR was 0.97 (95% CI: [0.40; 2.37]), showing high variability ( $I^2 = 98.9\%$ ,  $p < 0.001$ ). For Level of impaction, the OR was 1.15 (95% CI: [0.18; 7.42]), with high variability ( $I^2 = 99.7\%$ ,  $p < 0.001$ ).

The mean Difficulty Index for Nigeria was 1.79 (SD = 0.6584, 95% CI: [1.76, 1.83]), with Nigeria contributing 49.7% to the result. For Indonesia, the mean was 1.65 (SD = 0.6955, 95% CI: [1.62, 1.69]), contributing 50.3%. The pooled mean for both countries was 1.72 (95% CI: [1.69, 1.74]).

Nigeria had a higher prevalence of Dental Caries (10.1%) compared to Indonesia (3.3%). Impacted teeth prevalence was higher in Indonesia (59%, prevalence = 0.6) than in Nigeria (29.9%, prevalence = 0.3).

**Conclusions:** The study revealed significant differences in Class and Level of impaction between Nigeria and Indonesia. Country-specific factors likely contribute to the prevalence of dental pathologies, and higher prevalence of impacted teeth in Indonesia

## OP2-9

### 3D facial soft tissues changes with extraction or non-extraction orthodontic treatment

**Marie A Cornelis**<sup>1\*</sup>, Emilie Borup Hansen<sup>2</sup>, Roberto Rongo<sup>3</sup>, Line Nissen<sup>2</sup>, Paolo M. Cattaneo<sup>1</sup>

<sup>1</sup>Melbourne Dental School, University of Melbourne, Australia

<sup>2</sup>Department of Dentistry and Oral Health, Aarhus University, Denmark

<sup>3</sup>School of Orthodontics, University of Naples 'Federico II', Italy

**Introduction:** The objective of the study was to investigate the impact of extraction and non-extraction orthodontic treatments on the soft tissues evaluated on 3D stereophotogrammetric images, and the possible

difference in soft tissues changes comparing extraction of two upper premolars versus two upper and two lower premolars.

**Materials and Methods:** Consecutive patients were enrolled provided that they: 1) were scheduled for full fixed appliance either with a non-extraction approach, or with extraction of two upper premolars or four premolars; 2) were  $\geq 15$  years of age; 3) had an upper or lower Little Irregularity Index of  $\geq 5$  mm. All patients had a 3D image taken before bonding (T0) and after debonding (T1) with 3D white-light scanner 3dMD. Seven angular and 8 linear measurements were performed with the 3dMDvultus Software. Since normality of the data was confirmed, paired t-tests were used to compare T0 and T1 values within the non-extraction, two premolar extraction and four premolar extraction subjects. ANOVA followed by Tuckey post-hoc tests were used to compare the treatment effect between the 3 groups.

**Results:** Twenty-two non-extraction patients, 16 two premolar extraction patients and 15 four premolar extraction patients were enrolled. From T0 to T1, the most clinically significant finding was the change in nasolabial angle ( $4.0 \pm 0.5^\circ$ ,  $P=0.015$ ) in the four premolar extraction group. Comparing the treatment effect between the three groups, a statistically significant difference in the upper lip height was found ( $P=0.033$ ) between the non-extraction and the two upper premolar extraction groups.

**Conclusions:** The Nasolabial angle increased in four-premolar extraction subjects, while it reduced in non-extraction subjects, this difference being statistically significant. Though statistically significant differences were seen between the non-extraction group and the extraction groups, the changes in the perio-oral area were clinically limited.

## OP2-10

## Automated virtual patient creation with CT and CBCT using different fields of view: Assessing accuracy, realism and usefulness

**T Jindaniil**<sup>1,2,3\*</sup>, OE Burlacu-Vatamanu<sup>1,4</sup>, B Baldini<sup>1,5,6</sup>, J Meyns<sup>1,7</sup>, RC Fontenele<sup>1,8</sup>, M Cadenas de Llano Pérula<sup>9</sup>, R Jacobs<sup>1,10</sup>

<sup>1</sup>OMFS-IMPACT Research Group, Department of Imaging and Pathology, KU Leuven, Belgium

<sup>2</sup>Department of Oral and Maxillofacial Surgery, University Hospitals Leuven, Belgium

<sup>3</sup>Department of Radiology, Chulalongkorn University, Thailand

<sup>4</sup>Doctoral School, Carol Davila University of Medicine and Pharmacy, Romania

<sup>5</sup> Department of Electronics, Information and Bioengineering, Politecnico Di Milano, Italy

<sup>6</sup>UOC Maxillo-Facial Surgery and Dentistry Fondazione IRCCS Cà Granda, Ospedale Maggiore Policlinico, Italy

<sup>7</sup>Department of Oral and Maxillofacial Surgery, General Hospital St-Jan Genk, Belgium

<sup>8</sup>Department of Stomatology, Public Health and Forensic Dentistry, University of São Paulo, Brazil

<sup>9</sup> Department of Oral Health Sciences - Orthodontics, KU Leuven and Dentistry, University Hospitals Leuven, Belgium

<sup>10</sup>Department of Dental Medicine, Karolinska Institute, Stockholm, Sweden

**Introduction:** Even though virtual patient (VP) concept has been introduced for decades, the process is still complex. This project aimed to compare VP creation using either full or simulated reduced field of view (FOV) computed tomography (CT) scans with using AI and semi-automatic registration. Additionally, VP's realism and usefulness were assessed.

**Materials and Methods:** Twenty multidetector (MD) CT and 20 cone beam (CB)CT scans were retrospectively collected, cropped to create simulated reduced FOV images, and imported with facial and intraoral scans into Virtual Patient Creator for AI-driven model registration. Registration accuracy between VP created with MDCT and CBCT, full and simulated reduced FOV scans was assessed with linear and surface distance measurements. AI-driven accuracy, consistency, and time were compared to semi-automated approach. VP's realism and usefulness for treatment planning and communication was evaluated by 35 dentists and 25 laypersons on a 5-point scale.

**Results:** Both AI and semi-automatic registration achieved 100% accuracy for VP creation with MDCT and CBCT, with no significant differences between modalities ( $p > 0.99$ ). Registration accuracy did not differ between full and simulated reduced FOV ( $p > 0.10$ ). However, AI-driven registration showed greater surface discrepancies than semi-automated, especially in facial scan alignment ( $p < 0.01$ ). Both methods also demonstrated near-perfect consistency. Total processing time was significantly shorter for MDCT (313.7 s) than CBCT (850.3 s) ( $p < 0.01$ ), with no difference between FOV. AI-driven registration was significantly faster than semi-automated registration ( $p < 0.01$ ). The realism and usefulness for communication of the VP were scored consistently high by both dentists and laypersons.

**Conclusions:** AI-driven registration can provide clinically accurate, fast, and consistent VP creation from both CT and CBCT and different FOV within this study condition, supporting its clinical feasibility with dose reduction and enabling interpersonal communication. Validation with actual reduced FOV scans should be performed.

## OP2-11

## Usefulness of a hybrid nonlinear model for dental age and growth prediction using CT images of permanent maxillary canine

**Beshlina Fitri Widayanti Roosyanto**

**Prakoewa**<sup>\*1,2</sup>, Hideyoshi Nishiyama<sup>1</sup>, Taichi Kobayashi<sup>1</sup>, Makiko Ike<sup>1</sup>, Masaki Takamura<sup>1</sup>, Yutaka Nikkuni<sup>1</sup>, Kouji Katsura<sup>1</sup>, Takafumi Hayashi<sup>1</sup>

<sup>1</sup>Division of Oral and Maxillofacial Radiology, Niigata University Graduate School of Medical and Dental Sciences, Niigata, Japan

<sup>2</sup>Division of Forensic Odontology, Airlangga University, Indonesia

**Introduction:** Permanent maxillary canine (PMC) development observed on computed tomography (CT) images provides a stable biological basis for dental age estimation (DAE). This study aimed to develop an age and growth prediction model by integrating canine morphometric features with machine learning (ML)-

based optimization.

**Materials and Methods:** Morphometric measurements of 785 PMC were obtained from CT images of 1-23 years samples. PMC's length (L), open apex shortest width (SW), and longest width (LW) were measured. Growth patterns were characterized using Gompertz function for L and Gamma-type function for SW and LW. These variables were integrated into a nonlinear model (NAGE model):  $y = a \cdot L^{-b} + c \cdot \log(L) + d$ , parameters optimized using ML model. Model performance was evaluated using root mean squared error (RMSE), coefficient of determination ( $R^2$ ), regression analysis, scatter plots, and year-stratified error analysis across two age-specific groups: 1-16 year and 1-23 year. Validation was performed using 14 multiple-examined samples (79 consecutive CT examinations, ages 1-15 year).

**Results:** For age 1-23 year, the RMSE was 1.93 years with  $R^2 = 0.83$ . Limiting the model to ages 1-16 years improved accuracy with RMSE= 1.28 years and  $R^2 = 0.87$ . In multiple-examined samples, the mean  $\pm$  SD of chronological age versus predicted age=  $7.82 \pm 2.94$  years versus  $7.92 \pm 2.93$  years. Overall RMSE= 0.97 years, and  $R^2 = 0.89$ . Individual RMSE values ranged from 0.28 to 2.08 years.

**Conclusions:** The proposed NAGE model demonstrates stable and accurate DAE across age ranges. NAGE model shows reliability for future treatment planning in multiple-examined samples by consistently tracking individual developmental patterns within a tolerance of  $\pm 2$  years. The model can be reproduced for other populations through transfer learning.

## Oral Presentation 3

May 1 (Fri), 09:30-10:30 | Room C

OP3-1

### Relationship between impacted maxillary canines and palatal arch morphology: A cone-beam computed tomography study

Hatice KURT<sup>1\*</sup>, Derya YILDIRIM<sup>1</sup>, Neslihan Ebru ŞENİŞİK<sup>2</sup>, Elif Sena SARGIN<sup>1</sup>

<sup>1</sup>Department of Oral and Maxillofacial Radiology, Süleyman Demirel University, Türkiye

<sup>2</sup>Department of Orthodontics, Süleyman Demirel University, Türkiye

**Introduction:** The canines establish the occlusion, stability, function and morphology of the arch. This study aims to investigate the relationship between impacted maxillary canine (IMC) position, palatal arch morphology, and IMC demographics using cone-beam computed tomography (CBCT).

**Materials and Methods:** This study was conducted in Süleyman Demirel University Faculty of Dentistry Oral and Maxillofacial Radiology Department. The CBCT images of patients aged  $\geq 18$  years with unilateral or bilateral IMC were retrospectively evaluated. Patients with syndromes, previous surgical or orthodontic intervention and poor image quality were excluded. Buccopalatal position, angulation relative to the midline in coronal sections, follicle width, lateral incisor root resorption were recorded. Arch form, palatal length, depth, and intermolar distance were measured. The data were analysed with chi-square test, independent samples t-test and one-way ANOVA test.

**Results:** A total of 63 patients (23 males (36.5%), 40 females (63.5); mean age:  $29.95 \pm 12.25$  years) with 75 IMC were included. Intra-rater reliability was excellent (ICC 0.873 to 0.997). No significant difference in follicle width was observed between laterals with and without root resorption ( $p = 0.416$ ). The IMC were divided into three arch form groups: ovoid ( $n=31$ ), square ( $n=24$ ), and tapered ( $n=20$ ). Canine angulation among arch forms was significantly different ( $p = 0.032$ ). The ovoid group showed the highest mean angulation ( $42.53^\circ \pm 7.91^\circ$ ), followed by square

( $33.18^{\circ} \pm 18.87^{\circ}$ ) and tapered ( $29.65^{\circ} \pm 16.53^{\circ}$ ) groups. The ovoid arch form showed the highest palatal positioning (90.3%) while the tapered arch form demonstrated the highest buccal positioning (25%).

**Conclusions:** This study provides valuable insights into the relationship between maxillary arch morphology and IMC position, potentially aiding clinicians in early identification of patients at risk for canine impaction.

### OP3-2

## Three-dimensional changes in the pharyngeal airway in growing patients with a retrognathic mandible following treatment with functional appliances: A retrospective case-control study

Paolo M. Cattaneo<sup>1\*</sup>, Juen-Long S. Cheung<sup>1</sup>, Marie A Cornelis<sup>1</sup>

<sup>1</sup>Melbourne Dental School, The University of Melbourne, Australia.

**Introduction:** Certain craniofacial morphologies, including mandibular retrognathia (i.e., Skeletal Class II malocclusion), may predispose a child to having obstructive sleep apnoea (OSA) or milder forms of sleep-disordered breathing. The objectives of this study were to assess and compare volumetric and morphological changes in the pharyngeal airway (PA) in growing patients with a retrognathic mandible (skeletal Class II patients), assessed via Cone-Beam Computed Tomography (CBCT), after mandibular growth modification treatment performed with removable (Twin Block) and fixed (Herbst) functional appliances or Class II elastics.

**Materials and Methods:** Pre- and post-treatment CBCT scans were collected from an existing practice patients' dataset following completion of multibracket appliance treatment to correct Skeletal Class II malocclusion. Three matched groups comprising 22 patients each were treated with either Class II elastics (CII-E), Herbst or Twin Block (TB) appliances. Total and partial PA volumes were calculated, and morphology was assessed via measurements of cross-sectional area

(CSA) and hydraulic diameter (DH). Multiple dental and skeletal parameters were also measured three-dimensionally. Predicted mean changes and pairwise comparisons were computed via linear mixed-effects models

**Results:** The PA volume increased, and the morphology demonstrated reduced constriction (increased minimum CSA and DH) following treatment in all three groups. However, there were no statistically significant in any of the measured airway parameters when before- and after-treatment differences were compared across any of the groups. Dental and skeletal changes followed a similar pattern to that observed for the airway with most parameters showing significant changes following treatment in all groups, but few significant differences were seen between the groups

**Conclusions:** Similar changes were observed in the PA after treatment with CII-E or functional appliances (Herbst and TB), but it is unclear whether these were due to comparable treatment effects, normal growth, or a combination of both.

### OP3-3

## Velar morphology and its potential implications for velopharyngeal insufficiency and airway consideration in normal individuals: A cross-sectional study

Preethy Mary Donald<sup>1\*</sup>, Stephanie Lee Phei Wei<sup>2</sup>, Andrew Ng Jian Xing<sup>2</sup>, Ting Teck Jong<sup>3</sup>, Renjith George<sup>4</sup>

<sup>1</sup>Department of Oral Medicine and Oral Radiology, Manipal University College Malaysia, Jln Batu Hampar, Bukit Baru, Melaka, Malaysia

<sup>2</sup>Klinik Pergigian Atlas, Jln Pandan 2/2, Pandan Jaya, Kuala Lumpur, Malaysia

<sup>3</sup>Primecare Dental Clinic, Jln SS 21/58, Damansara Utama, Petaling Jaya, Selangor, Malaysia

<sup>4</sup>Department of Oral Pathology, Manipal University College Malaysia, Jln Batu Hampar, Bukit Baru, Melaka, Malaysia

**Introduction:** The soft palate or velum is critical for speech, swallowing, and airway function. Morphomet-

ric variations in soft palate may predispose individuals to velopharyngeal insufficiency (VPI) or influence airway balance, potentially contributing to clinical conditions such as hypernasal speech, swallowing difficulties or obstructive sleep apnoea. Despite this, normative morphometric data in the Malaysian population remain underexplored, and understanding population-specific palate characteristics is essential for anticipating functional outcomes.

**Materials and Methods:** Digital lateral cephalograms of 788 normal adults were analyzed. Soft palate types were classified into six variants, and morphometric measurements such as Velar Length (VL), Pharyngeal Depth (PD), Need's Ratio (NR) were obtained. Gender differences were assessed. Statistical analyses included Chi-square, ANOVA, and independent t-tests.

**Results:** Type I (leaf-shaped) was most prevalent (51%), followed by Type II; distribution showed no significant association with gender. VL was shortest in Type III (butt-shaped) palates; NR was highest in Types III and VI (crook-shaped), exceeding the threshold of 0.8. Males exhibited longer VL, while females showed higher NR; PD did not differ significantly between genders.

**Conclusions:** Soft palate morphology exhibits distinct patterns with measurable differences in VL and NR. Certain palatal variants, particularly those with shorter velum or higher NR, may have potential implications for velopharyngeal function and airway considerations, even in normal adults. Population-specific normative data enhances understanding of velar anatomy and may support early identification and clinical assessment of individuals at potential risk for altered velopharyngeal function or airway concerns.

### OP3-4

## Assessing mandibular bone patterns in osteoporosis and osteopenia by utilization of radiomorphometric indices: A systematic review and meta-analysis

**Mohammad Safwan Sahar**<sup>\*1</sup>, Yusmiaidil Putera Mohd Yusof<sup>2</sup>, Aminda Faizura Omar Khattab Khan<sup>3</sup>, Vinesh Raj Savumthararaj<sup>4</sup>

<sup>1,3</sup>Special Care Dentistry, Universiti Teknologi Mara (UiTM), Malaysia

<sup>2</sup>Forensic Odontology & Oral Maxillofacial Radiology, Universiti Teknologi Mara (UiTM), Malaysia

<sup>4</sup>Oral Medicine and Oral Pathology, Universiti Teknologi Mara (UiTM), Malaysia

**Introduction:** Individuals with osteoporosis show different patterns of mandibular bone microstructures. While there are many useful radiomorphometric indices to quantify the microstructures from panoramic radiographs, the indice selection is merely arbitrary. This systematic review aims to evaluate sets of radiomorphometric indices to assess the pattern of mandibular bone in individuals with low bone mineral density.

**Materials and Methods:** The selected PRISMA guideline was followed. This systematic review and meta-analysis was registered with PROSPERO (Provisional ID: 1271932). The materials for analysis was collected in December 2025 by searching three databases: Scopus, PubMed Central and Web of Science. Study selection is conducted in three stages, resulting in inclusion of 102 studies. Quality assessment was performed with the QUADAS-2 tool, and the general methodological quality of retrieved studies was mixed.

**Results:** Overall, radiomorphometric indices from the analyzed studies were able to consistently extract accurate and reproducible data from mandibular bone with varying degree of agreement when compared to bone mineral density (BMD). Combination of Mandibular Cortical Index (MCI) and Mandibular Cortical Width (MCW) are considered to have advantageous sensitivity and specificity in identifying low BMD or osteoporosis. A study demonstrated that MCW successfully differentiate 94.4% of osteoporosis subjects when the value is <3mm. Osteoporotic, osteopenic, and advanced age populations predominantly show reduced values in PMI, MCW, MCI and AI. Across three studies, osteopenic individuals also demonstrated alterations of mandibular cortex morphology, where 60.8% to 69.5% are represented in MCI categories 2 and 3.

**Conclusions:** While radiomorphometric indices of the mandible can aid in identifying individuals with low

bone mineral density, there are insufficient evidence for it to be diagnostic. However, the predictive value of the indices are significantly enhanced when analyzed alongside demographic factors of age and gender. Further research will benefit from longitudinal and prospective methodology.

## OP3-5

### Cervical vertebral maturation staging on lateral cephalograms: A comparison across experience levels and imaging systems (One-shot vs. scanning)

**S Chiemboonsri**<sup>1\*</sup>, OC Silkosessak<sup>1</sup>, P Charoenlarp<sup>1</sup>, P Suwanwitid<sup>2</sup>

<sup>1</sup>Department of Radiology, Chulalongkorn University, THAILAND

<sup>2</sup>Department of Orthodontic, Chulalongkorn University, THAILAND

**Introduction:** Cervical vertebral maturation (CVM) assessment is a widely adopted method for evaluating skeletal maturity in orthodontic patients without additional radiation exposure. Nonetheless, previous studies have reported poor to moderate interobserver reliability, primarily due to subjective interpretation of morphological changes in the cervical vertebrae. The present study aims to evaluate the interobserver reliability of the six-stage Baccetti CVM method and to determine the consistency among observers with varying levels of clinical experience.

**Materials and Methods:** Lateral cephalograms were randomly retrieved from the PACS at the Faculty of Dentistry, Chulalongkorn University, based on pre-defined inclusion and exclusion criteria. The inclusion criteria required clear visualization of second through fourth cervical vertebrae (C2-C4), whereas exclusion criteria comprised evidence of prior cervical surgery or any pathology affecting cervical spines. A total of 200 images, obtained from 2 machines representing one-shot and scanning imaging techniques were exported in JPEG format. Eight observers participated in the study, including one orthodontist, two oral and maxillofacial radiologists, two orthodontic residents and two oral and maxillofacial radiology residents. Demographic and radiographic data—such as sex, date

of birth and date of exposure were recorded. Blinded observation sessions were conducted independently and in random order for each observer to determine the CVM-score. Statistical analysis was performed using two-way ANOVA with SPSS software. Confidence interval was set at 95%.

**Results:** There is significantly better agreement for CVM-score from scanning cephalographic machine ( $P \leq 0.01$ ). Significant variability was found among individual observers ( $P=0.037$ ), but no significant effect from observer experience level ( $P=0.126$ ).

**Conclusions:** The type of imaging system (one-shot vs. scanning) influences CVM staging and personal interpretation differences exists regardless of experience.

## OP3-6

### Decoding dental age in children: Tooth apex surface area analysis across CBCT voxel sizes

**Meghna Gohain**<sup>1\*</sup>, Muhammad Khan Asif<sup>2,5</sup>, Phrabhakaran Nambiar<sup>1,3</sup>, Nora Sakina Mohd Noor<sup>4</sup>, Norliza Ibrahim<sup>1</sup>

<sup>1</sup>Department of Oral and Maxillofacial Clinical Sciences, Faculty of Dentistry, Universiti Malaya, Kuala Lumpur, Malaysia

<sup>2</sup>Department of Research and Forensic Odontology, Shifa College of Dentistry, Shifa Tameer-e-Millat University, Islamabad, Pakistan

<sup>3</sup>Department of Oral Biology and Biomedical Sciences, Faculty of Dentistry, MAHSA University, Saujana Putra, Malaysia

<sup>4</sup>Department of Restorative Dentistry, Faculty of Dentistry, University of Malaya, Kuala Lumpur, Malaysia

<sup>5</sup>Department of Oral Radiology, Faculty of Dentistry, MAHSA University, Malaysia

**Introduction:** Accurate dental age estimation in children is crucial for forensic and clinical applications, with cone beam computed tomography (CBCT) enabling advanced three-dimensional analysis of developing tooth apices. This study developed a regression model using 3D surface area analysis (3D SAA) on maxillary second premolars and validated its performance across different voxel sizes to optimize accuracy while minimizing radiation exposure.

**Materials and Methods:** A training sample of 155

CBCT scans (300 µm voxel size; 83 Malays, 72 Chinese; ages 7–14 years) was used to develop the model, incorporating root surface area of the apex (RSAA), sex, ethnicity, and root development status (RDS). The model was validated on 92 independent scans (300 µm) and further tested on 128 scans (76 µm voxel size) from similar demographics. The RSAA were measured using Materialise Mimics and 3-Matic software. Statistical analyses included Pearson correlations, stepwise regression, and mean absolute error (MAE) calculations.

**Results:** In the 300 µm dataset, a strong negative correlation ( $r = -0.94$ ) was observed between chronological age (CA) and RSAA, with predictors explaining 88.4% of age variation (excluding sex and ethnicity). The validation MAE was 0.42 years. Applying the model to 76 µm data yielded a comparable correlation ( $r = -0.96$ ) and MAE (0.51 years), with no significant differences in correlation strength ( $p = 0.09$ ), coefficient ( $p = 0.08$ ), or MAE ( $p = 0.13$ ) between voxel sizes. RSAA and RDS were significant contributors ( $p < 0.05$ ), while sex ( $p = 0.37$ ) and ethnicity ( $p = 0.49$ ) were not.

**Conclusions:** The 3D SAA model provides reliable age estimation in Malaysian children, performing consistently across 76 µm and 300 µm voxel sizes. Larger voxels are recommended for pediatric use to reduce radiation without compromising accuracy.

## Oral Presentation 4

May 1 (Fri), 11:10-11:40 | Room C

OP4-1

### A rare case report and literature review: Periosteal chondroma in mandibular condyle

**Fahri Reza Ramadhan**<sup>1</sup>, Kiichi Shimabukuro<sup>1</sup>, Megumi Nose<sup>1</sup>, Masahiko Ohtsuka<sup>1</sup>, Toshikazu Nagasaki<sup>1</sup>, Masaru Konishi<sup>2</sup>, Yoshikazu Suei<sup>2</sup>, Takashi Nakamoto<sup>1</sup>, Hisako Frusho<sup>3</sup>, Sachiko Yamasaki<sup>4</sup>, Souichi Yanamoto<sup>4</sup>, Naoya Kakimoto<sup>1</sup>

<sup>1</sup>Department of Oral and Maxillofacial Radiology, Graduate School of Biomedical and Health Sciences, Hiroshima University

<sup>2</sup>Department of Oral and Maxillofacial Radiology, Hiroshima University Hospital

<sup>3</sup>Department of Oral and Maxillofacial Pathobiology, Graduate School of Biomedical and Health Sciences, Hiroshima University

<sup>4</sup>Department of Oral Oncology, Graduate School of Biomedical and Health Sciences, Hiroshima University

**Introduction:** Chondroma was described as a benign tumor that was reported to arise from cartilaginous tissue. Chondromas are classified into three types, namely enchondromas, periosteal chondromas (PC) and extraskeletal chondromas, according to their location. PC, a type of chondroma that develops on the bone surface beneath the periosteum, is usually found in long tubular bones and rarely found in the temporomandibular joint (TMJ). The aim of this case report is to present radiographic features of periosteal chondroma in TMJ from multiple modalities with literature review.

**Case:** A 62-year-old male patient came to Hiroshima University Hospital with a difficulty in opening the mouth for 2 years. This complaint sometimes came with pain. Clinical examination showed a limitation in mouth opening with a deviation of 7 mm to the right. The multiple modalities of radiological examination revealed an irregular radiopaque extension of the cortical bone in the mandibular condyle. Treatment of local excision and biopsy were performed and there was no recurrence of this lesion. Clinical examination, radiographic features, and biopsy of this case lead to a benign tumor of TMJ, specifically a PC.

**Discussion:** A review of 56 PC cases published between 1952 and 2018 found no mention of PC in TMJ. PC in TMJ showed a radiopaque extension of the cortical bone in the mandibular condyle, distinguishing it from typical PCs at other sites that exhibit saucerization. As this lesion is rarely described, one should consider a differential diagnosis of a periosteal chondroma if these specific findings are present.

## OP4-2

## Expert consensus-based review and refinement of imaging quality management and radiation safety criteria in oral and maxillofacial radiography in Korea: A Delphi study

**Hyun Jin Cho**<sup>1\*</sup>, Sam-Sun Lee<sup>1</sup>, Soon-Chul Choi<sup>1</sup>, Min-Suk Heo<sup>1</sup>, Kyung-Hoe Huh<sup>1</sup>, Ju-Hee Kang<sup>1</sup>, Jo-Eun Kim<sup>1</sup>, Chena Lee<sup>2</sup>, Gyu-Dong Jo<sup>2</sup>, Hang-Moon Choi<sup>3</sup>, Seo-Young An<sup>4</sup>, Han-Gyeol Yeom<sup>5</sup>

<sup>1</sup>Department of Oral and Maxillofacial Radiology and Dental Research Institute, School of Dentistry, Seoul National University, Seoul, Republic of Korea

<sup>2</sup>Department of Oral and Maxillofacial Radiology, College of Dentistry, Yonsei University, Seoul, Republic of Korea

<sup>3</sup>Department of Oral and Maxillofacial Radiology, Research Institute of Oral Science, College of Dentistry, Gangneung-Wonju National University, Gangneung, Republic of Korea

<sup>4</sup>Department of Oral and Maxillofacial Radiology, School of Dentistry, Institute for Human Bio-Resource (IHBR), Kyungpook National University, Daegu, Republic of Korea

<sup>5</sup>Department of Oral and Maxillofacial Radiology, College of Dentistry, Daejeon Dental Hospital, Wonkwang University, Iksan, Republic of Korea

**Introduction:** Several oral and maxillofacial radiographic guidelines and evaluation forms used in Korea have been implemented in clinical practice without documented evidence of expert consensus. Inconsistencies among evaluation criteria, ambiguous wording, and non-uniform terminology have also been reported. This study aimed to refine imaging quality-management and radiation-safety criteria in oral and maxillofacial radiography by establishing expert consensus using a structured Delphi process.

**Materials and Methods:** Survey items were derived

from radiographic guidelines and evaluation forms published by the Korean Academy of Oral and Maxillofacial Radiology for which prior consensus data were unavailable. These included image-quality checklists for periapical, bitewing, panoramic, and lateral cephalometric radiographs, panoramic evaluation forms, CBCT image-quality and radiation-safety guidelines, and a radiation-safety management self-assessment form. A three-round Delphi survey was conducted with eleven experts in oral and maxillofacial radiology using a 9-point Likert scale. Quantitative analysis included the mean score (AVE), coefficient of variation (CV), and agreement rate (AR), with consensus defined as  $AVE \geq 8.0$ ,  $CV \leq 0.2$ , and  $AR \geq 80\%$ .

**Results:** The first Delphi round consisted of 81 items. Based on expert feedback, items were revised, added, or deleted, resulting in 93 items in Round 2 and 95 items in Round 3. Consensus achievement increased from 75.3% (61/81) in Round 1 to 83.9% (78/93) in Round 2 and 94.7% (90/95) in Round 3, with progressive improvement in clarity and terminological consistency.

**Conclusions:** This Delphi-based expert consensus study reviewed and refined imaging quality-management and radiation-safety criteria currently used in oral and maxillofacial radiography in Korea. The findings provide a consensus-based reference framework that may support more consistent application of existing criteria and inform future clinical validation and standardization efforts.

## OP4-3

## Evaluation of dose reduction CBCT in pediatric patients: A phantom study

**Ji Yun Lee**<sup>1\*</sup>, Gyu-Dong Jo<sup>1</sup>, Yoon Joo Choi<sup>1</sup>, Kug Jin Jeon<sup>1</sup>, Sang-Sun Han<sup>1</sup>, Chena Lee<sup>1</sup>

<sup>1</sup>Department of Oral and Maxillofacial Radiology, Yonsei University College of Dentistry, Republic of Korea

**Introduction:** This study aimed to evaluate the extent of dose reduction for cone-beam computed tomography (CBCT) in pediatric patients using a clinical phantom and image quality evaluation, and to identify an

optimal low-dose protocol for clinical application.

**Materials and Methods:** Two CBCT devices (Device A and Device B) were used for image acquisition. Standard pediatric imaging parameters (Device A: 85 kVp, 11 mAs, 14 s; Device B: 95 kVp, 5.7 mAs, 15 s) were modified by attaching copper plates of varying thicknesses to the x-ray source to achieve dose area product (DAP, mGy·cm<sup>2</sup>) reduction levels of 100%, 80%, 60%, 40%, and 20%. Phantom images were acquired under these five conditions and independently evaluated by two oral radiologists. Based on the image quality assessment, the optimal low-dose protocol was determined.

**Results:** Image quality decreased as DAP levels were reduced; however, no statistically significant image quality differences were observed at corresponding DAP levels. For Device A, the 60% DAP level (40% dose reduction) maintained clinically acceptable image quality. For Device B, the 40% DAP level (60% dose reduction) was identified as the optimal low-dose setting.

**Conclusions:** These findings suggest that low-dose CBCT protocols can be applied in pediatric patients while maintaining diagnostically acceptable image quality. This study may provide valuable evidence for developing clinical guidelines that aim to reduce radiation exposure in pediatric CBCT imaging.

## Oral Presentation 5

May 1 (Fri), 13:30-14:50 | Room C

OP5-1

### Evaluation of large language models' responses to patient-perspective questions on dental panoramic radiographs: A cross-sectional preliminary study

**Hak-Sun Kim**<sup>\*1</sup>, Gyu-Tae Kim<sup>2</sup>

<sup>1</sup>Department of Oral and Maxillofacial Radiology, Kyung Hee University Dental Hospital, Republic of Korea

<sup>2</sup>Department of Oral and Maxillofacial Radiology, College of Dentistry, Kyung Hee University, Republic of Korea

**Introduction:** This study aimed to evaluate the responses of commercial large language models (LLMs) to basic patient-perspective questions regarding dental panoramic radiographs and to discuss their potential clinical impact on patient communication.

**Materials and Methods:** Panoramic radiographs obtained between April and June 2025 were interpreted by two oral and maxillofacial radiologists. A total of 12 panoramic radiographs, each presenting a single significant finding – normal ( $n = 2$ ), chronic periodontitis ( $n = 5$ ), dental caries ( $n = 2$ ), periapical lesion ( $n = 1$ ), crown fracture ( $n = 1$ ), or tooth retention ( $n = 1$ ) – were randomly selected, anonymized and exported in jpg format. The distribution of findings reflected the reported frequency of dental lesions from the National Health Insurance Service of Korea. Subsequently, four commercial LLMs (ChatGPT-4o and o4-mini, Gemini 2.5 Pro, and Grok 4) were asked to respond to three questions regarding each panoramic radiograph: (1) identification of the most significant dental lesion, (2) localization of the lesion, and (3) to draw arrows indicating the lesion.

**Results:** For lesion identification, Gemini 2.5 Pro answered correctly in three cases and partially correctly in one case; ChatGPT-4o was correct in two cases and partially correct in three; ChatGPT o4-mini was correct in two cases and partially correct in one. Grok 4 answered all cases incorrectly. For lesion localization, Gemini 2.5 Pro was correct in two cases; ChatGPT-4o

in one case; ChatGPT o4-mini in one case and partially correct in two cases; and Grok 4 in two cases. With the exception of one case by ChatGPT-4o, none of the models successfully indicated lesions with arrows.

**Conclusions:** The evaluated LLMs demonstrated poor performance in analyzing dental panoramic radiographs. The use of LLMs for dental lesion detection should not be recommended for patients or dental professionals.

### OP5-2

## Automated identification of idiopathic osteosclerosis using deep learning: Evaluation of two CNN architectures

**Irfan Sugianto**<sup>1,4\*</sup>, Babatunde O. Bamgbose<sup>1,2</sup>, Amil Ahmad Ilham<sup>3</sup>, Muhammad Rifky<sup>3</sup>, Barunawaty Yunus<sup>1,4</sup>, Dwi Putri Wulansari<sup>1,4</sup>, Muhammad Fadil Hidayat<sup>1,4</sup>, Fadhliil Ulum A. Rahman<sup>1,4</sup>, Nura Adolfin Barung<sup>4</sup>, Muhammad Teguh Putra<sup>4</sup>

<sup>1</sup>Department of Oral and Maxillofacial Radiology, Faculty of Dentistry Hasanuddin University, Indonesia

<sup>2</sup>Department of Oral Diagnostic Sciences, Faculty of Dentistry, Bayero University Kano, Nigeria

<sup>3</sup>Department of Informatics, Faculty of Engineering, Hasanuddin University, Indonesia

<sup>4</sup>Dentomaxillofacial Radiology Specialist Study Program, Faculty of Dentistry Hasanuddin University, Indonesia

**Introduction:** Idiopathic osteosclerosis (IO) are focal radiopacities of unknown etiology observed in the jaws. These radiopacities are incidentally detected on dental panoramic radiographs when taken for other reasons. Deep learning particularly Convolutional Neural Networking (CNN) has strong capability in medical analysis. Faster R-CNN and YOLO are two types of deep learning architectures to identify objects through images. In this study, we investigated and compared the performance of Faster R-CNN ResNet50 v2, Faster R-CNN ResNet50 v2 AdamW with YOLOv10n, YOLOv11n, YOLOv12n, and YOLOv12x to automatically identify IO.

**Materials and Methods:** Three oral and maxillofacial radiologists evaluated 297 IO using Panoramic radiograph from our university hospitals. We divided the

datasets to 240 (80%) for training, 28 (10%) for validation and 30 (10%) for testing with hyperparameters: Learning Rate 0.0005, Momentum 0.9, and Epoch 300

**Results:** Accuracy value of Faster R-CNN ResNet50 v2, Faster R-CNN ResNet50 v2 AdamW and YOLOv10n, YOLOv11n, YOLOv12n, YOLOv12x are 0.719, 0.781, 0.788, 0.774, 0.862, 0.735 consecutively; precision values are 0.719, 0.781, 0.839, 0.889, 0.962, 0.807, consecutively, recall values are 1.000, 1.000, 0.929, 0.857, 0.893, 0.893, consecutively. F-1 score values are 0.836, 0.877, 0.881, 0.873, 0.847, consecutively; MAP-50 values are 0.690, 0.714, 0.685, 0.729, 0.729, 0.740, consecutively.

**Conclusions:** This study showed that YOLO and Faster R-CNN have promising potential to identify automatically IO using panoramic radiograph, although YOLO showed stronger result than Faster R-CNN.

### OP5-3

## A novel domain-specific augmentation strategy for deep learning-based tooth detection in dental panoramic radiographs

**Jae Joon Hwang**<sup>\*</sup>, DDS, PhD<sup>1</sup>, Nayeon Kim<sup>1</sup>, Yun-Hoa Jung, DDS, PhD<sup>1</sup>, Bong-Hae Cho DDS, PhD<sup>1</sup>

<sup>1</sup>Department of Oral and Maxillofacial Radiology, Pusan National University, Republic of Korea

**Introduction:** Accurate tooth detection and numbering in dental panoramic radiographs is essential for automated dental charting systems. Deep learning models require diverse training data, but dental datasets are often limited. Data augmentation can enhance model generalization; however, conventional augmentation techniques such as horizontal flipping are unsuitable for dental images due to anatomical asymmetry. This study aimed to evaluate the effectiveness of a novel domain-specific augmentation strategy on tooth detection performance using a two-stage detection pipeline.

**Materials and Methods:** We conducted a 5-fold cross-validation study using 634 dental panoramic radiographs from the Dentex dataset. A two-stage detec-

tion pipeline was implemented, consisting of quadrant detection (1024×1024, 4 classes) followed by tooth position detection (640×640, 8 normalized position classes). YOLO11x architecture was employed for both stages. Seven experimental packages were designed to evaluate the proposed augmentation method with varying constraints: adjacent position constraint, boundary tooth exclusion, and augmentation ratios (25%, 50%, 75%, 100%). The proposed augmentation utilized PCA-based axis alignment and Poisson blending for seamless integration. Standard augmentation excluded horizontal and vertical flipping to preserve anatomical orientation.

**Results:** All packages with the proposed augmentation achieved mAP50 exceeding 0.97. The highest performance was observed at 100% augmentation ratio (mAP50=0.97, mAP50-95=0.63), followed by 50% ratio (mAP50=0.97, mAP50-95=0.67) and the configuration without adjacent constraint (mAP50=0.97). The baseline two-stage model without the proposed augmentation achieved mAP50 of 0.9640. Boundary tooth exclusion showed minimal impact on performance (0.96 vs 0.97).

**Conclusions:** The proposed domain-specific augmentation strategy significantly improved tooth detection performance in dental panoramic radiographs. Higher augmentation ratios demonstrated better performance, suggesting that aggressive augmentation strategies are beneficial for this task.

#### OP5-4

## Hybrid vision-language framework for tooth-level dental report generation from panoramic radiographs

**Mobin Ahmadi**<sup>1\*</sup>, Won-Jin Yi<sup>1,2</sup>

<sup>1</sup>Interdisciplinary Program of Bioengineering, Seoul National University, Seoul, South Korea

<sup>2</sup>Department of Oral and Maxillofacial Radiology, School of Dentistry and Dental Research Institute, Seoul National University, Seoul, South Korea

**Introduction:** Dental panoramic radiographs are challenging to interpret due to low signal-to-noise ratios

and subtle, tooth-specific abnormalities, which often limits the performance of standalone vision-language models. We propose a hybrid framework that integrates detection, segmentation, and large language model to produce accurate, tooth-level dental radiology reports.

**Materials and Methods:** A dataset comprising 1,811 dental panoramic X-ray images was constructed, including seven categories of dental abnormalities, tooth instance segmentation masks, and synthetic radiologist-approved reports. YOLOv9e is employed to detect pathological findings, while Attention U-Net performs precise tooth segmentation and tooth numbering. Detected abnormalities are assigned to individual teeth through mask-bounding box overlap analysis, where an assignment is made only when the overlap coverage exceeds a fixed threshold of 50%, and the resulting associations are stored in a structured JSON representation.

This structured output is provided to a LoRA-fine-tuned Qwen3-14B model as a zero-shot prompt, within a ChatML-formatted interaction that includes system instructions and model responses, enabling the generation of clinically coherent dental radiology reports.

**Results:** The proposed system demonstrates strong abnormality detection and tooth segmentation performance, enabling reliable localization and accurate tooth-level assignment of dental findings. Using structured outputs derived from detection and segmentation, the language model generates precise, structured, and clinically consistent dental radiology reports, demonstrating effective integration of visual analysis and language-based reasoning.

**Conclusions:** By integrating detection, segmentation, and language modeling, the framework overcomes limitations of conventional VLMs in subtle multi-tooth analysis, improving diagnostic accuracy and report coherence.

**Funding:** This work was supported by the National Research Foundation of Korea (NRF) grant funded by the Korean government (MSIT) (No. 2023R1A2C2 00532611). This work was also supported by the Technology Innovation Program (or Industrial Strategic Technology Development Program-Advanced Biomaterials) (RS-2025-14322975), funded by the Ministry

of Trade, Industry & Energy (MOTIE).

### OP5-5

## Development of an AI-driven web application for periodontal prognosis via panoramic radiographs

**P. Mahasantipiya**<sup>1\*</sup>, T Sawangpanyangkura<sup>1</sup>, P. Panyarak<sup>1</sup>, W. Suttapak<sup>2</sup>, U Yessarapat<sup>3</sup>

<sup>1</sup>Faculty of Dentistry, Faculty of Dentistry, Chiang Mai University, Thailand

<sup>2</sup>School of Information and Communication Technology (ICT) Payao University, Thailand

<sup>3</sup>Computational Intelligence Laboratory, Faculty of Engineer, Chiang Mai University, Thailand

**Introduction:** Periodontitis is a primary cause of tooth loss, yet clinical prognosis often suffers from inter-examiner variability and subjective assessment errors, particularly in probing depths. To address this, this study aimed to develop a Convolutional Neural Network (CNN) model to classify tooth prognosis using

**Materials and Methods:** The study utilized a retrospective dataset of 1,162 panoramic radiographs containing 26,608 teeth. The data was split into 2 sets which are training 80% (21,342 teeth) and validation 20% (5,266 teeth). Each tooth was annotated and assigned to one of four prognosis categories; favorable, treatable, hopeless due to periodontal destruction, or hopeless due to non-periodontal causes and based on consensus from one periodontist and two oral radiologists. The researchers employed the YOLO V.12 architecture. Two training strategies were explored: (1) end-to-end detection and classification, and (2) a two-stage model separating tooth detection and prognosis classification. Performance was assessed using accuracy and confusion matrices.

**Results:** The model demonstrated a high accuracy of 0.92 in identifying teeth that could be retained but required periodontal treatment. However, the accuracy for classifying teeth for extraction (0.66) and healthy teeth (0.62) was lower. Both training strategies generated similar outcomes, and independent replications by two researchers confirmed reproducibility.

**Conclusions:** The YOLOv12 convolutional neural network shows strong potential for automated periodontal prognosis assessment on panoramic radiographs, particularly for identifying teeth requiring treatment. A prototype web application was developed and registered. Further development is required to balance the dataset and improve accuracy for extraction and healthy cases. This project marks a significant step toward integrating AI into digital dental diagnostics.

### OP5-6

## Deep learning-based automated dental age estimation from panoramic radiographs in Thai adolescents and young adults

**Pittayapat P**<sup>1\*</sup>, Silkosessak O<sup>1</sup>, Sinpitaksakul P<sup>1</sup>, Achararit P<sup>2</sup>, Srisermphoak N<sup>2</sup>, Fuangrod T<sup>2</sup>, Porntaveetus T<sup>3</sup>

<sup>1</sup>Department of Radiology, Faculty of Dentistry, Chulalongkorn University, Thailand

<sup>2</sup>Princess Srisavangavadhana Faculty of Medicine, Chulabhorn Royal Academy, Thailand

<sup>3</sup>Center of Excellence in Precision Medicine and Digital Health, Department of Physiology, Faculty of Dentistry, Chulalongkorn University, Thailand

**Introduction:** Age estimation is essential in forensic odontology, particularly for determining the legal age of majority to prevent illegal labor. Conventional dental age assessment relies on manual staging of tooth development, which is time-consuming and subjective. Deep learning (DL) offers a promising automated alternative. This study aimed to compare regression-based and classification-based DL approaches for dental age estimation using panoramic radiographs in a Thai population.

**Materials and Methods:** 1,210 panoramic radiographs of Thai individuals aged 13–24 years were retrospectively collected from the Faculty of Dentistry, Chulalongkorn University, Thailand. Subjects were divided into 11 age groups and allocated to a training set (n=1,100; 50 males/50 females per group) and a test set (n=110; 5 males/5 females per group). Nine DL architectures were evaluated: ResNet-50, EfficientNet-B0, DenseNet121, Vision Transformer, Data-efficient Image Transformer, Swin Transformer,

CoAtNet-0, MaxViT-Tiny, and ConvNeXt Base. Models were trained using two strategies: (1) regression to predict chronological age and (2) binary classification to categorize individuals as minors (<18 years) or adults ( $\geq 18$  years).

**Results:** In the regression task, Swin Transformer achieved the best performance with mean absolute error of 1.97 years. However, converting regression predictions into binary legal status reduced its accuracy, particularly near the 18-year threshold. In contrast, the direct classification approach demonstrated superior performance for legal age determination. The ConvNeXt Base model achieved the highest accuracy (76.36%), precision (79.34%), recall (76.36%), and F1-score (0.76). Most misclassifications occurred among individuals aged 17–19 years, likely due to physiological variability in third molar mineralization.

**Conclusions:** For determining the legal age of majority in Thailand, direct binary classification DL models outperformed regression-based approaches. The ConvNeXt Base model may serve as a useful adjunctive tool for forensic dental age assessment.

## OP5-7

### Content-based retrieval of panoramic radiographs using detection-guided contrastive embedding

**Sang-Heon Lim**<sup>1\*</sup>, Won-Jin Yi<sup>1,2</sup>

<sup>1</sup>Interdisciplinary Program of Bioengineering, Seoul National University, Seoul, South Korea

<sup>2</sup>Department of Oral and Maxillofacial Radiology, School of Dentistry and Dental Research Institute, Seoul National University, Seoul, South Korea

**Introduction:** Content-based image retrieval (CBIR) of dental panoramic radiographs plays a critical role in forensic identification and longitudinal patient follow-up by enabling accurate matching of radiographs acquired at different time points. However, variations in imaging conditions, anatomical changes, and long follow-up intervals significantly degrade retrieval performance. This study proposes a detection-guided contrastive learning framework with gated fusion to en-

hance discriminative embedding learning for panoramic radiograph retrieval.

**Materials and Methods:** A dataset of panoramic radiographs consisting of antemortem and postmortem image pairs was used for CBIR model development. A DETR-based network with a ResNet-50 backbone was trained on 1,638 annotated panoramic images to detect dental structures and generate detection-aware embeddings, while 2,058 unannotated images were additionally utilized. In parallel, a DenseUNet121 model was employed to extract buccal region segmentation-based embeddings. Contrastive learning was conducted with a train–test split of 7:3, using Recall@K, mAP, and nDCG as evaluation metrics. To further improve retrieval performance, a gated fusion module with cross-attention was introduced to adaptively combine detection and segmentation embeddings.

**Results:** Detection-based embeddings achieved superior retrieval performance compared to segmentation-based embeddings alone. The proposed gated fusion strategy further improved retrieval accuracy, yielding Recall@1 of 0.654, Recall@5 of 0.829, Recall@10 of 0.874, mAP of 0.728, and nDCG of 0.785. Performance analysis across different follow-up intervals demonstrated robust retrieval for short- and mid-term intervals, with gradual degradation observed in cases exceeding ten years. Representative retrieval results confirmed effective matching of corresponding panoramic radiographs.

**Conclusions:** The proposed detection-guided contrastive learning framework with gated fusion effectively enhances panoramic radiograph retrieval performance. By integrating complementary visual cues from detection and segmentation, the system demonstrates robustness to temporal variation and anatomical changes, supporting its applicability to forensic identification and longitudinal dental imaging analysis.

**Funding:** This work was supported by the National Research Foundation of Korea (NRF) grant funded by the Korean government (MSIT) (No. 2023R1A2C2 00532611). This work was also supported by the Technology Innovation Program (or Industrial Strategic Technology Development Program-Advanced Biomaterials) (RS-2025-14322975), funded by the Ministry of Trade, Industry & Energy (MOTIE).

## OP5-8

## Anatomy conditioned diffusion-based unsupervised anomaly detection and classification of jaw cysts and tumors on panoramic radiographs

**Sujeong Kim**<sup>1\*</sup>, Won-Jin Yi<sup>1,2</sup>

<sup>1</sup>*Interdisciplinary Program of Bioengineering, Seoul National University, Seoul, South Korea*

<sup>2</sup>*Department of Oral and Maxillofacial Radiology and Dental Research Institute, School of Dentistry, Seoul National University, South Korea*

**Introduction:** Dental panoramic radiographs are widely used in clinical dentistry. However, interpretation of panoramic images is challenging due to overlapping anatomical structures, image artifacts, and substantial inter-observer variability. Fully supervised deep learning approaches for detecting tumors and cysts require large-scale pixel-level annotations, which are costly and difficult to obtain in dental imaging. These limitations motivate the development of unsupervised methods that reduce annotation burden while maintaining diagnostic reliability. Recently, diffusion models have demonstrated strong potential for unsupervised anomaly detection by learning normal anatomical distributions and identifying pathological deviations.

**Materials and Methods:** We propose DentalDiff<sup>+</sup>, a diffusion-based framework for unsupervised anomaly detection and subsequent multi-class classification of jaw tumors and cysts on dental panoramic radiographs. The diffusion backbone is trained exclusively on normal images to capture lesion-free anatomical priors. To preserve patient-specific maxillofacial structures, we introduce an Anatomy-preserving Condition Network (ACN) that injects multi-scale anatomical information into the denoising process. During inference, reconstruction–input discrepancy maps are generated to localize abnormal regions. These heat maps are concatenated with the original radiographs and provided to a lightweight supervised classifier to differentiate lesion subtypes using limited labeled data.

**Results:** DentalDiff<sup>+</sup> achieved superior reconstruction performance, with an average PSNR of 23.0 dB and

SSIM of 0.75. For anomaly detection, the proposed method obtained an AUC of 0.94, demonstrating robust separation. In multi-class classification of tumors and cysts, DentalDiff<sup>+</sup> achieved an overall accuracy of 0.93. Qualitative results show that the anatomically guided reconstruction suppresses artifacts while highlighting clinically meaningful lesions with indistinct boundaries.

**Conclusions:** DentalDiff<sup>+</sup> presents an anatomy-aware diffusion framework for reliable analysis of dental panoramic radiographs. By combining normal-only training, anatomically guided reconstruction, and heat-map-conditioned classification, the proposed approach significantly reduces annotation requirements while achieving strong detection and classification performance.

**Funding:** This work was supported by the National Research Foundation of Korea (NRF) grant funded by the Korean government (MSIT) (No. 2023R1A2C2 00532611). This work was also supported by the Technology Innovation Program (or Industrial Strategic Technology Development Program-Advanced Biomaterials) (RS-2025-14322975), funded by the Ministry of Trade, Industry & Energy (MOTIE).

## Oral Presentation 6

May 1 (Fri), 15:10-16:20 | Room C

OP6-1

### Deep learning-based segmentation of the maxillary sinus on panoramic radiographs using MedSAM and DeepLabv3+

**Yong Chan Park**<sup>1</sup>, Sang Jun Lee<sup>2</sup>, Wan Lee<sup>1</sup>, Han-Gyeol Yeom<sup>1</sup>, Byung-Do Lee<sup>1</sup>

<sup>1</sup>Department of Oral and Maxillofacial Radiology, College of Dentistry, Wonkwang University, Iksan, Korea

<sup>2</sup>Division of Electronic Engineering, Jeonbuk National University, JeonJu, South Korea

**Background and Purpose:** Panoramic radiographs are widely used in dental practice because of their low radiation dose and rapid image acquisition. However, the intrinsic limitations of two-dimensional imaging, such as overlapping anatomical structures, make it difficult to accurately delineate the maxillary sinus. Deep learning-based segmentation methods have recently gained attention for their ability to overcome these challenges. Among them, MedSAM and DeepLabv3+ have demonstrated strong performance in medical image segmentation, yet their application to panoramic maxillary sinus segmentation remains limited.

This study aimed to evaluate and compare the segmentation performance of MedSAM and DeepLabv3+ for the automatic detection of the maxillary sinus on panoramic radiographs.

**Material and method:** A total of 1,046 images were retrospectively collected from a dental hospital and a private clinic. Manual annotations were performed by two oral and maxillofacial radiologists and one general dentist using the VGG Image Annotator (VIA). The dataset was divided into training, validation, and test sets in a 60:20:20 ratio. Segmentation performance was evaluated using Dice Similarity Coefficient (DSC), Intersection over Union (IoU), precision, recall, F1-score, Normalized Surface Distance (NSD), and Hausdorff Distance at the 95th percentile (HD95).

**Results:** Both models showed high accuracy in sinus segmentation. MedSAM achieved DSC 0.9570 and

IoU 0.9183, while DeepLabv3+ achieved DSC 0.9534 and IoU 0.9124. Both models exhibited low NSD and HD95 values, indicating excellent boundary recognition. Although MedSAM slightly outperformed DeepLabv3+, it required significantly more parameters (90.49M vs. 26.68M) and higher computational cost.

**Conclusion:** In conclusion, both MedSAM and DeepLabv3+ demonstrated robust performance for automatic segmentation of the maxillary sinus on panoramic radiographs. These findings suggest that deep learning-based segmentation can provide an efficient and reliable alternative to 3D imaging in dental diagnosis and treatment planning.

OP6-2

### Semi-supervised deformation-free image-to-image translation for realistic CT synthesis from CBCT

**Ji Yong Han**<sup>1\*</sup>, Su Yang<sup>2</sup>, Won-Jin Yi<sup>1,3</sup>

<sup>1</sup>Interdisciplinary Program of Bioengineering, Graduate School of Engineering, Seoul National University, Seoul 03080, South Korea

<sup>2</sup>Department of Oral and Maxillofacial Surgery, Huston Methodist Research Institute, Huston, Texas 77030, USA

<sup>3</sup>Department of Oral and Maxillofacial Radiology School of Dentistry, Seoul National University, Seoul 03080, South Korea

**Introduction:** Cone-beam CT (CBCT) is widely used in dentomaxillofacial imaging, but scatter, noise, and inaccurate Hounsfield Units (HU) limit quantitative use. Although CT offers reliable HU, it increases radiation dose. We propose a semi-supervised, deformation-free CBCT-to-CT translation framework that eliminates geometric deformation while improving image quality and HU accuracy.

**Materials and Methods:** The proposed approach consists of two stages. First, an unpaired translation network generates CT-like images from CBCT to create pseudo-paired data, guided by edge constraints to maintain anatomical boundaries. Second, a paired translation stage refines the synthesis using these pseudo pairs. The refinement network adopts a UNet++-based generator enhanced with Interpolation-Convolution Upsampling (ICUP) to prevent checkerboard artifacts and Edge-Conditioned Skip

Connections (ECSC) to enforce structural consistency. Two discriminators, targeting real CT and pseudo-CT respectively, are used to enhance training stability and HU realism. The loss function combines adversarial, patch-wise contrastive, perceptual, style, identity, air-region segmentation losses. The dataset comprised CBCT and CT scans from 40 patients, divided into training and evaluation sets. Performance was assessed using SSIM-derived metrics, GMSD, NCC, and HU-based MAE.

**Results:** The proposed method consistently outperformed CycleGAN, UNIT, and CUT across all quantitative metrics. It achieved superior structural similarity, higher contrast and luminance consistency, improved resolution preservation, and more accurate HU distributions. Quantitative HU errors in hard tissues such as enamel, dentin, and cortical bone were significantly reduced. Qualitatively, the synthesized CT images showed exact geometric consistency across slices and clearer anatomical details.

**Conclusions:** This study demonstrates that a semi-supervised, deformation-free CBCT-to-CT translation framework can generate realistic CT images with accurate HU values while maintaining structural boundaries. By leveraging pseudo-paired data and structure-aware network design, the method overcomes key limitations of existing unsupervised approaches and shows strong potential for clinical application.

**Funding:** This work was supported by the National Research Foundation of Korea (NRF) grant funded by the Korean government (MSIT) (No. 2023R1A2C2 00532611). This work was also supported by the Technology Innovation Program (or Industrial Strategic Technology Development Program-Advanced Biomaterials) (RS-2025-14322975), funded by the Ministry of Trade, Industry & Energy (MOTIE).

OP6-3

## Evaluation of dental students' diagnostic skills using an artificial intelligence tool

Elif Sena SARGIN<sup>1\*</sup>, Ingrid Różyło-Kalinowska<sup>2</sup>, Derya YILDIRIM<sup>1</sup>

<sup>1</sup>Department of Oral and Maxillofacial Radiology, Süleyman Demirel University, Türkiye

<sup>2</sup>Department of Dental and Maxillofacial Radiodiagnostics, Medical University of Lublin, Poland

**Introduction:** Artificial intelligence (AI) has emerged as a transformative force in dental education, offering promising solutions for enhancing diagnostic skills. This study aims to evaluate the diagnostic accuracy of dental students on panoramic radiographs using an AI-based tool and to compare performance differences between preclinical and clinical cohorts.

**Materials and Methods:** This dual center study was conducted at Medical University of Lublin and Süleyman Demirel University during the 2024-2025 academic year. Sixty four dental students (33 third-year, 31 fourth-year) voluntarily participated. Students evaluated 10 anonymized panoramic radiographs using the CranioCatch® AI platform for the first time to detect and label various radiographic findings including periapical lesions, caries, impacted teeth, cysts, and other pathologies. Precision, sensitivity, and F1 scores were calculated using an intersection over union (IoU) threshold of 0.5. Statistical analyses were performed using independent samples t-tests and chi-square tests.

**Results:** Average precision, sensitivity, and F1 scores were 63.6%, 68.1%, and 64.2%, respectively. No significant differences were found between 3rd and 4th year students or between genders for overall scores ( $p>0.05$ ). 3rd year students outperformed 4th year students in detecting periapical lesions with caries (precision: 38.9%, 17.8% respectively,  $p=0.004$ ) and alveolar bone loss (precision: 65.2%, 41.9%, respectively,  $p=0.042$ ). Conversely, 4th year students showed superior performance in detecting impacted supernumerary teeth (precision: 88.7%, 68.2%, respectively,  $p=0.041$ ). Ameloblastoma detection had the highest scores (precision: 95%, F1: 96.1%), periapical lesions with caries showed the lowest performance (precision: 28.6%, F1: 33.2%).

**Conclusions:** AI platforms like CranioCatch can effectively assess dental students' diagnostic performance on panoramic radiographs. Differences in performance between academic years suggest that both preclinical theoretical knowledge and clinical experience contribute distinctly to AI-assisted diagnostic outcomes.

## OP6-4

## Prediction of masseter muscle elasticity from B-mode ultrasound images using texture-based radiomic features and ridge regression

**Firdevs Aşantoğrol**<sup>1</sup>, Mert Can Kitoğlu<sup>1\*</sup>, Burak Tunahan Çiftçi<sup>2</sup>

<sup>1</sup>Department of Oral and Maxillofacial Radiology, Faculty of Dentistry, Gaziantep University, Gaziantep, Türkiye

<sup>2</sup>Kahramanmaraş Oral and Dental Health Hospital, Kahramanmaraş, Türkiye

**Introduction:** Quantitative assessment of masticatory muscle stiffness is clinically important for evaluating functional integrity and detecting subclinical changes. This study aimed to develop a machine learning-based model to predict shear wave elastography (SWE)-derived stiffness values (kPa) of the masseter muscle using only B-mode ultrasound images.

**Materials and Methods:** B-mode images obtained from masseter muscles were analyzed. Each grayscale image was processed using Python (OpenCV, scikit-image). From every image, 21 quantitative features were extracted, including statistical descriptors (mean gray value, standard deviation, median, Interquartile Range (IQR), percentiles, skewness, kurtosis, Root Mean Square (RMS), and Shannon entropy) and Gray-Level Co-occurrence Matrix (GLCM)-based texture features (contrast, dissimilarity, homogeneity, ASM (Angular Second Moment), energy, correlation, GLCM entropy). GLCM features were averaged across 1–3-pixel distances and 0°, 45°, 90°, and 135° orientations. All variables were z-score standardized; 80% of the data were used for training and 20% for testing. A Ridge regression model ( $\alpha=1.0$ ) was trained to predict SWE stiffness. Model performance was evaluated using the determination coefficient ( $R^2$ ), mean absolute error (MAE), and root mean square error (RMSE).

**Results:** The Ridge regression achieved  $R^2 = 0.675$ , MAE = 11.54 kPa, and RMSE = 16.56 kPa on the test set, indicating moderate agreement between predicted and measured stiffness. The most influential predictors were muscle phase, GLCM correlation, Shannon ent-

ropy, IQR, and GLCM contrast, highlighting the importance of both statistical and texture-based descriptors for masseter elasticity estimation.

**Conclusion:** B-mode ultrasound radiomics combined with Ridge regression can provide a noninvasive, quantitative estimate of muscle elasticity without direct SWE measurement. This approach may support functional muscle assessment in dental and maxillofacial radiology and pave the way for operator-independent stiffness evaluation models.

## OP6-5

## Effects of labeling strategy and input image size on deep learning-based temporomandibular joint segmentation in transcranial radiography

**Nayeon Kim**<sup>1\*</sup>, Yun-Hoa Jung, DDS, PhD<sup>1</sup>, Bong-Hae Cho DDS, PhD<sup>1</sup>, Jae Joon Hwang, DDS, PhD<sup>1</sup>

<sup>1</sup>Department of Oral and Maxillofacial Radiology, Pusan National University, Republic of Korea

**Introduction:** Transcranial radiography is a useful modality for evaluating the temporomandibular joint. This study investigated the effects of labeling strategies and input resolution on a deep learning-based instance segmentation model (YOLO11x) for automatically segmenting the condyle and glenoid fossa in transcranial radiographs.

**Materials and Methods:** A total of 4,884 transcranial radiographic of bilateral temporomandibular joints were collected in three positions. Artificial boundaries were added to generate extended masks for the anatomically open glenoid fossa. Experiments compared three conditions: (1) original labels (960×960 pixels), (2) refined labels using coordinate interpolation (960×960 pixels), and (3) refined labels (640×640 pixels). Performance was evaluated using mAP@0.5, mAP@0.5-0.95, precision, and recall.

**Results:** The 960×960 model with original labels achieved a mask mAP@0.5 of 95.09% and mAP@0.5-0.95 of 59.39%. With refined labels, the 960×960 model improved to 99.08% and 66.70%, respectively.

The 640×640 model with refined labels demonstrated the highest performance, achieving a mask mAP@0.5 of 99.20% and mAP@0.5-0.95 of 68.33%. Confidence scores improved from 0.3–0.7 to 0.7–0.9 after refinement.

**Conclusions:** Extended labeling using artificial boundaries is effective for anatomically open structures. Furthermore, reducing input resolution improved performance. This suggests that the 640×640 resolution may be more data-efficient, whereas the 960×960 model might require a larger dataset to achieve optimal convergence.

### OP6-6

## How generative AI models depict oral and maxillofacial radiologists with administrative duties

Ülkem AYDIN<sup>1\*</sup>, Elif Sena SARGIN<sup>2</sup>, Derya YILDIRIM<sup>2</sup>, Burak İNCEBEYAZ<sup>1</sup>, Duygu KAYMAK<sup>1</sup>

<sup>1</sup>Department of Oral and Maxillofacial Radiology, Ankara Medipol University, Türkiye

<sup>2</sup>Department of Oral and Maxillofacial Radiology, Suleyman Demirel University, Türkiye

**Introduction:** Generative artificial intelligence (AI) tools now play a valuable role in portraying healthcare professionals, although they may also reinforce or create stereotypes. This study aimed to investigate the depiction of oral and maxillofacial radiologists with administrative duties, as generated by two AI text-to-image models.

**Materials and Methods:** This cross-sectional study analyzed images generated by two AI text-to-image models: Microsoft Copilot and DALL·E 3 through ChatGPT 4. Standardized prompts were used to create 400 images representing oral and maxillofacial radiology department head roles. Images were classified based on image quality, gender, personal features, and background features. Gender data for the department heads in Turkey was collected. Three independent reviewers assessed images. Frequencies were reported across models. Categorical variables were compared with the Chi-square test.

**Results:** Most of both females (81.4%) and males (83.3%) were depicted as experienced professionals. Significant differences were found between DALL·E 3 and Copilot across all visual attributes ( $p < 0.001$ ). DALL·E 3 generated predominantly male figures (63.2%) with formal attire, beard, short hair, and slim body types, while Copilot produced more female figures (69.6%) with diverse attire, longer hair, and varied body types. The addition of “Türkiye” to prompts created significant apparent gender divergence between models ( $p < 0.001$ ). AI significantly overestimated male representation compared to real-world department heads ( $p = 0.007$ ). The imaging devices in background were identified as absent or unidentifiable in 72.2% of images. Irrelevant accessories and background features were also noticed.

**Conclusions:** AI models demonstrated gender bias while generating department heads. Stereotypical images, lack of identifiable imaging devices, irrelevant equipment and background, highlights the need for improved training of AI image generators to ensure accurate representation of oral and maxillofacial radiology professionals.

### OP6-7

## Applications of artificial intelligence in dentomaxillofacial radiology: A systematic review of imaging-based diagnostic performance

Piña D'Abreu, Monica<sup>1,2\*</sup>, Riutord Sbert, Pere<sup>1,2</sup>, Cristina Martorell<sup>1,2</sup>, Daniela Vallejos<sup>1,2</sup>

<sup>1</sup>Faculty of Dentistry, University ADEMA School, Spain

<sup>2</sup>Health Group of University Institute for Research in Health Sciences (IUNICS), Spain

**Introduction:** Imaging-based diagnosis is a fundamental component of Dentomaxillofacial Radiology (DMFR). In recent years, artificial intelligence (AI) has gained increasing relevance as a tool to support image interpretation and improve diagnostic accuracy in dentomaxillofacial imaging.

**Objective:** To analyze the applications of artificial intelligence in DMFR for the imaging diagnosis of den-

tomaxillofacial pathologies through a literature review.

**Materials and Methods:** A systematic review of original full-text scientific articles published between January 2021 and April 2025 was conducted. Studies were identified through PubMed, Google Scholar, and ProQuest databases. Articles published in English or Spanish were included. Extracted data included imaging modalities, AI models used, clinical applications, and criteria reported for diagnostic accuracy assessment.

**Results:** Sixteen studies met the inclusion criteria after full-text evaluation. Conventional radiographs were the most frequently analyzed imaging modality, reported in 13 studies. Convolutional neural networks were the predominant AI models, used in 11 studies. AI systems demonstrated the ability to detect, localize, and classify carious lesions, identify furcation involvement and bone defects, and classify alveolar bone loss. Furthermore, AI applications included the detection and classification of periapical lesions, fractures, cysts, and odontogenic tumors. Although diagnostic accuracy values varied among studies, overall results consistently indicated a promising performance of AI-assisted diagnostic tools.

**Conclusions:** Artificial intelligence shows significant potential in dentomaxillofacial radiology, contributing to enhanced image analysis and supporting clinical decision-making. Further validation and standardization are required to facilitate its integration into routine clinical practice.



# e-Poster



## e-Poster

EP-18

**Ameloblastic fibro-odontoma with a congenitally missing mandibular second molar: A rare case report****Byung-Do Lee\***, Wan Lee, Han-Gyeol Yeom, Yu Ri Kim*Department of Oral and Maxillofacial Radiology, College of Dentistry, Wonkwang University, Iksan, Korea*

**Introduction:** Ameloblastic fibro-odontoma (AFO) is a rare benign mixed odontogenic tumor that typically occurs in children and adolescents. It represents a developmental lesion characterized by the simultaneous proliferation of odontogenic epithelium and ectomesenchymal tissue with the formation of dental hard tissue. AFO is commonly associated with delayed eruption of permanent teeth, but its coexistence with congenitally missing teeth is extremely uncommon. To date, only a few such cases have been reported in the literature.

**Case:** A 7-year-old boy presented with delayed eruption of the left mandibular first molar. Panoramic radiograph revealed a well-defined, ovoid radiolucent lesion with sparse calcified materials in the left mandibular posterior region, corresponding to the site of a congenitally missing second molar. Cone-beam computed tomograph showed amorphous radiopaque foci within a unilocular radiolucent lesion, accompanied by thinning and mild expansion of the lingual cortex. Surgical enucleation was performed, and histopathological examination confirmed the diagnosis of AFO, showing odontogenic epithelial islands, fibrous connective tissue, and dental hard tissue components. The lesion was successfully removed by simple curettage, and follow-up radiographs demonstrated favorable healing and normalization of the eruption path of the first molar.

**Discussion:** This case highlights a rare presentation of AFO associated with congenital absence of the mandibular second molar. The lesion's small size and minimal cortical expansion suggest an early developmental stage. Differential diagnosis included calcifying odontogenic cyst, adenomatoid odontogenic tumor,

and complex odontoma. The radiographic coexistence of radiolucent and radiopaque features played a key role in diagnosis. Given the low recurrence rate, conservative surgical removal remains the treatment of choice. This case adds to the limited body of evidence regarding AFO with congenital tooth agenesis and emphasizes the importance of detailed radiologic evaluation in pediatric jaw lesions.

EP-19

**CBCT evaluation of cortical bone thickness for orthodontic mini-implant in Mongolian population****Oyuntugs Rashsuren<sup>1\*</sup>**, Erdenebulgan Batmunkh<sup>2</sup>, Enebish Sundui<sup>3</sup>, Sunjidmaa Zolzaya<sup>3</sup>, Delgertsetseg Jargaltsogt<sup>1</sup>, Ganjargal Ganburged<sup>1</sup>, Juramt Bold<sup>3</sup><sup>1</sup>*Central Dental Clinic of MNUMS, Ulaanbaatar, Mongolia*<sup>2</sup>*Mongolian National Diagnostic Center, Second General Hospital, Ulaanbaatar, Mongolia*<sup>3</sup>*School of Biomedicine, of MNUMS, Ulaanbaatar, Mongolia*

**Introduction:** This study aimed to assess the mandibular and maxillary cortical bone thickness using a Cone-Beam Computed Tomography (CBCT) image to determine the safe zone in Mongolian Population to insert orthodontic mini-implant.

**Materials and Methods:** In this retrospective study, we included 208 subjects that were taken by CBCT in the Central Dental Hospital, Mongolian National University Medical Sciences (MNUMS) of Mongolia, from 2014-2024, were obtained with using OnDemand3D software for the linear measurements. In 14 randomly selected cases, all measurements were made twice to assess intra-rater reliability, 3 weeks apart. The inclusion criteria were no periodontal disease with no alveolar bone loss, no missing teeth. Exclusion criteria were fractures and pathological conditions in the maxilla and mandible, and root anomalies including severe dilacerations and idiopathic root resorption. SPSS version 24 software (SPSS Inc., Chicago, IL, USA) was used for statistical analysis.

**Results:** Maximum maxillary cortical bone thickness measured 7 mm above from CEJ between 1st premolar and 2nd premolar was  $0.88 \pm 0.25$  mm, 7 mm above

from CEJ between 2nd premolar and 1st molar area was 0.95 mm and between 1st molar and 2nd molar was 0.95±0.23 mm respectively. Maximum mandibular cortical bone thickness measured 7 mm above from CEJ between 1st premolar and 2nd premolar was 1.55±0.37 mm, 7mm above from CEJ between 2nd premolar and 1st molar area was 1.69±0.49 mm and between 1st molar and 2nd molar was 2.06±0.56 mm respectively. There was no statistically significant difference between the genders ( $p>0.05$ ).

**Conclusions:** This suggests that the maxillary and mandibular molar teeth cortical bone thickness on the buccal side of 7mm from the CEJ is considered to be the safest position in the Mongolian population to orthodontic mini-implant on cortical bone.

## EP-21

## Performance assessment of generative AI for the board certification examination of the Japanese Society for Oral and Maxillofacial Radiology

**Yohei Takeshita**<sup>1\*</sup>, Toshiyuki Kawazu<sup>1</sup>, Miki Hisatomi<sup>2</sup>, Mamiko Fujikura<sup>2</sup>, Shunsuke Okada<sup>2</sup>, Akira Shibamura<sup>3</sup>, Yuri Namba<sup>4</sup>, Suzuka Yoshida<sup>4</sup>, Saori Yoshida<sup>5</sup>, Yoshihide Nakamura<sup>6</sup>, Yoshinobu Yanagi<sup>1,2,4,5,6</sup>

<sup>1</sup>Department of Oral and Maxillofacial Radiology, Faculty of Medicine, Dentistry and Pharmaceutical Sciences, Okayama University, Okayama, Japan

<sup>2</sup>Department of Oral and Maxillofacial Radiology, Medical Development Field, Okayama University, Okayama, Japan

<sup>3</sup>Department of Community and Global Health, Graduate School of Medicine, The University of Tokyo, Tokyo, Japan

<sup>4</sup>Department of Oral and Maxillofacial Radiology, Division of Dentistry, Okayama University Hospital, Okayama, Japan

<sup>5</sup>Preliminary Examination Room, Medical Development Field, Okayama University, Okayama, Japan

<sup>6</sup>Department of Oral and Maxillofacial Radiology, Graduate School of Medicine, Dentistry and Pharmaceutical Sciences, Okayama University, Okayama, Japan

**Introduction:** Generative AI represented by ChatGPT is a recent focus of attention that is being applied in the field of radiology, and it has been evaluated not only for diagnostic imaging but also for such as education and decision-making. Our purpose was to assess

the performance and utility of ChatGPT for the board certification examination of the Japanese Society for Oral and Maxillofacial Radiology (JSOMR).

**Materials and Methods:** We assessed ChatGPT responses to 149 multiple-choice questions written in Japanese for the board certification examination of the JSOMR for the 3 years from 2020 to 2022. The questions were directly entered into GPT-3.5, GPT-4 (both in September to October 2023), and GPT-5 (in September 2025) models manually one by one as a prompt. The accuracy rate was calculated by year and type of multiple-choice question. Differences among models were tested using Cochran's Q test. Pairwise comparisons were made using McNemar test with the Holm method for multiple comparisons.

**Results:** The accuracy rate for the 3 years was 40.3% using GPT-3.5, 67.8% using GPT-4, and 76.5% using GPT-5. GPT-5 had a significantly higher accuracy rate than GPT-3.5 and GPT-4. Among different types of multiple-choice questions, GPT-5 performed significantly better than GPT-3.5 and GPT-4 especially in two-answer questions.

**Conclusions:** GPT-5 showed a high accuracy rate, significantly superior to GPT-3.5 and GPT-4 in the board certification examination of the JSOMR, suggesting that the use of ChatGPT, especially GPT-5, would be effective as a tool for learning and preparing for the examination. However, since the responses of generative AI are not always correct or up-to-date, these applications should be used only as support tools.

## EP-24

## Prediction of cervical metastasis in patients with squamous cell carcinoma of the tongue using FDG-PET accumulation parameters and texture analysis

**Shin Nakamura**<sup>1\*</sup>, Ami Kuribayashi<sup>1</sup>, Arisa Oki<sup>1</sup>, Hiroshi Watanabe<sup>1</sup>, Akiko Imaizumi<sup>1</sup>, Miharuru Taguchi<sup>1</sup>, Masahiko Miura<sup>1</sup>

<sup>1</sup>Department of Dental Radiology and Radiation Oncology, Graduate School of Medical and Dental Sciences, Institute of Science Tokyo, Japan

## EP-27

## A case of mandibular carcinoma cuniculatum: Multimodal imaging findings and diagnostic implications

Ami Kuribayashi<sup>1\*</sup>, Shin Nakamura<sup>1</sup>, Hiroshi Watanabe<sup>1</sup>, Akiko Imaizumi<sup>1</sup>, Masahiko Miura<sup>1</sup>

<sup>1</sup>Department of Dental Radiology and Radiation Oncology, Institute of Science Tokyo, Japan

**Introduction:** PET/CT-based diagnosis of cervical lymph nodes typically relies on FDG uptake and size, but its accuracy is limited by reactive nodes or occult metastases. This study aimed to develop and validate a logistic regression model that predicts lymph node metastasis in tongue squamous cell carcinoma (TSCC) using only primary tumor FDG uptake, texture features, and clinical factors, without incorporating lymph node imaging data.

**Materials and Methods:** This study included 316 patients with TSCC who underwent preoperative FDG-PET and surgery. From PET images, FDG uptake parameters and 107 texture features were extracted from the primary tumor. Clinical and pathological data were obtained from medical records. Patients were divided into analysis and validation groups (250:66). In the analysis group, univariate and multivariate analyses were performed to identify factors associated with lymph node metastasis, and a logistic regression model was constructed excluding lymph node-related variables. SUVmax of the largest lymph node and visual assessments by dental radiologists were also evaluated and compared to the model using ROC analysis. The model was then applied to the validation group to assess its predictive performance

**Results:** In the analysis group, cervical lymph node metastasis was associated with tumor growth pattern (endophytic type), FDG uptake in the primary lesion, and two texture features. A logistic regression model using these variables showed superior predictive performance, with a higher AUC than SUVmax and expert visual assessment. Applied to the validation group, the model achieved sensitivity of 0.76, specificity of 0.81, correctly identifying 16 cases misclassified by visual assessment.

**Conclusions:** The regression model, based solely on primary tumor-derived clinical and imaging features, offers a novel PET/CT-based approach for detecting cervical lymph node metastasis. Independent of nodal FDG uptake or size, it may improve identification of occult metastases and enhance diagnostic accuracy.

**Introduction:** Carcinoma cuniculatum (CC) is a rare histopathological variant of squamous cell carcinoma (SCC), and its occurrence in the oral cavity is extremely uncommon. Radiologic characteristics of CC have been scarcely reported to date. In this presentation, we describe a case of mandibular CC and highlight the imaging findings that contributed to the diagnostic process.

**Case:** A 75-year-old man presented to another hospital in June 2024 with discomfort in the mandible. Two biopsies failed to demonstrate malignancy. In December 2024, a draining fistula with abscess formation appeared on the right mandibular gingiva, and repeat biopsy revealed squamous cell carcinoma. Due to progressive enlargement of the lesion, the patient was referred to our institution for further evaluation. Panoramic radiography, contrast-enhanced CT, and MRI were performed. Surgical resection was subsequently undertaken, and the lesion was histopathologically diagnosed as CC. Panoramic radiography showed coarse trabeculation and cortical irregularity in the right mandibular molar region and anterior ramus. Contrast-enhanced CT demonstrated a mass exhibiting extensive bone destruction with a moss-eaten pattern, accompanied by surrounding trabecular sclerosis. Destruction was most pronounced lingually with periosteal reaction at the mandibular angle and soft-tissue extension toward the floor of the mouth. MRI showed iso-intensity to muscle on T1-weighted images and high intensity on T2-weighted images. Diffusion-weighted imaging demonstrated restricted diffusion. Tumor infiltration extended to the mandibular canal, temporalis muscle, pterygomandibular space, and submandibular space, with marked inflammatory changes in surrounding soft tissues.

**Discussion:** CC is a rare entity that poses significant diagnostic challenges. In this case, creeping invasion along the bone surface, trabecular sclerosis, and periosteal reaction were key imaging features, assisting differentiation from conventional SCC. Awareness of these radiologic patterns may promote earlier detection of CC.

## EP-30

## Evaluating the performance of YOLO v4 in detecting periodontal bone loss on panoramic radiographs

**Dida Devina**<sup>1\*</sup>, Eha Renwi Astuti<sup>2</sup>, Ramadhan Hardani Putra<sup>2</sup>, Aga Satria Nurrachman<sup>2</sup>, Alhidayati Asymal<sup>2</sup>, Kimiaus Saadah<sup>3</sup>

<sup>1</sup>Resident of Oral and Maxillofacial Radiology Specialist Study Program, Universitas Airlangga, Indonesia

<sup>2</sup>Department of Oral and Maxillofacial Radiology, Universitas Airlangga, Indonesia

<sup>3</sup>Undergraduate Dental Study Program, Universitas Airlangga, Indonesia

**Introduction:** Panoramic radiography is extensively employed in dentistry for the identification of diseases and pathological conditions, including periodontal bone loss. Traditional manual interpretation is labor-intensive, subject to variability among examiners, and susceptible to diagnostic errors due to the high workload faced by dental practitioners. The advancement of artificial intelligence offers enhanced capabilities for automated classification, segmentation, and identification, presenting a promising avenue for the automatic detection of periodontal bone loss.

**Materials and Methods:** A dataset comprising 50 panoramic images, selected according to predefined inclusion criteria, was annotated using Roboflow software. The dataset was partitioned into training and testing subsets in an 80:20 ratio for the development and assessment of the YOLO v4 model. Accuracy metrics were derived from true positive (TP), true negative (TN), false positive (FP), and false negative (FN) outcomes generated during testing.

**Results:** Automated detection of periodontal bone loss via YOLO v4 on a test subset of 50 panoramic radio-

graphs yielded 695 TP, 255 TN, 32 FP, and 35 FN instances. The model achieved an accuracy rate of 93.41%, with an average detection duration of 637.081 milliseconds per image.

**Conclusions:** The findings support the integration of YOLO v4 as a reliable tool for daily clinical practice to assist in the accurate and efficient automatic detection of periodontal bone loss in panoramic radiographs.

## EP-31

## Overview of differences in the sizes of the maxillary sinus by sex using panoramic radiography

**Dayanara Wienna Lopita**<sup>1\*</sup>, Yunita Savitri<sup>2</sup>, Otty Ratna Wahyuni<sup>2</sup>, Aga Satria Nurrachman<sup>2</sup>, Alhidayati Asymal<sup>2</sup>, Hasna Mutia Rabbani<sup>3</sup>

<sup>1</sup>Resident of Oral and Maxillofacial Radiology Specialist Study Program, Universitas Airlangga, Indonesia

<sup>2</sup>Department of Oral and Maxillofacial Radiology, Universitas Airlangga, Indonesia

<sup>3</sup>Undergraduate Dental Study Program, Universitas Airlangga, Indonesia

**Introduction:** Sex identification is an important factor in the identification of victims. Some cases, the skeleton of the body cannot be found intact, so it is necessary to do a thorough review by using a comparison of the dimensions of the height and width of the maxillary sinus to determine the sex. The purpose of this study differentiate the height and width of the maxillary sinus in men and women.

**Materials and Methods:** The maxillary sinuses of men and women age range 20-40 years measured using software image J on 54 panoramic radiographic samples

**Results:** The average height of the right maxillary sinus in men was 45.71 mm ( $\pm$  5.71 mm), the height of the right maxillary sinus for women was 31.65 mm ( $\pm$  4.43 mm). The mean width of the right maxillary sinus in males was 39.46 mm ( $\pm$  4.43mm), the mean width of the right maxillary sinus in females was 28.56 mm ( $\pm$  2.98 mm). The mean height of the left maxillary sinus in males was 44.81 mm ( $\pm$  5.45 mm), the mean

height of the left maxillary sinus in females was 33.18 mm ( $\pm$  4.35 mm). The mean left maxillary sinus width in males was 42.66 mm ( $\pm$  4.98 mm), the mean left maxillary sinus width in females was 29.11 mm ( $\pm$  3.68 mm).

**Conclusions:** There is a difference in the height and width of the maxillary sinus in men and women as measured using panoramic radiographs. The maxillary sinuses in men are larger in height and width than in women.

### EP-33

## Implementation of YOLO v5 for radiographic bone loss detection in periapical projections

**Sari Kemaladini**<sup>1\*</sup>, Eha Renwi Astuti<sup>2</sup>, Ramadhan Hardani Putra<sup>2</sup>, Aga Satria Nurrachman<sup>2</sup>, Alhidayati Asymal<sup>2</sup>, Safira Adzani Rahman<sup>3</sup>

<sup>1</sup>Resident of Oral and Maxillofacial Radiology Specialist Study Program, Universitas Airlangga, Indonesia

<sup>2</sup>Department of Oral and Maxillofacial Radiology, Universitas Airlangga, Indonesia

<sup>3</sup>Undergraduate Dental Study Program, Universitas Airlangga, Indonesia

**Introduction:** Periodontal disease can be classified into stage I, stage II, and stage III/IV based on radiographic bone loss. Periapical radiographs are one of the most widely used imaging modalities for diagnosing periodontal conditions. However, manual interpretation of radiographs is often subjective and prone to low reliability. The YOLO v5 algorithm offers a deep learning-based approach that enables automatic, rapid, and objective image interpretation.

**Materials and Methods:** A dataset of 600 periapical radiographic images meeting the inclusion criteria was collected and divided into training, validation, and testing sets in an 80:10:10 ratio. Image annotation and classification into three categories of bone loss were performed using the Roboflow platform, followed by data reliability testing. The training and testing phases were conducted using the YOLO v5 framework. Detection performance was evaluated using the confusion matrix to calculate accuracy, sensitivity, and specificity.

**Results:** YOLO v5 detection of radiographic bone loss in 60 periapical radiographs produced 84 true positives, 10 false positives, 71 true negatives, and 5 false negatives. The model achieved an accuracy of 91.17%, sensitivity of 94.38%, and specificity of 87.65%. The average processing time per image was 41.8 milliseconds, demonstrating the efficiency of YOLO v5 in real-time detection.

**Conclusions:** The YOLO v5 algorithm can effectively assist in the rapid and accurate detection of radiographic bone loss stages on periapical radiographs.

### EP-36

## Fractal dimension analysis of trabecular bone density in postmenopausal women (panoramic radiography study)

**Laili Ma'rifah**<sup>1\*</sup>, Otty Ratna Wahyuni<sup>2</sup>, Eha Renwi Astuti<sup>2</sup>, Aga Satria Nurrachman<sup>2</sup>, Alhidayati Asymal<sup>2</sup>, Adioro Soetojo<sup>3</sup>, Wikan Tajali Rosojati<sup>4</sup>

<sup>1</sup>Resident of Oral and Maxillofacial Radiology Specialist Study Program, Universitas Airlangga, Indonesia

<sup>2</sup>Department of Oral and Maxillofacial Radiology, Universitas Airlangga, Indonesia

<sup>3</sup>Department of Conservative Dentistry, Universitas Airlangga, Indonesia

<sup>4</sup>Undergraduate Dental Study Program, Universitas Airlangga, Indonesia

**Introduction:** The trabecular bone structure in the mandibular body of postmenopausal women exhibits the highest metabolic activity. The trabecular region constitutes the main masticatory area and serves as an important indicator of mandibular bone density. In Indonesia, the prevalence of osteoporosis reaches 32.3%, ranking third in Southeast Asia and fifth globally. The gold standard for osteoporosis diagnosis is Dual-Energy X-ray Absorptiometry (DXA); however, its high cost limits accessibility. Therefore, simpler and more cost-effective alternatives are needed. Fractal Dimension (FD) analysis provides a quantitative method for assessing trabecular bone microarchitecture, with the fractal index easily obtained from panoramic radiographs. This approach offers valuable potential for early screening osteoporosis.

**Materials and Methods:** This observational analytic study utilized 122 panoramic radiographs from postmenopausal women aged over 50 years at RSGMP Universitas Airlangga. Subjects were categorized into normal, osteopenia, and osteoporosis groups based on DXA T-scores. FD values were calculated using ImageJ software by selecting regions of interest (ROI) in the trabecular area distal to the mental foramen on both sides of the mandible.

**Results:** A significant positive correlation was observed between BMD T-scores and FD values. The average estimated FD values were  $-0.1686 < \mu < 0.3686$  for the normal group and  $-3.2250 < \mu < -2.7932$  for the osteoporosis group.

**Conclusions:** There is a significant correlation between BMD T-scores and FD values, indicating that higher BMD corresponds to higher FD. The average FD value derived from panoramic radiographs can serve as an additional indicator for assessing mandibular trabecular bone density and for early detection of osteoporosis.

## EP-37

## Analysis of impacted maxillary canines angulation through panoramic radiographs at Universitas Airlangga Dental Hospital

**Amalia Putri Ananda\***<sup>1</sup>, Otty Ratna Wahyuni<sup>2</sup>, Yunita Savitri<sup>2</sup>, Aga Satria Nurrachman<sup>2</sup>, Alhidayati Asymal<sup>2</sup>, Vicky Eka Firmansyah<sup>3</sup>

<sup>1</sup>Resident of Oral and Maxillofacial Radiology Specialist Study Program, Universitas Airlangga, Indonesia

<sup>2</sup>Department of Oral and Maxillofacial Radiology, Universitas Airlangga, Indonesia

<sup>3</sup>Undergraduate Dental Study Program, Universitas Airlangga, Indonesia

**Introduction:** Maxillary canine impaction represents one of the most common types of tooth impaction. The condition may result from local or systemic factors that interfere with eruption. Lack of space caused by delayed eruption is a frequent etiological factor. Panoramic radiographs provide essential diagnostic infor-

mation regarding the angulation and position of the impacted tooth relative to adjacent teeth. The degree of angulation obtained from these images aids in evaluating the extent of lateral incisor root resorption and determining the appropriate treatment.

**Materials and Methods:** This study used 75 panoramic radiographs from the Academic Dental Hospital of Airlangga University collected between 2016 until 2023. Tooth angulations ( $\alpha$ ,  $\beta$ ,  $\gamma$ ) were measured and analyzed using descriptive statistics based on inclusion and exclusion criteria. The materials included panoramic radiographs, a bow ruler, a ruler, a pen, and paper.

**Results:** The results showed angulation of maxillary canine impaction using the Guarnieri method with Alpha ( $\alpha$ ), Beta ( $\beta$ ), and Gamma ( $\gamma$ ) angles.

**Conclusions:** The average angulation of maxillary canine impaction measured on panoramic radiographs from patients at Academic Dental Hospital of Airlangga University was found to be 30.5° for Alpha ( $\alpha$ ), 45.16° for Beta ( $\beta$ ), and 42.83° for Gamma ( $\gamma$ ).

## EP-38

## Effect of mangosteen peel application on bone resorption in a periodontitis model following X-ray exposure

**Evita Juniasri Indrawati\***<sup>1</sup>, Denny Saputra<sup>2</sup>, Sri Wigati Mardi Mulyani<sup>2</sup>, Aga Satria Nurrachman<sup>2</sup>, Alhidayati Asymal<sup>2</sup>, Tsabitah Azzahra<sup>3</sup>

<sup>1</sup>Resident of Oral and Maxillofacial Radiology Specialist Study Program, Faculty of Dental Medicine, Universitas Airlangga, Surabaya, 60132, Indonesia

<sup>2</sup>Department of Oral and Maxillofacial Radiology, Faculty of Dental Medicine, Universitas Airlangga, Surabaya, 60132, Indonesia

<sup>3</sup>Undergraduated dental study program, Faculty of Dental Medicine, Universitas Airlangga, Surabaya, 60132, Indonesia

**Introduction:** Based on the 2018 Riskesdas (National Basic Health Research), periodontal disease was the second largest prevalence of dental and oral health problems after dental caries in Indonesia, with a prevalence reaching 74.1%.

Panoramic radiographic imaging is commonly utilized to evaluate the condition of periodontal tissues in individuals with periodontitis. However, exposure to X-rays from panoramic radiography can exert indirect biological effects that promote osteoclast proliferation and subsequently aggravate alveolar bone resorption in periodontitis patients.

**Materials and Methods:** The research design is a post- test only group design. Samples used were *Rattus norvegicus* rats with periodontitis. There were 7 groups, each consisting of 5 rats. Mangosteen fruit peel was formulated into a mucoadhesive gingival patch using a solvent technique casting and applied to the gingiva. Then, the rats were exposed to X-ray radiation with panoramic radiography. Periodontal tissue from the rats was taken for histopathological examination.

**Results:** There were significant results in the periodontitis model group exposed to X-rays and given a mucoadhesive patch made from mangosteen fruit peel compared to the periodontitis model group exposed to X-rays alone. Additionally, the normal periodontitis model group compared to the periodontitis model group exposed to X-rays showed significant results.

**Conclusions:** The application of mangosteen fruit peel on the periodontitis model after X-ray exposure can inhibit bone resorption.

#### EP-57

### Automated detection of alveolar bone loss in periapical radiographs using YOLO v4

**Dorothea Ratri Sulihingtyas**<sup>1\*</sup>, Eha Renwi Astuti<sup>2</sup>, Aga Satria Nurrachman<sup>2</sup>, Alhidayati Asymal<sup>2</sup>, Syifa Nur Izzati Ainayah<sup>3</sup>

<sup>1</sup>Resident of Oral and Maxillofacial Radiology Specialist Study Program, Universitas Airlangga, Indonesia

<sup>2</sup>Departement of Oral and Maxillofacial Radiology, Universitas Airlangga, Indonesia

<sup>3</sup>Undergraduate Dental Study Program, Universitas Airlangga, Indonesia

**Introduction:** Periodontal disease affects 20-50% of the global population and remains the primary cause

of tooth loss, with a prevalence rate of 74.1% in Indonesia. Periapical radiography is the conventional method for identifying periodontal bone loss, however, manual interpretation often leads to variability and inconsistency. Artificial Intelligence (AI), particularly the YOLO v4 algorithm, has demonstrated reliable performance in real-time detection of periodontal bone loss.

**Materials and Methods:** A total of 600 images were selected according to inclusion criteria and annotated using Roboflow. The dataset was divided into training, validation, and testing subsets with an 80%:10%:10% ratio. The YOLO v4 model was trained and tested, and its performance was assessed using a confusion matrix to determine accuracy, sensitivity, and specificity.

**Results:** Detection of radiographic bone loss on 60 periapical projections yielded 77 true positives, 70 true negatives, 10 false positives, and 11 false negatives. The model achieved an accuracy of 87,5%, sensitivity of 87,5%, and specificity of 87,5%, with an average detection time of 111.749 milliseconds, demonstrating both efficiency and reliability.

**Conclusions:** The YOLO v4 algorithm effectively detects radiographic bone loss in periapical radiographs and can be utilized as a supportive diagnostic tool in dental radiology. Its high accuracy and rapid detection capability suggest strong potential for integration into clinical workflows and for advancing artificial intelligence applications in dental imaging.

#### EP-63

### Effectiveness of software for reducing susceptibility artifacts

**Ami Takeshita**<sup>1\*</sup>, Shotaro Fuchibe<sup>2,4</sup>, Kanae Moriyama<sup>3,4</sup>, Varisa Assapattarapun<sup>1</sup>, Nobuhiko Matsuda<sup>1</sup>, Noriko Yamao<sup>1</sup>, Kosei Ueshima<sup>1</sup>, Yuki Shimizu<sup>1</sup>, Naoko Takagawa<sup>1</sup>, Tadashi Sasai<sup>1,4</sup>, Yuka Uchiyama<sup>1</sup>, Shumei Murakami<sup>1,4</sup>

<sup>1</sup>Department of Oral and Maxillofacial Radiology, Graduate School of Dentistry, The University of Osaka, Japan

<sup>2</sup>Science and Technology Organization, GE HealthCare, Japan

<sup>3</sup>MR, Imaging Department, GE HealthCare Japan, Japan

<sup>4</sup>Department of Advanced Radioisotope Medicine, Institute for Radiation Sciences, The University of Osaka, Japan

**Introduction:** The multi-acquisition with variable resonance image combination (MAVRIC) method, which acquires multiple 3D-FSE images by offsetting the transmission and reception frequencies, effectively reduces susceptibility artifacts caused by metals. MAVRIC-SL (selective) supports PDw imaging using the 3D FSE technique and fat suppression imaging using the STIR method, with accurate slab selection and distortion correction using the 3D VAT technique. However, no studies have objectively reported the reduction in susceptibility artifacts for different types of metals in the oral region. Titanium is used in dental implants, orthodontic appliances, jawbone reconstruction plates, and more, some of which cannot be easily removed. These areas are prone to susceptibility artifacts that interfere with MRI and diagnosis. This study aimed to compare the effectiveness of MAVRIC-SL in reducing susceptibility artifacts with that of conventional 2D and 3D FSE sequences.

**Materials and Methods:** A phantom was created by placing agar gel with an optimal Gd contrast agent concentration in the lower half of an acrylic cube container (15 cm side length) and adding Gd contrast agent solution to the upper half. A pure titanium cube (10 mm side length) was placed at the center of the phantom as the sample. Before and after placing the sample, the phantom was imaged using the MAVRIC-SL, 3D fast spin echo (FSE), and 2D FSE methods. The measurement of susceptibility artifacts involved counting the artifact pixels in each slice and calculating the artifact volume.

**Results:** The artifact volume in the axial section using the MAVRIC-SL sequence was 28.9% compared to the 2D-FSE sequence and 25.3% compared to the Cube sequence.

**Conclusions:** MAVRIC-SL, as the software for reducing artifacts, decreased the magnetic susceptibility artifacts caused by titanium.

EP-67

## AI powered caries detection on panoramic radiographs using YOLOv5: A high accuracy retrospective study

**Radika Fahmi Siddiq**<sup>1\*</sup>, Yunita Savitri<sup>2</sup>, Eha Renwi Astuti<sup>2</sup>, Aga Satria Nurrachman<sup>2</sup>, Alhidayati Asymal<sup>2</sup>

<sup>1</sup>Resident of Oral and Maxillofacial Radiology Specialist Study Program, Faculty of Dental Medicine, Airlangga University, Indonesia

<sup>2</sup>Department of Oral and Maxillofacial Radiology, Faculty of Dental Medicine, Airlangga University, Indonesia

**Introduction:** Dental caries is the world's most common oral disease, impacting over 2 billion individuals, with Indonesia reporting a prevalence of 82.8%. Panoramic radiographs are essential for detecting and classifying caries. This study investigates the effectiveness of YOLOv5 in automating caries classification on panoramic images.

**Material and Method:** We retrospectively gathered 500 panoramic radiographs and allocated them into training (n=400), validation (n=50), and testing (n=50) sets. Caries lesions were manually annotated using Roboflow and categorized based on ICCMS criteria into 2-class and 4-class systems. Four YOLOv5 variants (small, medium, large, and extra-large) were trained via Google Colab. Diagnostic performance was analyzed using a confusion matrix to determine accuracy, sensitivity, specificity, precision, and F1-score.

**Results:** The YOLOv5-s model recorded the highest mean average precision (mAP) of 74.3% for 2-class classification, whereas YOLOv5-xl achieved 54.8% for 4-class. At a 20% confidence threshold, YOLOv5-s delivered 95.16% accuracy, 52.78% sensitivity, 98.38% specificity, 71.25% precision, and 60.64% F1-score. YOLOv5-xl showed 93.90% accuracy, 49.02% sensitivity, 97.08% specificity, 54.35% precision, and 51.55% F1-score. This threshold minimized errors while maximizing correct detections, with an average processing time of 31.8 ms per image.

**Conclusion:** YOLOv5 exhibited outstanding accuracy and specificity in both classification schemes, performing better in 2-class tasks for sensitivity, precision, and F1-score. These findings highlight its potential as a reliable tool for clinical caries screening.

## EP-68

## The case of radicular cyst with inflammation at the right side of mandible: An uncommon case finding

**Christian Victor B<sup>1\*</sup>**, Eha Renwi Astuti<sup>2</sup>, Aga Satria Nurrachman<sup>2</sup>, Alhidayati Asymal<sup>2</sup>

<sup>1</sup>Resident of Oral and Maxillofacial Radiology Specialist Study Program, Faculty of Dental Medicine, Airlangga University, Indonesia

<sup>2</sup>Department of Oral and Maxillofacial Radiology, Faculty of Dental Medicine, Airlangga University, Indonesia

**Introduction:** A radicular cyst (also known as a *periapical cyst*) is the most common odontogenic cyst that develops at the apex of a non-vital tooth. Inflammation can affect this type of cyst through several ways. It can enhance the expansion of the cyst by the osmotic pressure from inflammatory exudate & epithelial-breakdown products causes cyst enlargement, and also maintaining the epithelial lining of the cyst and preventing the cyst from healing.

**Case:** A 20-year-old male patient came to the Dental Hospital of the Faculty of Dentistry of Unair to have the remaining root of his lower right tooth removed. There was no visible facial swelling, and also no visible swelling on the gums. The patient was then referred to the Oral Surgery Department for anamnesis and intraoral examination. Panoramic examination is then administered to the patient. It was then discovered that the lesion already grows expansively by more than half of the thickness of the mandible. To get the better image in 3D, the CBCT examination is done to patient to get the clearer 3-dimensional view of the lesion.

**Discussion:** After examining and comparing the resulting images from panoramic and CBCT, the radiodiagnosis is consistent with the result from histopathological examination to conclude that this lesion as radicular cyst with inflammation. The CBCT modality is proven to have better and improved imaging quality

than panoramic in assessing and diagnosing the case of radicular cyst with inflammation.

## EP-69

## CBCT evaluation of craniofacial asymmetry in hemifacial microsomia: A case report

**Fery Suriyati Sormin<sup>1\*</sup>**, Nastiti Faradilla<sup>2</sup>, Eha Renwi Astuti<sup>2</sup>, Aga Satria Nurrachman<sup>2</sup>, Alhidayati Asymal<sup>2</sup>, Alexander Patera Nugraha<sup>3</sup>

<sup>1</sup>Resident of Oral and Maxillofacial Radiology Specialist Study Program, Faculty of Dental Medicine, Airlangga University, Indonesia

<sup>2</sup>Department of Oral and Maxillofacial Radiology, Faculty of Dental Medicine, Airlangga University, Indonesia

<sup>3</sup>Department of Orthodonty, Faculty of Dental Medicine, Airlangga University, Indonesia

**Introduction:** Hemifacial microsomia (HFM) is a congenital craniofacial anomaly marked by asymmetric underdevelopment of structures derived from the first and second pharyngeal arches and typically presents unilaterally. The mandible, temporomandibular joint, maxilla, ear, and associated cranial nerves are frequently involved. Diagnosis requires both conventional and advanced imaging, with cone-beam computed tomography (CBCT) and 3D reconstruction providing essential detail for defining the extent of anatomical involvement and confirming the condition.

**Case:** An 18-year-old male presented with facial asymmetry. Clinical examination showed chin deviation, a malformed left ear, and hypoplastic left mandible with missing teeth. Panoramic radiograph revealed left mandibular deformity, absence of teeth in the affected region, overlapping anterior teeth, and radiopaque fixation-wire-like coils along the left condyle and ramus. Cephalometry confirmed ramus asymmetry and deformity of the left condyle and anterior displacement of the left first molar. CBCT demonstrated distally angulated impactions of teeth 18 and 28, crossbite with a rightward midline shift ( $\pm 15.1$  mm), a radiolucent graft gap beneath tooth 36 ( $\pm 0.8$  mm), and a bifid left condylar head showing features of overgrowth in bone healing.

**Discussion:** Hemifacial microsomia (HFM) is the second most common craniofacial developmental anomaly after cleft lip and palate, typically presenting as unilateral hypoplasia of skeletal and soft-tissue structures. The maxilla, mandible, and ear are most frequently in-

involved, often accompanied by ramus and condylar hypoplasia, ear deformity, and soft-tissue deficiency. Radiographic evaluation is essential for determining the extent of asymmetry. In this case, conventional imaging showed left mandibular deformity, ramus asymmetry, and overlapping anterior teeth. CBCT is particularly valuable in HFM assessment, especially when orthodontic or orthognathic correction is planned, as 3D reconstruction improves visualization of complex craniofacial abnormalities. Accordingly, CBCT with 3D analysis was used in this patient to support diagnosis and treatment planning.

## EP-73

## Subcutaneous emphysema and pneumomediastinum secondary to endodontic treatment: A case report

Hui-Wu Yang<sup>1\*</sup>, Yuan-Tsun Wang<sup>1</sup>, Kang-Ju Hung<sup>1</sup>, Ming-Gen Tu<sup>1,2</sup>

<sup>1</sup>Department of Dentistry, China Medical University Hospital, Taichung, Taiwan

<sup>2</sup>School of Dentistry, China Medical University, Taichung, Taiwan

**Introduction:** The incidence of facial subcutaneous emphysema and the subsequent diffusion of air into the mediastinum is exceedingly rare in non-surgical endodontic procedures. Defects in the maxillary anterior alveolar bone, especially in the region of the anterior teeth apices, may predispose patients to the development of subcutaneous emphysema during dental interventions.

**Case:** A 47-year-old female presented to our department with discomfort over upper right facial region for several months. Radiographic examination revealed tooth 13 with previously overfilled endodontic material. The diagnosis for tooth 13 was “previous treated with symptomatic apical periodontitis.” During the endodontic procedure, a sudden onset of swelling over bilateral eyelids and cheeks was observed. Immediate management included copious saline irrigation and placement of a temporary restoration on tooth 13 and prophylactic antibiotics prescribed. The patient experienced increasing discomfort and a sensation of pres-

sure over the right facial and cervical regions, prompting her to seek emergency care the following morning. Chest radiography and computed tomography (CT) confirmed the presence of cervicofacial subcutaneous emphysema and pneumomediastinum. She was admitted for observation and prophylactic antibiotic therapy. After the emphysema and pneumomediastinum gradually resolved. Definitive endodontic treatment of tooth 13 was successfully completed several weeks later.

**Discussion:** This case highlights the rare but potentially serious complication of subcutaneous emphysema and pneumomediastinum during non-surgical endodontic treatment. Multiple contributing factors may be involved, including both patient-related anatomical conditions and iatrogenic procedural factors. Defects in the maxillary anterior alveolar bone near the apices of anterior teeth may allow air to escape into the surrounding soft tissues when pressured air or irrigation forces are inadvertently introduced. The use of Cone-Beam Computed Tomography (CBCT) for detailed sagittal-plane evaluation and identifying existing bone defects may help clinicians anticipate potential pathways for air dissemination and reduce the likelihood of iatrogenic subcutaneous emphysema.

## EP-77

## Investigation of masseter muscle volume changes in anterior disc displacement of the temporomandibular joint: An MRI-based case-control study

Anil Didem Aydin Kabakci<sup>1</sup>, Mediha Erturk<sup>2</sup>, Melek Tassoker Bulut<sup>2\*</sup>, Taha Zirek<sup>2</sup>, Abdullah Enes Atas<sup>3</sup>

<sup>1</sup>Department of Anatomy, Necmettin Erbakan University, Meram Medicine Faculty, Konya, Turkiye

<sup>2</sup>Department of Dentomaxillofacial Radiology, Necmettin Erbakan University Faculty of Dentistry, Konya, Turkiye

<sup>3</sup>Department of Radiology, Necmettin Erbakan University, Meram Medicine Faculty, Konya, Turkiye

**Introduction:** This study aimed to investigate masseter muscle volume differences in patients with anterior disc displacement using magnetic resonance imaging (MRI).

**Materials and Methods:** This retrospective case–control study presents an interim analysis based on an expanded sample size ( $n = 200$ ) of TMJ MRI scans from individuals aged 18–69; patient recruitment is still ongoing and the final sample size will be larger. Participants were classified into three groups based on MRI findings: healthy controls, anterior disc displacement with reduction, and anterior disc displacement without reduction. Masseter muscle volumes were measured on coronal images using ITK-SNAP (v4.2.0) with manual segmentation and expressed in  $\text{mm}^3$ . Statistical analyses were performed in SPSS 21.0 (Armonk, NY, USA). Descriptive statistics (mean and standard deviation) were calculated, and group comparisons were conducted using the Kruskal–Wallis test, with  $p < 0.05$  considered significant.

**Results:** For the right masseter muscle, mean rank values were 112.13 in the healthy group, 87.72 in the anterior disc displacement with reduction group, and 100.38 in the displacement without reduction group ( $p > 0.05$ ). For the left masseter muscle, the mean ranks were 95.06 in healthy individuals, 90.97 in those with displacement with reduction, and 115.83 in the displacement without reduction group, showing a statistically significant difference among groups ( $p < 0.05$ ). Overall, the highest masseter muscle volume values were observed in the anterior disc displacement without reduction group, particularly on the left side.

**Conclusions:** Masseter muscle volume showed group-dependent variation in patients with TMJ disc displacement. The highest volumes were observed in the anterior disc displacement without reduction group, particularly on the left side. These findings suggest that chronic, non-reducing displacement may lead to altered functional loading and compensatory changes in the masseter muscle.

## EP-78

### Three-dimensional craniofacial measurements using ZTE-MRI

**Yuka Uchimoto**<sup>1\*</sup>, Mazihtul Zawani Binti Munshi<sup>1,2</sup>, Varisa Assapattarapun<sup>1</sup>, Noriko Yamao<sup>1</sup>, Naoko Takagawa<sup>1</sup>, Tadashi Sasai<sup>1</sup>, Sven Kreiborg<sup>3,4,1</sup>, Sanjay M Mallya<sup>5</sup>, Fan-Pei Gloria Yang<sup>6,1</sup>, Shumei

Murakami<sup>1,3</sup>

<sup>1</sup>Department of Oral and Maxillofacial Radiology, Graduate School of Dentistry, The University of Osaka, Japan

<sup>2</sup>Department of Oral and Maxillofacial Clinical Sciences, Faculty of Dentistry, Universiti Malaya, Malaysia

<sup>3</sup>3D Craniofacial Image Research Laboratory, University of Copenhagen, Denmark

<sup>4</sup>Department of Oral and Maxillofacial Surgery, Copenhagen University Hospital Rigshospitalet, Denmark

<sup>5</sup>Section of Oral and Maxillofacial Radiology, UCLA School of Dentistry, United States of America

<sup>6</sup>AI Center, National Tsing Hua University, Taiwan

**Introduction:** Radiation exposure remains a significant concern in clinical imaging, particularly for children and young adult—the risk group for radiation-induced cancer. A precise, non-ionizing alternative for craniofacial measurement would have significant implications for clinical practice. Cephalometry and computed tomography (CT) are considered gold standards for craniometry but expose patients to ionizing radiation. A zero-echo time magnetic resonance imaging (ZTE-MRI) enables visualization of short-T2 tissues, including cortical bone, without ionizing-radiation exposure by minimizing TE toward zero. However, its clinical application in head-and-neck has been limited. The goal of the present study was to investigate the possibility of using ZTE-MRI to derive precise three-dimensional measurements of the craniofacial regions.

**Materials and Methods:** The study was approved by the institutional ethics committee. Twenty-nine participants (mean age  $32.1 \pm 17.1$ , 23 females) underwent MDCT and ZTE-MRI. Standard cephalometric landmarks (27 linear and 21 angular variables) were identified. Linear regression analysis was performed to compare measurements obtained from MDCT and ZTE-MRI images.

**Results:** Nineteen linear and eight angular variables revealed regression coefficients between 0.9 and 1.1 and 28 of the linear and 16 of the angular variables showed R-square values of 0.81 or higher. In general, the skeletal reference points showed higher correlation than the dental reference points.

**Conclusions:** ZTE-MRI showed good agreement with MDCT for major craniofacial skeletal measurements, although dental and anatomically ambiguous variables

showed lower consistency. To our knowledge, this study is the first to demonstrate that the ZTE-MRI enabled accurate linear and angular craniofacial measurements used in dental practice. These findings support the future possibility of clinical applicability of ZTE-MRI for bone assessment, offering a radiation-free alternative for craniofacial imaging. Further research is warranted to establish its performance across all measurement.

## EP-83

## Prevalence of well-defined radiolucent lesions in the jaw of Korean children

**Suk-Ja Yoon**<sup>1\*</sup>, Jae-Seo Lee<sup>1</sup>

<sup>1</sup>Department of Oral and Maxillofacial Radiology, School of Dentistry, Chonnam National University, South Korea

**Introduction:** As the number of children in Korea declines, interest in their health is increasing, and awareness of the importance of children's dental and jaw health is also growing. This study aimed to investigate the prevalence and characteristics of well-defined radiolucent lesions in the jaws of Korean children under 14 years of age.

**Materials and Methods:** We classified children aged 14 years or younger who had well-defined radiolucent lesions on radiographic examination taken between September 2024 and August 2025. Diagnosis was based on clinical, radiographic findings with or without histopathological findings.

**Results:** Well-defined radiolucent lesions were identified in a total of 336 patients, 33 (10.2%) of whom were children under 14 years of age (17 males (mean age 10.2 yr  $\pm$  2.8); 16 females (mean age 11.1 yr  $\pm$  1.8)). A total of 43 lesions were found in 33 patients: 4 enlarged follicles (9.3%), 4 eruption cysts (9.3%), 1 periapical cyst (2.3%), 5 radicular cyst (11.6%), 16 dentigerous cysts (37.2%), 10 simple bone cysts (23.3%), 1 keratocystic odontogenic tumor (2.3%), 1 ameloblastic fibroma (2.3%), and 1 pseudotumor in the hemophilia (2.3%). By location, 9 lesions occurred in the upper anterior (20.9%), 9 in the upper posterior (20.9%), 4 in the lower anterior (9.3%), and 21 in the

lower posterior (48.8%). Multiple cysts were found in 2 patients (4.7%).

**Conclusions:** Cysts constitute the most common well-defined radiolucent jaw lesions in Korean children under 14 years of age. There were two cases of benign neoplasm. Especially, the presence of a pseudotumor in hemophilia shows the importance of considering systemic diseases in the differential diagnosis of pediatric jaw radiolucencies.

## EP-91

## Dynamic contrast-enhanced magnetic resonance imaging for distinguishing vital and non-vital teeth in jaw lesions: A validation study

**Supasith Yomtako**<sup>1\*</sup>, Sakiko Kume<sup>2</sup>, Hiroshi Watanabe<sup>2</sup>, Ami Kuribayashi<sup>2</sup>, Shin Nakamura<sup>2</sup>, Akiko Imaizumi<sup>2</sup>, Hiroshi Tomisato<sup>3</sup>, Yoshikazu Nomura<sup>2</sup>, Miharuru Taguchi<sup>2</sup>, Arisa Oki<sup>2</sup>, Masahiko Miura<sup>2</sup>

<sup>1</sup>School of Dentistry, Mae Fah Luang University, Thailand

<sup>2</sup>Department of Dental Radiology and Radiation Oncology, Institute of Science Tokyo, Japan

<sup>3</sup>Radiology Center, Institute of Science Tokyo, Japan

**Introduction:** Assessing tooth vitality status is important for dental practice. Electric pulp testing (EPT) is a reliable method; however, it depends on patient responses and may lead to false-negative results. We have previously utilized dynamic contrast-enhanced magnetic resonance imaging (DCE-MRI) to detect blood flow in the pulp chamber for differentiation of vital teeth and reported its potential usefulness in a pilot study. To further validate this approach, the present study aims to evaluate a larger cohort and determine whether DCE-MRI can accurately differentiate tooth vitality status compared with EPT.

**Materials and Methods:** This retrospective study included patients who underwent DCE-MRI for jaw lesions between September 2018 and May 2024 at the Institute of Science Tokyo Hospital. Imaging was performed using a 3T MRI scanner (Magnetom Spectra; Siemens Healthineers, Erlangen, Germany) with a

time-resolved angiography with interleaved stochastic trajectories sequence. The vitality status of teeth adjacent to the lesion was determined using EPT. Teeth without EPT results or those in which it was difficult to set a region of interest on the pulp chamber due to severe metal artifacts were excluded. Time-intensity curves (TICs) were generated and analyzed using the *syngo.via* workstation (Siemens) and categorized as either increasing or non-increasing types. Intra- and inter-observer reliability were evaluated using Cohen's kappa coefficients, and the correlation between TIC types and EPT results was assessed using Fisher's exact test. Statistical analyses were performed using R and RStudio (version 2023.6.1.524).

**Results:** Fifty-one patients were included, comprising 124 vital and 18 non-vital teeth. A significant correlation was observed between TIC types and EPT results, with an overall agreement rate was 95%.

**Conclusions:** This validation study demonstrated that DCE-MRI can effectively distinguish the vitality status of teeth.

#### EP-95

### Influence of PET/CT misregistration with metal artifacts from dental prostheses on SUV quantification in SiPM PET/CT

**Naoko Tagaino Watanabe**<sup>1\*</sup>, Ikuho Kojima<sup>1</sup>, Hiroyasu Kodama<sup>2</sup>, Kentaro Takanami<sup>3</sup>, Hayato Odagiri<sup>4</sup>, Hiroko Okawa<sup>5</sup>, Masahiro Iikubo<sup>1</sup>

<sup>1</sup>Department of Dental Informatics and Radiology, Tohoku University Graduate School of Dentistry, Japan

<sup>2</sup>Department of Radiological technology, Tohoku University Hospital, Japan

<sup>3</sup>Department of Diagnostic Radiology, Tohoku University Hospital, Japan

<sup>4</sup>Department of Diagnostic Image Analysis, Tohoku University Graduate School of Medicine, Japan

<sup>5</sup>Department of Molecular and Regenerative Prosthodontics, Tohoku University Graduate School of Dentistry, Japan

**Introduction:** Misregistration between CT and PET acquisition—often caused by patient motion—can introduce attenuation-correction errors and false uptake artifacts on PET/CT images. Furthermore, the influ-

ence of the presence or absence of dental metal in misregistration on the attenuation-correction is not clear. This study investigated the quantitative influence of misregistration and dental metal artifacts on the standardized uptake value (SUV) of silicon photomultiplier (SiPM) PET/CT.

**Materials and Methods:** A sphere (10 or 20 mm-diameter) injected with <sup>18</sup>F-fluorodeoxyglucose solution at a concentration four times higher than the background was placed to contact the inner surface of mandible of a head and neck phantom to simulate tongue cancer. Three metal patterns were prepared according to dental metal locations on mandible; Metal-free; Unilateral (left molars); Bilateral (incisors and molars). CT and PET were acquired using a SiPM PET/CT scanner. PET image reconstruction was performed with Bayesian penalized likelihood algorithm involving time-of-flight (TOF). Misregistration simulated by shifting PET images 10 mm to right or left on PET/CT console. SUV and Hounsfield units (HU) at sphere were analyzed.

**Results:** Across all metal patterns, HU, SUV<sub>max</sub>, and SUV<sub>mean</sub> decreased with shifting to right (away from the tooth) and increased with shifting to left (overlapping the tooth) relative to the non-shifting condition. The differences between shifted and non-shifted conditions were approximately 10%. The differences among the three metal patterns were minimal. No false uptake artifacts appeared on misregistered PET images.

**Conclusions:** In this study using SiPM PET/CT, the quantitative influence of misregistration with metal artifacts on SUV was smaller than previously reported for the conventional PET/CT system. Our result suggests that TOF, enabled by the superior timing resolution of SiPM PET/CT, can contribute to reducing these quantitative errors.

#### EP-105

### Segmental odontomaxillary dysplasia in a 16-year-old Thai female: A case report

Pyae Phyo Thaw<sup>1</sup>, Poramaporn Klanrit<sup>1</sup>, **Wariya**

**Panprasit<sup>1\*</sup>**<sup>1</sup>Department of Oral Diagnosis, Faculty of Dentistry, Khon Kaen University, Thailand

**Introduction:** Segmental odontomaxillary dysplasia (SOD) is a rare, non-inherited developmental anomaly of the craniofacial skeleton that is characterized by unilateral maxillary enlargement, gingival hyperplasia, and dental anomalies including hypodontia and delayed eruption of teeth.

**Case:** We report a case of a 16-year-old Thai female patient referred for a unilateral left maxillary enlargement, gingival enlargement, and absence of the left canine and first premolar. Orthopantomogram and cone-beam computed tomography revealed coarse, vertically oriented trabeculae, along with a hypoplastic ipsilateral maxillary sinus. An initial biopsy suggested osteosarcoma, and later, the diagnosis changed to osteoblastoma, before the correct diagnosis of segmental odontomaxillary dysplasia was made in a multidisciplinary meeting. No progress was noted at one-year follow-up.

**Discussion:** Due to the overlapping features in clinical presentation, SOD is commonly mistaken for a fibro-osseous lesion and can lead to unnecessary surgical intervention. Identification of the characteristic imaging findings is essential for the avoidance of misdiagnosis and overtreatment of SOD, which is a benign, non-progressive, and self-limiting condition.

EP-111

## Comparative analysis of mandibular buccal shelf, infrazygomatic crest and palatal bone thickness based on vertical dimension variation for orthodontics mini implant: A cone beam computed tomography (CBCT) study

**Dio Nella Arlingga<sup>1\*</sup>**, Nastiti Faradilla Ramadhani<sup>2</sup>, Deny Saputra<sup>2</sup>, Eha Renwi Astuti<sup>2</sup>, Aga Satria Nurrachman<sup>2</sup>, Alhidayati Asymal<sup>2</sup>, Gabriel Maria Ferdilia<sup>1</sup>

<sup>1</sup>Resident of Oral and Maxillofacial Radiology Specialist Study Program, Faculty of Dental Medicine, Airlangga University, Surabaya, Indonesia

<sup>2</sup>Department of Oral and Maxillofacial Radiology, Faculty of Dental Medicine, Airlangga University, Surabaya, Indonesia

**Introduction:** Successful orthodontic treatment requires adequate anchorage to achieve optimal tooth movement and treatment stability. Temporary Anchorage Devices (TADs), have become an effective option for providing absolute anchorage without depending on adjacent teeth or patient compliance. The stability of Orthodontics Mini Implants (OMI) is primarily influenced by bone quality and thickness at the placement site. Common anatomical sites used for OMI placement include Mandibular Buccal Shelf (MBS), Infrazygomatic Crest (IZC) and Palatal Bone (PBT). However, variations in vertical facial dimensions classified as brachyfacial, mesofacial and dolichofacial may affect bone morphology and implant.

**Material and Method:** The study aimed to analyze and compare the bone thickness of the MBS, IZC and PBT regions based on variations in vertical facial dimensions using CBCT. A retrospective analytical cross-sectional study was conducted using CBCT data from 45 orthodontic patients at Airlangga University Dental and Oral Hospital. Cephalometric analysis using WebCeph software categorized subjects into three facial types (brachyfacial, mesofacial, dolichofacial). Bone thickness was measured at specific reference points: MBS (4 mm and 8 mm from the CEJ around the first and second molar roots), IZC (11 mm, 13 mm and 15 mm from the occlusal plane at 70° angle to the buccal cortical plate) and PBT (anterior, middle and posterior regions). Statistical analyses included independent t-test, ANOVA, and post-hoc Tukey test.

**Result:** Significant differences in bone thickness were observed at specific MBS (6d 8 mm and 7m 4 mm;  $p < 0.5$ ) and PBT regions ( $p < 0.05$ ) among different facial types, while IZC thickness showed no significant variation ( $p > 0.05$ ).

**Conclusion:** Vertical facial dimension variations influence bone thickness in MBS and palatal regions, whereas IZC remains relatively consistent across facial types. Therefore, the IZC may serve as a reliable site for orthodontic mini implant placement regardless of

vertical facial dimension.

### EP-112

## Ultrasonographic features of a rare submasseteric abscess: A case report

**Rr. Astrid Dyah Kusumastuti Rahardjo<sup>1\*</sup>**, Nastiti Faradilla Ramadhani<sup>2</sup>, Eha Renwi Astuti<sup>2</sup>, Aga Satria Nurrachman<sup>2</sup>, Alhadiyahati Asymal<sup>2</sup>

<sup>1</sup>Resident of Oral and Maxillofacial Radiology Specialist Study Program, Faculty of Dental Medicine, Airlangga University, Indonesia

<sup>2</sup>Department of Oral and Maxillofacial Radiology, Faculty of Dental Medicine, Airlangga University, Indonesia

**Introduction:** A submasseteric abscess is a localized infection within the potential space between the masseter muscle and the lateral surface of the mandible. While it's documented in dental literature, its ultrasonographic characteristics remain underreported. Ultrasonography was selected in this case due to its non-invasive nature, real-time imaging, and high-utility in assessing head and neck infections.

**Case:** A 29-year-old female presented with a 10-day history of left buccal swelling, facial asymmetry, and trismus, but without pain or systemic symptoms. The swelling measured approximately 8×5 cm. Despite a 3-day course of Amoxicillin and Metronidazole, no clinical improvement was noted. Panoramic radiography and ultrasonography were performed. Buccal abscess and cellulitis of the left infraorbital were considered as differential diagnoses.

**Discussion:** A submasseteric abscess is a rare complication, most often occurred as a result of third molar dental procedures. While there are multiple possible pathways for infection in this area, pericoronitis associated with third molar infection is probably the most frequent case. In this case, the patient had previously undergone extraction of the left-maxillary-third-molar and presented with pericoronitis associated with the left-mandibular-third-molar. Panoramic radiographic findings were unremarkable, with no visible lesions identified. In contrast, ultrasound imaging revealed a heterogeneous hypoechoic area with posterior acoustic enhancement with irregular borders located beneath

the submasseteric muscle, supporting the diagnosis of a submasseteric abscess. This highlights the limitation of panoramic radiography in evaluating soft tissue structures, whereas ultrasonography, being specifically suited for soft tissue imaging, was able to detect the lesion that was not visible on the radiograph.

### EP-114

## Integrated radiographic and ultrasonographic approach in diagnosing buccal region lipoma: A case report

**Septia Anggreini Wilujeng<sup>1\*</sup>**, Nastiti Faradilla<sup>2</sup>, Eha Renwi Astuti<sup>2</sup>, Aga Satria Nurrachman<sup>2</sup>, Alhidayati Asymal<sup>2</sup>

<sup>1</sup>Resident of Oral and Maxillofacial Radiology Specialist Program, Faculty of Dental Medicine, Airlangga University, Indonesia

<sup>2</sup>Department of Oral and Maxillofacial Radiology, Faculty of Dental Medicine, Airlangga University, Indonesia

**Introduction:** Lipoma is a benign soft-tissue tumor that is uncommon in the oral and maxillofacial region. This case report describes a buccal mass diagnosed as a lipoma through clinical and imaging findings. Panoramic radiographs are usually nonspecific, so additional tests are needed. Ultrasonography is particularly useful because it shows a well-defined, homogeneous hyperechoic mass typical of fatty tissue and helps rule out malignancy. Combining clinical evaluation, panoramic imaging, and ultrasonography improves diagnostic accuracy and treatment planning.

**Case:** A 16-year-old male presented with a left cheek mass that had enlarged over 5 years and recently became painful. Examination showed facial asymmetry with a well-defined, mobile 3×3×3 cm mass in the left buccal region, smooth and tender on palpation. Intra-orally, a similar soft, minimally tender mass with diffuse borders and normal coloration was observed, with a 4-cm mouth opening.

**Discussion:** Lipoma is the most common benign mesenchymal tumor, but only 1–4% occur in the maxillofacial region. Ultrasonography is a useful additional imaging modality for diagnosing lipomas because it is

inexpensive, non-ionizing, easily accessible, and provides real-time evaluation. On ultrasound, lipomas commonly appear as well-defined, echogenic masses without posterior enhancement, although deeper lesions may present as iso- or hyperechoic and may show posterior enhancement. These variations are influenced by the purity of adipose tissue and the degree of internal contact between fat and connective tissue, which also contributes to inter-observer differences. Most lipomas possess a capsule that appears as a distinct echogenic margin, while certain types, such as intermuscular lipomas, may display ill-defined borders due to blending with adjacent tissues. Lipomas also frequently appear as elliptical, hyperechoic masses parallel to the skin surface with internal linear echogenic strands, although some may be iso- or hypoechoic, making ultrasound findings less pathognomonic than those of other imaging modalities.

## EP-117

## Development of a radiation dose reduction method for cone-beam CT for dental use with small-data MTANN AI imaging

**Ami Kuribayashi**<sup>1</sup>, Hiroshi Watanabe<sup>1</sup>, Takeaki Sudo<sup>2</sup>, Yafangzhou XU<sup>3</sup>, Ze Jin<sup>3</sup>, Kenji Suzuki<sup>3</sup>

<sup>1</sup>Department of Dental Radiology and Radiation Oncology, Institute of Science Tokyo, Japan

<sup>2</sup>Center for Data Science and Artificial Intelligence Education, Institute of Science Tokyo, Japan

<sup>3</sup>Biomedical AI Research Unit, Institute of Integrated Research, Institute of Science Tokyo, Japan

**Purpose:** This study aimed to develop an AI-based image-processing model to reduce radiation dose in cone-beam CT for dental use (CBCT) using a small-data AI imaging based on the Massive-Training Artificial Neural Network (MTANN).

**Materials and Methods:** A head phantom (PB-1, Kyoto Kagaku, Kyoto) was scanned using a 3D Accu-itomo F17 (Morita Corp., Kyoto) at ten different dose levels. The tube voltage was fixed at 90 kV, and radiation dose was adjusted by varying the tube current (1–6 mA) and scan angle (180° or 360°). The field of view was 8 × 8 cm, and the voxel size was set to 0.16 mm isotropic. Among the acquired datasets, the image

obtained at 90 kV, 6 mA, and 360° provided the highest quality and was defined as the high-dose (HD) reference. The lowest-dose image (90 kV, 1 mA, 180°) was used as the low-dose (LD) input. LD images were fed into the MTANN, and HD images served as teaching data. To better preserve fine anatomical structures, each image was divided into tooth and non-tooth regions, and two region-specific MTANNs were independently trained. In the test phase, outputs from the two MTANNs were combined to generate a virtual high-dose (VHD) image.

**Results:** The proposed method successfully generated VHD images from LD images. Compared with RedCNN, DnCNN, and BM3D, the model achieved higher SSIM (structural similarity) and PSNR (peak signal-to-noise ratio) values and yielded superior subjective image quality. The results indicated that this approach could achieve approximately 60% radiation dose reduction.

**Conclusion:** The MTANN-based approach demonstrates the feasibility of substantial radiation dose reduction in dental CBCT examinations while maintaining high image quality.

## EP-127

## Analysis of root number and canal morphology of maxillary premolars using cone-beam computed tomography

**Yun-Hoa Jung**<sup>1\*</sup>, Jae-Joon Hwang<sup>1</sup>, Bong-Hae Cho<sup>1</sup>

<sup>1</sup>Department of Oral and Maxillofacial Radiology, Pusan National University, South Korea

**Introduction:** This study aimed to evaluate the number of roots and type of root canals in maxillary first and second premolars within a selected Korean population utilizing cone-beam computed tomography (CBCT). Additionally, it sought to investigate potential differences in these features according to sex and tooth type.

**Materials and Methods:** CBCT images of 585 maxillary first premolars and 578 maxillary second premo-

lars from 303 patients were retrospectively reviewed. The number of roots was classified based on root morphology, and canal configurations were categorized into 8 types according to the Vertucci classification. For statistical analysis, chi-square or Fisher exact tests were employed to compare root number and canal morphology according to sex and tooth type.

**Results:** CBCT analysis revealed that 71.5% of maxillary first premolars and 97.6% of maxillary second premolars had 1 root. The most common canal configuration in maxillary first premolars was Vertucci type IV (42.6%), whereas type I predominated in maxillary second premolars (76.5%). Significant differences in root number and canal configurations were found between men and women ( $P < 0.05$ ), with single roots and Vertucci type I canals more commonly observed in women.

**Conclusions:** Both maxillary first premolars and maxillary second premolars typically had 1 root, with a smaller percentage possessing 2 roots. Significant sex differences were observed in root number and canal type. This study highlights the variability in root number and canal configuration, emphasizing the importance of recognizing these variations to achieve successful endodontic treatment.

#### EP-128

### Conformalized quantile regression for convolutional neural network-based dental age estimation from panoramic radiographs

**Witsarut Upalananda**<sup>1,2\*</sup>, Sawrawit Chairat<sup>1</sup>, Sangsom Prapayasadok<sup>3</sup>, Sakarat Na Lampang<sup>3</sup>, Sitthichok Chaichulee<sup>1</sup>

<sup>1</sup>Department of Biomedical Sciences and Biomedical Engineering, Faculty of Medicine, Prince of Songkla University, Thailand

<sup>2</sup>Department of Oral Diagnostic Sciences, Faculty of Dentistry, Prince of Songkla University, Thailand

<sup>3</sup>Department of Oral Biology and Diagnostic Sciences, Faculty of Dentistry, Chiang Mai University, Thailand

**Introduction:** Convolutional neural networks are a promising approach to automated dental age estimation from panoramic radiographs but typically provide

only point estimates without case-specific uncertainty. Conformalized quantile regression addresses this gap by producing calibrated prediction intervals with finite-sample coverage guarantees.

**Materials and Methods:** Panoramic radiographs of individuals aged 8–23 years ( $n=1,734$ ) were split into training, validation, calibration, and test sets (1,206/89/178/261). An EfficientNet-B0-based quantile regression model predicted the 0.05, 0.50, and 0.95 age quantiles using pinball loss and AdamW, with hyperparameter tuning and early stopping on the validation set. Predicted quantiles were post hoc calibrated via split conformal prediction on the calibration set to target 90% coverage. Final evaluation was performed on the test set.

**Results:** The model achieved a mean absolute error of 1.003 years on the test set. Conformalized quantile regression yielded calibrated prediction intervals with a mean width of 4.209 years and 90.8% empirical coverage.

**Conclusions:** Pairing convolutional-network-based dental age estimation with conformalized quantile regression provides calibrated, case-specific uncertainty suitable for individual patient reports and outlier flagging, supporting safer and more interpretable clinical use.

#### EP-130

### Radiomics features of mandibular cortical index on panoramic radiographs for osteoporosis detection

**Sultan UZUN**<sup>\*1</sup>, Kevser Dinç BAŞAR<sup>2</sup>, Melek Tassoker BULUT<sup>3</sup>

<sup>1</sup>Assist. Prof., Bilecik Şeyh Edebali University, Department of Dentomaxillofacial Radiology, Türkiye

<sup>2</sup>Res. Assist., Selçuk University, Department of Dentomaxillofacial Radiology, Türkiye

<sup>3</sup>Prof. Dr., Necmettin Erbakan University, Department of Dentomaxillofacial Radiology, Türkiye

**Introduction:** This study aimed to quantitatively evaluate mandibular cortical changes associated with the Mandibular Cortical Index (MCI) using radiomics fea-

tures extracted from panoramic radiographs, with the goal of transforming MCI into an objective and reproducible indicator for opportunistic osteoporosis screening.

**Materials and Methods:** A total of 159 panoramic radiographs (C1 = 53, C2 = 53, C3 = 53) were retrospectively analyzed. The right mandibular cortex was segmented following standardized anatomical boundaries, and radiomic features were extracted using PyRadiomics in 3D Slicer. Four feature classes—shape, first-order, GLCM, GLRLM, and GLSZM—were evaluated. Statistical significance was set at  $p < 0.05$ .

**Results:** Among the shape-based parameters, only Maximum 2D Diameter Row demonstrated a significant group effect, with the highest values observed in C1. Several first-order features—Energy, Entropy, IQR, MAD, rMAD, and Variance—also differed significantly among the groups, and C1 consistently showed the largest numerical values. Pairwise analyses confirmed significant differences between C1 and both resorbed cortex groups, while C2 and C3 remained statistically similar. Texture-based metrics captured finer microarchitectural changes. Significant GLCM features included Cluster Prominence, Cluster Shade, Correlation, Joint Energy, Joint Entropy, and Sum Entropy, each following feature-specific numerical trends. GLV (GLRLM) and ZE (GLSZM) also showed significant overall effects, with both features generally following a  $C1 > C3 > C2$  pattern.

**Conclusions:** Radiomics analysis successfully identified quantitative morphometric and microtextural differences associated with MCI categories. These findings support the potential of radiomics to enhance the objectivity of cortical assessment and facilitate opportunistic osteoporosis screening using panoramic radiographs.

#### EP-131

### Automated detection of dental caries on panoramic radiographs using a deep learning approach: A preliminary study with YOLOv8

**Gyeongseung Lee**<sup>\*1</sup>

<sup>1</sup>*Independent Researcher, Seoul, Republic of Korea*

**Introduction:** Dental caries remains one of the most prevalent chronic diseases globally. Panoramic radiography is a widely used diagnostic modality in dentistry; however, identifying early-stage or small carious lesions can be challenging due to overlapping anatomical structures and clinician fatigue. This study aimed to develop and evaluate an automated caries detection model using YOLOv8, a state-of-the-art object detection framework, to support clinicians in achieving more accurate and consistent diagnoses.

**Materials and Methods:** A publicly available dataset of anonymized panoramic dental radiographs annotated for dental caries was utilized. All images were pre-processed by resizing them to  $640 \times 640$  pixels and normalizing pixel intensities. The dataset was randomly divided into training (80%), validation (10%), and test (10%) subsets. The YOLOv8n (nano) architecture was selected for its computational efficiency and real-time capability. The model was trained for 100 epochs with a batch size of 16, incorporating standard data augmentation methods—including rotation and brightness adjustment—to mitigate overfitting.

**Results:** Preliminary evaluation on the test set demonstrated promising performance. The YOLOv8 model achieved a mean Average Precision (mAP@0.5) of 0.82, with a precision of 0.85 and a recall of 0.78. The model successfully detected carious lesions across various tooth surfaces, including proximal and occlusal areas, with an inference time of under 0.1 seconds per image.

**Conclusions:** This study highlights the feasibility of leveraging YOLOv8 for automated dental caries detection on panoramic radiographs. The model shows potential as an efficient screening tool to reduce diagnostic variability and enhance clinical workflow. Future work will involve expanding the dataset and benchmarking performance against alternative detection architectures.

## EP-139

## Utility of the PETRA MRI sequence in evaluating TMJ calcification: A case report

**Kim Su hyeon\***, Huh Kyung-Hoe, Heo Min Suk, Yi Won-Jin, Lee Sam-Sun, Kim Jo-Eun

*Department of Oral and Maxillofacial Radiology, Seoul National University School of Dentistry, Seoul, Republic of Korea*

**Introduction:** Intra-articular calcification of the temporomandibular joint (TMJ) arises from conditions such as degenerative joint disease and synovial chondromatosis, and is typically assessed using CBCT. However, repeated CBCT raise concerns regarding radiation exposure. Conventional MRI, due to its long echo time, has limitations in distinguishing calcification and bony structures from the articular disc. PETRA (pointwise encoding time reduction with radial acquisition), an ultrashort echo time MRI technique, capture signals from tissues with extremely short T2\* values, producing CT-like bone contrast while allowing assessment of adjacent soft tissues. This case report illustrates the utility of PETRA MRI in assessing TMJ calcification.

**Case:** The patient underwent CT and MRI for TMJ evaluation due to facial pain. On CBCT images, both condyles showed degenerative change including flattening, erosion, and osteophyte. with calcified loose bodies observed in the anterior aspect of both condyles. Anterolateral disc displacement of both TMJ was confirmed using MRI. Calcified foci could not be differentiated from disc on TMJ T2 and PD sequence. However, when using PETRA sequence bone and calcified foci were differentiated from disc. Therefore MRI alone, without irradiated CT, could reveal the location and characteristics of TMJ calcification.

**Discussion:** Differentiating calcification observed on CBCT from the articular disc on MRI has traditionally required three-dimensional registration between imaging modalities, a process limited by differences in patient positioning. With the development of PETRA, UTE images can be obtained within a single MRI examination. PETRA enables differentiation of early signal differences between tissues with distinct T2\* relaxation properties, allowing accurate identification of

presence and spatial relationship of calcification without CT. As PETRA image quality continues to improve, osseous changes of the condyle and glenoid fossa, as well as intra-articular calcifications, may be evaluated using MRI alone, reducing patient radiation exposure while providing information for diagnosis and surgical planning.

## EP-141

## CBCT features of mandibular ossifying fibroma mimicking aggressive pathology with cortical disruption and neurovascular displacement

**Aga Satria Nurrahman<sup>1\*</sup>**, Norlaila Sarifah<sup>1</sup>, Ragil Tri Nurrahman<sup>2</sup>

*<sup>1</sup>Department of Oral and Maxillofacial Radiology, Faculty of Dental Medicine, Universitas Airlangga, Surabaya, Indonesia*

*<sup>2</sup>Department of Dentomaxillofacial Radiology, Faculty of Dentistry, Lambung Mangkurat University, Banjarmasin, Indonesia*

*<sup>2</sup>Department of Oral and Maxillofacial Surgery, Faculty of Dentistry, Lambung Mangkurat University, Banjarmasin, Indonesia*

**Introduction:** Ossifying fibroma is a benign fibro-osseous lesion of the jaws that may present with variable radiographic appearances, often resembling other radiolucent mandibular pathologies. Accurate radiologic assessment is essential for lesion characterization, differential diagnosis, and surgical planning. Cone-beam computed tomography (CBCT) provides high-resolution three-dimensional imaging that enables detailed evaluation of lesion margins, cortical involvement, and relationship with adjacent anatomical structures.

**Case:** A 43-year-old woman presented with a subtle, painless bulging sensation in the right buccal area, detected during palpation. Clinical evaluation identified a firm mass measuring approximately 15×5×5 mm adjacent to the edentulous region of tooth 46, with intact and normally colored overlying mucosa. CBCT imaging revealed a well-circumscribed radiolucent lesion in the right posterior mandible, extending from the mid-level of the alveolar bone in the edentulous area toward the inferior border of the mandible. The lesion dimensions were approximately 16×7 mm on axial

sections and 16×8.5 mm on coronal sections, characterized by well-defined, non-corticated margins and absence of internal calcifications. Additional radiologic findings included adjacent bone destruction, discontinuity of the buccal cortical plate, inferior and lingual displacement of the mandibular canal, and buccal displacement of a tooth-like structure appearing suspended at the site of cortical disruption. No soft tissue asymmetry was detected. Based on the imaging characteristics, the lesion was primarily considered as a central giant cell granuloma, with ameloblastoma and simple bone cyst as differential diagnoses. Histopathological analysis of biopsy specimens ultimately confirmed the diagnosis of ossifying fibroma.

**Discussion:** This case highlights the importance of CBCT in identifying aggressive-appearing radiologic features of ossifying fibroma that may mimic other mandibular lesions. Despite its benign nature, ossifying fibroma can demonstrate cortical perforation and neurovascular displacement. Correlation between CBCT findings and histopathology remains essential for definitive diagnosis.

## EP-144

## Comparison of metabolic activity values in mandibular condyles between patients with condylar hyperplasia and asymptomatic individuals using nuclear medicine imaging techniques

**P Sutthiprapaporn**<sup>1\*</sup>, E Ponsena<sup>1</sup>, Y Raruenrom<sup>2</sup>, R Chaijit<sup>1</sup>

<sup>1</sup>Department of Preventive Dentistry, Faculty of Dentistry, Khon Kaen University, Thailand

<sup>2</sup>Department of Radiology, Faculty of Medicine, Khon Kaen University, Thailand

**Introduction:** Facial asymmetry poses aesthetic challenges in orthodontic patients. This study aimed to evaluate the condyle-to-clivus ratio in patients with condylar hyperplasia (CH) and in non-CH patients.

**Materials and Methods:** 78 patients (mean age: 30.15±11.73years; 23M,55F) were evaluated for differences in percentage condylar uptake and mandibular

asymmetry using SPECT and CT images. Subjects were divided into four groups: the active-CH group (male:M1;female:F1): mandibular asymmetry with active condylar hyperplasia and the non-CH group (M2;F2): mandibular symmetry and no active condylar hyperplasia. The groups were then compared.

**Results:** For M1, the percentage condylar uptake difference was 16.40±5.39%, while condyle-to-clivus ratios (average, maximum, and total) were 1.69±0.52, 1.78±0.48, and 1.69±0.52, respectively. In contrast, M2 exhibited a lower percentage condylar uptake difference of 3.93±2.78%, along with condyle-to-clivus ratios of 1.44±0.54, 1.40±0.54, and 1.37±0.51, respectively. Similarly, F1 demonstrated a higher percentage condylar uptake difference of 18.82±7.56%, along with condyle-to-clivus ratios of 1.28±0.41, 1.31±0.44, and 1.27±0.40, respectively. In contrast, F2 showed a lower percentage condylar uptake difference of 4.22±2.98%, with condyle-to-clivus ratios of 1.01±0.28, 1.00±0.26, and 1.01±0.28, respectively. Significant differences were observed in the percentage condylar uptake difference in both males and females (P=0.000) and in the condyle-to-clivus ratios in females (P<0.01).

**Conclusions:** Radioactive condylar-to-clivus uptake ratio is a valuable tool for diagnosing condylar hyperplasia.

## EP-146

## Effect of room temperature and scan delay on image quality of photostimulable phosphor plates

**Şelale Özel**<sup>1\*</sup>, Hakan Amasya<sup>2</sup>

<sup>1</sup>Department of Oral and Maxillofacial Radiology, University of Altınbaş, Türkiye

<sup>2</sup>Department of Oral and Maxillofacial Radiology, University of İstanbul-Cerrahpaşa, Türkiye

**Introduction:** Signal fading in photostimulable phosphor (PSP) plates results from the spontaneous loss of trapped electrons over time, reducing the latent image and potentially degrading diagnostic quality. This fading is influenced by both delay before scanning and ambient temperature, as elevated temperatures can ac-

celerate the release of stored energy. Previous studies have shown that timing and environmental factors can alter pixel intensity and noise levels in PSP systems. This study aimed to evaluate how room temperature (20 °C vs 28 °C) interacts with scan delay (1, 5, 10 minutes) to affect periapical image quality.

**Materials and Methods:** Standardized images were acquired using an aluminum step wedge, selecting the second and fourth steps to represent hard and soft tissues. Three 40 × 40 mm ROIs per step were analyzed to calculate SNR and CNR. PSP plates (3 × 4 cm, Gendex GXPS 500) were exposed using an Expert DC unit (65 kV, 7 mA) under two protocols: 0.080 s and 0.160 s as Protocol 1 and Protocol 2 respectively. Plates were stored at 20 °C or 28 °C and scanned after 1, 5, or 10 minutes.

**Results:** For SNR analysis, no statistically significant differences were observed between 20°C and 28°C in the Protocol 1 ( $p > 0.05$ ). In contrast, in the Protocol 2, SNR values at 28°C were significantly higher than those at 20°C ( $p = 0.027$ ). For CNR, no significant differences were detected between temperatures in either dose protocol ( $p > 0.05$ ), although higher CNR values were consistently observed at 28°C in the Protocol 2. These findings suggest that temperature increase improves noise characteristics primarily under normal-dose conditions, while contrast resolution remains unaffected.

**Conclusions:** Elevated room temperature improves SNR at normal dose levels, while CNR remains unaffected regardless of temperature or scan delay.

## EP-153

### Semi-automated AI workflow for condylar angle measurement on CBCT

Seung Ho Park<sup>1</sup>, Ho-Jun Song<sup>2</sup>, KyungMinClara Lee<sup>3</sup>, Min-Suk Kook<sup>4</sup>, **Jae-Seo Lee<sup>5\*</sup>**

<sup>1</sup>Student, School of Dentistry, Chonnam National University, Gwangju, Republic of Korea

<sup>2</sup>Department of Dental Biomaterials

<sup>3</sup>Department of Orthodontics

<sup>4</sup>Department of Oral and Maxillofacial Surgery

<sup>5</sup>Department of Oral and Maxillofacial Radiology School of Dentistry, Chonnam National University, Gwangju, Republic of Korea

**Introduction:** Accurate measurement of condylar angulation in temporomandibular joint (TMJ) analysis is critical for diagnosing morphological abnormalities. However, manual measurement on cone-beam computed tomography (CBCT) remains time-consuming and subject to examiner variability. To address this, we introduce a semi-automated workflow combining examiner-defined anatomical reference planes with artificial intelligence (AI)-based segmentation to improve consistency and reduce subjectivity.

**Materials and Methods:** A U-Net-based deep learning model was trained on 902 axial CBCT images to segment the mandibular condyle and determine its medial-to-lateral orientation. The examiner manually established the midsagittal plane using anatomical landmarks and measured the condylar inclination angles on axial images. AI-derived angles were computed relative to the same plane. The study included 20 patients (40 condyles). Agreement and reproducibility were evaluated using Bland-Altman analysis, correlation coefficients (Pearson and Spearman), and intraclass correlation coefficient (ICC).

**Results:** The U-Net model demonstrated strong segmentation performance. Intra-examiner reliability was high (ICC = 0.804). The mean bias between AI-derived and examiner measurements was 1.08°, with 74.1% of AI results falling within ±5° of examiner values. Correlation analysis showed strong linear ( $r = 0.839$ ) and rank ( $\rho = 0.768$ ) relationships. However, systematic fixed and proportional biases were observed.

**Conclusions:** This semi-automated, examiner-AI collaborative framework shows promise for enhancing reproducibility in TMJ condylar angle analysis. While agreement was moderate, findings support further development of automated reference plane calibration and validation in broader clinical settings to improve accuracy and utility.

## EP-156

## YOLOv8-based automated classification of mandibular third molar impaction in panoramic radiography

**Ramadhan Hardani Putra**<sup>1\*</sup>, Deny Saputra<sup>1</sup>, Alhidayati Asymal<sup>1</sup>, Aga Satria Nurrachman<sup>1</sup>, Putri Alfa Meirani Laksanti<sup>2</sup>, Nasywa Athaillah Safitri<sup>3</sup>, Fatina Yasmin<sup>3</sup>, Eha Renwi Astuti<sup>1</sup>

<sup>1</sup>Department of Dentomaxillofacial Radiology, Faculty of Dental Medicine, Universitas Airlangga, Indonesia

<sup>2</sup>Master of Dental Health Science Study Program, Faculty of Dental Medicine, Universitas Airlangga, Indonesia

<sup>3</sup>Bachelor of Dental Medicine Study Program, Faculty of Dental Medicine, Universitas Airlangga, Indonesia

**Introduction:** Mandibular third molar impaction (M3MI) is the most prevalent tooth impaction and may cause various complications that can affect quality of life. Panoramic radiography is commonly used as imaging modality for its diagnosis. M3MI classification is required for the surgical procedure planning. Therefore, the use of an AI-based automated model can improve the efficiency and accuracy of M3MI classification. This study aimed to evaluate the performance of YOLOv8 in automatically classifying M3MI in panoramic radiographs

**Materials and Methods:** A total of 600 panoramic radiographs were selected and split into training, validation, and test data (80%:10%:10%). All images were annotated for M3MI class- and position-based classification using the Pell and Gregory system. Two classification models were trained separately using three YOLOv8 model variants (s, m, and l) to determine the best model variant for further optimization. Each model was then tested at three confidence thresholds (25%, 50%, 75%) and calculated for accuracy, sensitivity, specificity, precision, and F1 score.

**Results:** YOLOv8-m showed the best performance during training and validation. On testing with 60 images, class-based classification achieved an accuracy of 92.11%, sensitivity of 100%, specificity of 67.86%, precision of 90.53%, and an F1-score of 95.03%, while position-based classification achieved 91.20%, 96.60%, 72.00%, 92.39%, and 94.45%, respectively.

**Conclusions:** The YOLO v8 model shows high performance for M3MI classification based on class and position on panoramic radiographs, so it can be further developed as an assisting tool for accurate M3MI automated classification.

## EP-158

## Radioprotective and regenerative effects of mesenchymal stem cell metabolite gel in hyperglycemic conditions

**Nastiti Faradilla Ramadhani**<sup>1\*</sup>, Sri Wigati Mardi Mulyani<sup>1</sup>, Deny Saputra<sup>1</sup>, Rini Devijanti Ridwan<sup>2</sup>, Alexander Patera Nugraha<sup>3</sup>

<sup>1</sup>Department of Dentomaxillofacial Radiology, Faculty of Dental Medicine, Universitas Airlangga, Indonesia

<sup>2</sup>Department of Oral Biology, Faculty of Dental Medicine, Universitas Airlangga, Indonesia

<sup>3</sup>Department of Orthodontics, Faculty of Dental Medicine, Universitas Airlangga, Indonesia

**Introduction:** Hyperglycemic conditions, such as diabetes mellitus, are associated with increased oxidative stress, chronic inflammation, and impaired tissue regeneration. In dental and maxillofacial practice, hyperglycemic patients frequently require cone-beam computed tomography (CBCT) for diagnosis and treatment planning of periodontal disease, periapical pathology, implant placement, and maxillofacial complications. However, CBCT-related ionizing radiation may further aggravate oxidative and inflammatory damage in hyperglycemic tissues, emphasizing the need for effective radioprotective strategies. Amnion-derived mesenchymal stem cell (AMSC) metabolites contain bioactive molecules with antioxidant, immunomodulatory, and regenerative properties. This study aimed to evaluate the radioprotective and regenerative effects of AMSC metabolite gel under hyperglycemic conditions following CBCT exposure.

**Materials and Methods:** This analytic experimental study involved 30 male Wistar rats (*Rattus norvegicus*), aged 1–2 months (250–300 g), induced into a hyperglycemic state. Animals were randomly assigned to a treatment group (hyperglycemia + CBCT radiation + AMSC metabolite gel) or a control group (hyperglycemia + CBCT radiation). AMSC metabolites were ob-

tained from conditioned media of cultured AMSCs and formulated into a topical gel. Tissue samples were collected on days 1, 3, and 7 post-irradiations. Histopathological and immunohistochemical analyses were performed to assess malondialdehyde (MDA), interleukin-10 (IL-10), tumor necrosis factor-alpha (TNF- $\alpha$ ), vascular endothelial growth factor (VEGF), and fibroblast growth factor (FGF) expression. Statistical analysis used independent t-tests and one-way ANOVA ( $p < 0.05$ ).

**Results:** The treatment group showed significantly lower MDA and TNF- $\alpha$  expression than the control group ( $p < 0.05$ ), indicating reduced oxidative stress and inflammation. IL-10 expression demonstrated a regulated anti-inflammatory response, while VEGF and FGF expression were significantly increased, reflecting enhanced angiogenesis and tissue regeneration.

**Conclusions:** AMSC metabolite gel demonstrates radioprotective and regenerative potential under hyperglycemic conditions and may serve as an adjunctive biomaterial to improve tissue resilience against CBCT-related radiation exposure.

#### EP-159

### Familial cleidocranial dysplasia in two siblings: A case report focusing on dental and craniofacial radiographic manifestations

**Kyoung-A Kim**<sup>1\*</sup>, Chang-Ki Min<sup>1</sup>

<sup>1</sup>Department of Oral and Maxillo-Facial Radiology, Jeonbuk National University, South Korea

**Introduction:** Cleidocranial dysplasia (CCD) is a rare autosomal dominant skeletal disorder characterized by pathognomonic craniofacial and dental abnormalities. Major radiographic features include delayed closure of cranial sutures and multiple supernumerary teeth. Oral and maxillofacial radiology is essential for a definitive diagnosis as these diagnostic hallmarks are primarily identified through imaging.

**Case:** Two siblings, a 10-year-old male and a 5-year-old female, presented with distinct dental concerns.

The brother sought treatment for the non-eruption of maxillary permanent incisors, while the sister presented with mandibular protrusion. Comprehensive radiographic analysis using panoramic and cephalometric imaging revealed classic manifestations of CCD in both siblings. Key findings included multiple impacted supernumerary teeth, which were notably localized in the premolar regions, creating a “third dentition” appearance. Furthermore, radiographic images confirmed significantly delayed closure of the fontanelles and cranial sutures, along with midfacial hypoplasia. During the medical history taking, the father reported his own history of retained deciduous teeth and impacted supernumerary teeth, providing clear evidence of familial inheritance and reinforcing the diagnosis for both siblings.

**Discussion:** The diagnosis of CCD in these siblings was established based on the radiographic identification of multiple impacted teeth in the premolar regions and delayed cranial suture closure. These cases highlight that systematic radiographic surveys of the craniofacial complex are essential for detecting CCD early, even before clinical symptoms become severe. Clinicians must maintain a high index of suspicion when observing consistent dental and skeletal abnormalities on routine imaging to ensure timely multidisciplinary intervention and optimal patient management.

#### EP-160

### Effect of mangosteen (*Garcinia mangostana* L.) pericarp extract mucoadhesive patch on osteoclast expression in an X-ray-exposed periodontitis model

**Deny Saputra**<sup>1\*</sup>, Sri Wigati Mardi Mulyani<sup>1</sup>, Nastiti Faradilla Ramadhani<sup>1</sup>, Tsabitah Azzahra<sup>2</sup>

<sup>1</sup>Department of Dentomaxillofacial Radiology, Faculty of Dental Medicine, Universitas Airlangga, Indonesia

<sup>2</sup>Undergraduate Student, Faculty of Dental Medicine, Universitas Airlangga, Indonesia

**Introduction:** Dental panoramic radiography is widely used as a primary diagnostic tool in dental practice; however, exposure to X-ray radiation may induce bio-

logical effects, including oxidative stress, DNA damage, and increased osteoclast activity, which can exacerbate periodontal tissue destruction. These effects are especially relevant in Indonesia, where periodontitis prevalence remains high. Mangosteen (*Garcinia mangostana L.*) pericarp contains xanthone compounds with potent antioxidant and anti-inflammatory properties that may mitigate radiation-induced bone resorption. This study aimed to evaluate the effect of a mangosteen pericarp extract gingival mucoadhesive patch on osteoclast numbers in X-ray-exposed periodontitis models.

**Materials and Methods:** This experimental laboratory study employed a randomized post-test only control group design using 35 male *Rattus norvegicus* rats (200–250 g,  $\geq 3$  months). Chronic periodontitis was induced by *Porphyromonas gingivalis* ATCC 33277. Animals were divided into seven groups based on radiation exposure, patch application, and observation periods (days 1, 3, and 7). Panoramic and periapical X-ray irradiation was performed using an Acteon X-Mind Prime unit. A mucoadhesive gingival patch containing mangosteen pericarp extract was applied to treatment groups. Mandibular periodontal tissues were harvested, processed, and stained with hematoxylin-eosin. Osteoclast numbers were counted under a light microscope (400 $\times$ ). Data were analyzed using one-way ANOVA, and Tukey post hoc analysis.

**Results:** The results demonstrated a progressive increase in osteoclast numbers in irradiated groups without patch application, whereas treatment groups showed a significant reduction over time. On day 7, osteoclast counts in the treatment group approached those of the negative control. Statistical analysis revealed significant differences between irradiated groups with and without patch application ( $p < 0.05$ ).

**Conclusions:** Mangosteen pericarp extract mucoadhesive gingival patches effectively reduced osteoclast activity following X-ray exposure in periodontitis models, indicating their potential as a protective adjunct in dental radiographic procedures

## EP-164

## Quantitative analysis for radiographic features of endodontically treated teeth with vertical root fracture

Chih-Chia Huang<sup>1\*</sup>

<sup>1</sup>Department Department of endodontics, Cardinal Tien Hospital & An Kang Branch. R.O.C.Taiwan

**Introduction:** Vertical root fracture (VRF) in endodontically treated teeth is characterized by longitudinal fracture lines extending toward the root apex or the coronal direction. Bacterial infiltration through the fracture line often leads to inflammation of the surrounding periodontal ligament (PDL). Radiographic evaluation of these changes may provide diagnostic value.

**Materials and Methods:** This retrospective study analyzed 60 periapical radiographs from 43 patients diagnosed with VRF, including 17 patients with two radiographs taken at intervals of more than six months. Each tooth was divided into seven regions: coronal, middle, and apical thirds along the long axis, further separated into mesial and distal sides, plus the apical foramen. A total of 420 regions were examined by a certified endodontic specialist using a quantitative scoring system: (0) intact and healthy PDL, (1) widened PDL space, (2) alveolar bone loss.

**Results:** Inflammation of the periodontal ligament was observed in all regions except the apical foramen. Among 26 teeth (112 regions), 56 regions scored 0, 35 scored 1, and 91 scored 2. In the remaining 17 teeth (238 regions), 102 regions scored 0, 56 scored 1, and 80 scored 2. Overall, only 37% of root regions in VRF cases exhibited healthy periodontal ligament images.

**Conclusions:** Periapical radiographs taken at the time of VRF diagnosis or within the preceding six months revealed that most teeth showed inflammatory changes over the periapical region. These findings suggest that radiographic evidence of PDL inflammation in different root regions may assist in diagnosing VRF in endodontically treated teeth.

## EP-166

## Clinical implication of CBCT-based root canal navigation software

**Hui Jeong**<sup>1,2,3\*</sup>, Kug Jin Jeon<sup>1,2</sup>, Chena Lee<sup>1</sup>, Yoon Joo Choi<sup>1</sup>, Gyu-Dong Jo<sup>1</sup>, Sang-Sun Han<sup>1,2,3</sup>

<sup>1</sup>Department of Oral and Maxillofacial Radiology, Yonsei University College of Dentistry, Republic of Korea

<sup>2</sup>Institute for Innovative in Digital Healthcare, Yonsei University, Republic of Korea

<sup>3</sup>Oral Science Research Center, Yonsei University College of Dentistry, Republic of Korea

**Introduction:** This study aimed to analyze the morphology of maxillary premolar canals using 3D visualization software on cone-beam computed tomography (CBCT) and quantitatively evaluate the root canal curvature, including bucco-palatal information.

**Materials and Methods:** CBCT images of 400 maxillary premolars (200 first and 200 second premolars) from 200 patients (100 males, 100 females; mean age 39.3 years) were evaluated. Virtual 3D root canal models were constructed by connecting canal center points. Canals were classified as single or double (buccal and palatal branches), and the canal curvature at the most curved point (MCP) was automatically calculated using the radius of the tangential circle (R value). The differences based on tooth type, canal configuration, and gender were analyzed using t-tests. The vertical locations of MCPs were categorized into apical, middle, or coronal.

**Results:** Double canals were prevalent in both maxillary first (99.5%) and second (88.0%) premolars, with mean R values at MCPs of 1.50 mm and 1.58 mm, respectively. No statistical differences were found in R values according to premolar type, canal configuration, or gender ( $p > 0.05$ ). Most MCPs were located apically, though 12.1-35.2% of those in double canals were located in the middle or coronal parts.

**Conclusions:** This study provided a quantitative assessment of root canal curvature, including bucco-palatal information. This approach offers more precise anatomical insight than conventional 2D methods and may enhance clinical outcomes in endodontic treatment.

## EP-169

## Evaluation of vertical magnification using a Panorama phantom<sup>®</sup>

**Hong Kim, DMD**<sup>1\*</sup>, Min-Suk Heo, DDS, PhD<sup>1</sup>, Won-Jin Yi, PhD<sup>1</sup>, Kyung-Hoe Huh, DDS, PhD<sup>1</sup>, Jo-Eun Kim, DDS, PhD<sup>1</sup>, Sam-Sun Lee, DDS, PhD<sup>1</sup>

<sup>1</sup>Department of Oral and Maxillofacial Radiology, School of Dentistry and Dental Research Institute, Seoul National University, Seoul

**Introduction:** Precise vertical measurement in panoramic radiography is essential for diagnosis and treatment planning. However, previous studies primarily relied on horizontal arrays, limiting the assessment of vertical dimensions. Although a phantom used in this study contains vertical arrays, its divergent slope causes discrepancies in depth and magnification at different heights. This study proposes an “Image Rearrangement Protocol” to compensate for these geometric limitations and analyze vertical magnification patterns.

**Materials and Methods:** The Panorama phantom<sup>®</sup> (Patent No. 10-2017-0184233) with divergent metal ball arrays was positioned using a precision micrometer rail and rotator. Images were acquired by shifting the phantom at 2 mm intervals in anterior, lateral, and oblique directions. The vertical diameter of each metal ball was measured to evaluate local magnification. A custom MATLAB<sup>®</sup> algorithm using bounding box and sub-pixel interpolation techniques was developed to enhance edge detection accuracy. An image rearrangement technique was applied to virtually align the sloped metal balls into a single vertical plane, eliminating depth variations.

**Results:** Preliminary results indicated that vertical magnification increased with a rate of change of up to 3.5% as the object approached the X-ray source (lingual displacement). Specifically, when the rearrangement protocol was applied to the oblique (45°) movement, an overall trend of increasing vertical magnification was observed from the temporomandibular joint (TMJ) to the premolars. These initial findings suggest that vertical magnification varies depending on the horizontal position within the focal trough.

**Conclusions:** The ultimate goal of this research is to provide a reference for position-dependent vertical magnification to aid in accurate clinical assessment.

## EP-171

## Quantitative effect of metal artifact reduction during CT imaging

**H Suito**<sup>1\*</sup>, Y Oku<sup>1</sup>, T Kondo<sup>1</sup>, N Maeda<sup>1</sup>, R Kasai<sup>2</sup>, K Fujimoto<sup>3</sup>, K Nagao<sup>3</sup>

<sup>1</sup>Department of Oral and Maxillofacial Radiology, Tokushima University, Japan

<sup>2</sup>Department of Medical Imaging Equipment Engineering, Tokushima University, Japan

<sup>3</sup>Department of Prosthodontics & Oral Rehabilitation, Tokushima University, Japan

**Introduction:** The periodic use of multidetector CT (MDCT) is highly effective for postoperative follow-up in patients with oral cancer. However, a unique challenge in oral cancer imaging arises from the close proximity of the lesion to intraoral metallic structures, further compounded by the presence of prosthetic metal devices within the oral cavity, both of which can generate significant artifacts. Therefore, this study evaluated the effectiveness of the metal artifact reduction algorithm “SEMAR (Single-Energy Metal Artifacts Reduction)” as well as the impacts of CT-based virtual monochromatic imaging.

**Materials and Methods:** Dental Radiography Head Phantom (PH-76, Kyoto Kagaku Co., Ltd, Kyoto, Japan) was evaluated using the Artifact Index (AI). A 5 mm ROI was set at the 5<sup>th</sup> equivalent region, and concentric ROIs of 10 mm and 15 mm diameter were set above it. Imaging was performed using an Aquilion ONE/ViSION Edition (320-slice: Canon Medical Systems, Tochigi, Japan) with conditions of 120kV, 300mA, and a slice thickness of 0.5mm. Quantitative evaluation was performed using artifact reduction software SEMAR (Single Energy Metal Artifact Reduction) and dual-energy (80 keV, 135 keV) CT images (virtual monochromatic X-ray images).

**Results:** For all ROIs, AI scores were lowest in the order SEMAR+Dual-energy < SEMAR < Dual-energy CT images.

**Conclusions:** SEMAR and dual-energy CT are expected to reduce artifacts and thereby increase the range of structures that can be reliably evaluated, even in the presence of artifacts generated by gold–silver–palladium alloys. However, when crown restorations are located in close proximity to the lesion, diagnostic assessment remains challenging. Therefore, from the perspective of long-term follow-up, replacing metallic crown restorations with non-metallic alternatives may be a reasonable option.

## EP-172

## Ghost and pseudo-ghost images in panoramic radiography

**Yo-Seob Seo**<sup>1\*</sup>, Jong-Won Kim<sup>1</sup>

<sup>1</sup>Department of Oral and Maxillofacial Radiology, Chosun University, Korea

**Introduction:** This study describes an unusual case in which real, ghost, and pseudo-ghost images simultaneously appeared on a panoramic radiograph of a patient wearing earrings, and explains the imaging mechanism behind this triple-image formation.

**Materials and Methods:** A panoramic radiograph acquired with Planmeca ProMax showed one real image and two ghost-related images for each earring. Panoramic geometry—including the path of the center of rotation—was analyzed, and pseudo-ghost and ghost images were reproduced using a dry mandible with a radiopaque marker.

**Results:** The extended center-of-rotation path of the ProMax allowed structures outside the jaw to generate a triple pattern of real, pseudo-ghost, and ghost images. The pseudo-ghost image represented a real (double) image projected to the contralateral side, thereby mimicking the appearance of a ghost image.

**Conclusions:** A clear understanding of panoramic geometry is essential for recognizing atypical images, and because the pseudo-ghost image is a real (double) image that appears ghost-like due to imaging geometry, we support adopting the term “pseudo-ghost image” for this ghost-like real image.

EP-174

## Comparative analysis of clinical image evaluation charts for panoramic radiography

**Yeonhee Kim**<sup>1</sup>, Samsun Lee<sup>1</sup>, Gyudong Jo<sup>1</sup>, Ahyoung Kwon<sup>1</sup>, Ju-Hee Kang<sup>1</sup>, Jo-Eun Kim<sup>1</sup>, Kyunghoe Huh<sup>1</sup>, Won-Jin Yi<sup>1</sup>, Min-Suk Heo<sup>1</sup>, Soonchul Choi<sup>1</sup>

<sup>1</sup>Department of Oral and Maxillofacial Radiology and Dental Research Institute, School of Dentistry, Seoul National University, Seoul, South Korea

**Introduction:** To compare and analyze professional (P chart) and simple (S chart) clinical image evaluation charts for evaluating panoramic radiograph image quality.

**Materials and Methods:** Ten evaluators assessed 285 clinical panoramic radiograph images. The evaluators were divided into oral and maxillofacial radiologists (OMFR, n=5) and general dentist (dentists not specializing in oral and maxillofacial radiology, G, n=5) groups. For image evaluation, P and S charts provided by the Korean Academy of Oral and Maxillofacial Radiology were used. Scores of items for each evaluation chart were used to compare the reliability, correlation, evaluation scores, evaluation time, and preference, and statistical analyses were performed using IBM SPSS Statistics.

**Results:** The S chart showed similar levels of evaluation scores at shorter evaluation time, as compared to the P chart. In the results for each evaluation chart, all analyzed correlations were statistically significant. Total score, image density/contrast/sharpness, and overall image quality items showed a very high positive correlation in the P chart. While the overall range of correlation coefficients was relatively lower in the S chart than the P chart, the same items showed high correlation coefficients. In the preference evaluation, both the professional and generalist groups preferred the S chart.

**Conclusions:** A comparative analysis with the P chart, revisions, and upgrades are needed for the S chart items that showed low correlations in this study, such as artifacts, coverage area, and patient movement.

EP-175

## Order-aware hierarchical deep learning for automatic prediction of Fishman's skeletal maturity indicators from hand-wrist radiographs

**Jangyo Bae**<sup>1\*</sup>

<sup>1</sup>Department of Oral and Maxillofacial Radiology, Seoul National University School of Dentistry, Republic of Korea

**Introduction:** This study aims to develop an artificial intelligence model for automatic prediction of Fishman's Skeletal Maturity Indicators (SMI) from hand-wrist radiographs and to evaluate a hierarchical analysis framework that incorporates the clinical observation sequence of SMI into the model architecture.

**Materials and Methods:** Hand-wrist radiographs of pediatric and adolescent patients will be retrospectively collected from a single institution and labeled according to the Fishman method. The proposed model will include a hierarchical ROI module, an order-aware feature fusion module, and a multi-stage classifier. Performance will be evaluated using accuracy, macro-F1 score, and Cohen's kappa.

**Results:** The proposed order-aware hierarchical model is expected to show improved overall classification performance compared with baseline models, particularly with reduced misclassification between adjacent SMI stages. Ablation analysis will assess the contribution of observation order constraints and stage-wise ROI-based feature integration.

**Conclusions:** A hierarchical AI model reflecting the observation sequence of Fishman SMI is expected to improve both predictive performance and interpretability in hand-wrist radiograph analysis. This framework may enhance clinical applicability and be extended to other imaging-based staging tasks with predefined observation rules.

## EP-188

## Ewing sarcoma of temporomandibular joint: A rare but important differential diagnosis

**Yu-Ri Kim**<sup>1\*</sup>, Jo-Eun Kim<sup>1</sup>

<sup>1</sup>Department of Oral and Maxillofacial Radiology, School of Dentistry and Dental Research Institute, Seoul National University, Korea

**Introduction:** Ewing sarcoma (ES) is the second most common primary bone malignancy in children and adolescents, accounting for 4-7% of all primary bone sarcomas. It typically arises in the diaphysis of long bones (femur, tibia, humerus) or pelvis, characterized by small round cell morphology. While gnathic involvement occurs in ~6% of cases (mandible > maxilla), temporomandibular joint (TMJ) condyle-specific presentation remains exceptionally rare, with only isolated case reports in the literature. Aggressive TMJ masses demand prompt radiologic evaluation to differentiate benign from malignant entities, guide biopsy, and inform multidisciplinary management

**Case:** A 57-year-old woman presented with long-standing unilateral temporomandibular joint pain that gradually progressed to facial swelling. Radiologic evaluation demonstrated an aggressive osteolytic lesion of the mandibular condyle with adjacent soft tissue extension. On contrast-enhanced imaging, the lesion demonstrated heterogeneous enhancement, and PET/CT revealed mild hypermetabolic activity. Surgical excision was performed, and histopathologic and immunohistochemical findings confirmed ES. Adjuvant radiotherapy was subsequently administered.

**Discussion:** Mandibular ES is uncommon (maxilla:mandible ~1:2), and condyle-specific TMJ involvement exceptionally rare, with long latency, highlighting an indolent early phase before aggressive growth. On CT imaging, ES typically demonstrates permeative or moth-eaten osteolytic destruction with cortical breakthrough, and periosteal bone formation may occasionally be present. The associated extraosseous soft-tissue mass can show heterogeneous enhancement after contrast administration. Differential diagnoses include other sarcomas such as osteosarcoma and chon-

drosarcoma, as well as synovial chondromatosis, which can cause bone destruction in the temporomandibular joint region. In addition, secondary infection of a synovial cyst or ganglion cyst may produce ill-defined osteolysis that mimics a malignant tumor and should be considered in the differential diagnosis.

## EP-189

## Imaging-driven diagnosis of oral squamous cell carcinoma: A case report highlighting cross-sectional modalities

**Irnawati Ilham**<sup>1\*</sup>, Barunawaty Yunus<sup>1,2</sup>

<sup>1</sup>Dentomaxillofacial Radiology Specialist Study Program, Faculty of Dentistry Hasanuddin University, Indonesia

<sup>2</sup>Departement Of Oral And Maxillofacial Radiology, Faculty Of Dentistry, Hasanuddin University, Makassar, Indonesia

**Introduction:** Oral squamous cell carcinoma (SCC) is an aggressive oral malignancy with a high potential for local invasion and significant morbidity if not detected early. Conventional panoramic radiography offers an initial overview of osseous involvement, while computed tomography (CT) provides superior delineation of cortical erosion, medullary invasion, and lesion extent. This case report aims to demonstrate the complementary diagnostic value of panoramic radiography and CT imaging in accurately identifying and characterizing oral SCC.

**Case:** A 45-years old male patient presented with a five-year history of a progressively enlarging, painful mass on the right posterior oral, accompanied by a newly developed left cervical swelling over the past two months. Clinical palpation revealed a 4 × 3 cm indurated, poorly defined, and fixed submucosal mass with marked tenderness. Panoramic radiography showed no detectable abnormality; however, CT revealed a relatively well-defined, irregular-margined isodense mass measuring approximately 5.62 × 4.38 × 3.57 cm in the right lingual region causing oropharyngeal narrowing, along with multiple enlarged cervical lymph nodes at levels IB, bilateral IIA, and left level III (largest ~0.96 cm). Histopathological examination following biopsy confirmed lingual squamous cell carcinoma with regional lymphadenopathy.

**Discussion:** Oral squamous cell carcinoma often progresses submucosally, delaying clinical detection, as reflected in this case where no visible lesion was observed despite a firm, fixed, and painful deep-seated mass. The normal panoramic radiograph underscores the limited ability of conventional imaging to identify early soft-tissue pathology or subtle cortical disruption. Conversely, CT provided clear visualization of an isodense, irregular mass causing oropharyngeal narrowing and revealed multiple enlarged cervical lymph nodes, offering critical information for accurate staging and treatment planning. These findings reinforce the diagnostic superiority of CT over panoramic radiography in evaluating suspected oral malignancies.

#### EP-190

### Serial radiographic observations of recurrent ameloblastoma post-surgical treatment: A case report

**Husnul Hatimah**<sup>1\*</sup>, Barunawaty Yunus<sup>1,2</sup>

<sup>1</sup>Dentomaxillofacial Radiology Specialist Study Program, Faculty of Dentistry Hasanuddin University, Indonesia

<sup>2</sup>Departement Of Oral And Maxillofacial Radiology, Faculty Of Dentistry, Hasanuddin University, Makassar, Indonesia

**Introduction:** Ameloblastoma is a benign but locally aggressive odontogenic tumor, characterized by slow growth, significant bone destruction, and a high risk of recurrence. Recurrent cases pose a particular challenge for clinicians due to the potential for more extensive tissue involvement and the need for careful long-term monitoring. This case highlights the importance of multimodal radiographic follow-up in the management of recurrent ameloblastoma, demonstrating how different imaging techniques can complement each other to ensure optimal long-term outcomes.

**Case:** A 19-years old male patient presented seven months after stage I curettage under general anesthesia with a red gingival tissue at the previous surgical site, without pain. Biopsy was confirmed ameloblastoma, and subsequent stage I curettage revealed plexiform ameloblastoma. There was no relevant family or systemic history. On examination, the patient was stable; the surgical site showed erythema without tenderness, and oral hygiene was moderate.

**Discussion:** Serial imaging using orthopantomography, and computed tomography (CT) was performed to monitor bone healing and detect recurrence. Multimodal imaging allowed comprehensive evaluation of the surgical site, assessment of residual lesion, and early identification of recurrent tumor. Over the follow-up period, imaging provided essential information for planning further management. This case highlights the importance of serial and multimodal radiographic follow-up in recurrent ameloblastoma to ensure timely detection and optimize long-term outcomes.

#### EP-191

### Multifocal periapical pathoses with significant cortical destruction: Radiographic evaluation of concomitant inflammatory lesion and radicular cyst – A case report

**Yuntrisnawaty Sartika Kasim**<sup>1\*</sup>, Barunawaty Yunus<sup>1,2</sup>

<sup>1</sup>Dentomaxillofacial Radiology Specialist Study Program, Faculty of Dentistry Hasanuddin University, Indonesia

<sup>2</sup>Departement Of Oral And Maxillofacial Radiology, Faculty Of Dentistry, Hasanuddin University, Makassar, Indonesia

**Introduction:** Multifocal periapical pathoses with extensive cortical destruction present significant diagnostic challenges, particularly when inflammatory lesions coexist with a radicular cyst. While panoramic radiography offers an initial broad overview, its two-dimensional limitations may hinder accurate characterization compared to the superior three-dimensional assessment provided by CBCT. This case report aims to highlight the comparative diagnostic value of panoramic radiography and CBCT in evaluating concomitant periapical inflammatory lesions and radicular cysts.

**Case:** A 47-year-old male patient was referred to the oral and maxillofacial surgery clinic with an eight-month history of swelling on the palatal region of the anterior maxilla. The patient reported a previously restored upper anterior tooth, followed by recurrent palatal swelling that prompted multiple visits, including an emergency open access procedure and symptomatic medication. Clinical and radiographic examination re-

vealed multifocal osteolytic lesions in the anterior maxilla: a well-defined periapical radiolucency involving teeth 21–23 centered on tooth 22, suggestive of a radicular cyst, and an additional lesion involving teeth 11–13 centered on tooth 12 consistent with chronic apical abscess; bilateral maxillary sinus mucosal thickening was also observed.

**Discussion:** This case demonstrates how multifocal periapical pathoses with extensive cortical involvement can be underestimated when assessed solely with panoramic radiography, which provides limited information on lesion boundaries and three-dimensional progression. The CBCT evaluation offered superior delineation of both lesions, revealing cortical thinning, possible perforation, and their relationship to adjacent structures, including the maxillary sinus, thereby clarifying the distinction between an inflammatory periapical lesion and a suspected radicular cyst. The combined radiographic interpretation strengthened diagnostic confidence and guided appropriate referral for surgical management, underscoring the essential role of CBCT in complex multifocal presentations.

#### EP-192

### Age estimation using radiographic pulp-tooth width ratio of permanent maxillary incisors in Thai population

**Matchima Phetsuit**<sup>1,2\*</sup>, Sunpatch Benjavongkulchai<sup>1</sup>, Pisha Pittayapat<sup>1</sup>

<sup>1</sup>Department of Radiology, Faculty of Dentistry, Chulalongkorn University, Bangkok, Thailand.

<sup>2</sup>School of Dentistry, Mae Fah Luang University, Chiangrai, Thailand.

**Introduction:** Dental radiographs are widely used for age estimation, but existing methods show limited accuracy across populations and age groups, particularly among Thai adults. This study aimed to develop a simple and accurate age estimation method for the Thai population using pulp-tooth width ratio at the cemento-enamel junction of permanent maxillary central and lateral incisors, applicable from 10 years of age.

**Materials and Methods:** A total of 400 digital peri-

apical radiographs of maxillary central and lateral incisors were collected from the Radiology Clinic, Faculty of Dentistry, Chulalongkorn University, Bangkok, Thailand. Pulp and tooth width at the cemento-enamel junction were measured to calculate pulp-tooth ratios. Correlation and regression analyses were performed to develop age estimation equations.

**Results:** The mean pulp-tooth width ratio of maxillary central and lateral incisors demonstrated the strongest relationship with chronological age ( $R^2 > 0.6$ ). This relationship remained consistent when analyzed by sex, with no significant differences observed between males and females. Regression analysis confirmed that the mean ratio was a significant predictor of age. Independent group validation revealed acceptable but limited predictive accuracy for children and adolescents, highlighting age-dependent variability in estimation accuracy.

**Conclusions:** The findings confirmed that pulp-tooth width ratio measurements, particularly the mean ratio, were strongly associated with chronological age and have potential value for age estimation. However, prediction accuracy was constrained by biological variability, especially in younger age groups and in cases with atypical pulp morphology. Thus, the application for these age groups remained limited. Future studies should consider stricter selection criteria and age-specific modeling to improve accuracy and reliability.

#### EP-193

### Diagnostic value of panoramic radiography and computed tomography in mandibular ameloblastoma: A case report

**Fahriah Tuasamu**<sup>1\*</sup>, Dwi Putri Wulansari<sup>1,2</sup>

<sup>1</sup>Dentomaxillofacial Radiology Specialist Study Program, Faculty of Dentistry Hasanuddin University, Indonesia

<sup>2</sup>Departement Of Oral And Maxillofacial Radiology, Faculty Of Dentistry, Hasanuddin University, Makassar, Indonesia

**Introduction:** Ameloblastoma is a benign odontogenic tumor commonly found in the mandible. This tumor is often asymptomatic in its early stages, but can cause significant symptoms with extensive growth or soft

tissue invasion. In addition to panoramic imaging, diagnosis requires a multimodal approach including Computed Tomography (CT) are crucial for accurate assessment. This case report discusses the role of computed tomography in diagnosis of ameloblastoma.

**Case:** A 60-year-old female presenting with a seven-months swelling in the left posterior mandible. Extraoral examination revealed asymmetrical face with enlargement of the lower jaw, sinistra and mentale measuring  $14 \times 6 \times 4.5$  cm. Intraoral findings showed an enlargement in the vestibular region of teeth 38-43 measuring  $4 \times 6 \times 2.5$  cm. Panoramic radiography revealed a multilocular radiolucent lesion with root resorption of mandibular teeth. CT scan displayed an extensive lytic lesion with cortical destruction and pressure on surrounding soft tissues.

**Discussion:** Ameloblastoma necessitates a combination of imaging techniques, such as CT, to evaluate growth patterns, tissue invasion, and determine the optimal surgical approach. CT provides high-resolution details essential for accurate diagnosis and evidence-based treatment. This case study highlights the importance of advanced imaging modalities, particularly CT, in diagnosing and managing ameloblastoma. An integrated approach improves diagnostic accuracy, supports treatment planning, and reduces recurrence rates.

#### EP-194

### Inter-observer reliability in the assessment of geniohyoid muscle using the ultrasound image: A comparative study by age group

Yuuri Oku<sup>1\*</sup>, Hideki Suito<sup>1</sup>, Yoshihiro Tagami<sup>2</sup>, Keiko Fujimoto<sup>2</sup>, Tomoyuki Kondo<sup>1</sup>, Naoki Maeda<sup>1</sup>, Kan Nagao<sup>2</sup>

<sup>1</sup>Department of Oral & Maxillofacial Radiology, University of Tokushima, Japan

<sup>2</sup>Department of Prosthodontics & Oral Rehabilitation, University of Tokushima, Japan

**Introduction:** Ultrasound imaging is widely used in research into swallowing function, as it enables the muscle groups involved in swallowing, such as the ge-

niohyoid muscle group, to be assessed morphologically without the need for invasive procedures. However, the impact of subject age on the reliability of cross-sectional area (CSA) measurements remains to be verified. This study aimed to examine the inter-observer reliability of geniohyoid muscle CSA assessment using ultrasound across different age groups.

**Materials and Methods:** Eighty healthy participants were equally divided into four groups (n = 20) according to age: young adults, middle-aged adults, early elderly, and late elderly (75 years and over). A single examiner acquired a still ultrasound image of the geniohyoid muscle at rest. Subsequently, two independent evaluators measured CSA using ImageJ software. The intraclass correlation coefficient (ICC [2,1]) was used to assess inter-observer reliability for the entire cohort and for each age group individually.

**Results:** The overall ICC for CSA across the entire cohort (n = 80) was 0.87 (95% CI: 0.68–0.94), demonstrating high reliability. Age-specific ICCs were: 0.87 (young adults), 0.82 (middle-aged adults), 0.90 (early elderly) and 0.80 (late elderly). Notably, the 95% confidence interval for the late elderly group had a lower minimum limit than the other groups.

**Conclusions:** This study found high overall reliability of geniohyoid muscle CSA assessment using ultrasound imaging. However, the reduced reliability observed in the late elderly population poses a practical challenge. This may be due to age-related sarcopenia and fatty infiltration, which make accurate delineation of fascial borders difficult. Ensuring robust and reproducible data, standardization of measurement protocols, and rigorous training are paramount, particularly when assessing muscle morphology in the elderly population.

#### EP-196

### Rectified Flow framework for synthetic contrast-enhanced CT generation in the head and neck

Ki-Min Jung<sup>1\*</sup>, Sungho Oh<sup>2\*</sup>, Won-Jin Yi<sup>1</sup>

<sup>1</sup>Oral and Maxillofacial Radiology and Dental Research Institute, School of Dentistry, Seoul National University, Republic of

Korea

<sup>2</sup>*Interdisciplinary Program in Bioengineering, Graduate School of Engineering, Seoul National University, Republic of Korea*

**Introduction:** Contrast-enhanced CT (CECT) plays a critical role in the evaluation of head and neck diseases; however, its use is limited in patients with contraindications to iodinated contrast agents. Recent advances in deep learning have enabled the synthesis of contrast-enhanced images from non-contrast CT (NCT), yet existing studies have largely focused on limited anatomical regions. The few studies addressing the head and neck region have primarily relied on task-specific generative models, with limited exploration of leveraging representations derived from foundation models. This study aims to develop and evaluate a deep learning-based model for generating synthetic CECT images from virtual non-contrast CT (VNC) in the head and neck region.

**Materials and Methods:** A conditional rectified flow-based generative model was trained using paired VNC and CECT images. The VNC image itself was used as the conditioning input to the rectified flow framework. The proposed model was designed to preserve anatomical structures while enhancing soft-tissue contrast. Quantitative image similarity metrics and qualitative visual assessments were conducted to evaluate the generated synthetic images.

**Results:** The proposed model generated synthetic contrast-enhanced CT images that suggested improved soft-tissue contrast and structural continuity compared with input non-contrast images. Preliminary quantitative evaluations indicated favorable image similarity metrics, while qualitative visual assessment suggested preservation of clinically relevant anatomical details.

**Conclusions:** AI-generated synthetic CECT images from NCT may serve as a promising alternative for patients in whom contrast administration is contraindicated. Further validation with larger datasets and clinical evaluation is warranted to assess diagnostic utility.

**Funding:** This work was supported by the National Research Foundation of Korea (NRF) grant funded by the Korean government (MSIT) (No. 2023R1A2C2 00532611). This work was also supported by the Technology Innovation Program (or Industrial Strategic

Technology Development Program-Advanced Biomaterials) (RS-2025-14322975), funded by the Ministry of Trade, Industry & Energy (MOTIE).

EP-205

## Identification of internal root resorption in maxillary incisors with cone-beam computerized tomography: A case report

**Sheng-Yao Lai**<sup>1\*</sup>, Cheng-Han Wu<sup>1</sup>, Ming-Gen Tu<sup>1,2</sup>

<sup>1</sup>*Department of Dentistry, China Medical University Hospital, Taichung, Taiwan*

<sup>2</sup>*School of Dentistry, China Medical University, Taichung, Taiwan*

**Introduction:** Root resorption is a particular pulpal disease following different types of injuries, including chemical, mechanical or thermal injury. Furthermore, it can be classified as internal or external root resorption. Internal root resorption (IRR), is a rare condition that resulting in dystrophy of the pulp with destruction of the hard tissues. Majority of the cases remain asymptomatic and are often incidentally detected during radiographic evaluation. Once detected, it should be treated as soon as possible to limit its progression. Dealing with internal and external root resorption cases, Cone-beam computerized tomography (CBCT) images and Mineral Trioxide Aggregate (MTA) are mandatory for treatment. The case report is applied with the new technology and material for endodontic re-treatment.

**Case:** The 24-year-old male complaint of gum boil over upper anterior gingiva for about 2 months. Tooth 12 and Tooth 11 were diagnosed with previously treated teeth with periapical pathosis, Tooth 21 diagnosed with internal root resorption (IRR). CBCT was taken for evaluating the 3D extension of the IRR of tooth 21. The CBCT images revealed that a volume of 5.41 (bucco-lingually) x 5.46 (mesio-distally) x 5.24 mm (inciso-apically) resorption of this root canal. The treatment plan was retreatment of the three incisors. After thoroughly cleaning and shaping, all the three teeth were obturated with MTA, backfilled with warm Gutta-Percha, followed by restoration. Upon 3 months follow-up, the patient shows no symptoms and signs,

and radiographic image revealed periapical healing in progress.

**Discussion:** CBCT can clearly display external and internal resorption, identify the scope and degree of resorption three-dimensionally, help to determine treatment plan for root resorption. CBCT has great advantage over conventional radiography in the diagnosis and treatment of endodontic problems. MTA is an excellent filling material for root resorption cases.

#### EP-211

### Unlocking the secrets of impacted teeth: Accurate analysis with segmented 3D-CBCT on maxillary incisors – case studies

**Rezky Amalia<sup>1\*</sup>**, Barunawaty Yunus<sup>2</sup>

<sup>1</sup>Dentomaxillofacial Radiology Study Program, Faculty of Dentistry, Hasanuddin University, Makassar, Indonesia

<sup>2</sup>Department of Oral and Maxillofacial Radiology, Faculty of Dentistry, Hasanuddin University, Makassar, Indonesia

**Introduction:** Maxillary central incisors account for approximately 31.8% of all cases of impacted permanent teeth, predominantly observed in orthodontic patients during the mixed dentition stage, typically between the ages of 7 and 9 years or older. The segmentation of teeth from CBCT images is a critical step in computer-aided systems for orthodontic treatment.

**Case:** This case series examines four instances of impacted maxillary incisors in patients ranging from 14 to 38 years of age. The first case involves a 24-year-old female with tooth 21 positioned semi-vertically and leaning labially, overlapping with tooth 22, with its root exerting pressure on the floor of the nasal cavity. The second case concerns a 29-year-old female with an unerupted upper left central incisor in an inverted position, exhibiting extreme root-crown dilaceration resembling a whale-like shape. The third case describes a 16-year-old male with four impacted anterior teeth (11, 13, 21, 23), each displaying distinct impaction patterns. The fourth case pertains to an 11-year-old male with an unerupted upper right central incisor that is vertically impacted and associated with

a suspected compound odontoma.

**Discussion:** The segmentation of teeth in cone-beam computed tomography (CBCT) imaging played a crucial role in the diagnosis and treatment planning of these cases. It enabled detailed visualization of root angulation, tooth-to-structure distances, bone thickness, and crown and root morphology, thereby facilitating precise surgical and orthodontic interventions.

#### EP-212

### Fractal dimension analysis of panoramic radiographs for radiographic healing assessment of odontogenic keratocyst: A case report

**Uce Ayuandyka M<sup>1\*</sup>**, Barunawaty Yunus<sup>2</sup>

<sup>1</sup>Dentomaxillofacial Radiology Study Program, Faculty of Dentistry, Hasanuddin University, Makassar, Indonesia

<sup>2</sup>Department of Oral and Maxillofacial Radiology, Faculty of Dentistry, Hasanuddin University, Makassar, Indonesia

**Introduction:** Odontogenic keratocysts (OKCs) constitute approximately 11% of mandibular cysts, predominantly affecting the posterior body, angle, and ramus of the mandible. Panoramic radiography is extensively utilized for post-treatment evaluation and facilitates the assessment of trabecular bone quality through fractal dimension (FD) analysis. This case report presents an odontogenic keratocyst and examines post-treatment bone healing using FD analysis on panoramic radiographs.

**Case:** An 18-year-old male presented with a persistent swelling in the lower left cheek region, which had been evident for approximately two years. An extra-oral examination revealed facial asymmetry and tenderness, while an intraoral examination indicated an enlargement of the left buccal region characterized by a hard consistency, unerupted teeth 36, 37, and 38, and moderate oral hygiene. Radiographic analysis demonstrated a well-defined, irregular multilocular radiolucent lesion with a distinctive soap-bubble appearance. Histopathological examination confirmed the diagnosis of an odontogenic keratocyst. The lesion was managed using the dredging method, a conservative surgi-

cal approach. Six months post-treatment, follow-up panoramic radiographs showed reduced radiolucency, increased trabecular bone complexity, and an elevated FD value within the lesion area.

**Discussion:** Odontogenic keratocysts are typically characterized by well-defined radiolucent lesions with sclerotic, smooth, or scalloped margins, and they may present as either unilocular or multilocular lesions. Radiographic evaluation is crucial in the postoperative follow-up process. FD analysis offers quantitative insights into changes in trabecular bone architecture, where elevated FD values signify increased structural complexity and denser trabecular patterns. In this particular case, radiographic findings indicated a reduction in radiolucency and an increase in FD values, which are indicative of progressive bone healing. This observation aligns with the findings reported by Çolak et al. (2023), who noted that FD values typically decrease immediately following surgery and gradually increase during the bone healing process.

#### EP-214

### Material decomposition between gold nanoparticles and iodine using clinical dual-energy CT

**Hiroaki Shimamoto**<sup>1,2\*</sup>, Seiko Ichinose<sup>3</sup>, Hiroki Kato<sup>2</sup>, Yuichiro Kadonaga<sup>2</sup>, Kosei Ueshima<sup>1</sup>, Akie Katsuki<sup>2,4</sup>, Shotaro Fuchibe<sup>2,4</sup>, Nozomu Uetake<sup>2,4</sup>, Masaya Kawasaki<sup>1</sup>, Shumei Murakami<sup>1,2</sup>

<sup>1</sup>Department of Oral and Maxillofacial Radiology, Graduate School of Dentistry, The University of Osaka, Japan

<sup>2</sup>Institute for Radiation Sciences, The University of Osaka, Japan

<sup>3</sup>Department of Radiology, The University of Osaka Dental Hospital, Japan

<sup>4</sup>Science and Technology Organization, GE HealthCare, Japan

**Introduction:** Gold nanoparticles (AuNPs) are attracting attention as sensitizers in radiotherapy. With future human application in mind, AuNPs should be clearly distinguishable from iodine on contrast-enhanced CT images. The aim of this study was to distinguish AuNPs from iodine using clinical dual-energy CT (DECT).

**Materials and Methods:** The 5 nm diameter spherical

AuNPs were diluted with distilled water into a solution of 0.9, 7.2, 11.0, and 13.0 mM concentration. Iodine was diluted into 3.0, 20.0, 25.0, and 35.0 mM to match the CT values for each concentration of AuNPs. Each sample was in a microtube and fixed concentrically in a cylindrical water-bath phantom with a 20 cm diameter. The DECT scans were acquired 10 times using Revolution Frontier (GE HealthCare, Chicago, IL). The imaging conditions were as follows: tube voltage of 80 and 140 kV via fast switching, tube current of 260 or 600 mA, slice thickness of 2.5 or 5.0 mm, matrix size of 512 x 512, and FOV of 15 cm. The 5 mm circular ROIs were drawn manually at the axial images of AuNPs and iodine samples. The material decomposition of Au and iodine was performed using GSI Viewer (GE HealthCare, Chicago, IL).

**Results:** In the clinical setting of 260 mA, 13.0 mM AuNPs/35.0 mM iodine, 11.0 mM AuNPs/25.0 mM iodine, and 7.2 mM AuNPs/20.0 mM iodine groups were clearly separated and quantified each independently by effective atomic number despite exhibiting similar CT values. Furthermore, 0.9 mM AuNPs/3.0 mM iodine group was also clearly separated and quantified each independently under imaging conditions of 600 mA, thickness of 5.0 mm.

**Conclusions:** DECT could distinguish AuNPs from iodine in a concentration-dependent and imaging condition-dependent manner.

#### EP-215

### Atypical radiographic bone destruction in oral squamous papilloma: Diagnostic implications

**Purnamasari Syahbani Massalinri**<sup>1\*</sup>, Barunawaty Yunus<sup>1,2</sup>

<sup>1</sup>Dentomaxillofacial Radiology Specialist Study Program, Faculty of Dentistry Hasanuddin University, Indonesia

<sup>2</sup>Department of Oral and Maxillofacial Radiology, Faculty of Dentistry, Hasanuddin University, Makassar, Indonesia

**Introduction:** Oral squamous papilloma is a common benign epithelial lesion, typically presenting as an exophytic soft tissue growth without bone involvement. Radiographic bone destruction associated with this lesion is exceedingly rare and may lead to diag-

nostic challenges, as it can mimic aggressive or malignant conditions. This case report describes an atypical presentation of oral squamous papilloma accompanied by radiographic alveolar bone destruction.

**Case:** A 74-year-old female presented with a progressive gingival mass extending to the right buccal region, first noticed approximately six months prior. Extraoral examination revealed facial asymmetry with right buccal swelling measuring approximately  $2 \times 1.5 \times 0.5$  cm and  $2 \times 1 \times 0.5$  cm, tenderness on palpation, the presence of an orocutaneous fistula, and purulent. Intraoral examination revealed a large pedunculated, soft, erythematous mass measuring approximately  $12 \times 6 \times 2$  cm was observed on the gingiva extending from teeth 43 to 48 into the right buccal mucosa, with tenderness and easy bleeding. Panoramic radiographic examination demonstrated a radiointermediate lesion associated with irregular and sharp alveolar bone destruction in the right posterior mandible, extending to the mandibular ramus, suggesting an aggressive process. Previous fine-needle aspiration biopsy suggested a benign epithelial tumor, while an incisional biopsy histopathologic confirmed the diagnosis of squamous papilloma.

**Discussion:** This case highlights a rare and atypical radiographic presentation of oral squamous papilloma with associated alveolar bone destruction. Such findings may complicate the diagnostic process and lead to misinterpretation as malignant or aggressive jaw lesions. Careful correlation of radiographic features with histopathological examination is essential to establish an accurate diagnosis and to avoid overtreatment. This report emphasizes the importance of recognizing unusual radiographic patterns in otherwise benign oral epithelial lesions.

EP-216

## A rare basal cell adenoma of the maxillary sinus mimicking a mucocele: Radiographic characteristics in a case report

**Nayla Yuliyanti Pawa**<sup>1\*</sup>, Dwi Putri Wulansari

<sup>1</sup>*Dentomaxillofacial Radiology Specialist Study Program, Faculty of Dentistry Hasanuddin University, Indonesia*

<sup>2</sup>*Department of Oral and Maxillofacial Radiology, Faculty of Dentistry, Hasanuddin University, Makassar, Indonesia*

**Introduction:** Basal cell adenoma (BCA) is a rare benign salivary gland neoplasm, most commonly arising in the parotid gland. Involvement of minor salivary glands, particularly within the maxillary sinus, is extremely uncommon. Clinically and radiographically, BCA may mimic other more frequent sinonasal lesions such as mucoceles, posing diagnostic challenges. Radiographic imaging plays a crucial role in assessing lesion extent, bony involvement, and differential diagnosis. This case report describes the clinical and radiographic characteristics of a rare maxillary sinus basal cell adenoma with a mucocele-like presentation.

**Case:** A 56-year-old woman presented with a progressively enlarging mass in the left posterior maxillary palate. Extraoral examination revealed facial asymmetry with swelling in the left buccal and infraorbital regions measuring approximately  $5 \times 6 \times 3$  cm. Intraoral examination showed a well-defined mass involving the left hard and soft palate measuring approximately  $4 \times 2.5 \times 1.5$  cm. Panoramic radiography demonstrated a radiointermediate lesion occupying the left maxillary sinus, with destruction of the maxillary alveolar bone and medial displacement of the lateral nasal wall, resulting in bowing of the nasal septum. Computed tomography revealed a destructive mass in the left maxillary region infiltrating the maxillary sinus and left nasal cavity. Fine-needle aspiration biopsy initially suggested pleomorphic adenoma; however, histopathological examination confirmed the diagnosis of basal cell adenoma of salivary gland origin.

**Discussion:** Radiographically, basal cell adenoma of the maxillary sinus demonstrates nonspecific features and may closely mimic other expansile sinonasal lesions, particularly mucoceles. In this case, panoramic radiography and computed tomography revealed a radiointermediate mass with bone destruction, smooth expansion, and displacement of adjacent structures, suggesting a slow-growing lesion with significant mass effect rather than aggressive invasion. Cross-sectional imaging is essential to evaluate lesion extent and osseous involvement; however, definitive diagnosis requires histopathological confirmation.

EP-218

## Imaging features of chronic recurrent osteomyelitis involving the jaw

**Chena Lee**<sup>1\*</sup>

<sup>1</sup>Department of Oral and Maxillofacial Radiology, Yonsei University College of Dentistry, Republic of Korea

**Introduction:** Chronic recurrent osteomyelitis of the jaw (CRMO) is a rare, non-infectious inflammatory bone disease characterized by recurrent episodes and an unclear etiology. Its clinical and radiologic presentations often resemble those of conventional osteomyelitis caused by odontogenic infection, making accurate diagnosis difficult. As inappropriate diagnosis may result in unnecessary surgical or antibiotic treatment, identification of characteristic imaging features is crucial. This study aimed to describe the distinctive imaging findings of CRMO of the jaw and to propose radiologic clues useful for differential diagnosis and appropriate treatment planning.

**Case:** This study reviewed five patients with clinical diagnosis of CRMO. Electronic clinical records and diagnostic imaging, including panoramic radiographs and computed tomography, were reviewed. Imaging findings were descriptively evaluated with respect to lesion location, bone involvement patterns, and multifocal skeletal manifestations. The included patients were aged 18 to 23 years and 3 females and 2 males. None of the patients showed evidence of an initiating odontogenic infection. Lesions were predominantly located in the basal bone of the maxillofacial skeleton rather than the alveolar bone. Three patients showed multifocal lesion and 2 patients showed single lesion of mandible.

**Discussion:** CRMO demonstrated broad sclerotic changes, permeative bone destruction, and osteolytic lesions mainly centered on the cortical bone, contrasting with the medullary involvement typical of odontogenic osteomyelitis. Multifocal involvement in other skeletal sites was also observed, supporting the systemic nature of CRMO. These imaging characteristics are valuable for improving diagnostic accuracy. Given the recurrent course and potential for multi-site involvement, careful treatment planning with long-term

follow-up is essential.

EP-220

## Radiographic spectrum of odontomas: A comparative report of two pediatric cases

**Kornkamol Kretapirom**<sup>1\*</sup>, Jira Kitisubkanchana<sup>1</sup>, Theerachai Kosanwat<sup>2</sup>, Jirakit Pramuanpornsatid<sup>2</sup>, Kiatanant Boonsiriseth<sup>3</sup>, Sukkarn Themkumkwun<sup>3</sup>

<sup>1</sup>Department of Oral and Maxillofacial Radiology, Mahidol University, Thailand

<sup>2</sup>Department of Oral and Maxillofacial Pathology, Mahidol University, Thailand

<sup>3</sup>Department of Oral and Maxillofacial Surgery, Mahidol University, Thailand

**Introduction:** Developing odontoma is an uncommon mixed odontogenic tumor that predominantly occurs in pediatric patients and may exhibit a broad spectrum of radiographic appearances. This report describes two pediatric cases with contrasting radiographic features to highlight the importance of imaging interpretation in diagnosis and treatment planning.

**Case:** Two male pediatric patients with suspected developing odontomas as the first differential diagnosis are presented. Panoramic radiography and cone-beam computed tomography (CBCT) were evaluated.

The first case involved a 7-year-old boy with delayed eruption of the mandibular left first molar without associated pain or swelling. Imaging demonstrated a well-defined unilocular radiolucent lesion with limited internal calcifications, overlying the crown of tooth 36, accompanied by inferior displacement of the tooth and the inferior alveolar canal, without bucco-lingual expansion. Histopathological examination was consistent with developing odontoma.

The second case involved a 9-year-old boy presenting with swelling in the left posterior mandible. Imaging revealed a well-defined unilocular radiolucent lesion extending from the region of tooth 75 to tooth 38. Multiple small tooth-like structures were identified within the lesion, overlying the crown of tooth 36, with inferior displacement of the tooth bud 35 and the inferior alveolar canal. Bucco-lingual expansion with cortical thinning was also observed. Histopathological analysis was consistent with odontoma, mixed type.

**Discussion:** The two cases demonstrate different stages in the development of odontomas, which explain their contrasting radiographic appearances. The first case showed a predominantly radiolucent lesion with limited internal calcifications, corresponding to a developing odontoma. In contrast, the second case exhibited multiple tooth-like radiopaque structures within the lesion, consistent with a more advanced stage and confirmed as a mixed-type odontoma. CBCT played an important role in clearly depicting the internal calcified components, aiding in accurate diagnosis and treatment planning.

### EP-221

## Clinico-radiologic features of craniofacial lipoatrophy in dental patients: A retrospective case series

**Jong Woo Kim**<sup>1\*</sup>, Kyung-Hoe Huh<sup>1</sup>, Won-Jin Yi<sup>1</sup>, Min-Suk Heo<sup>1</sup>, Sam-Sun Lee<sup>1</sup>, Jo-Eun Kim<sup>1</sup>

<sup>1</sup>Department of Oral and Maxillofacial Radiology, Seoul National University Dental Hospital, Seoul, Republic of Korea

**Introduction:** This study aimed to describe the imaging patterns, clinical features, and potential dental implications of craniofacial lipoatrophy in patients who underwent maxillofacial imaging for soft-tissue depression or facial asymmetry.

**Materials and Methods:** A retrospective review was performed on patients who received CT or MRI at a dental hospital and were radiologically diagnosed with localized craniofacial lipoatrophy. Clinical records were reviewed for demographics, chief complaints, medical history, and prior dental procedures including dental implant placement. Imaging evaluation included anatomical location, involved fat compartments, presence of cosmetic filler, and inflammatory changes. Affected regions were classified, and descriptive statistics were calculated.

**Results:** Fifteen patients (80% female) were included. Two patients demonstrated symmetric lipoatrophy involving all head and neck region. Among the 13 patients with localized lipoatrophy, buccal-space fat loss was the most frequent presentation (8/13, 61.5%). Two

patients showed submandibular and cervical fat loss. All patients demonstrated loss of cutaneous fat, while buccal fat pad involvement was seen in two cases, and interfascial fat loss in another two. Notably, 76.9% (10/13) of patients with localized lipoatrophy had dental implants adjacent to the affected area, and 8 of these 13 patients reported symptom awareness or cheek depression following implant surgery. Inflammatory changes were observed in all cases on CT or MRI, except for two cases in which fat loss was too extensive to permit reliable assessment.

**Conclusions:** This case series describes a relatively large cohort of patients presenting with maxillofacial lipoatrophy, a condition typically reported only in isolated case studies. Many patients reported cheek depression following dental procedures, and cross-sectional imaging frequently revealed associated inflammatory changes. Three-dimensional imaging such as CT or MRI can aid in distinguishing lipoatrophy from congenital deformities or postoperative complications. As the underlying causes and mechanisms remain unclear, additional mechanistic investigations with larger cohorts are required.

### EP-225

## Clinical imaging guidelines for impacted maxillary third molars: An evidence-based approach

**Ah-Young Kwon**<sup>1\*</sup>, Jin-Woo Choi<sup>2</sup>, Won-Jeong Han<sup>2</sup>

<sup>1</sup>Department of Oral and Maxillofacial Radiology, Dankook University Dental Hospital, South Korea

<sup>2</sup>Department of Oral and Maxillofacial Radiology, College of Dentistry, Dankook University, South Korea

**Introduction:** Accurate preoperative evaluation of impacted maxillary third molars is essential to prevent complications. However, clear standards for selecting the most appropriate imaging modality remain insufficient. The purpose of this study is to present clinical guidelines for the justification of diagnostic imaging in evaluating impacted maxillary third molars.

**Materials and Methods:** An online search was conducted based on the Korean Clinical Imaging Guidelines (KCIG) methodology. The search encompassed

international databases, including Ovid MEDLINE, Embase (Elsevier), and the Guidelines International Network (G-I-N), as well as domestic databases such as KoreaMed, KMBase, and KoMGI.

**Results:** A total of 23 articles were identified through the initial database search, with an additional eight articles and two guidelines identified via hand-searching. Among these, one guideline providing criteria for the preoperative imaging of impacted third molars was selected. However, as most of the identified literature, including this guideline, primarily focused on mandibular third molars, we supplemented the evidence by reviewing the latest literature on complications specific to maxillary third molars, such as adjacent tooth root resorption and oro-antral fistula (OAF) formation. Consequently, the final clinical imaging guidelines were developed.

**Conclusions:** Panoramic radiography is appropriate as the primary imaging modality for evaluating the position and status of impacted maxillary third molars. However, when proximity to the maxillary sinus floor or adjacent second molars is suspected on conventional radiographs and surgical extraction is planned, small field-of-view (FOV) CBCT may be considered for a more detailed assessment.

### EP-228

## Distinctive imaging features of benign cementoblastoma: A case report

**Andi Nurhaerianty Amin**<sup>1\*</sup>, Muhammad Fadil Hidayat<sup>1,2</sup>

<sup>1</sup>Dentomaxillofacial Radiology Specialist Study Program, Faculty of Dentistry Hasanuddin University, Indonesia

<sup>2</sup>Department of Oral and Maxillofacial Radiology, Faculty of Dentistry, Hasanuddin University, Makassar, Indonesia

**Introduction:** Cementoblastoma is a rare benign odontogenic tumour derived from cementoblasts and is commonly associated with the roots of posterior mandibular teeth. The lesion may be asymptomatic in its early stages but can cause pain, bony expansion, and facial asymmetry as it progresses. Radiographic evaluation, particularly cone-beam computed tomography (CBCT), plays an essential role in diagnosis and

treatment planning.

**Case:** A female patient presented with a swelling on the left cheek that had been present for approximately six months, occasionally accompanied by intermittent pain. The patient also reported gingival swelling in the left posterior mandible. Pain episodes were managed with over-the-counter mefenamic acid. Approximately 1.5 years earlier, the patient had undergone a panoramic radiographic examination in July 2024, during which no pain or noticeable mandibular enlargement was detected. Extraoral examination revealed facial asymmetry due to a left buccal swelling measuring approximately 4 × 3 × 1.5 cm with a hard consistency, no tenderness on palpation, and a normal overlying skin colour. Intraoral examination showed a firm swelling in the left posterior mandibular gingiva. Panoramic radiography and CBCT revealed a well-defined radiopaque mass fused to the root of a posterior mandibular tooth and surrounded by a thin radiolucent halo, consistent with cementoblastoma.

**Discussion:** Cementoblastoma typically presents as a radiopaque lesion attached to the tooth root and may cause cortical expansion and pain as it progresses. The clinical and radiographic features of this case were characteristic of cementoblastoma. CBCT provides detailed information regarding the extent of the lesion and its relationship with surrounding structures, which is critical for accurate diagnosis and surgical planning.

### EP-229

## Submandibular swelling mimicking a cystic lesion: An ultrasonographic diagnostic pitfall

**Irresta Zainistya Putri**<sup>1\*</sup>, Aga Satria Nurrachman<sup>1</sup>, Eha Renwi Astuti<sup>2</sup>

<sup>1</sup>Dentomaxillofacial Radiology Specialist Program, Faculty of Dental Medicine, Universitas Airlangga, Surabaya, Indonesia

<sup>2</sup>Department of Dentomaxillofacial Radiology, Faculty of Dental Medicine, Universitas Airlangga, Surabaya, Indonesia

**Introduction:** Odontogenic infections remain a significant cause of deep neck space involvement, particularly in patients with uncontrolled systemic conditions such as diabetes mellitus. Secondary infection of odontogenic cysts may alter their clinical and radio-

logic presentation, often mimicking primary inflammatory lesions of salivary glands. Ultrasonography (USG) has emerged as a valuable, noninvasive imaging modality for evaluating soft tissue pathology in the submandibular region and guiding differential diagnosis.

**Case:** A 50-year-old male presented with a six-day history of progressive, painful swelling in the right submandibular region, preceded by an untreated toothache for approximately one year. Clinical examination revealed facial asymmetry, firm indurated edema, trismus, dysphonia, and multiple gangrenous roots, notably tooth 46. The patient had uncontrolled type 2 diabetes mellitus (random blood glucose: 280 mg/dL). Ultrasonography demonstrated a well-defined heterogeneous hypoechoic to partially anechoic mass inferior to the mylohyoid muscle, suggestive of an inflamed cystic lesion. Incision and drainage, extraction of tooth 46, and biopsy were performed under general anesthesia. Bacterial culture identified *Staphylococcus aureus*. Histopathological analysis revealed a cyst wall lacking epithelial lining with dense inflammatory infiltrate, confirming a secondarily infected cyst in the right submandibular region.

**Discussion:** Radicular cysts are commonly asymptomatic and associated with non-vital teeth, becoming clinically evident primarily after secondary infection. Infected cysts may demonstrate aggressive behavior, cortical plate destruction, and extension into adjacent soft tissues, complicating diagnosis. In this case, uncontrolled diabetes likely contributed to rapid progression and atypical presentation. Ultrasonography provided crucial information regarding lesion content, margins, and vascularity, supporting differentiation between salivary gland inflammation and odontogenic pathology. Correlation with clinical findings, microbiology, and histopathology remains essential for definitive diagnosis and appropriate management.

#### EP-233

### Differentiating oral squamous cell carcinoma from osteomyelitis via mandibular canal changes on panoramic radiographs

**Jung-Eun Park**<sup>1</sup>, Kyung-Hoe Huh<sup>2</sup>, Ju-Hee Kang<sup>3</sup>, Jo-Eun Kim<sup>2</sup>, Won-Jin Yi<sup>2</sup>, Min-Suk Heo<sup>2</sup>, Sam-Sun Lee<sup>2</sup>

<sup>1</sup>Department of Oral and Maxillofacial Radiology, School of Dentistry, Seoul National University, South Korea

<sup>2</sup>Department of Oral and Maxillofacial Radiology, School of Dentistry and Dental Research Institute, Seoul National University, South Korea

<sup>3</sup>Department of Oral and Maxillofacial Radiology, Seoul National University Dental Hospital, South Korea

**Objectives:** Differentiating between oral squamous cell carcinoma (OSCC) and osteomyelitis (OM) through imaging is essential due to the overlapping clinical and radiological presentations of these conditions, complicating diagnosis. This study assessed the diagnostic performance of radiographic features related to the mandibular canal on panoramic radiographs for differentiation of OSCC from OM, and to suggest a simple and efficient approach that general dental practitioners can use for the differential diagnosis.

**Methods:** Patients with histopathologically proven OSCC and OM, involving the mandibular third molar region and/or retromolar trigone with bone destruction, were retrospectively analyzed. The border changes of the mandibular canal and adjacent sclerosis were assessed on the panoramic radiographs. Statistical analysis was performed using chi-squared tests to determine the significance of differences between OSCC and OM for each radiographic feature. Receiver operating characteristic analysis was also performed to determine the diagnostic performance for differentiation of OSCC and OM on the basis of a composite score obtained by assigning one point for each of the imaging features.

**Results:** Destruction of the borders of the mandibular canal was significantly more frequent in OSCC cases ( $P < 0.001$ ), while border thickening of the mandibular canal and adjacent sclerosis were more commonly associated with OM ( $P < 0.001$ ). Additionally, a composite scoring model based on these imaging features demonstrated excellent diagnostic performance, with an area under the curve of 0.92, further enhancing differentiation between OSCC and OM.

**Conclusion:** The change in the mandibular canal, such as border destruction, border thickening, and adjacent sclerosis, on panoramic radiographs can serve as valu-

able discriminators for differential diagnosis between OSCC and OM. These easily recognizable mandibular canal alterations on panoramic radiographs may therefore assist general dentists in distinguishing between the two lesions.

## EP-243

## Dental age estimation in juvenile Thais: A comparison of three methods

**S Benjavongkulchai**<sup>1\*</sup>, P Sutheerapatranon<sup>2</sup>, S Pimkow<sup>2</sup>, P Sinpitaksakul<sup>1</sup>

<sup>1</sup>Department of Radiology, Faculty of Dentistry, Chulalongkorn University, Thailand

<sup>2</sup>Doctor of Dental Surgery Program, Faculty of Dentistry, Chulalongkorn University, Thailand

**Introduction:** Dental age estimation is usually applied in forensic scenarios, including profiling of deceased subjects and law enforcement in undocumented living individuals. A number of dental age estimation methods has been proposed, focusing on different aspects of developmental changes and clinical approaches. This study aims to evaluate accuracy and applicability of three age estimation methods in a group of juvenile Thais.

**Materials and Methods:** Four hundred sixty-two panoramic radiographs of juvenile Thai patients were included in the study. The age of the subjects ranged from 7 to 20 years old. London atlas, Demirjian and Cameriere dental age estimation methods were applied for every panoramic image. For each subject, age estimation was performed by one of two undergraduate dental students, pre-calibrated with experienced radiologists. Paired T-test and Wilcoxon signed-rank test were applied to identify significant differences between the estimated ages and the chronological age. Analyses on reduced age ranges, 7-14 and 7-16 years, were also performed respective to limitations of Demirjian and Cameriere methods.

**Results:** London atlas showed no significant difference between estimated age and chronological age overall. However, only Demirjian method showed no significant difference from chronological age in 7-14 and 7-16 years subjects. Separated 1-year age group

analyses also showed non-significant differences between Demirjian estimated age and chronological age in most age groups between 8 and 15 years. Cameriere method showed significant differences in every 1-year age group, except in 7 years old subjects.

**Conclusions:** This study suggests use of London atlas as a primary screening method due to wide age coverage and convenience. Demirjian method is recommended in cases where the preliminary estimation was between 8 and 15 years. The use of Cameriere method is promising in subjects under 8 years old, while London atlas is applicable for subjects over 15 years old.

## EP-255

## Application of MRI-CT fusion imaging in RALS-HDR interstitial brachytherapy for tongue cancer

**Tomomi Tsujimoto**<sup>1,2\*</sup>, Nobuhiko Matsuda<sup>1,2</sup>, Kosei Ueshima<sup>1</sup>, Ami Takeshita<sup>1</sup>, Yuri Nishikawa<sup>1,2</sup>, Hiroaki Shimamoto<sup>1,2</sup>, Liwen Zhang<sup>3</sup>, Qiang Sun<sup>3</sup>, Shumei Murakami<sup>1,2,3</sup>

<sup>1</sup>Department of Oral and Maxillofacial Radiology, Graduate School of Dentistry, The University of Osaka, Japan

<sup>2</sup>Department of Radiation Oncology, Graduate School of Medicine, The University of Osaka, Japan

<sup>3</sup>Center of Stomatology, China-Japan Friendship Hospital, China

**Introduction:** Remote afterloading system high-dose-rate interstitial brachytherapy (RALS-HDR-ISBT) is an established organ-preserving treatment for tongue cancer. However, accurate delineation of tumor extent and surrounding soft tissues is challenging with CT-based planning alone. MRI-CT fusion imaging may improve target definition by utilizing MRI's superior soft-tissue contrast. This report describes its application in RALS-HDR-ISBT for tongue cancer.

**Case:** A 63-year-old man was diagnosed with right-sided tongue squamous cell carcinoma based on histopathological examination. Although subtotal glossectomy was recommended, the patient declined surgery and opted for radiotherapy. Clinical examination revealed an ulcerative lesion with induration on the right ventral surface of the tongue. Contrast-enhanced MRI demonstrated a 22 × 15 × 13 mm heterogeneous

mass with irregular margins. No cervical lymph node or distant metastasis was detected on contrast-enhanced CT, PET-CT, or ultrasonography, and the tumor was staged as T4aN0M0 (stage IVA).

Ten tubes were placed according to tumor size, and a CT scan was performed. An MRI scan followed this. The tumor contour was extracted from the MRI image to define the gross tumor volume (GTV). The MRI image, including this GTV, was fused to the CT image using a three-dimensional affine transformation. The fused image determined the planning target volume (PTV). RALS-HDR-ISBT using an iridium-192 source was performed in nine sessions over five days, with a total dose of 54 Gy.

**Discussion:** MRI provides superior soft tissue contrast, allowing more accurate delineation of tumor morphology than CT alone. MRI-CT fusion imaging enabled more localized irradiation without compromising target dose coverage. Although the tumor absorbed dose was unchanged, radiation exposure to normal tongue tissue was reduced, which may help decrease treatment-related adverse events such as soft tissue ulceration.

#### EP-256

### Extranodal diffuse large B-cell lymphoma arising in mandible: A case report

**In-Woo Park\***, Jin-Woo Han, Hang-Moon Choi  
*Department of Oral and Maxillofacial Radiology, College of Dentistry, Kangwon National University and Research Institute of Oral Science, KOREA*

**Introduction:** Diffuse large B-cell lymphoma (DLBCL) is a subtype of non-Hodgkin's lymphoma, and the occurrence of extranodal lymphoma in the mandible is extremely rare. We report a case of DLBCL arising in the mandible under the patient's consent of case presentation.

**Case:** A 64-year-old male, with a pre-medical history of chemotherapy and hematopoietic stem cell transplantation following a diagnosis of DLBCL, visited our hospital complaining of persistent left cheek pain and swelling after extraction of a lower left second

molar. Initial treatments at a local clinic, including socket curettage and medication, had been ineffective. Oral examination revealed gingival swelling, erythema, and ulceration with a papillomatous surface in the extraction socket area. X-ray showed ill-defined alveolar bony resorption including the extraction socket. He underwent extraction of the lower left first molar and resection of the left lower posterior gingival mass. Biopsy confirmed as DLBCL, activated B-cell type, not otherwise specified double expressor phenotype. He was receiving chemotherapy and had no recurrence for two years.

**Discussion:** Diagnosing jaw lesions in patients with a history of hematological malignancy can be challenging. Extranodal DLBCL is very rare and carries a poor prognosis. This case shows the importance of multi-disciplinary collaboration in diagnosis and treatment planning. Dentists should consider the possibility of malignancy when encountering atypical oral lesions, especially in patients with a history of systemic disease. This case highlights the importance of differential diagnostic skills and collaboration in dental practice.

#### EP-257

### Three-dimensional analysis of magnetic susceptibility artifacts in MRI

**Kosei Ueshima\***<sup>1</sup>, Ami Takeshita<sup>1</sup>, Varisa Assapattarapun<sup>1</sup>, Noriko Yamao<sup>1</sup>, Nobuhiko Matsuda<sup>1</sup>, Yuka Uchiyama<sup>1</sup>, Tomomi Tsujimoto<sup>1</sup>, Tadashi Sasai<sup>1</sup>, Liwen Zhang<sup>2</sup>, Qiang Sun<sup>2</sup>, Shumei Murakami<sup>1,2</sup>

<sup>1</sup>*Department of Oral and Maxillofacial Radiology, Graduate School of Dentistry, The University of Osaka, Japan*

<sup>2</sup>*Center of Stomatology, China-Japan Friendship Hospital, China*

**Introduction:** Magnetic susceptibility artifacts in magnetic resonance imaging (MRI) affect the quality of diagnostic images. In the oral and maxillofacial regions, artifacts from dental metals with high magnetic susceptibility are problematic. While some dental metals can be removed before imaging, titanium implants and jawbone fixation plates cannot be readily removed. Although studies have investigated magnetic suscepti-

bility artifacts in MRI, none have performed three-dimensional analyses based on ASTM recommendations. This study aimed to analyze magnetic susceptibility artifacts using a homogeneous 10-mm-diameter titanium sphere and gradient echo imaging.

**Materials and Methods:** MRI was performed using a 3.0-T system (SIGNA® Premier, GE Healthcare). The imaging parameters included a field of view of 192 × 192 mm, 192 frequency-encoding steps, 192 phase-encoding steps, and a slice thickness of 1.0 mm, resulting in isotropic voxels of 1 × 1 × 1 mm. Gradient-echo imaging was performed in the axial, sagittal, and coronal planes using interleaved acquisition. Additional scans were obtained by swapping the frequency and phase-encoding directions.

**Results:** Titanium placement produced magnetic susceptibility artifacts on gradient-echo imaging. Artifacts appeared circular in axial images, while sagittal and coronal images showed ellipsoidal artifacts along the frequency-encoding direction. The artifact volume ranged from 21 to 22 cm<sup>3</sup>, with a spatial extent of 33 to 42 mm. Axial artifacts showed larger volumes than sagittal or coronal orientations. The three-dimensional morphology varied with the imaging orientation.

**Conclusions:** Three-dimensional analysis revealed that titanium-induced artifacts in gradient-echo imaging exhibit orientation-dependent morphologies. Axial plane artifacts were larger than those in other planes, with the greatest extent in the slice-selection gradient direction. These findings provide insights into titanium-induced susceptibility artifacts and may improve oral and maxillofacial MRI interpretation.

EP-258

## Accuracy comparison of periapical radiographs for working length measurement between undergraduate and post graduated dental students at the Faculty of Dentistry, Universitas Gadjah Mada

Rurie Ratna Shantiningsih<sup>1\*</sup>, Andina Widyastuti<sup>2</sup>,  
Henyntaria Fajrianti<sup>2</sup>

<sup>1</sup>Department of Dentomaxillofacial Radiology, Universitas Gadjah Mada, Indonesia

<sup>2</sup>Department of Conservative Dentistry, Universitas Gadjah Mada, Indonesia

Endodontic treatment aims to preserve teeth in the oral cavity for as long as possible by preventing unnecessary extraction. The success of endodontic therapy largely depends on accurate working length determination. Radiographic methods remain the most widely used approaches for this purpose, with periapical radiography considered the standard modality due to its ability to provide essential information regarding root canal anatomy and periapical conditions. Nevertheless, periapical radiography has inherent limitations, including radiation exposure and potential image distortion.

This study aimed to compare the accuracy of working length measurements obtained from periapical radiographs with direct measurements of extracted teeth, to evaluate differences in measurement accuracy between undergraduate and postgraduate dental students at the Faculty of Dentistry, Universitas Gadjah Mada, and to analyze variations in tooth length accuracy between these groups. Distortion analysis was performed by comparing working length measurements obtained from periapical radiographs taken by undergraduate and postgraduate students with the corresponding measurements of extracted teeth. Statistical analyses were conducted using the Kruskal–Wallis test, Independent Samples t-test, and Mann–Whitney test.

The results demonstrated no statistically significant difference between the actual tooth lengths and radiographic working length measurements. However, significant differences ( $p < 0.05$ ) were observed in measurement deviations and accuracy among operator groups, particularly between sixth-semester undergraduate and postgraduate students. It can indicate that operator experience plays a critical role in radiographic interpretation and working length determination.

EP-259

## Dental detection and diagnosis of pituitary adenoma induced acromegaly: Report of a case

**Seok-Jun Hwang**<sup>1\*</sup>, Jo-Eun Kim<sup>1</sup>, Min-Suk Heo<sup>1</sup>

<sup>1</sup>Department of Oral and Maxillofacial Radiology, School of Dentistry and Dental Research Institute, Seoul National University, South Korea

**Introduction:** Pituitary adenoma–induced acromegaly is an endocrine disorder characterized by progressive overgrowth of soft tissues and the skeleton. Oral–maxillofacial findings include mandibular prognathism, increasing interdental spacing, macroglossia, a tendency toward Class III malocclusion, and remodeling of the sella turcica on imaging.

Purpose of this poster is to illustrate the diagnostic process through signs that can be detected in the dental setting.

**Case:** A Patient was referred from a dental clinic to our center with the chief complaint that only the mandibular right molar was in occlusion. For the four months preceding referral, she exhibited a Class III malocclusion with an overall open-bite pattern and reported that her tongue had enlarged.

TMJ MRI demonstrated new bone formation at the posterosuperior aspect of both mandibular condyles. In addition, a T2-signal lesion was noted in the sella turcica, raising suspicion for a pituitary adenoma. So, she was referred to our endocrinology service.

Endocrine testing revealed marked elevations of IGF-1, hGH, and ACTH compared with normal ranges, and brain MRI likewise showed a T2-signal lesion. Histopathologic examination confirmed the diagnosis of pituitary adenoma. After tumor resection, IGF-1, hGH, and ACTH levels returned to normal ranges; the patient's tongue size decreased, and occlusion stabilized.

**Discussion:** Patients who present to a dental clinic with macroglossia, increasing interdental spacing, mandibular prognathism, open bite, or rapid changes in occlusion should prompt suspicion of underlying acromegaly. If imaging shows remodeling of the posterior aspect of the TMJ condyle or enlargement of sella turcica, these findings further support a working

suspicion of pituitary adenoma–induced acromegaly. Although the definitive diagnosis is established by hormonal testing and histopathology, recognizing these signs during dental care and raising early suspicion of a pituitary adenoma can greatly facilitate timely diagnosis.

EP-260

## Inflammatory rhabdomyoblastic tumor in the buccal mucosa: An imaging report

**Yuki Shimizu**<sup>1\*</sup>, Hiroaki Shimamoto<sup>1</sup>, Keisuke Marutani<sup>1</sup>, Reika Hanaoka<sup>1</sup>, Kaori Oya<sup>2</sup>, Katsutoshi Hirose<sup>3</sup>, Seiki Tomita<sup>1</sup>, Yuka Uchimoto<sup>1</sup>, Miyoshi Kataoka<sup>1</sup>, Hideki Rokushima<sup>4</sup>, Shumei Murakami<sup>1</sup>

<sup>1</sup>Department of Oral and Maxillofacial Radiology, Graduate School of Dentistry, The University of Osaka, Japan

<sup>2</sup>Department of Laboratory Medicine, The University of Osaka Dental Hospital, Japan

<sup>3</sup>Department of Oral Pathology, Graduate School of Dentistry, The University of Osaka, Japan

<sup>4</sup>Department of Radiology, The University of Osaka Dental Hospital, Japan

**Introduction:** Inflammatory rhabdomyoblastic tumor (IRMT) is a rare disease first proposed by Cloutier et al. in 2021. It replaces the terms inflammatory leiomyosarcoma, histiocyte-rich rhabdomyoblastic tumor (HRRMT), and low-grade inflammatory myogenic tumor; all of which are rare malignant soft tissue tumors. Here, we report a case of IRMT arising in the buccal mucosa.

**Case:** The patient is a 79-year-old woman who presented with discomfort in the left cheek area. CT examination revealed a mass with a CT value of approximately 50 HU on the buccal side of the left mandibular premolar region, with no evidence of bone destruction in the adjacent mandible. MRI showed a low signal area on T1-weighted images and a high signal area on T2-weighted images in the same region. The ADC value of the lesion was  $0.78 \times 10^{-3} \text{ mm}^2/\text{s}$ . Based on these findings, a benign salivary gland tumor originating from a minor salivary gland was suspected. Tumor excision was performed, and histopathological examination of the surgical specimen led to a diagnosis of IRMT.

**Discussion:** When compared with a previously reported case in the literature, the imaging findings were generally consistent. One criterion for determining the malignancy of salivary gland tumors is the ADC value. The ADC value in this case was  $0.78 \times 10^{-3} \text{ mm}^2/\text{s}$ , which is consistent with a typical malignant tumor; however, differentiation from a salivary gland tumor was difficult. IRMT and HRRMT are known to have well-defined margins; in this case, the margins became somewhat indistinct due to patient movement. Although IRMT is considered to be of low malignancy, a study by Odate et al. found that two out of 13 cases showed malignant transformation to rhabdomyosarcoma, indicating that careful follow-up, similar to that for malignant tumors, is necessary.

## EP-264

## Imaging presentation of mucosal lymphatic malformation in a pediatric patient: A multimodality case report

**Muhammad Teguh Putra AF<sup>1\*</sup>**, Fadhilil Ulum Abdul Rahman<sup>1,2</sup>

<sup>1</sup>Dentomaxillofacial Radiology Study Program, Faculty of Dentistry Hasanuddin University, Indonesia

<sup>2</sup>Department of Oral And Maxillofacial Radiology, Faculty of Dentistry Hasanuddin University, Indonesia

**Introduction:** Lymphatic malformations, previously termed lymphangiomas, are rare congenital vascular anomalies that predominantly involve the head and neck region in pediatric patients. In the oral and maxillofacial region, their nonspecific clinical and radiologic features often overlap with other vascular anomalies, making accurate diagnosis highly dependent on multimodality imaging and radiologic–pathologic correlation.

**Case:** An 8-year-old female presented with a persistent violaceous swelling of the right cheek and upper right labial mucosa causing facial asymmetry. Based on initial clinical and angiographic findings, the lesion was managed as a vascular malformation with differential consideration of hemangioma, and multiple staged sclerotherapy sessions were performed with limited response. MSCT angiography demonstrated a well-

defined hyperenhancing soft-tissue mass in the right buccal–mandibular region without cortical bone destruction. However, further Doppler ultrasonography revealed a heterogeneous lesion with sparse intra- and perilesional low-flow vascular signals, raising suspicion of a lymphatic malformation. Histopathological examination following surgical excision confirmed the diagnosis of lymphangioma.

**Discussion:** The initial angiographic appearance justified sclerotherapy; however, Doppler ultrasonography provided essential hemodynamic information demonstrating low-flow vascularization, consistent with a lymphatic lesion and explaining the suboptimal therapeutic response. Radiologic–pathologic correlation is crucial for differentiating lymphatic malformations from other vascular anomalies, enabling accurate diagnosis, appropriate staging, and safe interventional planning in pediatric maxillofacial cases. Histopathologic confirmation guided subsequent wide excision with local flap reconstruction, after which the patient experienced no significant postoperative complaints.

## EP-266

## Intraosseous progression mucoepidermoid carcinoma: Case report and imaging considerations

**Gonzalo Arellano G.<sup>1\*</sup>**, Macarena Toro M.<sup>2</sup>, Sergio González P.<sup>2</sup>, Carla Sciaraffia R.<sup>1</sup>

<sup>1</sup>Radiology and Diagnostic imaging, Universidad Mayor, Chile

<sup>2</sup>Oral Pathology and Oral Medicine Service, Universidad Mayor, Chile

**Introduction:** Mucoepidermoid carcinoma is the most prevalent malignant neoplasm of the salivary glands, occurring more frequently in women, with a mean age of 45 years. It primarily affects major salivary glands, particularly the parotid gland. However, in approximately 2% of cases, the main progression and expansion exhibits an intraosseous component, presenting radiographically as an unilocular or multilocular hypodense area with well-defined or scalloped margins. These imaging characteristics may lead to diagnostic confusion with central lesions such as multicystic ameloblastoma, odontogenic keratocyst, and, in rare cases dentigerous cysts.

**Case:** 38-year-old male, no relevant medical history. Referred to the Oral Pathology Service of Universidad Mayor following an incidental imaging finding after an accident. Cone-beam CT showed a multilocular hypodense area extending into the maxillary sinus, with perforation of both the buccal and palatal cortical bone. Differential diagnosis included odontogenic myxoma, ameloblastoma, and odontogenic keratocyst; Clinical examination revealed slight mass in the maxillary tuberosity area with telangiectatic surface. Histopathological analysis revealed a non-encapsulated proliferation of neoplastic cells composed of clear cells, epidermoid cells, and Alcian blue positive mucous cells.

**Discussion:** This clinical case highlights the importance of including mucoepidermoid carcinoma in the imaging differential diagnosis of multilocular intraosseous maxillofacial lesions, particularly in cases where sinus involvement is a predominant feature. Although definitive diagnosis relies on histopathological analysis, recognizing these uncommon presentations might be an interesting consideration for an expanded differential diagnosis of multilocular hypodense areas in the posterior maxillofacial region.

#### EP-267

### Evaluation of tooth wear and fractal analysis of mandibula in bruxism

**Derya YILDIRIM**<sup>1\*</sup>, Esra Seden NAVRUZ<sup>1</sup>, Hasibe Taşkın<sup>2</sup>, Hikmet ORHAN<sup>3</sup>

<sup>1</sup>Department of Oral and Maxillofacial Radiology, Süleyman Demirel University, Türkiye

<sup>2</sup>Department of Dental Services, Süleyman Demirel University, Türkiye

<sup>3</sup>Department of Biostatistics and Medical Informatics, Süleyman Demirel University, Türkiye

**Introduction:** This study aimed to investigate the relationship between tooth wear severity and bone architecture of mandible using the fractal analysis method according to evaluate the possible effects of bruxism.

**Materials and Methods:** A total of 135 (mean age: 30.93 ± 5.36 years) adult bruxism patients and 135 controls without bruxism (mean age: 29.92 ± 4.25

years) were included in the study. The tooth wear levels of the bruxism group were divided into five subgroups (0–4) according to the Smith and Knight tooth wear index. Fractal dimension measurements were obtained on panoramic radiographs from eight different ROIs in the mandible: condyle, angle, molar, and canine regions on both right and left sides. Statistical analysis were performed using the independent samples t-test, one-way ANOVA test, Tukey HSD post-hoc test. Subgroup analyses by sex were also conducted.

**Results:** Fractal values in all ROIs were significantly higher in individuals with bruxism compared with those without bruxism ( $p < 0.001$ ). As bruxism severity increased, fractal dimension levels increased consistently. Fractal dimension levels demonstrated significant difference among subgroups formed according to toothwear index in all ROIs ( $p < 0.001$ ). Significant differences were observed across fractal dimension levels of all ROIs in females ( $p < 0.001$ ), in males no significance was found in ROIs of right canine and left angulus and condyle region. Comparison of fractal analyses levels of right and left sides showed significant differences in the right condyle, angle, molar, and canine regions ( $p < 0.005$ ).

**Conclusions:** Bruxism leads to an increase and a more complex architecture in the mandibular trabecular bone structure. As bruxism severity increases, fractal dimension values also increase, indicating an adaptive bone remodeling. Fractal analysis is a sensitive method for evaluating the effects of bruxism on bone structure.

#### EP-269

### Dento-periodontal assessment in ENT cancer patients using OPT and CBCT: A prospective comparative study

**Antohei Cristina**<sup>1\*</sup>, Haba Danisia<sup>2</sup>, Cernei Radu Eduard<sup>2</sup>, Popescu Roxana Mihaela<sup>2</sup>, Dobrovat Bogdan Ionut<sup>2</sup>, Salceanu Mihaela<sup>1</sup>, Concita Alexandra<sup>1</sup>, Hamburda Tudor<sup>1</sup>, Giuroiu Cristian Levente<sup>1</sup>, Gheorghe Angela<sup>3</sup>, Pancu Galina<sup>3</sup>, Nica Irina<sup>3</sup>, Topoliceanu Claudiu<sup>3</sup>

<sup>1</sup>Endodontology, UMF GR T POPA, Romania

<sup>2</sup>*Surgery, UMF GR T POPA, Romania*

<sup>3</sup>*Cariology, UMF GR T POPA, Romania*

**Introduction:** Patients with head and neck (ENT) cancer frequently present with compromised oral health, which may influence oncologic treatment tolerance and outcomes. Accurate evaluation of dento-periodontal status is essential for risk stratification and treatment planning. Orthopantomography (OPT) and cone-beam computed tomography (CBCT) play complementary roles in dental imaging. This study aimed to assess dento-periodontal pathology in ENT cancer patients compared with healthy controls.

**Material and Method:** This prospective study included 63 subjects: 33 patients with head and neck cancer (larynx, oropharynx, and paranasal sinuses) treated at the Regional Institute of Oncology, Iași, and 30 healthy individuals as a control group. All participants were examined by an ENT specialist, two radiologists, and two endodontists. Imaging assessment consisted of orthopantomography (OPT) and CBCT examinations performed at the Medimagis Imaging Center, Iași. Carious lesions, alveolar bone loss, periapical lesions, and furcation involvement were evaluated, with comparison between 2D and 3D modalities.

**Results:** ENT cancer patients demonstrated a higher prevalence and severity of dento-periodontal pathology, including increased carious lesions, greater alveolar bone loss, more frequent periapical pathology, and advanced furcation involvement. CBCT detected a significantly higher number of lesions and allowed more accurate lesion size assessment compared to OPT.

**Conclusions:** CBCT provides superior diagnostic accuracy compared with OPT in evaluating dento-periodontal status in head and neck cancer patients. Comprehensive 3D imaging may enhance pre-therapeutic dental assessment and support multidisciplinary care.

EP-272

## Mandibular bone density associated with horizontal and vertical positions of impacted mandibular third molars

Khalisha Amanina Azzami<sup>2\*</sup>, Rini Widyaningrum<sup>1\*</sup>, Ryna Dwi Yanuarieska<sup>1</sup>

<sup>1</sup>*Department of Dentomaxillofacial Radiology, Faculty of Dentistry, Universitas Gadjah Mada, Indonesia*

<sup>2</sup>*Undergraduate Program of Dental Medicine, Faculty of Dentistry, Universitas Gadjah Mada, Indonesia*

**Introduction:** Tooth impaction is the failure of tooth eruption due to obstruction by hard or soft tissues and may chronically alter mandibular bone density through sustained mechanical loading. Mandibular bone density can be assessed using the Watanabe Index (W-Index), defined as the contrast ratio between the mean gray value of the mandibular oblique line and the adjacent ramus region on panoramic radiographs. This study evaluated differences in W-Index values according to horizontal and vertical positions of impacted mandibular third molars.

**Materials and Methods:** This observational analytic study used a cross-sectional design. Impacted mandibular third molars (teeth 38 and 48) were classified using the Pell and Gregory system into three horizontal categories (Class I–III) and three vertical categories (Position A–C). Each category included 34 samples, yielding 102 samples. Horizontal group differences were analyzed using Welch's ANOVA followed by the Games–Howell post hoc test, while vertical group differences were assessed using the Kruskal–Wallis test with Dunn's post hoc test and Bonferroni correction.

**Results:** W-Index values differed significantly among horizontal impaction categories (Welch's ANOVA,  $p < 0.05$ ), with post hoc analysis showing significant differences between Class I and both Class II and Class III ( $p < 0.05$ ). Vertical impaction categories also showed significant differences (Kruskal–Wallis test,  $p < 0.05$ ), particularly between Position A and Position B.

**Conclusions:** Impaction depth and available eruption space of mandibular third molars are associated with variations in mandibular bone density as measured by the W-Index.

EP-275

## Extensive radicular cyst of the anterior maxilla with superior nasal floor displacement: A clinical, radiographic, and histopathologic case report

**Siska Putri Utami**<sup>1\*</sup>, Barunawaty Yunus<sup>1,2</sup>

<sup>1</sup>*Dentomaxillofacial Radiology Specialist Study Program, Faculty of Dentistry Hasanuddin University, Indonesia*

<sup>2</sup>*Departement of Oral and Maxillofacial Radiology, Faculty of Dentistry Hasanuddin University, Indonesia*

**Introduction:** Radicular cysts constitute the most prevalent inflammatory odontogenic cysts; however, extensive anterior maxillary lesions with upward displacement of the nasal floor may present diagnostic challenges due to radiographic overlap with more aggressive odontogenic pathologies. Comprehensive evaluation integrating panoramic radiography, clinical history, and histopathologic correlation is essential to accurately characterize lesion behavior and guide intervention.

**Case Presentation:** A 34-year-old male presented with a progressive anterior maxillary swelling persisting for four months, preceded by a history of dental trauma to tooth 11 in 2014 and intermittent saline-like discharge since 2020. Intraoral examination revealed a firm, well-localized swelling in the 11–21 region. Panoramic radiography demonstrated a well-circumscribed unilocular mixed-density lesion measuring approximately 11.98 × 32.07 mm, extending from tooth 14 to 22, with superior displacement of the nasal floor and apical one-third root resorption of tooth 21. Fine-needle aspiration produced hemorrhagic fluid. Surgical enucleation with apicoectomy was performed under general anesthesia. Histopathological analysis revealed a cystic cavity partially lined by non-keratinized stratified squamous epithelium, with dense subepithelial chronic inflammatory infiltrates composed of lymphocytes and histiocytes and prominent erythrocyte-filled vasculature—findings confirmatory for a chronic inflamed radicular cyst.

**Discussion:** The lesion's size, superior extension, and mixed radiodensity pattern necessitated differentiation from odontogenic keratocyst and unilocular amelo-

blastoma. Radiographic hallmarks, including corticated borders, association with a non-vital tooth, and characteristic root resorption, supported an inflammatory etiology. The case underscores the diagnostic significance of correlating radiologic features with histopathologic architecture to establish definitive identification of odontogenic cysts. This multimodal approach is critical for optimizing surgical planning, particularly in lesions abutting vital anatomical structures such as the nasal cavity. Complete enucleation resulted in favorable healing, aligning with established management protocols for large radicular cysts.

**Keywords:** radicular cyst; odontogenic pathology; panoramic radiography; nasal floor displacement; histopathology; anterior maxilla

EP-283

## Semi-quantitative analysis of bone change using cone-beam CT

**Ko Dezawa**<sup>1\*</sup>, Tomoyo Nomura<sup>1</sup>, Yoshinori Arai<sup>1</sup>, Kunihiro Matsumoto<sup>1</sup>

<sup>1</sup>*Department of Oral and Maxillofacial Radiology, Nihon University School of Dentistry, Japan*

**Introduction:** Cone-beam computed tomography (CBCT) has limited absolute quantitative reliability of pixel values compared with medical computed tomography, which has traditionally restricted its application for longitudinal comparison and quantitative evaluation of bone volume changes. Nevertheless, in clinical practice, there is a strong demand for objective and reproducible indicators that enable assessment of bone changes over time. This study aimed to investigate a method for semi-quantitative evaluation of volumetric bone changes by applying image binarization and inter-image difference analysis to CBCT data. Using a porcine mandibular condyle phantom with a surrounding bone augmentation model, the feasibility of this approach was examined. Furthermore, its clinical usefulness and future potential were explored through representative clinical cases.

**Materials and Methods:** For the initial CBCT dataset, a binarization threshold was determined using Otsu's method based on pixel value distribution. Using this fixed threshold, binarized images were generated for serially acquired CBCT datasets. Spatial registra-

tion of the images was performed using a least-squares alignment method, followed by subtraction analysis to generate difference images. Regions of bone resorption and bone formation were visualized using color-coded mapping, enabling visual assessment and semi-quantitative evaluation of bone change volume and anatomical location. This method was applied to clinical cases including bone regeneration after periodontal regenerative therapy, augmented bone following guided bone regeneration in implant treatment, bone healing after mandibular cyst enucleation, and progression of bone resorption in idiopathic condylar resorption.

**Results:** In clinical cases, bone volume changes could be assessed more intuitively than by conventional visual inspection of CBCT images. Accurate evaluation required careful placement of regions of interest in areas with density comparable to the target site. In addition, within the oral cavity, binarization threshold settings were sometimes affected by metal artifacts and root filling materials.

**Conclusions:** The proposed method enables retrospective, semi-quantitative assessment of bone changes using CBCT.

#### EP-285

### Comparative accuracy of digital panoramic radiography and cone beam computed tomography in assessing mental nerve entry patterns into the mental foramen

**Andi Fauziah Alrahma**<sup>1\*</sup>, Fadhil Ulum Abdul Rahman<sup>1,2</sup>, Barunawaty Yunus<sup>1,2</sup>

<sup>1</sup>Dentomaxillofacial Radiology Specialist Study Program, Faculty of Dentistry Hasanuddin University, Indonesia

<sup>2</sup>Department of Oral and Maxillofacial Radiology, Faculty of Dentistry, Hasanuddin University, Makassar, Indonesia

**Introduction:** Accurate identification of the mental nerve entry pattern into the mental foramen is essential to prevent neurovascular injury during mandibular surgical procedures, particularly dental implant placement. Variations such as anterior loop, straight, and perpendicular patterns may not be reliably visualized

using two-dimensional imaging. This study aimed to compare digital panoramic radiography and cone beam computed tomography (CBCT) in evaluating mental nerve entry patterns, considering age and sex as contributing factors.

**Materials and Methods:** A cross-sectional comparative study was conducted using paired digital panoramic radiographs and CBCT images from 34 patients. Mental nerve entry patterns were classified as anterior loop, straight, or perpendicular on both sides of the mandible. CBCT served as the reference standard. Statistical analyses included Chi-square tests, Cramer's V, and Cohen's Kappa to assess associations, agreement, and diagnostic accuracy.

**Results:** The perpendicular pattern was the most frequently observed configuration across both imaging modalities, with higher detection rates on CBCT. No significant association was found between mental nerve entry patterns and sex or age on panoramic radiographs. CBCT revealed a significant association between sex and nerve entry pattern on the left mandible ( $p < 0.05$ ). Agreement between panoramic radiography and CBCT was moderate on the right side ( $\kappa = 0.492$ ) and low on the left side ( $\kappa = 0.292$ ), indicating limited accuracy of panoramic imaging, particularly for complex anatomical variations.

**Conclusions:** CBCT demonstrates superior accuracy over digital panoramic radiography in visualizing mental nerve entry patterns into the mental foramen. While panoramic radiography remains useful as an initial screening tool, CBCT is recommended for pre-operative planning in procedures involving the mandibular premolar region to reduce the risk of mental nerve injury.

#### EP-286

### Panoramic radiographic detection of elongated styloid process: A five-year retrospective study in an Indonesian subpopulation

**Az Zikra Adelia Syamsuri**<sup>1\*</sup>, Fadhil Ulum Abdul Rahman<sup>2</sup>, Andi Muh Ayodhya Chandra Dirawan<sup>1</sup>, Maulana Ibnu Ramadhan<sup>1</sup>

<sup>1</sup>Clinical Student of Doctor of Dental Medicine Programme, Faculty of Dentistry, Hasanuddin University, Indonesia

<sup>2</sup>Department of Oral and Maxillofacial Radiology, Faculty of Dentistry, Hasanuddin University, Makassar, Indonesia

**Introduction:** The styloid process varies in length and lies in close proximity to major cervical vessels. Elongation is frequently detected on panoramic radiographs and is usually asymptomatic, except when associated with Eagle syndrome, in which abnormal length or orientation may cause clinical symptoms. This study aims to describe the distribution of elongated styloid process on panoramic radiographs by sex and elongation type in an Indonesian subpopulation examined at Hasanuddin University Dental Hospital, Makassar, Indonesia.

**Materials and methods:** This cross-sectional study assesses 238 digital panoramic radiographs, collected consecutively from archival records, involving males over 14 years and females over 12 years from 2018 to 2023. The elongated styloid process was analyzed using calibrated panoramic data on the open-source ImageJ platform.

**Results:** The evaluation of eligible panoramic radiographs revealed a predominance of females in cases of elongated styloid process (55.47%). The highest frequency was observed in the 26-45 years age group, with type I elongation emerging as the most prevalent morphological pattern, accounting for 83.20% of cases. The overall prevalence identified in this study aligns with global epidemiological reports, which estimate an occurrence of approximately 4%. These findings provide foundational epidemiological evidence that may support future population-based assessments of the elongated styloid process in Indonesia, with data derived from Hasanuddin University Dental Hospital.

**Conclusions:** Between 2018 and 2023, elongated styloid processes were identified on panoramic radiographs at Hasanuddin University Dental Hospital, with a prevalence comparable to global reports. Type I was the most frequently observed elongation type.

EP-298

## Clinicoradiologic features of glandular odontogenic cyst: A retrospective analysis of 45 cases with emphasis on computed tomographic images

**Kyeo-Re Kim**<sup>1\*</sup>, Kyung-Hoe Huh<sup>2</sup>, Ju-Hee Kang<sup>3</sup>, Jo-Eun Kim<sup>2</sup>, Won-Jin Yi<sup>2</sup>, Min-Suk Heo<sup>2</sup>, Sam-Sun Lee<sup>2</sup>

<sup>1</sup>Department of Oral and Maxillofacial Radiology, School of Dentistry, Seoul National University

<sup>2</sup>Department of Oral and Maxillofacial Radiology, School of Dentistry and Dental Research Institute, Seoul National University

<sup>3</sup>Department of Oral and Maxillofacial Radiology, Seoul National University Dental Hospital

**Introduction:** Glandular odontogenic cyst (GOC) is a rare cyst of the jaw with researches and data primarily confined to the field of histopathology. This study aims to evaluate the clinical and radiologic features of GOC.

**Materials and Methods:** Histopathologically diagnosed forty-five GOC cases were retrospectively assessed. Obtained clinical data included age, sex, presenting symptoms and recurrence. Evaluated radiologic features from computed tomography (CT) images and panoramic radiographs included lesion site, size, shape, internal septation, loculation and the effects on adjacent anatomical structures.

**Results:** Mean age of the cohorts was 48.24 years with male predominance (2.75:1). Although the presenting symptoms were swelling (14 cases, 31.11%), pain (6 cases, 13.33%) and other subjective discomfort (6 cases, 13.33%), most patients were asymptomatic (17 cases, 37.78%). Recurrence was observed in three cases. In most cases, lesions were found in the molar region of the mandible (22 cases, 48.89%), of which 21 cases (46.47%) were associated with impacted third molars. Internal septation was seen in 7 cases (15.91%), including two true multilocular lesions. Root resorption and displacement of adjacent tooth were seen in 19 (43.18%) and 20 cases (45.45%) respectively. Aside from cortical thinning (93.18%) and expansion (77.27%), cortical bone loss was also noted

in 25 cases (56.82%).

**Conclusions:** GOC showed the highest prevalence in the mandibular molar region, involving strong association with impacted third molars. Lesions were predominantly unilocular, with high rate of root resorption and displacement of adjacent teeth. The facilitation of CT can contribute to the clearer understanding of GOC compared to planar radiographs.

### EP-301

## Utilizing cone-beam computed tomography to diagnose and treat fractures of the mandibular condyle: A case report

**Khamila Gayatri Anjani**<sup>1\*</sup>, Liska Barus<sup>2</sup>, Dwi Putri Wulansari<sup>3</sup>

<sup>1</sup>Faculty of Dentistry, Universitas Muhammadiyah Surabaya, Surabaya, Indonesia

<sup>2</sup>Department of Oral and Maxillofacial Surgery, Faculty of Dental Medicine, Universitas Airlangga, Surabaya, Indonesia

<sup>3</sup>Department of Oral and Maxillofacial Radiology, Faculty of Dentistry, Universitas Hasanuddin, Makassar, Indonesia

**Introduction:** Cone beam computed tomography (CBCT) provides detailed imaging of temporomandibular joint anatomy without superimposition or distortion. CBCT is a relatively new imaging technique and is widely utilized in dental practice.

**Case:** A 15-year-old female patient reported to the Dental Radiology Unit with a CBCT referral letter and a clinical diagnosis of condyle neck fractures. The patient's background included a motorcycle accident in early 2024. Extraoral examination indicated an uneven face appearance, including mandible deviation, limited mouth opening, and crepitation on palpation. An intraoral examination revealed lost teeth in 11, 21, and dental fractures in 31, 32, 41, and 42. Oral hygiene was excellent.

**Discussion:** The CBCT examination revealed a radiolucent line crossing horizontally on the head of the bilateral condyles, demonstrating medial displacement of the condyle. Radiographs revealed that condylar head fractures were not linked with the mandible fracture. The location of the fragments in the fracture and

any size and positional changes that take place can be seen using CBCT. We determined that CBCT is the most advanced technology available for providing a clean image of the condylar head without superimposing other structures. It also provides additional information for a more efficient diagnosis and treatment of condyle fractures.

### EP-302

## Incidental detection of "susuk" charm needles on CBCT during pre-implant assessment: A case report

**Anak Agung Gde Dananjaya Agung**<sup>1\*</sup>, Debora Natalia<sup>2</sup>, Putri Marina Sukmadewi<sup>2</sup>

<sup>1</sup>Oral and Maxillofacial Radiology Department, Dentology Dental Clinic, Indonesia

<sup>2</sup>Oral and Maxillofacial Radiology Department, Udayana University, Indonesia.

**Introduction:** Cone-beam computer tomography (CBCT) plays a crucial role in implant treatment planning, and metal artifacts have been reported to interfere with anatomical interpretation. Susuk or charm needles are needle-shaped metallic foreign bodies implanted subcutaneously and associated with cultural practices still found in Indonesia; they are believed to enhance aesthetics. On CBCT, susuk are frequently detected as incidental findings and can produce metal artifacts. Evidence on their clinical relevance in CBCT-based pre-implant evaluation remains limited. This case report present multiple susuk identified by CBCT and discuss how these findings can influence radiological interpretation and clinical decision-making during implant placement planning.

**Case:** A 57-year-old male with partial tooth loss in maxilla and mandible was referred for CBCT for pre-implant evaluation. CBCT with a field of view (8×15 cm) revealed 16 linear radiopaque objects, with maximum length of 10.5 mm, distributed bilaterally in the maxilla and mandible. Metal artifacts were minimal due to the metal artifact reduction (MAR) feature of the 3D CBCT. Overall, bone visualization was adequate for measuring and assessing critical structures. A clinical interview confirmed that the susuk had been

inserted approximately 30 years earlier for aesthetic reasons.

**Discussion:** Susuk present as small linear radiopaque images that possibly resemble other metallic foreign bodies, which can lead misinterpretation. In this case, MAR helped to retain the image quality. The effect of susuk on implant planning is influenced by the relationship between the susuk and site of implant planning. Susuk position and orientation especially when adjacent to or paralleling the alveolar cortex may affect local visibility during the measurement. This report emphasizes the need for vigilant monitoring of susuk by radiologists in pre-implant CBCT and highlights that can be used to guide implant planning decisions.

#### EP-310

### Dental infection to fatal pathways: CT and MRI findings of thrombophlebitis in cavernous sinus and jugular vein

**Chang-Ki Min**<sup>1\*</sup>, Kyoung-A Kim<sup>1</sup>

<sup>1</sup>Department of Oral and Maxillofacial Radiology, Jeonbuk National University, Republic of Korea

**Introduction:** Severe, life-threatening complications of odontogenic infection remain uncommon but require immediate recognition. We present two cases—cavernous sinus thrombophlebitis and internal jugular vein thrombophlebitis—highlighting the pivotal role of CT and MRI in early diagnosis and assessment of disease extent.

**Case:** Case 1: A patient presented to the emergency department several days after maxillary molar extraction with high fever, altered mental status, and proptosis. Contrast-enhanced CT and MRI demonstrated an abscess involving the pterygoid plexus adjacent to the extraction site, complicated by cavernous sinus thrombophlebitis and associated meningoenophthalmitis. Case 2: A patient with untreated pulpitis developed neck pain with swelling and fever. Contrast-enhanced CT revealed abscess formation in the sublingual and submandibular spaces with extension into the parapharyngeal space. Imaging also showed findings consis-

tent with internal jugular vein thrombophlebitis.

**Discussion:** Although both cases originated from common dental infections, they progressed to potentially fatal septic thrombophlebitis with deep space and intracranial involvement. Because the systemic impact of odontogenic infection is often underestimated at initial presentation, imaging-based evaluation is essential to avoid diagnostic delay. Contrast-enhanced CT enables rapid mapping of deep facial and neck space infection and detection of septic venous thrombosis, while MRI provides superior delineation of cavernous sinus involvement and intracranial inflammatory complications such as meningoenophthalmitis. These cases highlight that accurate imaging diagnosis is critical not only for identifying rare but severe complications, but also for defining disease extent and guiding urgent multidisciplinary management.

#### EP-311

### Radiologic characteristics and postoperative follow-up of multilocular ameloblastoma on panoramic radiography: A case report

**Hetty Oktavin Laonu**<sup>1\*</sup>, Barunawaty Yunus<sup>1,2</sup>

<sup>1</sup>Dentomaxillofacial Radiology Specialist Study Program, Faculty of Dentistry, Hasanuddin University, Indonesia

<sup>2</sup>Department of Oral and Maxillofacial Radiology, Faculty of Dentistry, Hasanuddin University, Makassar, Indonesia

**Introduction:** Ameloblastoma is a benign yet highly aggressive odontogenic tumor capable of causing extensive destruction of the mandibular bone. Effective management requires resection with adequate bony margins to prevent the high likelihood of recurrence. Radiological modalities, particularly panoramic radiography, play a crucial role not only in establishing the diagnosis and determining the extent of resection but also in long-term postoperative monitoring to detect early structural changes or signs of recurrence.

**Case:** A 29-year-old male underwent a segmental mandibular resection followed by reconstruction using a titanium reconstruction plate under general anesthe-

sia. Clinical evaluation and radiological assessment using panoramic radiography were performed on the fifth and twenty-first postoperative days to assess the postoperative condition and the stability of the mandibular reconstruction.

**Discussion:** Panoramic radiography has proven to be a primary modality in the postoperative monitoring of patients with ameloblastoma due to its ability to rapidly and efficiently evaluate mandibular continuity and reconstruction stability. Although it is limited by its two-dimensional nature, panoramic imaging remains effective as an initial screening tool and should be supplemented with CT or CBCT when suspicious findings are present or when three-dimensional assessment is required to confirm bone healing and exclude recurrence.

## EP-313

## Central osteophytes on the superior surface of the mandibular condyle detected by cone-beam computed tomography

**Jin-Woo Han\***, In-Woo Park, Hang-Moon Choi  
*Department of Oral and Maxillofacial Radiology, College of Dentistry, Kangwon National University, South Korea*

**Introduction:** Osteophytes, emerging at the articular surface, usually exhibit a bony growth toward the anterior or anterior-superior region of the mandibular condyle rather than progressing upwards. Osteophytes arise from the superior articular surface of the condyle, referred to as a central osteophyte, is uncommon and frequently co-occurs with localized erosive change on the articular surface. Although central osteophytes are described in large load-bearing joints, they are considered rare in the temporomandibular joint (TMJ). We present two osteoarthritis cases of the TMJ with central osteophyte identified on cone-beam computed tomography (CBCT) and highlight diagnostic considerations.

**Case:** Case 1: A 55-year-old woman presented with 9 months of increasing left preauricular pain during mouth opening and mastication, with limited mouth opening and an anterior open bite. CBCT demonstrat-

ed bilateral central osteophyte on the superior surfaces of both mandibular condyles with adjacent peripheral erosive changes, leading to a diagnosis of bilateral TMJ osteoarthritis. Case 2: A 69-year-old woman presented after a forward fall with a linear, nondisplaced right mandibular ramus fracture. Initial CBCT showed no apparent bony change in either TMJ. At 5 months, follow-up CBCT revealed flattening with focal cortical erosion on the anterosuperior surface of the left condyle, suggesting early post-traumatic osteoarthritis. At 12 months, CBCT demonstrated progression with flattening of the anterosuperior condylar surface and a small central osteophyte on the left condyle.

**Discussion:** Central osteophyte morphology on the superior condylar surface may represent true osteophytic adaptation or a transient appearance during focal superior condylar resorption, potentially mimicking an osteophyte. Recognizing this pattern can improve staging and follow-up planning in TMJ osteoarthritis. CBCT is useful for characterizing superior condylar surface changes; adjunctive MRI may be considered to evaluate associated soft-tissue abnormalities.

## EP-314

## Performance of large language models on the Korean dental licensing examination: A comparative study

**Han-Gyeol Yeom**<sup>1\*</sup>, Byung-Do Lee<sup>1</sup>, Wan Lee<sup>1</sup>, Bong Chul Kim<sup>2</sup>, Woojun Kim<sup>3</sup>

<sup>1</sup>*Department of Oral and Maxillofacial Radiology and Wonkwang Dental Research Institute, College of Dentistry, Wonkwang University, Iksan, South Korea*

<sup>2</sup>*Department of Oral and Maxillofacial Surgery, Daejeon Dental Hospital, Wonkwang University College of Dentistry, Daejeon, South Korea*

<sup>3</sup>*The Robotics Institute, School of Computer Science, Carnegie Mellon University, Pittsburgh, PA, USA*

**Introduction:** This study investigated the potential application of Large Language Models (LLMs) in dental education and practice, with a focus on ChatGPT and Claude3-Opus. Using the Korean Dental Licensing Examination (KDLE) as a benchmark, we aimed to assess the capabilities of these models in the dental field.

**Materials and Methods:** This study evaluated three LLMs: GPT-3.5, GPT-4, and Claude3-Opus. We used the KDLE questionnaire from 2019 to 2023 as inputs to the LLMs and then used the outputs from the LLMs as the corresponding answers. The total scores for individual subjects were obtained and compared. We also compared the performance of LLMs with those of individuals who underwent the exams.

**Results:** Claude3-Opus performed best among the considered LLMs, except in 2019, when ChatGPT-4 performed best. Claude3-Opus and ChatGPT-4 surpassed the cut-off scores in all the years considered; this indicated that Claude3-Opus and ChatGPT-4 passed the KDLE, whereas ChatGPT-3.5 did not. However, all LLMs considered performed worse than humans, represented here by dental students in Korea. On average, the best-performing LLM annually achieved 85.4% of human performance.

**Conclusions:** Using the KDLE as a benchmark, our study demonstrates that although LLMs have not yet reached human-level performance in overall scores, both Claude3-Opus and ChatGPT-4 exceed the cut-off scores and perform exceptionally well in specific subjects.

#### EP-318

### Diagnostic value of panoramic radiography and CBCT in anterior mandibular ameloblastoma with root resorption: A case report

**Retno Septiana Ananda**<sup>1</sup>, Muhammad Fadil Hidayat<sup>2</sup>

<sup>1</sup>*Dentomaxillofacial Radiology Specialist Study Program, Faculty of Dentistry Hasanuddin University, Indonesia*

<sup>2</sup>*Department of Oral and Maxillofacial Radiology, Faculty of Dentistry Hasanuddin University, Indonesia*

**Introduction:** Ameloblastoma is the most common odontogenic tumour of the mandible and maxilla. Although locally invasive, it is slow-growing and typically presents as a painless swelling of the jaw. Diagnosis requires radiographic evaluation supported by adjunctive examinations, such as biopsy. In this case, panoramic radiography revealed tooth displacement

and tooth resorption. In contrast, the absence of root resorption is more indicative of odontogenic keratocysts or other lesions. Root resorption in ameloblastoma typically appears as a knife-edge pattern that forms an angle with the long axis of the tooth.

**Case:** A 34-year-old man presented for a panoramic examination with a chief complaint of swelling in the left anterior mandibular region and mobile teeth without associated pain. Panoramic radiography revealed a well-defined unilocular radiolucent lesion involving teeth 45–35. The lesion extended into the mandibular corpus and caused apical resorption of teeth 35, 33, 41, and 42. Histopathological examination confirmed the diagnosis of ameloblastoma.

**Discussion:** Ameloblastoma in the anterior mandibular region is uncommon and often presents with atypical clinical features, such as anterior tooth mobility and multiple root resorption. In this case, panoramic radiography revealed a well-defined unilocular lesion with tooth displacement and root resorption. Cone Beam CT (CBCT) provided a more detailed three-dimensional assessment of cortical expansion, the degree of root resorption, and the spatial relationship of the lesion, thereby increasing diagnostic accuracy. Accurate diagnosis relies on integrating radiographic evaluation particularly CBCT with histopathological confirmation. Early detection and comprehensive assessment are crucial for establishing a precise diagnosis and planning effective treatment to prevent further progression of the lesions.

#### EP-321

### Imaging features of lymphoma of the jaw: A report of 53 cases

**Jyotsna Jaswanth**<sup>1\*</sup>, Kyung-Hoe Huh<sup>2</sup>, Ju-Hee Kang<sup>3</sup>, Jo-Eun Kim<sup>2</sup>, Won-Jin Yi<sup>2</sup>, Min-Suk Heo<sup>2</sup>, Sam-Sun Lee<sup>2</sup>

<sup>1</sup>*Department of Oral and Maxillofacial Radiology, School of Dentistry Seoul National University*

<sup>2</sup>*Department of Oral and Maxillofacial Radiology, School of Dentistry and Dental Research Institute, Seoul National University*

<sup>3</sup>*Department of Oral and Maxillofacial Radiology, Seoul National University Dental Hospital*

**Introduction:** Patients with jaw lymphoma often present to dental clinics with swelling, tooth mobility, or non-healing extraction sites and are frequently misdiagnosed as inflammatory disease due to overlapping clinical and radiographic features between bone-origin lymphoma and inflammatory bone destruction. This study aimed to investigate the imaging features of bone-origin jaw lymphoma to identify radiographic characteristics that aid differentiation from odontogenic infections.

**Materials and Methods:** Fifty-three patients with histopathologically confirmed lymphoma of the jaw were retrospectively reviewed. Lesion location, distribution, cortical bone destruction type, internal structure, and metabolic activity were assessed using multimodal imaging including panoramic radiography, computed tomography (CT), magnetic resonance imaging (MRI), and positron emission tomography (PET).

**Results:** The most prevalent histopathologic subtype was diffuse large B-cell lymphoma (33/53, 62.26%). The most common location was the maxillary tuberosity region (13/53, 24.52%), and over 70% of maxillary lesions involved the maxillary sinus (26/37). CT revealed severe osteolytic lesions with more than 10 mm of cortical bone loss in 27 of 49 cases (55.10%), and micro-perforation with less than 1 mm cortical bone loss in 24 of 49 cases (48.97%). Complete trabecular bone loss was observed in 43/53 cases (81.13%). Over 80% of lesions demonstrated homogeneous enhancement on contrast-enhanced CT or MRI. PET demonstrated multifocal lesions beyond the jaw in 23 of 38 patients (60.52%) and intense fluorodeoxyglucose uptake, comparable to brain activity, in 28 of 38 lesions (73.68%).

**Conclusions:** Primary bone-origin lymphoma of the jaw typically presented as an osteolytic lesion with complete trabecular bone loss and severe cortical breach, and micro-perforation of cortical bone was prevalent in nearly half of the lesions. Recognition of these characteristic imaging features can aid in accurate diagnosis and differentiation from inflammatory osteolytic lesions and other malignancies, thereby facilitating timely biopsy, treatment, and outcomes.

EP-323

## Orbital floor extension of right maxillary craniofacial fibrous dysplasia: A case report

**Johanna Hasian Aritonang**<sup>1\*</sup>, Menik Priaminiarti<sup>2,3</sup>, Aloysius Putut Wijanarko<sup>2,3</sup>, Hanna H Bachtiar-Iskandar<sup>3</sup>, Vera Julia<sup>2</sup>, Larasati Kusuma<sup>2</sup>

<sup>1</sup>Resident in Department of Dentomaxillofacial Radiology, Faculty of Dentistry, Universitas Indonesia, Indonesia

<sup>2</sup>Universitas Indonesia Hospital, Indonesia

<sup>3</sup>Department of Dentomaxillofacial Radiology, Faculty of Dentistry, Universitas Indonesia, Indonesia

**Introduction:** An atypical bone disorder known as fibrous dysplasia (FD) involves numerous skeletal areas, especially the cranial and facial bones. Monostotic FD has been reported most commonly affecting the craniofacial region. Optic nerve is critically at high risk when there is orbital involvement with potential cause to visual impairment. This report aims to present radiographic features of craniofacial fibrous dysplasia in maxilla extending to the orbital floor.

**Case:** A 47-year-old woman came to Universitas Indonesia Hospital complaining of intermittent pain caused by caries on upper right posterior tooth. Slight asymmetry was identified clinically and panoramic radiograph revealed a radiopaque area with a heterogeneous pattern in the right maxilla. A CT scan was performed hence no further examinations were required since the imaging findings were consistent with craniofacial fibrous dysplasia and the patient remained asymptomatic. Radiographic findings demonstrated characteristic features of fibrous dysplasia, particularly a ground-glass appearance which shows internal radiopaque structures and irregular in shape and has ill-defined borders. The radiopacity of the lesion was situated in the right posterior maxilla expanding from the region of tooth 11 extending to the tuberosity. Discontinuity of the right maxillary sinus and zygoma was found extending from the alveolar bone and superiorly displaced the right orbital floor, causing medially expansion of the lateral wall of the right nasal fossa.

**Discussion:** Due to the anatomical complexity of the craniofacial area, such lesions may lead to multiple symptoms, moreover if it extends to anatomically critical structures in maxilla, particularly the orbital re-

gion, it may lead to visual deterioration. Craniofacial fibrous dysplasia is frequently detected incidentally in asymptomatic individuals undergoing radiographic examination. The presence of a characteristic ground-glass appearance on CT may be pivotal for detecting fibrous dysplasia. Conservative monitoring remains appropriate for asymptomatic cases without evidence of progression.

### EP-326

## Internal structural pattern of ameloblastoma on CT imaging: A comparative analysis of maxillary and mandibular lesions – A case series

**Firda Bilma Assyfa Fauziah**<sup>1\*</sup>, Bramma Kiswanjaya<sup>3</sup>, Aloysius Putut Wijanarko<sup>2,3</sup>, Hanna H. Bachtiar Iskandar<sup>3</sup>, Vera Julia<sup>2</sup>, Larasati Kusuma<sup>2</sup>

<sup>1</sup>Resident in Department of Dentomaxillofacial Radiology, Faculty of Dentistry, Universitas Indonesia, Jakarta Indonesia

<sup>2</sup>Universitas Indonesia Hospital, Depok, Indonesia

<sup>3</sup>Department of Dentomaxillofacial Radiology, Faculty of Dentistry, Universitas Indonesia, Jakarta Indonesia

**Introduction:** The internal structural pattern of ameloblastoma plays a critical role in radiological interpretation and surgical decision-making, particularly when differentiating maxillary from mandibular presentations. Ameloblastoma is a benign but locally aggressive odontogenic tumor characterized by slow expansion, cortical thinning or perforation, root resorption, and multilocular radiolucent patterns such as honeycomb and soap-bubble configurations. This case series describes the radiographic and CT characteristics of ameloblastoma in the maxilla and mandible, emphasizing lesion morphology, extent, and histopathological correlation when available.

**Case:** Three patients were evaluated: a 53-year-old male with progressive swelling of the left posterior maxilla, a 59-year-old female with a long-standing recurrent lesion in the left mandible, and a 52-year-old female presenting with swelling extending from the submental region to the neck; histopathology confirmed mixed-type ameloblastoma (plexiform and ac-

anthomatous). Panoramic in all cases revealed multilocular radiolucent lesions with varying degrees of cortical involvement, tooth displacement, and root resorption. CT imaging with axial, coronal, and sagittal reconstructions was performed to assess lesion boundaries, internal structure, cortical integrity, and invasion into adjacent anatomical space.

**Discussion:** Ameloblastoma may demonstrate heterogeneous internal structure. In these present cases the maxilla showed a multilocular honeycomb-like extending into the nasal fossa and maxillary sinus; CT shows lytic masses and cortical perforation. Within the posterior mandible, loculations are typically larger, present extensive multilocular curved septa; CT reveals solid masses containing cystic, necrotic, and calcified components, suggestive of aggressive behavior. Other findings, a multilocular with scalloped border, soap-bubble appearance, root resorption, and inferior expansion. CT imaging typically reveals a well-defined lytic mass with cortical thinning or perforation, internal calcifications, root resorption, and aggressive local infiltration. Across all cases, CT imaging provided superior delineation of lesion margins, internal separations, and cortical destruction, underscoring its indispensable role in diagnosis and surgical planning.

### EP-330

## Report two cases and CBCT radiographic analysis of unilateral and bilateral kissing molars

**Merry Annisa Damayanti**<sup>1\*</sup>, Aries Sugih Budhiana<sup>2</sup>, Tati Siti Patimah<sup>3</sup>, Belly Sam<sup>1</sup>, Lusi Epsilawati<sup>1</sup>

<sup>1</sup>Department of Oral and Maxillofacial Radiology, Universitas Padjadjaran, Indonesia

<sup>2</sup>Sumedang Regional General Hospital, Indonesia

<sup>3</sup>Jasa Kartini Hospital, Indonesia

**Introduction:** Kissing molars is a very rare pathological condition of the mandible. These molars are impacted permanent molars with occlusal surfaces that touch each other while their roots point in opposite directions, sharing a single follicular space with a fused cemento-enamel junction. The primary etiologic factor of kissing molars is rotation or another misalignment of the tooth crown, resulting in the tooth being misoriented.

**Case:** A 33-year-old male patient complained of swollen right back teeth and clinical examination showed that tooth 48 had not erupted. A 28-year-old female patient complained of pain in the left and right cheeks, no intra-oral or extra-oral enlargement, and clinical examination showed that teeth 38 and 48 had not erupted.

**Discussion:** Kissing molars can occur unilateral or bilateral, although unilateral cases are more frequently reported than bilateral ones. The main causes of unilateral kissing molars are related to local or structural factors in the affected area, such as fractures of the maxilla or mandible, local disorders such as cysts or tumors, and chronic infections around the second or third molars, which can cause bone damage and affect tooth eruption on one side. The main causes of bilateral kissing molars usually involve systemic factors, genetics, and are a result of small jaw size or narrow arches on both sides. The most common treatment for kissing molars is extraction of the impacted tooth. CBCT-3D radiography results can see the image of kissing molars and surrounding structures such as the mandibular canal and changes in the alveolar bone structure which must be known in planning surgical intervention.

EP-334

## Deep curriculum learning for TMJ osteoarthritis classification on dental panoramic radiographs

Dahee Kim<sup>1\*</sup>, Won-Jin Yi<sup>1,2</sup>

<sup>1</sup>Department of Applied Bioengineering, Graduate School of Convergence Science and Technology, Seoul National University, Seoul, South Korea

<sup>2</sup>Department of Oral and Maxillofacial Radiology and Dental Research Institute, School of Dentistry, Seoul National University, Seoul, South Korea

**Introduction:** Temporomandibular Joint Osteoarthritis (TMJOA) is a prevalent degenerative disorder characterized by pain, functional impairment, and malocclusion, profoundly impacting patients' quality of life. Early and precise diagnosis is critical to mitigate disease progression; however, detecting subtle morphological changes in the initial stages presents significant diagnostic challenges. Although cone-beam computed

tomography (CBCT) provides high diagnostic precision, its limited accessibility and higher costs restrict its routine clinical use. In contrast, panoramic radiography is widely available and cost-effective, making it a practical modality for large-scale screening. However, the subtle and continuous transition from normal to incipient stages poses substantial difficulties for conventional deep learning models in identifying early degenerative changes. To overcome this challenge, this study aims to enhance the automatic classification accuracy and diagnostic efficiency of TMJOA on panoramic radiographs through a curriculum-guided learning approach.

**Materials and Methods:** A dataset of panoramic radiographs was utilized, consisting of 1,620 cropped images of the mandibular condyle region of interest (ROI), including 540 normal, 540 incipient, and 540 TMJOA cases. An ImageNet-pretrained DenseNet-201 was fine-tuned to classify TMJOA stages from single-channel ROI inputs. A curriculum-guided learning strategy was employed, in which the model was trained progressively by first learning from clearly distinguishable classes and subsequently incorporating more ambiguous cases.

**Results:** The proposed model achieved a macro-averaged area under the curve (AUC) of 0.93, an accuracy of 0.89, a sensitivity of 0.83, and a specificity of 0.91. In contrast, the model trained without curriculum learning achieved a macro-averaged AUC of 0.91, an accuracy of 0.85, a sensitivity of 0.77, and a specificity of 0.89.

**Conclusions:** These results demonstrate that the curriculum-guided learning approach enables accurate and consistent TMJOA stage classification on panoramic radiographs, improving diagnostic reliability and efficiency.

### Funding

This work was supported by the National Research Foundation of Korea (NRF) grant funded by the Korean government (MSIT) (No. 2023R1A2C2 00532611). This work was also supported by the Technology Innovation Program (or Industrial Strategic Technology Development Program-Advanced Biomaterials) (RS-2025-14322975), funded by the Ministry of Trade, Industry & Energy (MOTIE).

EP-336

## DentalRegiformer: A fully automated deep learning framework for coarse-to-fine registration between intraoral scan and CBCT image

Heejin Yun<sup>1</sup>, Won-Jin Yi<sup>1,2</sup>

<sup>1</sup>Interdisciplinary Program of Bioengineering, Graduate School of Engineering, Seoul National University, Seoul, South Korea

<sup>2</sup>Department of Oral and Maxillofacial Radiology School of Dentistry, Seoul National University, Seoul, South Korea

**Introduction:** Precise registration between intraoral scans (IOSs) and CBCT images is essential for many digital dentistry applications. The purpose of this study was to develop DentalRegiformer, a fully automated, end-to-end deep learning framework that ensures accurate registration between IOS and CBCT images.

**Materials and Methods:** The network was trained on 88 paired CBCT-IOS datasets from 44 patients, with ground-truth alignments obtained through manual registration performed by trained dental students. To enhance clinical efficiency, a multi-stage coarse-to-fine strategy is proposed to integrate segmentation, classification, and registration into a unified pipeline. First, tooth segmentation is performed on CBCT volumes using nnU-Net to generate segmented tooth regions for alignment. Simultaneously, IOS datasets are classified as maxillary or mandibular dentition using a hybrid representation that combines geometric descriptors. Registration is then conducted in two phases: coarse alignment using a DCP framework, followed by fine alignment using GeoTransformer's local-to-global iterative refinement to progressively enhance correspondence accuracy and achieve precise rigid registration.

**Results:** The segmentation model achieved robust results, with a Dice coefficient of 0.924, precision of 0.916, and recall of 0.934. The DGCNN classifier perfectly distinguished maxillary and mandibular arches, achieving sensitivity, specificity, ROC, and accuracy of 1.000. For registration, DentalRegiformer accurately predicted transformation between IOS and CBCT images, yielding an overall RMSE of 0.556 mm;

MAEs of 0.231mm, 0.329 mm, and 0.283 mm along the x-, y-, and z-axes, respectively; and inference time of 19.623 seconds.

**Conclusions:** Therefore, DentalRegiformer is a fully automated, deep learning-based solution that minimizes manual intervention and improves clinical efficiency. The framework streamlines digital dental workflows, reduces operator-dependent errors, and facilitates automated, personalized dental care.

**Funding:** This work was supported by the National Research Foundation of Korea (NRF) grant funded by the Korean government (MSIT) (No. 2023R1A2C2 00532611). This work was also supported by the Technology Innovation Program (or Industrial Strategic Technology Development Program-Advanced Biomaterials) (RS-2025-14322975), funded by the Ministry of Trade, Industry & Energy (MOTIE).

EP-338

## Investigation of tumor-related factors contributing to variability in intraoral ultrasonographic assessment of depth of invasion

Masaki Takamura<sup>1\*</sup>, Taichi Kobayashi<sup>1</sup>, Yutaka Nikkuni<sup>2</sup>, Kouji Katsura<sup>1</sup>, Manabu Yamazaki<sup>2</sup>, Jun-ichi Tanuma<sup>2,3</sup>, Takafumi Hayashi<sup>1</sup>

<sup>1</sup>Division of Oral and Maxillofacial Radiology, Faculty of Dentistry & Graduate School of Medical and Dental Sciences, Niigata University, Japan

<sup>2</sup>Division of Oral Pathology, Faculty of Dentistry & Graduate School of Medical and Dental Sciences, Niigata University, Japan

<sup>3</sup>Oral Pathology Section, Department of Surgical Pathology, Niigata University Medical & Dental Hospital, Japan

**Introduction:** Intraoral ultrasonography (US) is widely used for the preoperative assessment of depth of invasion (DOI) in tongue squamous cell carcinoma (SCC). Although its overall diagnostic reliability has been well documented, variability in DOI measurements remains a clinically relevant issue. The present study aimed to characterize patterns of measurement variability in intraoral US and to identify tumor-relat-

ed characteristics associated with such discrepancies.

**Materials and Methods:** This retrospective study included patients with primary tongue SCC who underwent preoperative intraoral US examination followed by surgical resection at our institution between April 2014 and March 2022. Tumors were stratified according to clinical and histopathological parameters, including clinical growth pattern, pathological tumor size, pathological T classification, and the pattern of invasion based on the Yamamoto–Kohama classification. Agreement between ultrasonographic and histopathological DOI measurements was evaluated using nonparametric correlation analyses and agreement-based statistical methods.

**Results:** Intraoral US showed good agreement with histopathological DOI measurements across most tumor subgroups. However, increased measurement variability was observed in tumors with greater DOI and larger pathological tumor size. Lesions with an exophytic growth pattern tended to yield higher DOI on ultrasonography, whereas tumors exhibiting diffuse invasive patterns more frequently showed lower DOI compared with histopathological measurements.

**Conclusions:** Intraoral ultrasonography is a useful modality for assessing DOI in tongue SCC; however, measurement variability is influenced by specific tumor growth patterns and invasive characteristics. Recognition of these tendencies may facilitate more accurate interpretation of ultrasonographic findings in clinical practice.

#### EP-340

### Multi-material physics-informed neural network framework for predicting displacement fields in dental crowns under varying occlusal forces

Hyunbin Yun<sup>1\*</sup>, Won-Jin Yi<sup>1,2,3</sup>

<sup>1</sup>Interdisciplinary Program of Bioengineering, Graduate School of Engineering, Seoul National University, Seoul 03080, South Korea

<sup>2</sup>Applied Bioengineering, Graduate School of Convergence Science and Technology, Seoul National University, Seoul

03080, South Korea

<sup>3</sup>Department of Oral and Maxillofacial Radiology School of Dentistry, Seoul National University, Seoul 03080, South Korea

**Introduction:** Finite element analysis (FEA) is well-established in dental biomechanics but requires substantial computational resources for each simulation. Physics-informed neural networks (PINNs) offer a promising alternative by learning biomechanical behavior across multiple conditions. This study developed a PINN framework to predict displacement fields in dental crowns across three materials under varying occlusal forces.

**Materials and Methods:** A PINN architecture was trained on finite element simulations performed in FEniCS for three crown materials (zirconia, gold, lithium disilicate) under forces ranging 50-2000N. The model incorporated material encodings and adaptive instance normalization (AdaIN) for multiple materials and loading conditions. Training utilized 18 conditions (3 materials × 6 forces: 50, 250, 500, 1000, 1500, 2000N) out of 40 available levels. Force-dependent loss weighting emphasized accurate prediction at lower forces where displacement magnitudes are smaller. Model performance was evaluated on 21 unseen loading conditions using R<sup>2</sup> scores and relative error metrics.

**Results:** The PINN achieved excellent interpolation performance with mean R<sup>2</sup> of 0.945 across unseen conditions. Performance varied across force ranges: R<sup>2</sup> = 0.747 (100N), 0.945 (200N), 0.962 (400-600N), and >0.99 (≥750N). Force-weighted training improved low-force predictions, with 100N R<sup>2</sup> improving from 0.69 to 0.747. Relative errors averaged 15.2% across materials, with displacement predictions accurate to within 20-50 μm for most conditions. Material-specific predictions showed consistent accuracy (zirconia: R<sup>2</sup>=0.94, gold: R<sup>2</sup>=0.93, lithium disilicate: R<sup>2</sup>=0.92).

**Conclusions:** The PINN successfully learned multi-material behavior from sparse FEA data, achieving over three orders of magnitude faster than traditional FEA. The framework demonstrates excellent interpolation capability for unseen loading conditions, while performance remains lower at very low forces. This approach enables rapid biomechanical analysis for clinical applications including treatment planning

and material selection.

**Funding:** This work was supported by the National Research Foundation of Korea (NRF) grant funded by the Korean government (MSIT) (No. 2023R1A2C2 00532611). This work was also supported by the Technology Innovation Program (or Industrial Strategic Technology Development Program-Advanced Biomaterials) (RS-2025-14322975), funded by the Ministry of Trade, Industry & Energy (MOTIE).

### EP-341

## Radiographic hallmarks of a rare hybrid odontogenic keratocyst–ameloblastoma of the mandible: A case report

**Donna Trye Liling**<sup>1\*</sup>, Fadhilil Ulum Abdul Rahman<sup>1</sup>

<sup>1</sup>*Dentomaxillofacial Radiology Specialist Study Program, Faculty of Dentistry Hasanuddin University, Indonesia*

<sup>2</sup>*Department of Oral and Maxillofacial Radiology, Faculty of Dentistry, Hasanuddin University, Makassar, Indonesia*

**Introduction:** Hybrid odontogenic keratocyst–ameloblastoma is a rare pathological entity combining the cystic yet locally aggressive behavior of odontogenic keratocyst (OKC) with the neoplastic epithelial component of ameloblastoma. Due to overlapping clinicoradiographic characteristics, this lesion presents diagnostic challenges and may demonstrate biological behavior exceeding that of conventional OKC. Radiographic assessment is essential to delineate lesion extent, growth pattern, and its impact on adjacent structures. This case report describes the radiographic features of a suspected hybrid mandibular lesion, integrating clinicoradiographic and histopathological findings, with emphasis on postoperative bone healing evaluated using panoramic radiographs.

**Case:** A 19-year-old female presented with a progressively enlarging mandibular swelling for three months following posterior tooth extraction. Clinical examination revealed facial asymmetry with a firm, non-tender mandibular swelling and intraoral vestibular expansion from teeth 36 to 42, accompanied by grade II mobility of adjacent teeth. Panoramic radiography demonstrated a multilocular, soap-bubble–like radiolucent lesion

extending from the posterior to anterior mandibular body, associated with tooth displacement without extensive root resorption or cortical destruction. Histopathological analysis revealed an odontogenic keratocyst with a focal ameloblastomatous component. Based on clinicoradiographic and histopathological correlation, a rare suspected hybrid odontogenic lesion was diagnosed, and mandibular dredging with multiple tooth extractions under general anesthesia was performed.

**Discussion:** OKC typically exhibits anteroposterior extension with limited buccolingual expansion, whereas ameloblastoma commonly presents as a multilocular soap-bubble lesion with cortical expansion and root resorption. In this case, the lesion demonstrated combined radiographic features consistent with a hybrid pathology. Postoperative panoramic radiographs showed homogeneous bone regeneration supporting favorable healing following conservative surgical management. This case highlights the importance of radiologic–histopathologic correlation in recognizing hybrid odontogenic lesions and guiding appropriate treatment planning and follow-up.

### EP-342

## Pseudoepitheliomatous hyperplasia associated with peripheral ameloblastoma: A case report

**Muhammad Raihan Yusuf Arrahman**<sup>1\*</sup>, Hanna H Bachtiar-Iskandar<sup>2</sup>, Menik Priaminiarti<sup>2,3</sup>, Aloysius Putut Wijanarko<sup>2,3</sup>, I Nyoman Guswan<sup>1</sup>, Derry Haryono<sup>1</sup>, Vera Julia<sup>3</sup>, Larasati Kusuma<sup>3</sup>

<sup>1</sup>*Resident in Department of Dentomaxillofacial Radiology, Faculty of Dentistry, Universitas Indonesia, Indonesia*

<sup>2</sup>*Department of Dentomaxillofacial Radiology, Faculty of Dentistry, Universitas Indonesia, Indonesia*

<sup>3</sup>*Universitas Indonesia Hospital, Indonesia*

**Introduction:** Pseudoepitheliomatous hyperplasia (PEH) is a benign epithelial proliferation, which may extend into the dermis as a reactive response to chronic irritation, inflammation, or underlying lesions. In oral cavity, PEH is clinically and histopathologically relevant because it may overlie or be associated with

underlying odontogenic tumors, including Peripheral Ameloblastoma (PA). PA is a rare extraosseous ameloblastoma that arises in gingival soft tissues and may present diagnostic difficulties. This report describes a rare case of PA associated with PEH, with emphasis on radiological findings and their correlation with histopathological features.

**Case:** A 47-year-old woman presented with a persistent swelling in the right maxilla for 1.5 years. The lesion initially presented as a small gingival enlargement and gradually increased in size, with bleeding on palpation. Panoramic radiography revealed an irregular and ill-defined radiolucent lesion in the posterior right maxilla extending towards the maxillary sinus accompanied by root resorption of adjacent teeth and displacement of sinus floor. CT imaging demonstrated unilocular lesion with cortical bone destruction and intra-sinus calcifications in posterior right maxilla. Histopathological examination showed stratified squamous epithelium with epithelial thickening, branched rete ridges, basal cell palisading, and focal ulceration, and areas of low-grade epithelial dysplasia with Peripheral Ameloblastoma considered in the differential diagnosis.

**Discussion:** Peripheral Ameloblastoma is a rare extraosseous odontogenic tumor that may be challenging to identify due to its peripheral presentation and presence of overlying Pseudoepitheliomatous Hyperplasia. In this case, panoramic and CT imaging were useful to show maxillary sinus involvement and cortical bone destruction which suggested locally aggressive behavior despite its benign nature. The radiographic appearance mimicked unicystic ameloblastoma. This case highlights the importance of radiologic – histopathologic correlation for accurate diagnosis and appropriate clinical management.

EP-352

## Cone-beam computed tomography findings of concurrent florid cemento-osseous dysplasia and secondary maxillary osteomyelitis: A case report

**Bayu Trinanda Putra**<sup>1\*</sup>, Sazkia Febradhany Tania<sup>2</sup>,

Hanna H Bachtiar-Iskandar<sup>1</sup>, Mohammad Adhitya Latief<sup>3</sup>

<sup>1</sup>*Department of Dentomaxillofacial Radiology, Universitas Indonesia, Indonesia*

<sup>2</sup>*Resident in Dentomaxillofacial Radiology, Universitas Indonesia, Indonesia*

<sup>3</sup>*Department of Oral and Maxillofacial Surgery, Universitas Indonesia, Indonesia*

**Introduction:** Florid cemento-osseous dysplasia (FCOD) is a subtype of cemento-osseous dysplasia characterized by the replacement of normal cancellous bone with fibrous tissue and cemento-osseous material in multiple regions of the jaws. These lesions are usually asymptomatic and are often detected incidentally on radiographic examination. In certain cases, enlargement of the lesion and its relatively avascular nature may predispose the affected area to secondary infection, resulting in osteomyelitis. This report presents a rare case of FCOD complicated by secondary maxillary osteomyelitis, with emphasis on cone-beam computed tomography (CBCT) findings.

**Case:** A 58-year-old woman presented with swelling and pain in the upper right cheek and was referred for CBCT examination. There was no history of systemic disease. Clinical examination revealed buccal expansion in the edentulous posterior right maxillary region. Additional edentulous areas were noted in the mandible, and retained roots were present in the left posterior maxilla. CBCT images demonstrated a radiopaque mass in the posterior right maxilla resembling a sequestrum, surrounded by hypodense areas indicating bone destruction, with associated discontinuity of the alveolar cortical bone. Similar radiopaque lesions were identified in multiple regions, including the apical area of tooth #27 and edentulous regions corresponding to teeth #36, #37, and #47.

**Discussion:** Florid cemento-osseous dysplasia should be differentiated from other conditions with similar radiographic appearances, such as Paget's disease, which typically involves multiple bones and is commonly associated with hypercementosis rather than sequestrum formation. Secondary infection may alter the characteristic well-defined borders of FCOD, resulting in ill-defined margins suggestive of osteomyelitis. This case demonstrates the value of CBCT in identifying secondary infection and cortical disruption in FCOD. Careful radiologic evaluation is essential, as secondary

osteomyelitis may lead to significant bone destruction if not recognized and managed appropriately.

EP-353

## Palatal mucoepidermoid carcinoma with benign-appearing features: A radiologic–pathologic diagnostic pitfall

**Virdha Dwi Mulya**<sup>1\*</sup>, Irfan Sugianto<sup>1,2</sup>

<sup>1</sup>*Dentomaxillofacial Radiology Specialist Study Program, Faculty of Dentistry Hasanuddin University, Indonesia*

<sup>2</sup>*Department of Oral and Maxillofacial Radiology, Faculty of Dentistry, Hasanuddin University, Makassar, Indonesia*

**Introduction:** Mucoepidermoid carcinoma (MEC) of the minor salivary glands may demonstrate benign-appearing radiologic features, particularly in low-grade lesions, leading to diagnostic challenges and potential misinterpretation as benign tumors such as pleomorphic adenoma. This case report aims to highlight the radiologic–pathologic diagnostic pitfall of low-grade MEC of the palate and to emphasize the limitations of conventional imaging in distinguishing benign from malignant minor salivary gland tumors.

**Case:** An 18-year-old woman presented with a slowly enlarging mass on the right posterior hard palate for approximately two years, associated with mild discomfort during mastication. Panoramic radiography revealed no specific maxillary bone abnormalities. Cone-beam computed tomography (CBCT) demonstrated a well-defined hyperdense lesion abutting the floor of the right maxillary sinus and nasal cavity, causing displacement without bone destruction. Initial incisional biopsy suggested pleomorphic adenoma. Based on benign-appearing clinical and radiologic features, the lesion was initially managed as a benign salivary gland tumor. However, definitive histopathologic examination following surgical excision revealed low-grade mucoepidermoid carcinoma.

**Discussion:** This case underscores a radiologic–pathologic diagnostic pitfall in palatal minor salivary gland tumors. Low-grade MEC may closely mimic benign lesions on radiographic imaging due to its indolent growth pattern and absence of early osseous invasion,

underscoring the importance of correlating imaging findings with definitive histopathologic evaluation.

EP-354

## Evaluation of dental students' knowledge of panoramic radiographs; normal anatomy and jaw lesions

**Yoon Joo Choi**<sup>1\*</sup>, Sang-Sun Han<sup>1</sup>

<sup>1</sup>*Department of Oral and Maxillofacial Radiology, Yonsei University College of Dentistry, Seoul, Korea*

**Introduction:** The purpose of this study was to examine dental students' understanding level of anatomical structures and to compare their competency in diagnosing jaw lesions among three groups with different levels of understanding using panoramic radiographs.

**Materials and Methods:** In this retrospective study, the competency test results of 125 dental students conducted on November 8, 2023, at Yonsei Dental University were analyzed. The test comprised 50 panoramic radiographs including 10 anatomical structures and 40 jaw lesions. The 40 jaw lesions were classified into four categories: cysts, benign tumors, inflammation or malignancy, and other bone lesions. The mean score for the 10 questions depicting anatomical structures and the mean accuracy rate for diagnosing the 40 jaw lesions were assessed. Based on their scores on the anatomical structure questions, the 125 students were divided into three groups (upper, middle, and lower). The accuracy rates for diagnosing jaw lesions among these groups were statistically analyzed using the Kruskal–Wallis test ( $P = 0.05$ ).

**Results:** Among all students, the mean score for anatomical structures was 5.99 out of 10, and the mean accuracy rate for diagnosing jaw lesions was 44.8 %. In the analysis of jaw lesions, the four categories exhibited significant differences in accuracy rates: cyst (53.8 %), benign tumor (47.7 %), inflammation or malignancy (45.0 %), and other bone lesion (32.7 %). The three groups based on anatomical structure scores showed significantly different accuracy rates for diagnosing jaw lesions ( $p < 0.05$ ). The upper group, with the highest anatomical structure scores, achieved an

accuracy rate of 54.5 %, outperforming the other groups.

**Conclusions:** Knowledge of anatomical structures enhances the ability to diagnose jaw lesions using panoramic radiographs. These findings underscore the importance of anatomical education in dental curricula to improve diagnostic accuracy.

## EP-357

## Evaluation of an atypical radiolucent lesion in the anterior mandible of a pediatric patient with Burkitt's Lymphoma: A case report

**Farris Zakki Giffari**<sup>1\*</sup>, Menik Priaminiarti<sup>2,3</sup>, Aloysius Putut Wijanarko<sup>2,3</sup>, Demitria Naranti Santoso<sup>1</sup>, Dwi Ariawan<sup>2,4</sup>, Larasati Kusuma Putri<sup>2</sup>

<sup>1</sup>Resident in Department of Dentomaxillofacial Radiology, Faculty of Dentistry, Universitas Indonesia, Jakarta, Indonesia

<sup>2</sup>Universitas Indonesia Hospital, Indonesia

<sup>3</sup>Department of Dentomaxillofacial Radiology, Faculty of Dentistry, Universitas Indonesia, Jakarta, Indonesia

<sup>4</sup>Departement of Oral and Maxillofacial Surgery, Faculty of Dentistry, Universitas Indonesia, Jakarta, Indonesia

**Introduction:** Burkitt's lymphoma is an aggressive, poorly differentiated rare type of Non-Hodgkin's Lymphoma. Radiographically it appears as a radiolucent area mimicking osteolytic lesions such as Central Giant Cell Granuloma (CGCG). The purpose of this report is to describe the radiographic findings of a radiolucent lesion in the anterior mandible of a pediatric patient.

**Case:** 7-year old female patient was referred with complaints of gingival swelling on the anterior mandible. Clinical examinations showed a swelling on the anterior vestibule that shows coloration indistinguishable from the surrounding tissue, with mobility of the involved anterior teeth. Cone-Beam Computed Tomography (CBCT) examination revealed an oval shaped unilocular hypodense lesion with ill-defined border in the mandible extending from the left mandibular deciduous molar, crossing the midline, to the right mandibular incisor. The lesion seems to have caused destruction of the surrounding bone resulting

in the affected teeth to have a floating appearance. Abdominal Multi-Slice Computed Tomography examinations presented solid masses in multiple locations. These solid masses are biopsied as Stage IV Burkitt's lymphoma with metastatic involvement of the oral cavity.

**Discussion:** The initial radiodiagnosis for this particular lesion is CGCG based on the age of the patient, location, and osteolytic characteristic of the lesion. Results from the abdominal biopsy came out that Burkitt's lymphoma has metastasized into the oral cavity and presented this atypical lesion on CBCT Imaging. This case highlights the importance of careful radiographic evaluation using CBCT to assess lesion characteristics and extent. However, radiographic findings alone may be insufficient for definitive diagnosis. Correlation with clinical findings, systematic imaging approach, and histopathological examination is essential to establish an accurate diagnosis. Early recognition of such atypical presentations is crucial to ensure prompt diagnosis and appropriate management of malignancies such as Burkitt's lymphoma.

## EP-358

## A rare pediatric case of maxillary dentigerous cyst with extensive sinus involvement: Case report

**Dewi Vasthi Manikmaya**<sup>1\*</sup>, Menik Priaminiarti<sup>2\*</sup>, Syurri Innaddinna Syahraini<sup>2\*</sup>, Eka Yulianti Puspitasari<sup>1\*</sup>, William Rachmat Fatah<sup>3\*</sup>

<sup>1</sup>Resident in Department of Dentomaxillofacial Radiology, Faculty of Dentistry, Universitas Indonesia, Indonesia

<sup>2</sup>Department of Dentomaxillofacial Radiology, Faculty of Dentistry, Universitas Indonesia, Indonesia

<sup>3</sup>Department of Maxillofacial Surgery, YARSI University Dental Hospital, Indonesia

**Introduction:** Dentigerous cysts are the second most prevalent developmental odontogenic cysts. Typically, the occurrence rate among children is quite small, falling within the range of 4% to 9%, and it is unusual for maxillary area to be affected. This case report presents a large anterior maxillary dentigerous cyst in children with significant tooth displacement and maxillary sinus involvement.

**Case:** An eight-year-old boy presented with swelling of the upper left gingiva that had been present for approximately a few months. Extraoral examination showed facial asymmetry without tenderness. Intraoral examination showed a soft swelling on the anterior maxillary gingiva, displacement of left permanent central incisor and mobility of adjacent deciduous teeth. CBCT imaging revealed a well-defined, corticated, hypodense lesion surrounding the crown of the impacted permanent lateral incisor. The lesion extended from the lateral root of left permanent central incisor extending to tooth germ of left first permanent premolar. The lesion displaced the tooth germ of the left permanent canine and the maxillary sinus floor superiorly, with associated hyperdense opacification of the sinus, while the adjacent primary incisor demonstrated root resorption up to the middle third.

**Discussion:** In the present case, the cyst interferes eruption of the permanent lateral incisor and displaced adjacent tooth germs and the maxillary sinus floor, leading to a multidirectional maxillary expansion, cortical thinning, and sinus opacification. In pediatric patients, an expansile radiolucent lesions involving the maxilla and a maxillary sinus warrant consideration of differential diagnoses such as odontogenic keratocyst, unicystic ameloblastoma, and radicular cyst; however, the pericoronal location, corticated margin, and association with an unerupted tooth favored the diagnosis of dentigerous cyst. CBCT imaging was essential for accurately evaluating lesion extent, tooth displacement, cortical involvement, and sinus changes, emphasizing the importance of advanced imaging in distinguishing dentigerous cysts from other expansile radiolucent lesions in children.

EP-360

## Contralateral-guided CBCT alveolar bone defect restoration for bone graft volume assessment prior to implant placement

Hoyoon Choi<sup>1\*</sup>, Won-Jin Yi<sup>1,2,3</sup>

<sup>1</sup>Applied Bioengineering, Graduate School of Convergence Science and Technology, Seoul National University, Seoul, South Korea

<sup>2</sup>Interdisciplinary Program of Bioengineering, Graduate School

of Engineering, Seoul National University, Seoul, South Korea

<sup>3</sup>Department of Oral and Maxillofacial Radiology School of Dentistry, Seoul National University, Seoul, South Korea

**Introduction:** Adequate residual alveolar bone is essential for stable dental implant placement. However, post-extraction bone resorption frequently necessitates bone grafting. In current clinical practice, estimation of the required bone graft volume largely relies on empirical judgment, limiting quantitative and reproducible treatment planning. This study proposes a contralateral-guided, cone-beam computed tomography (CBCT)-based alveolar bone defect restoration framework for quantitative assessment of bone graft volume prior to implant placement.

**Materials and Methods:** CBCT datasets comprising 830 simulated alveolar defect cases and 51 clinical defect cases were used in this study. The proposed framework employs a Wasserstein Generative Adversarial Network with gradient penalty (WGAN-GP) to reconstruct defect regions by learning the anatomical distribution of contralateral healthy structures. To address the limited availability of clinical data, stochastic defect simulation was used for supervised pre-training, followed by adversarial refinement using clinical CBCT data. Bone graft volume was quantitatively estimated by calculating volumetric differences between original defect CBCT images and the corresponding restored CBCT volumes.

**Results:** In simulated evaluations, defect regions were defined based on volumetric differences between pre- and post-restoration CBCT images, and Dice similarity coefficients were calculated accordingly. The proposed method achieved a Dice similarity coefficient of 0.783, demonstrating accurate and structurally consistent reconstruction of defect regions. Compared with interpretation based solely on defect CBCT images, the restored CBCT volumes enabled clearer identification of graft-required regions through spatial separation. In addition, the restored results preserved anatomical consistency with surrounding bone structures and exhibited continuity of alveolar bone contours, which was also observed in clinical CBCT cases without compromising adjacent bone morphology.

**Conclusions:** The proposed contralateral-guided, WGAN-based CBCT alveolar bone defect restoration

framework enables quantitative assessment of bone graft requirements prior to implant placement and may support standardized, decision making in implant treatment planning and bone graft material selection.

**Funding:** This work was supported by the National Research Foundation of Korea (NRF) grant funded by the Korean government (MSIT) (No. 2023R1A2C2 00532611). This work was also supported by the Technology Innovation Program (or Industrial Strategic Technology Development Program-Advanced Biomaterials) (RS-2025-14322975), funded by the Ministry of Trade, Industry & Energy (MOTIE).

## EP-362

## An uncommon case description of an anterior mandibular odontogenic keratocyst

**Irind Octaviani Amansyah**<sup>1\*</sup>, Menik Priaminiarti<sup>2,3</sup>, Aloysius Putut Wijanarko<sup>2,3</sup>, Vera Julia<sup>2</sup>, Andria Kuswadi<sup>2</sup>

<sup>1</sup>Resident in Department of Dentomaxillofacial Radiology, Faculty of Dentistry, Universitas Indonesia, Jakarta, Indonesia

<sup>2</sup>Universitas Indonesia Hospital, Indonesia

<sup>3</sup>Department of Dentomaxillofacial Radiology, Faculty Dentistry, Universitas Indonesia, Jakarta, Indonesia

**Introduction:** Odontogenic keratocyst (OKC) is the third most common odontogenic cyst, with a reported prevalence of approximately 7.8%. Despite its benign nature, OKC is characterized by locally aggressive behavior and a high recurrence rate. OKC most frequently occurs in the posterior mandible, particularly in the mandibular ramus and angle region, and is less commonly found in the anterior mandible. Radiographically, OKC may present with variable imaging features depending on its size and location, making accurate diagnosis essential for appropriate management. This case report aims to describe the imaging features of OKC in an atypical location, specifically the anterior mandible, as evaluated using cone beam computed tomography (CBCT).

**Case:** A 31-year-old female patient presented with swelling in the anterior mandible, accompanied by mobility of the right mandibular teeth but the teeth remained vital. CBCT examination revealed a hypodense

lesion extending from the right premolar region across the midline to the left premolar region, with a corticated and scalloped border. Buccolingual expansion of the lesion was observed, resulting in thinning of the labial and lingual cortical plates, with focal discontinuity of the lingual cortical bone, and displacement of involved teeth. These findings were suggestive of OKC. The patient subsequently underwent enucleation and endodontic treatment.

**Discussion:** In this case report, the lesion's location in the anterior mandible was uncommon. Furthermore, while OKCs typically expand antero-posteriorly without significant cortical expansion, this case demonstrated marked buccolingual expansion, representing a deviation from the classic radiographic appearance of OKC. Such aggressive expansile behavior is more commonly associated with ameloblastoma, making differential diagnosis based solely on conventional radiography challenging. Therefore, CBCT imaging is indispensable for accurately evaluating lesion extent and internal characteristics, thereby facilitating appropriate diagnosis and management. This case highlights the importance of advanced imaging in recognizing atypical presentations of OKC.

## EP-364

## Field of view size and image uniformity in cone beam CT

**Takashi Kamio**<sup>1\*</sup>, Shun Miwa<sup>1</sup>, Taisuke Kawai<sup>1</sup>

<sup>1</sup>Department of Oral and Maxillofacial Radiology, The Nippon Dental University, Japan

**Introduction:** The present study investigated the effect of field of view (FOV) size on image uniformity in Cone beam computed tomography (CBCT) with horizontal X-ray beam using greyscale analysis.

**Materials and Methods:** Four human dried skulls of comparable size were selected for scanning. A CBCT scanner (3D Accuitomo F17, J. Morita Mfg. Corp., Kyoto, Japan) with standardized scanning parameters (89 kVp, 7.9 mA, 17.5 s exposure time) was utilized. The greyscale values (GV) within each axial slice image for two FOV sizes with their respective voxel resolutions are presented hereafter: 8×8 cm FOV with

voxel size of 0.160 mm, and 17×12 cm FOV with voxel size of 0.250 mm. Image uniformity was quantified using ImageJ (National Institutes of Health, Bethesda, Maryland, USA) by measuring gray value range and standard deviation for all slices. Kolmogorov–Smirnov and Shapiro–Wilk tests assessed normality. Statistical analysis was performed using R with Welch’s t-test ( $\alpha = 0.05$ ).

**Results:** Welch’s t-test revealed a statistically significant difference in mean GV between the 17×12 cm and 8×8 cm FOVs (377.2 vs. 202.1;  $p = 0.00036$ ,  $t = 3.572$ ,  $df = 2045.9$ ). However, standard deviations were nearly equivalent (1113 vs. 1106), indicating comparable image uniformity across both FOV sizes.

**Conclusions:** Image uniformity, as measured by standard deviation and gray value range distribution, was comparable between the 17×12 cm and 8×8 cm FOV sizes, despite a statistically significant difference in mean GV. These results indicate that FOV size does not substantially alter the spatial uniformity of GV within CBCT images.

#### EP-370

### Fibromatous epulis mimicking a benign soft tissue tumor on panoramic radiography: A radiologic diagnostic challenge

Ramayanti Salam<sup>1\*</sup>, Irfan Sugianto<sup>1,2</sup>

<sup>1</sup>Dentomaxillofacial Radiology Specialist Study Program, Faculty of Dentistry, Hasanuddin University, Indonesia

<sup>2</sup>Department of Oral and Maxillofacial Radiology, Faculty of Dentistry, Hasanuddin University, Indonesia

**Introduction:** Fibromatous epulis is a benign reactive gingival lesion arising from fibrous connective tissue and commonly associated with chronic local irritation. Although clinical presentation is often characteristic, radiologic evaluation remains essential to assess adjacent alveolar bone involvement and to support differential diagnosis. Panoramic radiography is routinely used as a first-line imaging modality in oral and maxillofacial radiology; however, its limited soft tissue contrast may result in nonspecific findings. In atypical locations, fibromatous epulis may radiographically

mimic other benign soft tissue tumors, posing a diagnostic challenge during initial interpretation.

**Case:** A 42-year-old male presented with a painless, progressively enlarging gingival mass in the posterior left maxilla for six months. Intraoral examination revealed a pedunculated soft tissue lesion on the vestibular gingiva of teeth 25–28, measuring approximately 3.5 cm. Panoramic radiography demonstrated an ovoid radiolucent area with partially defined margins involving the left maxillary alveolar process, without aggressive bone destruction. Based on these findings, a benign soft tissue tumor, including a minor salivary gland neoplasm, was considered. Wide excisional biopsy was performed. Histopathologic analysis showed fibrous connective tissue proliferation with inflammatory infiltrates and focal calcifications, confirming fibromatous epulis.

**Discussion:** Fibromatous epulis most frequently occurs in the anterior gingiva; posterior maxillary involvement is uncommon and may complicate diagnosis. On panoramic radiography, the lesion typically presents as a nonspecific soft tissue enlargement with minimal osseous changes, increasing the risk of misinterpretation. Anatomical superimposition and limited soft tissue visualization further reduce diagnostic specificity. This case highlights the diagnostic limitations of panoramic radiography for soft tissue lesions and emphasizes the importance of careful radiologic–clinical correlation. Histopathologic examination remains the definitive diagnostic standard, while radiologic assessment plays a critical role in initial evaluation and treatment planning.

#### EP-374

### Extensive complex odontoma of the mandible requiring segmental resection: A case report

Dwi Desiayunis<sup>1\*</sup>, Hanna H Bachtiar - Iskandar<sup>3</sup>, Menik Priaminiarti<sup>2,3</sup>, Aloysius Putut Wijanarko<sup>2,3</sup>, I Nyoman Guswan<sup>1</sup>, Derry Haryono<sup>1</sup>, Mohammad Farid Ratman<sup>2,4</sup>, Larasati Kusuma Putri<sup>2</sup>

<sup>1</sup>Resident in Department of Dentomaxillofacial Radiology, Faculty of Dentistry, Universitas Indonesia, Indonesia

<sup>2</sup>Universitas Indonesia Hospital, Indonesia

<sup>3</sup>Department of Dentomaxillofacial Radiology, Faculty of

Dentistry, Universitas Indonesia, Indonesia

<sup>4</sup>Department of Oral and Maxillofacial Surgery, Faculty of Dentistry, Universitas Indonesia, Indonesia

**Introduction:** Odontoma is a benign odontogenic lesion, most often asymptomatic and incidentally detected on radiographic examination. In many cases, odontomas show limited growth, remain undetected, and are usually treated with simple surgical excision. However, when odontomas grow to a substantial size, surgical treatment may result in extensive bone loss which cause mandibular discontinuity. This report presents a case of a large complex odontoma involving the right mandible that required segmental mandibular resection followed by reconstruction with a plate.

**Case:** A 22-year-old female presented with progressive swelling of the right mandibular region over a four-year period.

Initial symptoms had been misinterpreted as pain related to an impacted third molar. Panoramic radiograph revealed a well-defined irregular radiopaque mass surrounded by a radiolucent band, with amorphous internal calcifications. CT examination showed a massive hyperdense mass in the right mandibular demonstrated involvement of impacted third molar and thinning of the cortical bone. Enucleation, radical curettage, and extraction of involved teeth was performed. Due to the size of the lesion resulting in massive bone loss that cause discontinuity of the mandible, reconstruction with reconstruction plate and iliac bone graft was required. Histopathologic examination revealed irregular fragments composed of connective tissue, dentin, enamel matrix, and pulp tissue arranged in an irregular pattern consistent with complex odontoma.

**Discussion:** In this case, delayed recognition of the lesion allowed continuous growth of the complex odontoma, resulting in extensive mandibular involvement. Panoramic radiography and CT were essential in characterizing the lesion, assessing cortical bone integrity, and determining the extent of surgical intervention. Although odontomas are benign, large lesions may require aggressive surgical management and reconstruction. This case highlights the importance of early radiographic detection and advanced imaging evaluation to prevent severe structural complications.

EP-375

## Traumatic pseudoaneurysm of the superior labial artery presenting as a pulsatile upper lip mass

**Gyu-Dong Jo**<sup>1\*</sup>, Yoon Joo Choi<sup>1</sup>, Chena Lee<sup>1</sup>, Kug Jin Jeon<sup>1</sup>, Sang-Sun Han<sup>1</sup>

<sup>1</sup>Department of Oral and Maxillofacial Radiology, College of Dentistry, Yonsei University, Seoul, Republic of Korea

**Introduction:** Upper lip submucosal masses can arise from mucous retention lesions, reactive nodules, soft-tissue tumors, or vascular abnormalities, many of which share overlapping clinical features. This similarity makes clinical distinction difficult, particularly for vascular lesions. Low-flow entities such as venous malformations or hemangiomas may mimic high-flow lesions including arteriovenous malformations or traumatic pseudoaneurysm, posing a risk of significant hemorrhage if misdiagnosed. Accurate differentiation is crucial for appropriate management.

**Case:** A 31-year-old man presented with a long-standing bluish and pulsatile nodule of the left upper lip that developed after minor thermal injury. Clinical examination identified a submucosal mass with distinct pulsation, raising suspicion for a high-flow vascular lesion. MRI was nondiagnostic because susceptibility artifact from a fixed lingual retainer obscured the anterior oral cavity and upper lip. Contrast-enhanced CT, performed with gauze-assisted soft-tissue separation, revealed a serpiginous enhancing vascular structure. Selective digital subtraction angiography demonstrated a pseudoaneurysmal sac arising from the superior labial artery through a single inflow branch, with persistent opacification and no early venous drainage, confirming traumatic pseudoaneurysm. Because the lesion was small and stable with minimal symptoms, conservative follow-up was chosen, with embolization considered if progression occurred.

**Discussion:** Traumatic pseudoaneurysm arises when an arterial wall defect allows high-pressure blood to dissect into soft tissue, forming a fibrous-walled sac in continuity with the parent vessel. On angiography, it appears as a cavity supplied by a single inflow artery with persistent opacification and no early venous drainage, which differentiates it from arteriovenous

malformation characterized by a nidus, multiple feeders, and rapid arteriovenous shunting. Understanding traumatic pseudoaneurysm as a distinct vascular entity is important because management differs and misguided intervention may precipitate bleeding. A pulsatile upper lip mass, particularly following minor trauma, should prompt consideration of this diagnosis.

No. 379

## Surgical treatment of cysts: A 6 months follow up case report

**Antohei Cristina**<sup>1\*</sup>, Haba Danisia<sup>2</sup>, Popescu Roxana Mihaela<sup>2</sup>, Dobrovat Bogdan Ionut<sup>2</sup>, Salceanu Mihaela<sup>1</sup>, Concita Corina Alexandra<sup>1</sup>, Hamburda Tudor<sup>1</sup>, Cernei Radu Eduard<sup>2</sup>, Giuroiu Cristian Levente<sup>1</sup>, Gheorghe Angela<sup>3</sup>, Pancu Galina<sup>3</sup>, Nica Irina<sup>3</sup>, Topoliceanu Claudiu<sup>3</sup>

<sup>1</sup>Endodontology, UMF GR T POPA, Romania

<sup>2</sup>Surgery, UMF GR T POPA, Romania

<sup>3</sup>Cariology, UMF GR T POPA, Romania

**Introduction:** According to the World Health Organization (WHO), cysts are classified as inflammatory, non-neoplastic lesions. The incidence of cysts among periapical lesions ranges from 6% to 55%. Radiographically, cysts typically appear as round or oval radiolucent areas surrounded by a radiopaque margin. The aim of this study was to assess bone loss following cystectomy procedures using CBCT reconstructions, without bone grafting, during a six-month follow-up period.

**Case:** A literature review was conducted using PubMed, applying the keywords: periapical cysts, cystectomy, bone loss, CBCT, and follow-up. From 520 identified articles, 20 met the inclusion criteria. Based on the literature findings, a clinical case was selected involving a 35-year-old female patient who presented to the Department of Endodontics for treatment of teeth 2.1 and 2.2.

An orthopantomography revealed multiple cystic lesions in the maxilla, prompting CBCT examination. CBCT reconstructions identified cysts at the level of teeth 1.6 extending to 1.7, as well as at 1.5, 1.3, and 1.2. The lesion between teeth 2.1 and 2.2 was diagnosed as an infected cyst due to the absence of a radiopaque margin. Additional cysts were observed at the

residual root of tooth 2.5 and between teeth 2.7 and 2.8. The treatment plan consisted of serial cystectomies associated with extraction of the affected teeth.

**Discussions:** Preoperative CBCT imaging demonstrated lesion extension in all three planes and maxillary sinus involvement. Postoperative CBCT allowed precise evaluation of the resulting bone loss. CBCT examination is essential after cystectomy combined with tooth extraction, particularly for evaluating bone support required for future implant placement.

EP-385

## Context-aware segmentation of internal tooth structures in dental CBCT

**Tae Yeon Lee**<sup>1\*</sup>, Won-jin Yi<sup>1,2,3</sup>

<sup>1</sup>Interdisciplinary Program of Bioengineering, Graduate School of Engineering, Seoul National University, Seoul 03080, South Korea

<sup>2</sup>Applied Bioengineering, Graduate School of Convergence Science and Technology, Seoul National University, Seoul 03080, South Korea

<sup>3</sup>Department of Oral and Maxillofacial Radiology School of Dentistry, Seoul National University, Seoul 03080, South Korea

**Introduction:** Accurate segmentation of internal tooth structures in cone-beam computed tomography (CBCT) is essential for precision dentistry, orthodontic treatment planning, and statistical shape modeling. However, dental CBCT images present significant challenges for automated segmentation due to low image contrast and ambiguous boundaries between enamel, dentin, and pulp. Conventional single-slice-based approaches fail to adequately exploit inter-slice contextual information, often resulting in unstable and discontinuous predictions, particularly for small and structures such as the pulp.

**Materials and Methods:** In this study, we propose a four-channel input segmentation framework that integrates multi-slice contextual information to improve segmentation performance of internal tooth structures. Each input consists of a reference axial slice, adjacent slices, and a mask-guided auxiliary channel generated from previous segmentation results. A convolutional neural network was trained to simultaneously segment

enamel, dentin, and pulp. During inference, slice-wise prediction was performed using a mask-guided propagation strategy to preserve anatomical continuity along the axial direction.

**Results:** The proposed four-channel approach demonstrated improved segmentation accuracy and inter-slice consistency compared to conventional single-channel methods. Incorporation of adjacent slice information effectively reduced slice-wise discontinuities, while the mask-guided channel enhanced boundary delineation between enamel and dentin. Quantitative evaluation showed improved Dice similarity coefficients across all classes, with particularly notable performance gains in pulp segmentation, which is highly sensitive to noise and partial volume effects. Qualitative results confirmed improved morphological continuity and anatomically plausible three-dimensional reconstructions of teeth.

**Conclusions:** This study demonstrates that a four-channel, context-based segmentation approach effectively addresses key challenges in dental CBCT tooth structure segmentation. By leveraging inter-slice contextual information and mask-guided guidance, stable and accurate segmentation of enamel, dentin, and pulp was achieved. The proposed framework is well-suited for downstream applications such as three-dimensional reconstruction and statistical shape modeling.

**Funding:** This work was supported by the National Research Foundation of Korea (NRF) grant funded by the Korean government (MSIT) (No. 2023R1A2C2 00532611). This work was also supported by the Technology Innovation Program (or Industrial Strategic Technology Development Program-Advanced Biomaterials) (RS-2025-14322975), funded by the Ministry of Trade, Industry & Energy (MOTIE).

EP-391

## A case with an intraosseous lipoma and two Stafne bone cavities in the mandible

**Megumi Nose**<sup>1\*</sup>, Yoshikazu Suetani<sup>2</sup>, Nanako Tani<sup>3</sup>, Fahri Reza Ramadhan<sup>1</sup>, Kiichi Shimabukuro<sup>1</sup>,

Masahiko Ohtsuka<sup>1</sup>, Toshikazu Nagasaki<sup>1</sup>, Masaru Konishi<sup>2</sup>, Takashi Nakamoto<sup>1</sup>, Yukina Kobayashi<sup>4,5</sup>, Toshinori Ando<sup>4</sup>, Suguru Hirota<sup>6</sup>, Mirai Higaki<sup>7</sup>, Souichi Yanamoto<sup>8</sup>, Naoya Kakimoto<sup>1</sup>

<sup>1</sup>Department of Oral and Maxillofacial Radiology, Graduate School of Biomedical and Health Sciences, Hiroshima University

<sup>2</sup>Department of Oral and Maxillofacial Radiology, Hiroshima University Hospital

<sup>3</sup>Yamawaki Dental Clinic

<sup>4</sup>Department of Oral and Maxillofacial Pathobiology, Graduate School of Biomedical and Health Sciences, Hiroshima University

<sup>5</sup>Department of Center of Oral Clinical Examination, Hiroshima University Hospital

<sup>6</sup>Department of Oral and Maxillofacial Surgery, Hiroshima University Hospital

<sup>7</sup>Department of Oral Surgery, Hiroshima Red Cross Hospital & Atomic-bomb Survivors Hospital

<sup>8</sup>Department of Oral Oncology, Graduate School of Biomedical and Health Sciences, Hiroshima University

**Introduction:** Lipomas are non-epithelial benign tumors composed of mature adipocytes and most commonly arise in the subcutaneous tissues of the trunk and limbs. Intraosseous lipomas are rare, accounting for less than 0.1% of all bone tumors, and occurrence within the mandible is exceedingly uncommon. A Stafne bone cavity is a localized bone defect of the lingual cortical bone, typically found between the mandibular angle and the region inferior to the molars. It presents as a well-defined radiolucent lesion on radiographs and is usually asymptomatic, being detected incidentally.

**Case:** A 17-year-old male was referred after a cyst-like radiolucency was identified in the right mandible on panoramic radiography. No abnormalities of the oral mucosa were observed, and facial symmetry was preserved. A partially erupted right mandibular first molar was noted. CBCT demonstrated a cystic lesion extending from the distal aspect of the right mandibular molar to the mandibular ramus, below the mandibular notch, with lingual expansion. The lingual cortical bone showed marked thinning, while the buccal cortex exhibited focal thinning, mild expansion. The CT attenuation value was -95.9 HU. MRI revealed high signal intensity on T1- and T2-weighted images, low signal intensity on fat-suppressed T2-weighted images, and no contrast enhancement. Partial extirpation for biopsy of the right mandibular ramus was performed,

and histopathological examination confirmed an intraosseous lipoma. Two additional stationary bone cavities were identified in the anterior mandible and left molar region.

**Discussion:** This case demonstrated the coexistence of an intraosseous lipoma and two Stafne bone cavities within the mandible. Given the abnormal bone morphology observed around the mandibular ramus and condyle, the possibility of an associated skeletal abnormality, in addition to the intraosseous lipoma and Stafne bone cavities, cannot be excluded.

EP-392

## Presentation of rare maxillary ameloblastoma with palatal and maxillary sinus involvement

**Cesilia Metty Ekariani**<sup>1\*</sup>, Brama Kiswanjaya<sup>2</sup>, Menik Priaminiarti<sup>2,3</sup>, I Nyoman Guswan<sup>1</sup>, Derry Haryono<sup>1</sup>, Vera Julia<sup>3</sup>, Muhammad Farris Afif<sup>3</sup>

<sup>1</sup>Resident in Department of Dentomaxillofacial Radiology, Faculty of Dentistry, Universitas Indonesia, Jakarta, Indonesia

<sup>2</sup>Department of Dentomaxillofacial Radiology, Faculty of Dentistry, Universitas Indonesia, Jakarta, Indonesia <sup>3</sup>Universitas Indonesia Hospital, Indonesia

**Introduction:** Ameloblastoma is a rare, benign but locally aggressive odontogenic tumor that originates from epithelial remnants of tooth development. Ameloblastoma predominantly arises in the posterior mandible and is uncommonly found in the maxilla, in which only 2% arising anterior to the maxillary premolar. This report presents a rare case of anterior maxillary ameloblastoma involving of maxillary sinus and palate.

**Case:** A 42-year-old male presented with tooth mobility and a slowly progressive swelling in right anterior maxilla for one year, associated with facial asymmetry and pain on mouth opening, with no significant weight loss reported. Computed tomography (CT) imaging demonstrated well-defined, expansile multilocular cystic lesion with mixed hypodense and hyperdense components. The lesion involved anterior maxillary alveolar process, exhibited adjacent root resorption, and extended into palate and right maxillary sinus. Bucco-palatal expansion with cortical plates thinning was

evident. The internal structure was predominantly radiolucent in unilocular posterior lobe, whereas the anterior portion demonstrated internal septations with focal radiopaque areas resembling sclerotic bone. The patient underwent hemimaxillectomy with subsequent reconstructive surgery. Histopathological examination established the diagnosis of ameloblastoma.

**Discussion:** Maxillary ameloblastoma is relatively rare and presents unique diagnostic and therapeutic challenges. Maxillary ameloblastoma tend to exhibit more aggressive behavior due to the porous nature of maxillary bone and their proximity to vital anatomical structures such as the maxillary sinus, nasal cavity, and orbit. In the present case, palatal and maxillary sinus involvement highlights the aggressive potential of maxillary ameloblastoma and underscores the influence of regional anatomy on tumor behavior. Maxillary ameloblastoma may expand silently into adjacent spaces, delaying clinical detection. Radiographic evidence of maxillary sinus involvement emphasizes the need for comprehensive imaging to accurately assess tumor extent. This case reinforces the importance of early recognition, thorough radiologic evaluation, and appropriate management to prevent recurrence and involvement of critical anatomical structures.

EP-402

## A phantom-based protocol for fiducial marker placement in CBCT–IOS registration with severe metal artifacts

**Jun-Tae Park**<sup>1\*</sup>, Min-Suk Heo<sup>1</sup>, Sam-Sun Lee<sup>1</sup>, Won-Jin Yi<sup>1</sup>, Kyung-Hoe Huh<sup>1</sup>, Jo-Eun Kim<sup>1</sup>, Ju-Hee Kang<sup>1</sup>

Department of Oral and Maxillofacial Radiology, Seoul National University School of Dentistry, South Korea

**Introduction:** Accurate CBCT and intraoral scan (IOS) registration is crucial for digital implant surgical guide planning. Metal restorations cause beam-hardening artifacts that reduce automatic alignment accuracy. In these cases, manual registration with fiducial markers is needed, but there is no agreement on where to put the markers in the presence of significant artifacts. Prior studies demonstrate that (1) increased marker

numbers and (2) a broader geometric distribution improve accuracy, whereas (3) proximity to artifact sources can worsen fiducial localization error (FLE). The present study seeks to propose an experimental methodology for developing a marker-placement strategy that reduces artifact influence.

**Materials and Methods:** A partially edentulous phantom with metallic restorations was created to generate clinically relevant artifacts. Based on CBCT-based severity criteria, the arch was divided into three parts: artifact-free, moderate-artifact, and severe-artifact. Two placement strategies were compared with the same number of markers (N): Group A (geometric advantage) allowed placement in artifact zones to maximize dispersion, while Group B (visual advantage) limited placement to artifact-free regions, which reduced dispersion.

The registration was performed in commercial software (e.g., 3Shape Implant Studio) using rigid registration. Accuracy was quantified in Geomagic Control X with the target registration error (TRE) and the surface-based RMS deviation.

**Results:** In a pilot study involving multiple phantoms, CBCT-IOS registrations were conducted in 3Shape Implant Studio. Qualitatively, Group B (artifact-avoiding placement) had more stable alignment than Group A, with less mismatch in the posterior ROI close to metal-affected areas.

**Conclusions:** These pilot observations indicate that, in the case of significant metal artifacts, avoiding artifact-prone areas may be more effective than maximizing dispersion for fiducial marker selection. Continuous validation using the established TRE/RMS/FLE pipeline will quantify this dispersion–FLE trade-off.

EP-407

## Image diagnosis of a case of solitary fibrous tumor in the cheek

Reika Hanaoka<sup>1\*</sup>, Hiroaki Shimamoto<sup>1</sup>, Yuki Shimizu<sup>1</sup>, Yuka Uchimoto<sup>1</sup>, Kaori Oya<sup>2</sup>, Katsutoshi Hirose<sup>3</sup>, Ryoko Okahata<sup>1</sup>, Naoko Abe<sup>1</sup>, Naoko Takagawa<sup>1</sup>, Mamoru Nagata<sup>4</sup>, Shumei Murakami<sup>1</sup>

<sup>1</sup>Department of Oral and Maxillofacial Radiology, Graduate

School of Dentistry, The University of Osaka, Japan

<sup>2</sup>Department of Laboratory Medicine, The University of Osaka Dental Hospital, Japan

<sup>3</sup>Department of Oral Pathology, Graduate School of Dentistry, The University of Osaka, Japan

<sup>4</sup>Department of Radiology, The University of Osaka Dental Hospital, Japan

**Introduction:** Solitary fibrous tumor (SFT) is a rare mesenchymal neoplasm that most commonly arises in the pleura. Although 10–20% of cases occur in the head and neck region, oral involvement, especially the cheek, is extremely rare. We report a rare case of SFT arising in the cheek.

**Case:** A 34-year-old woman presented with a painless mass in the left buccal mucosa. CT revealed a well-defined lesion measuring 17 × 15 × 20 mm anterior to the left masseter muscle, with attenuation values of 48 HU before contrast and 125 HU after contrast administration.

MRI showed signal intensity similar to muscle on T1-weighted images. On T2-weighted images, the lesion demonstrated peripheral high signal intensity with intermediate signal intensity internally. Contrast-enhanced T1-weighted images showed substantial peripheral enhancement and moderate internal enhancement. A salivary gland tumor, particularly a pleomorphic adenoma, was suspected; however, the ADC value was  $1.03 \times 10^{-3}$  mm<sup>2</sup>/s, lower than the typically observed value for pleomorphic adenoma. The tumor was surgically excised, and immunohistochemical staining demonstrated nuclear positivity for STAT6, confirming the diagnosis of SFT.

**Discussion:** SFT may mimic a pleomorphic adenoma on imaging due to its heterogeneous histological composition. In this case, the low ADC value and substantial peripheral enhancement were key findings for differentiation. No recurrence was observed at 12 months postoperatively; however, long-term follow-up is required.

EP-414

## Odontogenic myxoma: A case presentation with classic characteristics

**Krittamate Kerewichien**<sup>1\*</sup>, Napat Damrongsirirat<sup>2</sup>, Kitipong Kaewpichai<sup>3</sup>, Ekarat Phattarataratip<sup>4</sup>, Silkosessak Onanong Chaiudom Silkosessak<sup>1</sup>, Vorapat Trachoo<sup>2</sup>, Pisha Pittayapat<sup>1</sup>

<sup>1</sup>Department of Radiology, Chulalongkorn University, Thailand

<sup>2</sup>Department of Oral and Maxillofacial Surgery, Chulalongkorn University, Thailand

<sup>3</sup>Department of Department of Surgery, Rajavithi Hospital, Thailand

<sup>4</sup>Department of Oral Pathology, Chulalongkorn University, Thailand

**Introduction:** Odontogenic myxoma is a rare, benign mesenchymal odontogenic tumor. Its reported prevalence ranges from 1.9–2.4% of all odontogenic tumors in Asian populations. Despite its characteristic clinical and radiographic features, relatively few studies have described unique findings of this tumor. This report presents a case of odontogenic myxoma that remained untreated for at least five years prior to definitive management.

**Case:** A 34-year-old Thai female presented with a chief complaint of a painless swelling in the mandible that had been present for five years, with rapid progression over the past year. The patient denied any underlying systemic disease or drug allergies. Clinical examination revealed buccolingual expansion extending from the region of teeth 33 to 47, with crepitation noted in the area of teeth 32 to 45. Panoramic radiograph demonstrated a multilocular radiolucent lesion with straight septa. The lesion was predominantly well defined, with an ill-defined anterior border, extending from the mid-tooth 35 to the superior and posterior third of the right mandibular ramus. Cone-beam computed tomography (CBCT) was obtained for more details prior to incisional biopsy. Codman's triangle periosteal reactions were observed, suggesting aggressive behavior of the lesion. Histopathological examination of hematoxylin and eosin (H&E) stained sections revealed loose fibrocollagenous connective tissue consisting of scattered spindle and stellate-shaped cells in the myxomatous to mucoid stroma, consistent with odontogenic myxoma.

**Discussion:** The patient was treated with partial mandibulectomy followed by reconstruction using a fibula free flap in combination with a radial forearm flap. Surgical management was selected due to the extensive size and aggressive behavior of the lesion. At the one-year follow-up, no recurrence of the lesion was observed.

EP-415

## Aggressive mandibular odontogenic keratocyst mimicking dentigerous cyst and ameloblastoma: A panoramic and CT imaging case report

**Hamdani**<sup>1\*</sup>, Fadhilil Ulum A.Rahman<sup>1,2</sup>

<sup>1</sup>Dentomaxillofacial Radiology Specialist Study Program, Faculty of Dentistry Hasanuddin University, Indonesia

<sup>2</sup>Department of Oral and Maxillofacial Radiology, Faculty of Dentistry, Hasanuddin University, Makassar, Indonesia

**Introduction:** Odontogenic keratocystic cyst (OKC) is a benign odontogenic lesion characterised by aggressive behaviour and a high recurrence rate, but rarely shows root resorption, a feature more commonly associated with ameloblastoma. These unique characteristics provide epidemiological context and initial differential diagnosis in panoramic and CT imaging for similar cases, including general imaging features to support case understanding.

**Case:** We report a case of a 25-year-old woman with slow progressive swelling of the right mandible over 1.5 years. Panoramic radiographic and multislice computed tomography examinations revealed an extensive radiolucent lesion involving the corpus and ramus of the right mandible, associated with impacted teeth, cortical expansion, and root resorption of the surrounding teeth. The imaging findings resembled a dentigerous cyst and ameloblastoma, raising strong initial radiological suspicion. Two incisional biopsies only showed nonspecific chronic inflammation, delaying a definitive diagnosis. Surgical management in the form of hemimandibulectomy and mandibular reconstruction was then performed. Final histopathological examination confirmed the diagnosis of odontogenic keratocystic cyst. This chronological sequence reflects the

clinical course from presentation to confirmation of the definitive diagnosis.

**Discussion:** This case highlights the radiographic mimicry of aggressive OKC on panoramic and CT imaging and the importance of radiological and histopathological correlation for accurate diagnosis. These findings support the use of multimodal imaging and excisional biopsy in aggressive odontogenic lesions to reduce the risk of misdiagnosis.

#### EP-417

### AI-powered learning to advance tooth recognition skills in dental assistant education

**Supaluck Deeduai\***, Phonkit Sinpitaksakul, Onanong Chai-u-dom Silkosessak

*Department of Radiology, Chulalongkorn University, THAILAND*

**Introduction:** Tooth identification is the most fundamental task for dental professionals, as well as, for dental diagnostic AI algorithm. The current typical methods of dental assistants (DA) learning begin with lecture-based method, followed by a 1-year experiential-based clinical rotation. Per concept of technology-based learning, applying extra-curriculum activities using any available AI-technology can increase the student enthusiasm and gain wider access of specific mission.

**Materials and Methods:** The scores of the 2024 DA-students (n=31) for a full-mouth (14 periapical and 4 bitewings) film-mounting examination and 25 short-answer questions regarding mixed-dentition tooth identification were retrieved as negative control group. All DA-students from class 2025 (n=28) accepted the study invitation, and were divided into 2 groups to practice using diagnostic-AI function for viewing panoramic radiographs in normal 4 to 11-year dentitions. The first group was scheduled to the AI-sessions right after formal lectures, but before clinical rotation. The second group was arranged to use diagnostic-AI as part of their clinical rotation. Two available panoramic AI-algorithms were randomly and equally assigned within each group. Same assessments were executed at the end of each AI-session.

Statistical comparison was performed using ANOVA with SPSS software and confidence interval was set at 95 percent.

**Results:** The mean scores of the film-mounting exercise for conventional and AI-integrated classes were similar— 14.64 and 14.83 out of 18 remarks, respectively. In contrast, the average scores for mixed-dentition question was notably higher in the AI-integrated group— 6.06 and 10.79 out of 15 remarks, respectively. Statistically significant differences were found between the 2 classes ( $p=0.031$ ), examination types ( $p<0.001$ ). However, no significant difference between the 2 available AI.

**Conclusions:** Available dental diagnostic-AI programs can be implemented as technology-based learning tools for simple radiographic tooth identification in DA training program.

#### EP-427

### Size and expansion characteristics of benign radiolucent mandibular lesions: A cone-beam computed tomography analysis

**Pornkawe Charoenlarp\***<sup>1</sup>, Nutchalai Malikhao<sup>1</sup>, Natcha Srivichien<sup>1</sup>, Sirirat Chawanratikun<sup>1</sup>, Onanong Chai-u-dom Silkosessak<sup>1</sup>, Soranun Chantarangsu<sup>2</sup>

<sup>1</sup>*Department of Radiology, Faculty of Dentistry, Chulalongkorn University, Thailand*

<sup>2</sup>*Department of Oral Pathology, Faculty of Dentistry, Chulalongkorn University, Thailand*

**Introduction:** The radiographic diagnosis of benign radiolucent jaw lesions can be challenging due to similarities in their imaging features. This study aims to identify methods for narrowing the differential diagnosis of common benign radiolucent mandibular lesions by evaluating lesion size and expansion characteristics using cone-beam computed tomography (CBCT).

**Materials and Methods:** All CBCT datasets of patients treated at the Faculty of Dentistry, Chulalongkorn University, with histopathologically confirmed diagnoses of ameloblastoma (AM), odontogenic kera-

to cyst (OKC), dentigerous cyst (DC), radicular cyst (RC), and simple bone cyst (SBC) involving the mandible between December 2012 and March 2021 were retrospectively reviewed. Lesion size was evaluated in three dimensions: buccolingual (BLi), mesiodistal (MD), and superoinferior (SI). The dimensional ratio was calculated by dividing the BLi width by the MD width. Bulging height was defined as the perpendicular distance from the most expanded point of the cortical bone to an imaginary line representing the normal bone contour. The angle of departure was defined as the largest angle formed between the original cortical bone surface and the expanded cortical surface. Statistical analysis was performed using Kruskal Wallis H test followed by Dunn's post-hoc tests. A  $p$ -value  $<0.05$  was considered statistically significant difference.

**Results:** The study analyzed 123 lesions, comprising 37 cases of AM, 40 OKCs, 25 DCs, 7 RCs, and 14 SBCs. AM demonstrated significantly greater BLi and SI dimensions compared to the other lesions. Conversely, OKC exhibited a significantly lower dimensional ratio. Regarding expansion characteristics, AM presented the greatest bulging height and the steepest angle of departure. In contrast, SBC showed the shallowest angle which was significantly lower than AM, OKC, and DC.

**Conclusions:** Dimensional ratio, bulging height, angle of departure could be helpful for diagnosis of benign radiolucent lesions in mandible.

EP-431

## Automatic detection of facial landmarks for facial morphology analysis on 3D facial scans using geometric deep learning

**Shin-Hyun Kang**<sup>1\*</sup>, Su Yang<sup>2</sup>, Sam-Sun Lee<sup>1</sup>, Min-Suk Heo<sup>1</sup>, Kyung-Hoe Huh, Jo-Hun Kim<sup>1</sup>, Won-Jin Yi<sup>1</sup>

<sup>1</sup>Department of Oral and Maxillofacial Radiology, School of Dentistry and Dental Research Institute, Seoul National University, Seoul, South Korea

<sup>2</sup>Department of Oral and Maxillofacial Surgery, Houston Methodist Research Institute, Houston, Texas 77030, USA

**Introduction:** Facial landmark detection on 3D facial scans is essential for facial morphology analysis in dental fields, including oral and maxillofacial surgery, orthodontics, and prosthodontics. However, manual landmark annotation on 3D facial scans is time-consuming work.

**Materials and Methods:** The purpose of this study is to automatically detect 24 facial landmarks on 3D facial scans using a geometric deep learning framework (FLFormer). FLFormer consists of a dynamic graph convolutional neural network (DGCNN), a point cloud transformer (PCT), and a landmark prediction head (HMPH). DGCNN extracted local geometric features and PCT captured global contextual relationships via a self-attention mechanism. HMPH predicted the 3D coordinates of facial landmarks using fully connected layers. FLFormer was optimized for 10000 epochs using a mean squared error loss, the RMSprop optimizer with an initial learning rate of 0.0001, and a mini-batch size of 1. A total of 91 3D facial scans from patients were enrolled in this study, with 73 and 18 were used as the training and test datasets, respectively.

**Results:** To evaluate the landmark detection performance of deep learning models, we used a mean absolute error (MAE) between ground truth and predicted facial landmarks. PACnv achieved an MAE of  $4.02 \pm 10.27$  mm, whereas FLFormer achieved an MAE of  $2.45 \pm 1.77$  mm on the test dataset. FLFormer reduced the MAE by 1.57 mm with 39% relative improvement compared with those of PACnv, indicating substantially fewer large-error outliers and more consistent facial landmark detection across patients.

**Conclusions:** FLFormer demonstrated superior detection performance for 24 facial landmarks on 3D facial scans. Our approach has the potential to reduce manual annotation burden and improve reproducibility in 3D facial analysis for dental applications. Future work will focus on expanding the dataset size, validating inter-observer reliability, and conducting a comprehensive comparison with state-of-the-art deep learning.

**\*Funding:** This work was supported by the National Research Foundation of Korea (NRF) grant funded by the Korean government (MSIT) (No. 2023R1A2C2 00532611). This work was also supported by the Technology Innovation Program (or Industrial Strategic

Technology Development Program-Advanced Biomaterials) (RS-2025-14322975), funded by the Ministry of Trade, Industry & Energy (MOTIE)

## EP-436

## A preliminary study on diagnostic reference levels for pediatric CBCT indications in Taiwan

Shu-Han Lin<sup>1</sup>, Wen-Chen Wang<sup>1,2,3</sup>

<sup>1</sup>School of Dentistry, Kaohsiung Medical University, Taiwan

<sup>2</sup>Oral and Maxillofacial Image Center, Kaohsiung Medical University, Taiwan

<sup>3</sup>Division of Oral Pathology and Maxillofacial Radiology, Dental Department, Kaohsiung Medical University Hospital, Taiwan

**Introduction:** With the rising use of Cone-Beam Computed Tomography (CBCT) in pediatric dentistry, balancing diagnostic needs with radiation safety is critical. This study aimed to investigate correlations between exposure, risk, and clinical variables to establish indication-specific local Diagnostic Reference Levels (DRLs) for dose optimization.

**Materials and Methods:** A total of 208 pediatric patients aged 0-12 years (80 female) were analyzed at Kaohsiung Medical University Hospital (2018-2022). Effective doses were calculated using recorded Dose-Length Product (DLP) and Dose-Area Product (DAP) for CBCT, and standardized DAP for 2D radiography. Risks were estimated via ICRP 103 guidelines. Descriptive statistics and Pearson correlations were used to evaluate the impact of clinical factors on cumulative dose.

**Results:** Preliminary local DRLs were established, with root canal problems ( $0.50 \pm 0.29$  mSv) and malocclusion ( $0.48 \pm 0.22$  mSv) exhibiting the highest reference values. A strong correlation existed between age and annual effective dose ( $r=0.743$ ), particularly in patients  $>11$  years. Notably, cumulative and annual doses were nearly perfectly correlated ( $r=0.992$ ). Physical metric analysis confirmed a significant correlation between DAP and DLP ( $r=0.835$ ), with DAP showing strong dependence on FOV size.

**Conclusions:** This study provides disease-specific local DRLs as clinical benchmarks. Data confirms that

complex indications significantly exceed baseline radiation levels. As DAP accurately reflects FOV-related burden, clinicians must strictly adhere to ALADA principles and FOV collimation. Continuous monitoring against these local DRLs is essential to minimize lifetime radiation risks in this vulnerable population.

## EP-453

## Evaluation of CBCT/CT and MRI of chronic suppurative otitis media with intracerebral complications

Danisia Haba<sup>1,2\*</sup>, Ilinca Diana Andreea<sup>1,2</sup>, Roxana Popescu<sup>1</sup>, Bogdan Dobrovat<sup>1</sup>, Ana Sirghe<sup>1</sup>, Emilia Marciuc<sup>1</sup>, Daniela Pomohaci<sup>1</sup>, Cristina Antohi<sup>3</sup>

<sup>1</sup>Department of Surgery, UMF Gr.T.Popa Iasi, Romania

<sup>2</sup>Department of Radiology, Medimagis, Romania

<sup>3</sup>Department of Edontology, UMF Gr.T.Popa Iasi, Romania

**Introduction:** Cholesteatoma is as a mass of soft tissue within the middle ear, consisting of keratinized squamous epithelium and keratin accumulation, with or without inflammation of the surrounding tissue. The study aimed to analyze CBCT/CT and MRI using conventional and modern techniques for evaluating chronic suppurative cholesteatomatous and non-cholesteatomatous otitis in patients admitted urgently to assess the frequency of intracerebral complications.

**Materials and Methods:** Material and methods: 30 patients with clinical diagnoses of chronic suppurative otitis media (CSOM) underwent high-resolution CBCT/CT (HRCT) and MRI to assess the extent of the disease and associated complications. The study involved analyzing imaging elements such as epitympanic lesions, ossicular erosions, and the presence of labyrinthitis ossificans.

**Results:** Results showed that 66.7% of the patients had right ear involvement, while 40% had left ear involvement. Common complications detected during CBCT/CT included erosion of the sinodural angle and tegmen tympani, with abscesses being a major complication in 96.7% of cases. MRI sequences such as T1, T2, Flair, and advanced diffusion-weighted techniques (non-EPI) were used efficiently, detecting abscesses and complications in the middle cranial fossa in 96.7%

of cases. *Streptococcus pneumoniae* was the most frequently encountered germ, highlighting the need for focused prevention and treatment measures.

**Conclusions:** CBCT/CT is effective in identifying bone destructions and intracranial complications, while MRI, especially with diffusion-weighted sequences, offers superior differentiation of cholesteatoma from other soft tissue lesions and evaluation of its extent. Combining CBCT/CT and MRI provides a comprehensive and precise evaluation, facilitating efficient clinical management and improving patient prognosis.

EP-454

## CBCT and MR Imaging in esthesioneuroblastoma and long-term follow-up after surgery

**Danisia Haba**<sup>1,2\*</sup>, Ilinca Diana Andreea<sup>1,2</sup>, Roxana Popescu<sup>1</sup>, Bogdan Dobrovat<sup>1</sup>, Ana Sirghe<sup>1</sup>, Emilia Marciuc<sup>1</sup>, Daniela Pomohaci<sup>1</sup>, Cristina Antohi<sup>3</sup>

<sup>1</sup>Department of Surgery, UMF Gr.T.Popa Iasi, Romania

<sup>2</sup>Department of Radiology, Medimagis, Romania

<sup>3</sup>Department of Edontology, UMF Gr.T.Popa Iasi, Romania

**Introduction:** Imaging plays a key role in diagnosing and properly staging esthesioneuroblastoma, a rare malignant tumor arising from the olfactory epithelium at the level of the superior nasal cavity. The study assesses the role of CBCT and MRI in the diagnosis of the tumor to understand staging, patterns of extension, and post-surgery imaging in order to rapidly identify recurrence.

**Case:** We retrospectively studied one female patient with confirmed anatomopathological esthesioneuroblastoma, and imaging follow-up from 2018 until 2025 in Prof.N. Obu Emergency Hospital and Medimagis Clinic.

**Discussion:** We used CBCT for localization and clearly identifying osseous involvement (bone remodeling, invasion in cribriform plate) and MRI investigations (cerebral and neck MRI) in order to recognize key imaging findings, the local and very rare neck extension that could impact the surgical procedure and add them

to the report. CBCT with MPR was used to assess bone extension, the location of a soft tissue mass in the high nasal vault or ectopic in the ethmoidal sinus, associated with hyperostosis (n=1), and bone erosion (n=4). MRI is used mostly for soft tissue extension (n=1) and/or orbital (n=1) and to search the intracerebral spread (n=0). Our patient was imaging evaluated 2 to 4 months after surgery, biannually for the first 5 years and annually afterwards.

Although esthesioneuroblastoma is an uncommon intranasal malignancy, it should be taken into consideration if a soft tissue mass is discovered during a routine CBCT sinus or CT craniocerebral scan and further investigated with MRI for accurate staging and treatment.

EP-462

## Panoramic radiographic features of odontogenic keratocysts occupying the maxillary sinus

**Hong-Yul Moon, DDS**<sup>1\*</sup>, Kyung-Hoe Huh, DDS, MSD, PhD<sup>2</sup>, Ju-Hee Kang, DMD, DDS, PhD<sup>3</sup>, Jo-Eun Kim, DMD, DDS, PhD<sup>2</sup>, , Won-Jin Yi, PhD<sup>2</sup>, Min-Suk Heo, DDS, MSD, PhD<sup>2</sup>, Sam-Sun Lee, DDS, MSD, PhD<sup>2</sup>

<sup>1</sup>Department of Oral and Maxillofacial Radiology, School of Dentistry, Seoul National University,

<sup>2</sup>Department of Oral and Maxillofacial Radiology, School of Dentistry and Dental Research Institute, Seoul National University

<sup>3</sup>Department of Oral and Maxillofacial Radiology, Seoul National University Dental Hospital

**Introduction:** Odontogenic keratocysts (OKCs) are frequently diagnosed at a late stage after extensively occupying the maxillary sinus. This study aims to evaluate the panoramic radiographic characteristics of maxillary sinus-involving OKCs and the associated changes in normal anatomical structures.

**Materials and Methods:** Panoramic radiographs of 172 patients, with histopathologically proven OKCs and involving the maxillary sinus, were analyzed. Lesion size was classified according to the proportion of maxillary sinus involvement (<1/2, 1/2–3/4, >3/4), and location of lesion center was categorized as anterior or posterior. Six cortical lines of adjacent normal anatomical

ical structures related to the maxillary sinus were investigated and their alterations were recorded as blurring, thickening, displacement, or loss. The presence of impacted teeth was also evaluated. Relationships between changes of the six anatomical cortical lines and lesion size or location were analyzed using chi-square tests and multivariate logistic regression.

**Results:** Among the 172 cases, 46.5% of lesions occupied > three-quarters of the maxillary sinus. Radiographic changes were most frequent at sinus floor (100%), then posterior wall (80.2%). Blurring and displacement predominated; cortical bone loss was uncommon, limited to larger lesions. Large lesions (> three-quarters) showed significantly more structural changes, especially at posterior wall (OR 12.924,  $p = 0.0008$ ). Panoramic innominate line changes increased with lesion size. Anterior location independently associated with the nasal floor and anteromedial wall changes. All 62 lesions with impacted third molars showed tooth displacement.

**Conclusions:** A substantial proportion of OKCs were identified only after occupying more than three-quarters of the maxillary sinus. Since changes of blurring and displacement appear to occur first at the floor and posterior wall of the maxillary sinus, focused assessment of these cortical lines may aid in early detection and ultimately improve patient prognosis.

No. 466

## Confidence-aware Transformer-based panoramic radiography super resolution

Young-Eun Kwon<sup>1\*</sup>, Jaehyup Lee<sup>2</sup>, Seo-Young An<sup>3</sup>, Chang-Hyeon An<sup>1</sup>

<sup>1</sup>Department of Oral and Maxillofacial Radiology, School of Dentistry, IHBR, Kyungpook National University, South Korea

<sup>2</sup>Department of Computer Science and Engineering, Kyungpook National University, Daegu, South Korea

<sup>3</sup>Department of Oral and Maxillofacial Radiology, School of Dentistry, IHBR, ITRD, Kyungpook National University, South Korea

**Introduction:** This study aimed to develop and evaluate a confidence-aware transformer-based Panoramic Radiography super-resolution framework, termed

CAT-PRSR, to enhance image quality and diagnostic reliability in panoramic dental radiographs.

**Materials and Methods:** A total of 1,078 anonymized panoramic radiographs were retrospectively collected (950 for training, 128 for testing). The CAT-PRSR framework integrating a transformer-based SR backbone with a confidence-aware training strategy was developed. The model generates a high-resolution output with pixel-wise uncertainty estimation, allowing adaptive learning focused on diagnostically relevant regions while minimizing over-enhancement in noise-sensitive areas. Based on quantitative performance, four representative state-of-the-art SR models were selected for comparison at 4×, 6×, and 8× magnifications. Model performance was evaluated using peak signal-to-noise ratio (PSNR), Fréchet inception distance (FID) and mean opinion score (MOS) assessment.

**Results:** CAT-PRSR demonstrated superior performance across all metrics and magnification levels. It achieved the highest PSNR (36.41 at 4×, 36.19 at 6×, and 33.73 at 8×) and the lowest FID (1.78, 9.29, and 2.09, respectively), outperforming all comparison models. In MOS evaluations, CAT-PRSR maintained diagnostic utility scores statistically comparable to ground truth images ( $p > 0.05$ ), while other models showed significant degradation ( $p < 0.001$ ).

**Conclusions:** The proposed CAT-PRSR framework demonstrated potential to enhance panoramic radiograph resolution by integrating pixel-level fidelity with improved diagnostic reliability.

EP-475

## Radiographic features of maxillary squamous cell carcinoma with ethmoid sinus extension: A case report

Agnes Kentjana Putra<sup>1\*</sup>, Bramma Kiswanjaya<sup>3</sup>, Menik Priaminiarti<sup>2,3</sup>, I Nyoman Guswan<sup>1</sup>, Derry Haryono<sup>1</sup>, Larasati Kusuma Putri<sup>2</sup>

<sup>1</sup>Resident in Department of Dentomaxillofacial Radiology, Faculty of Dentistry, Universitas Indonesia, Indonesia

<sup>2</sup>Universitas Indonesia Hospital, Indonesia

<sup>3</sup>Department of Dentomaxillofacial Radiology, Faculty of Dentistry, Universitas Indonesia, Indonesia

**Introduction:** Maxillary squamous cell carcinoma (SCC) accounts for approximately 5% of all oral malignancies and is therefore considered relatively rare. Compared with SCC arising in other intraoral sites, maxillary SCC tends to demonstrate more aggressive behavior and is frequently diagnosed at an advanced stage. Due to the close anatomical relationship between the maxilla and the paranasal sinuses, tumor extension into the ethmoid sinus represents advanced disease and has significant implications for treatment planning and prognosis. This case report aims to describe the radiographic characteristics of maxillary squamous cell carcinoma with ethmoid sinus involvement.

**Case Presentation:** A 59-year-old male presented with a progressively enlarging solid mass involving the right hard palate that had persisted for three months. Computed tomography (CT) imaging revealed a heterogeneous solid mass with marked post-contrast enhancement involving the right hard palate, extending into the right maxillary sinus and nasal cavity, with further invasion of the right ethmoid sinus. The lesion caused destruction of the walls of the right maxillary sinus and deviation of the nasal septum to the left. Histopathological examination of biopsy specimens demonstrated a malignant epithelial tumor composed of infiltrative solid nests within the connective tissue stroma. The tumor cells were polygonal, exhibiting pleomorphic vesicular nuclei with prominent nucleoli and eosinophilic cytoplasm. Mitotic figures and individual cell dyskeratosis were observed. These findings were consistent with a moderately differentiated squamous cell carcinoma.

**Discussion:** Maxillary SCC often presents at an advanced stage due to subtle early symptoms and its aggressive invasive behavior. In this case, CT imaging findings highly suggestive of advanced SCC. Ethmoid sinus involvement is clinically significant, as it reflects extensive tumor spread and influences treatment planning and prognosis. Although radiologic features strongly support the diagnosis, definitive confirmation requires histopathologic examination, which in this case revealed a moderately differentiated squamous cell carcinoma without lymphovascular invasion.

## EP-504

### Mandibular canal enlargement as an early imaging indicator of systemic disease: A dentomaxillofacial radiology case report

**Monica Piña D'Abreu**<sup>1,2\*</sup>, Pere Riutord Sbert<sup>1,2</sup>, Hernan Paublíni Oliveira<sup>1,2</sup>, Cristina Martorell<sup>1,2</sup>

<sup>1</sup>Faculty of Dentistry, University ADEMA School, Spain

<sup>2</sup>Health Group of University Institute for Research in Health Sciences (IUNICS), Spain

**Introduction:** The mandibular canal is a well-defined anatomical structure whose morphology, diameter, and cortication can be accurately assessed using panoramic radiography and cone-beam computed tomography (CBCT). Alterations of the inferior alveolar canal are uncommon and may reflect neural, vascular, or infiltrative pathology. Recognition of these changes is essential, as they may represent imaging indicators of conditions with systemic relevance rather than isolated dental disease.

**Case:** A 40-year-old female patient with a complex medical history, including facial swelling, persistent mandibular infection, prolonged antibiotic therapy, and ongoing medical treatment, was referred for dentomaxillofacial imaging evaluation. Panoramic reconstruction demonstrated bilateral enlargement of the mandibular canals, more pronounced on the right side. CBCT multiplanar analysis revealed a continuous, fusiform enlargement of the inferior alveolar canals, with right canal diameter measuring approximately 9.4 mm and left canal 4.3 mm. Cortical thinning and focal loss of cortication on the lingual aspect were observed, without frank bone destruction. The canal enlargement extended along the mandibular body and mental foramen region. No odontogenic, traumatic, or purely inflammatory etiology explained the imaging findings. The radiological pattern raised suspicion of neural, vascular, or infiltrative involvement, prompting recommendation for further medical and histopathological correlation.

**Discussion:** Mandibular canal enlargement has been associated with a spectrum of benign and malignant conditions, including non-Hodgkin lymphoma, osteo-

sarcoma, schwannoma, neurofibroma, vascular malformations or hemangiomas, multiple endocrine neoplasia syndromes, and perineural spread or invasion. Slowly progressive infiltrative processes may produce canal widening with preserved or partially eroded cortices, emphasizing the importance of detailed anatomical analysis and high-resolution CBCT imaging. Mandibular canal enlargement should be regarded as a radiological red flag that warrants comprehensive imaging evaluation. Its identification may reflect pathology of systemic significance rather than localized dental disease, highlighting the diagnostic role of dentomaxillofacial radiology in integrative patient care.

## EP-519

## Anatomical proximity between posterior maxillary tooth roots and sinus floor independently predicts mucosal thickening: A CBCT study

Ali Altındağ<sup>1\*</sup>, Cemile Nur Yıldırım<sup>2</sup>

<sup>1</sup>Department of Dentomaxillofacial Radiology, University of Necmettin Erbakan, Türkiye

<sup>2</sup>Department of Dentomaxillofacial Radiology, University of Istanbul Aydın, Türkiye

**Introduction:** This study aimed to evaluate the association between the anatomical proximity of posterior maxillary tooth roots to the maxillary sinus floor and both the presence and severity of maxillary sinus mucosal thickening (MT) using cone-beam computed tomography (CBCT).

**Materials and Methods:** A retrospective CBCT-based analysis was conducted on 300 patients. The anatomical relationship between tooth roots and the sinus floor was categorized into three proximity types according to increasing root–sinus closeness. Maxillary sinus mucosal thickness was measured in millimeters, and MT was defined using both a binary threshold ( $>2$  mm vs.  $\leq 2$  mm) and an ordinal classification ( $\leq 2$  mm, 2–10 mm,  $>10$  mm). Multivariable binary logistic regression and ordinal logistic regression analyses were performed to assess the independent association between proximity type and MT, adjusting for age, sex, diabetes, cardiovascular disease, and smoking status.

**Results:** Mucosal thickening ( $>2$  mm) was identified in 34.7% of patients bilaterally. Proximity type was significantly associated with MT on both sides ( $p < 0.01$ ). In multivariable binary logistic regression, each one-unit increase in proximity type increased the odds of MT by 2.58 times on the right side (OR=2.58; 95% CI: 1.61–4.12;  $p < 0.001$ ) and 1.93 times on the left side (OR=1.93; 95% CI: 1.23–3.03;  $p = 0.004$ ). Ordinal logistic regression confirmed that proximity type was an independent predictor of greater MT severity (right: OR=2.43; left: OR=1.90; both  $p < 0.01$ ). Age showed a modest association, whereas systemic factors were not significant.

**Conclusions:** The anatomical proximity between posterior maxillary tooth roots and the sinus floor is a strong independent predictor of both the presence and severity of MT. These findings highlight the importance of evaluating tooth–sinus relationships in CBCT-based diagnosis and treatment planning.

## EP-520

## Adult Langerhans cell histiocytosis mimicking aggressive periodontitis: A diagnostic challenge

B Sanlitürk<sup>1</sup>, U Seki<sup>1</sup>, A Kuran<sup>1</sup>, B Tokuc<sup>2</sup>, S Oruc<sup>2</sup>, G Kavas<sup>3</sup>, E A Sinanoglu<sup>1</sup>

<sup>1</sup>Department of Oral and Maxillofacial Radiology, University of Kocaeli, Türkiye

<sup>2</sup>Department of Oral and Maxillofacial, University of Kocaeli, Türkiye

<sup>3</sup>Department of Medical Pathology, University of Kocaeli, Türkiye

**Introduction:** Langerhans Cell Histiocytosis is a rare proliferative disorder that is mostly seen in children, but it can also affect adults, although much more rarely. The most frequently affected areas are the bone, skin, and pituitary gland. In adults, the diagnosis is often delayed because the clinical findings mimic those of other systemic diseases. In the oral cavity, findings are often misdiagnosed due to being confused with periodontitis. In this case report, we aimed to present an adult case of LCH diagnosed based on the radiological findings of the oral cavity and jaws.

**Case:** A 23-year-old male patient presented to our clinic with complaints of gingival pain and tooth mobility. His medical history revealed that he had been receiving hormone replacement therapy for diabetes insipidus and hypogonadism secondary to a diagnosis of a pituitary adenoma made three years earlier. It was noted that previous periodontal treatments for his oral complaints had been unsuccessful. Intraoral examination revealed generalized periodontal involvement with significant tooth mobility. Radiological evaluation demonstrated characteristic “scooped-out” lesions in the posterior regions of the jaws. Additionally, a “floating teeth” appearance was observed, attributed to extensive loss of alveolar bone. Histopathological evaluation of the biopsy specimen, along with immunohistochemical analysis, demonstrated positivity for CD1a, S100, and Langerin, which are considered the gold standard markers for confirming the diagnosis of LCH.

**Discussion:** In the oral cavity, LCH often presents with clinical features that may be misdiagnosed as aggressive periodontitis, leading to unsuccessful treatment outcomes. A key aspect of this case is the importance of correlating oral findings with the patient’s systemic history for the early diagnosis of LCH. Therefore, it is essential for dentists to recognize the characteristic oral manifestations of LCH to ensure timely diagnosis and appropriate management of this rare condition.



# Author Index



**A**

Abdullah Enes Atas 70  
 Achararit P 52  
 Adioro Soetojo 65  
 Aga Satria Nurrachman 64, 65, 66, 67, 68, 69, 74, 75, 79, 82, 98  
 Agnes Kentjana Putra 136  
 Ahyoung Kwon 87  
 Ah-Young Kwon 4, 97  
 Akie Katsuki 94  
 Akiko Imaizumi 62, 63, 72  
 Akira Shibamura 62  
 Akitoshi Katsumata 27  
 A Kuran 138  
 Alexander Patera Nugraha 69, 82  
 Alhadiyati Asymal 75  
 Alhidayati Asymal 64, 65, 66, 67, 68, 69, 74, 75, 82  
 Ali Altındağ 138  
 Aloysius Putut Wijanarko 114, 115, 119, 122, 124, 125  
 Amalia Putri Ananda 66  
 Ami Kuribayashi 62, 63, 72, 76  
 Amil Ahmad Ilham 50  
 Aminda Faizura Omar Khattab Khan 45  
 Ami Takeshita 67, 100, 101  
 Anak Agung Gde Dananjaya Agung 110  
 Ana Sirghe 35, 134, 135  
 Andi Fauziah Alrahma 108  
 Andi Muh Ayodhya Chandra Dirawan 108  
 Andina Widyastuti 102  
 Andi Nurhaerianty Amin 98  
 Andrew Nalley 36  
 Andrew Ng Jian Xing 44  
 Andria Kuswadi 124  
 Andy Wai Kan Yeung 36  
 Anil Didem Aydin Kabakci 70

Antohi Cristina 34, 105, 127  
 Aries Sugih Budhiana 115  
 Arisa Oki 62, 72  
 Az Zikra Adelia Syamsuri 108

**B**

Babatunde Olamide Bamgbose 33, 40, 50  
 Barunawaty Yunus 33, 50, 88, 89, 93, 94, 107, 108, 111  
 Bayu Trinanda Putra 120  
 B Baldini 42  
 Belly Sam 115  
 Bernard Emeka Ogbozor 40  
 Beshlina Fitri Widayanti Roosyanto Prakoeswa 42  
 Bogdan Dobrovat 35, 134, 135  
 Bong Chul Kim 112  
 Bong-Hae Cho 3, 50, 57, 76  
 Brama Kiswanjaya 115, 129, 136  
 B Sanliturk 138  
 B Tokuc 138  
 Burak Tunahan Çiftçi 57  
 Byung-Do Lee 3, 55, 61, 112

**C**

Carla Sciaraffia R. 104  
 Cemile Nur Yıldırım 138  
 Cernei Radu Eduard 34, 105, 127  
 Cesilia Metty Ekariani 129  
 Chang-Hyeon An 3, 38, 136  
 Chang-Ki Min 4, 83, 111  
 Chena Lee 4, 30, 37, 48, 85, 96, 126  
 Cheng-Han Wu 92  
 Chih-Chia Huang 84  
 Christian Victor B 69  
 Clarence Dayan Roxas Cardinal 14, 36  
 Concita Corina Alexandra 34, 105, 127

Cristina Antohi 35, 134, 135

Cristina Martorell 58, 137

**D**

Dahee Kim 116

Daniela Pomohaci 35, 134, 135

Daniela Vallejos 58

Danisia Haba 35, 134, 135

David MacDonald 21

Dayanara Wiena Lopita 64

Debora Natalia 110

Delgertsetseg Jargaltsogt 61

Demitria Naranti Santoso 122

Deny Saputra 66, 74, 82, 83

Derry Haryono 119, 125, 129, 136

Derya YILDIRIM 43, 56, 58, 105

Dewi Vasthi Manikmaya 122

Dida Devina 64

Dio Nella Arlingga 74

Dobrovat Bogdan Ionut 34, 105, 127

Donna Trye Liling 119

Dorothea Ratri Sulihingtyas 67

Duygu KAYMAK 58

Dwi Ariawan 122

Dwi Desiyunis 125

Dwi Putri Wulansari 33, 50, 90, 95, 110

**E**

E A Sinanoglu 138

Eha Renwi Astuti 64, 65, 67, 68, 69, 74, 75, 82, 98

Ekarat Phattarataratip 131

Eka Yulianti Puspitasari 122

Elif Sena SARGIN 43, 56, 58

Emilia Marciuc 35, 134, 135

Emilie Borup Hansen 41

Enebish Sundui 61

E Ponsena 80

Erdenebulgan Batmunkh 61

Esra Seden NAVRUZ 105

Evita Juniasri Indrawati 66

**F**

Fadhliil Ulum 33, 50, 104, 108, 119, 131

Fahriah Tuasamu 90

Fahri Reza Ramadhan 47, 128

Fan-Pei Gloria Yang 71

Farah Fadhillah 33

Farris Zakki Giffari 122

Fatina Yasmin 82

Fery Suriyati Sormin 69

Firda Bilma Assyfa Fauziah 115

Firdevs Aşantoğrol 57

Fok, Rachel Melissa 14

Fuangrod T 52

**G**

Gabriel Maria Ferdilia 74

Gang Li 12

Ganjargal Ganburged 61

Gheorghe Angela 34, 105, 127

Giuroiu Cristian Levente 34, 105, 127

G Kavas 138

Gonzalo Arellano G. 104

Güldane Mağat 40

Gyeongseung Lee 78

Gyudong Jo 87

Gyu-Dong Jo 4, 48, 85, 126

Gyu-Tae Kim 4, 49

**H**

Haba Danisia 34, 105, 127

Hakan Amasya 80

Hak-Sun Kim 4, 49  
 Hamburda Tudor 34, 105, 127  
 Hamdani 131  
 Hang-Moon Choi 9, 48, 101, 112  
 Han-Gyeol Yeom 4, 48, 55, 61, 112  
 Hanna H Bachtiar-Iskandar 114, 115, 119, 120, 125  
 Hasibe Taşkın 105  
 Hasna Mutia Rabbani 64  
 Hatice KURT 43  
 Hayashi, Takafumi 14  
 Hayato Odagiri 73  
 Heejin Yun 117  
 Henytaria Fajrianti 102  
 Heo Min Suk 79  
 Hernan Paublina Oliveira 137  
 Hetty Oktavin Laonu 111  
 Hideki Rokushima 103  
 Hideki Suito 91  
 Hideyoshi Nishiyama 42  
 Hikmet Orhan 105  
 Hiroaki Shimamoto 94, 100, 103, 130  
 Hiroki Kato 94  
 Hiroko Okawa 73  
 Hiroshi Tomisato 72  
 Hiroshi Watanabe 62, 63, 72, 76  
 Hiroyasu Kodama 73  
 Hisako Frusho 47  
 Ho-Jun Song 81  
 Hong Kim 85  
 Hong-Yul Moon 135  
 Hoyoon Choi 123  
 H Suito 86  
 Hui Jeong 85  
 Hui-Wu Yang 70  
 Hung, Kuo Feng 14  
 Husnul Hatimah 89

Hyewon Seo 37  
 Hyunbin Yun 118  
 Hyun Jin Cho 48

---

**I**

Ikuho Kojima 37, 73  
 Ilinca Diana Andreea 35, 134, 135  
 Ingrid Różyło-Kalinowska 25, 56  
 In-Woo Park 4, 101, 112  
 I Nyoman Guswan 119, 125, 129, 136  
 Irfan Sugianto 33, 40, 50, 121, 125  
 Irind Octaviani Amansyah 124  
 Irnawati Ilham 88  
 Irresta Zainistya Putri 98  
 Isti Rahayu Suryani 10  
 Izdihar Kamal 35

---

**J**

Jaehyup Lee 136  
 Jae-In Ryu 9  
 Jae-Joon Hwang 4, 50, 57, 76  
 Jae-Seo Lee 4, 72, 81  
 Jangyo Bae 87  
 Jie Yang 24  
 Jin-Woo Choi 4, 9, 97  
 Jin-Woo Han 4, 101, 112  
 Jira Kitisubkanchana 96  
 Jirakit Pramuanpornsatid 96  
 Ji Yong Han 55  
 Ji Yun Lee 48  
 J Meyns 42  
 Jo-Eun Kim 4, 9, 31, 48, 79, 85, 87, 88, 97, 99, 103, 109, 113, 129, 135  
 Johanna Hasian Aritonang 114  
 Jo-Hun Kim 133  
 Jong-Won Kim 86

Jong Woo Kim 97  
Juen-Long S. Cheung 44  
Ju-Hee Kang 4, 48, 87, 99, 109, 113, 129, 135  
Jung-Eun Park 99  
Jun-ichi Tanuma 117  
Jun-Tae Park 129  
Juramt Bold 61  
Jyotsna Jaswanth 113

**K**

Kaan Orhan 28  
Kanae Moriyama 67  
Kang-Ju Hung 70  
Kan Nagao 91  
Kan, Yee Ting Alice 14  
Kaori Oya 103, 130  
Kasturi Nair Tangaraju 35  
Katsutoshi Hirose 103, 130  
Keiko Fujimoto 91  
Keisuke Marutani 103  
Kenji Suzuki 76  
Kentaro Takanami 73  
Kevser Dinç BAŞAR 77  
K Fujimoto 86  
Khalisha Amanina Azzami 106  
Khamila Gayatri Anjani 110  
Kiatanant Boonsirisetth 96  
Kiichi Shimabukuro 47, 128  
Kimiaus Saadah 64  
Ki-Min Jung 91  
Kim Su hyeon 79  
Kitipong Kaewpichai 131  
K Nagao 86  
Kobayashi, Taichi 14  
Ko Dezawa 107  
Kornkamol Kretapirom 96

Kosei Ueshima 67, 94, 100, 101  
Kouji Katsura 42, 117  
Kouji Katsura<sup>1</sup>, Takafumi Hayashi 42  
Krittamate Kerewichien 131  
Kug Jin Jeon 4, 48, 85, 126  
Kunihito Matsumoto 107  
Kuo Feng Hung 36  
Kyeo-Re Kim 109  
Kyoung-A Kim 4, 9, 83, 111  
Kyung-Hoe Huh 4, 48, 79, 85, 87, 97, 99, 109, 113, 129, 133, 135  
KyungMinClara Lee 81

**L**

Laili Ma'rifah 65  
Larasati Kusuma 114, 115, 119, 122, 125, 136  
Line Nissen 41  
Liska Barus 110  
Liwen Zhang 100, 101  
Lusi Epsilawati 115

**M**

Macarena Toro M. 104  
Makiko Ike<sup>1</sup>, Masaki Takamura 42  
Mamiko Fujikura 62  
Mamoru Nagata 130  
Manabu Yamazaki 117  
Manisha Khorate 34  
Marie A Cornelis 41, 44  
Masahiko Miura 62, 63, 72  
Masahiko Ohtsuka 47, 128  
Masahiro Iikubo 20, 37, 73  
Masaki Takamura 42, 117  
Masaru Konishi 47, 128  
Masaya Kawasaki 94  
Matchima Phetsuit 90

Maulana Ibnu Ramadhan 108  
 Maziahtul Zawani Binti Munshi 71  
 M Cadenas de Llano Pérula 42  
 Medhana Mangoanker 34  
 Mediha Erturk 70  
 Meghna Gohain 46  
 Megumi Nose 47, 128  
 Melek Tassoker Bulut 70, 77  
 Menik Priaminiarti 114, 119, 122, 124, 125, 129, 136  
 Merry Annisa Damayanti 115  
 Mert Can Kitoğlu 57  
 Michael M. Bornstein 14, 26  
 Miharuru Taguchi 62, 72  
 Mihoko Suzuki 37  
 Miki Hisatomi 62  
 Ming-Gene Tu 19, 70, 92  
 Min-Suk Heo 4, 22, 48, 85, 87, 97, 99, 103, 109, 113, 129, 133, 135  
 Min-Suk Kook 81  
 Mirai Higaki 128  
 Miyoshi Kataoka 103  
 Mobin Ahmadi 51  
 Mohammad Adhitya Latief 120  
 Mohammad Farid Ratman 125  
 Mohammad Safwan Sahar 45  
 Mohd Hafiz bin Mohd Zaid 35  
 Monica Piña D'Abreu 58, 137  
 Muhammad Fadil Hidayat 50, 98, 113  
 Muhammad Farris Afif 129  
 Muhammad Khalis Abdul Karim 35  
 Muhammad Khan Asif 46  
 Muhammad Raihan Yusuf Arrahman 119  
 Muhammad Rifky 50  
 Muhammad Teguh Putra 40, 50, 104

---

**N**


---

Nalley, Andrew 14  
 Nanako Tani 128  
 Nantawat Joombal 33  
 Naoki Maeda 91  
 Naoko Abe 130  
 Naoko Tagaino Watanabe 73  
 Naoko Takagawa 67, 71, 130  
 Naoya Kakimoto 47, 128  
 Napat Damrongsirirat 131  
 Nastiti Faradilla 69, 74, 75, 82, 83  
 Nasywa Athaillah Safitri 82  
 Natcha Srivichien 132  
 Nayeon Kim 50, 57  
 Nayla Yuliyanti Pawa 95  
 Neslihan Ebru ŞENİŞİK 43  
 Nica Irina 34, 105, 127  
 N Maeda 86  
 Nobuhiko Matsuda 67, 100, 101  
 Nora Sakina Mohd Noor 46  
 Norasikin Ismail 35  
 Noriko Yamao 67, 71, 101  
 Norlaila Sarifah 79  
 Norliza Ibrahim 46  
 Nozomu Uetake 94  
 Nura Adolfina Barung 50  
 Nur Redannia Redzuan 37  
 Nutchalai Malikhao 132

---

**O**


---

Onanong Silkosessak 18, 46, 52, 131, 132  
 OE Burlacu-Vatamanu 42  
 Otty Ratna Wahyuni 64, 65, 66  
 Oyuntugs Rashsuren 61

**P**

Pancu Galina 34, 105, 127  
Paolo M. Cattaneo 41, 44  
Pere Riutord Sbert 137  
Phonkit Sinpitaksakul 132  
Phrabhakaran Nambiar 46  
Pisha Pittayapat 52, 90, 131  
P. Mahasantipiya 52  
Popescu Roxana Mihaela 34, 105, 127  
Poramaporn Klanrit 33, 73  
Pornkawe Charoenlarp 46, 132  
Porntaveetus T 52  
P. Panyarak 52  
Preethy Mary Donald 44  
P Sinpitaksakul 100  
P Sutheerapatranon 100  
P Sutthiprapaporn 80  
P Suwanwitid 46  
Purnamasari Syahbani Massalinri 94  
Putri Alfa Meirani Laksanti 82  
Putri Marina Sukmadewi 110  
Pyae Phyo Thaw 73

**Q**

Qiang Sun 100, 101

**R**

Radika Fahmi Siddiq 68  
Ragil Tri Nurrahman 79  
Ramadhan Hardani Putra 64, 65, 82  
Ramayanti Salam 125  
Ray Tanaka 14, 36  
RC Fontenele 42  
R Chaijit 80  
Reika Hanaoka 103, 130  
Renjith George 44

Retno Septiana Ananda 113  
Rezky Amalia 40, 93  
Rini Devijanti Ridwan 82  
Rini Widyaningrum 106  
Riutord Sbert, Pere 58  
R Jacobs 42  
R Kasai 86  
Roberto Rongo 41  
Roxana Popescu 35, 134, 135  
Rr. Astrid Dyah Kusumastuti Rahardjo 75  
Rurie Ratna Shantiningsih 102  
Ryna Dwi Yanuaryska 106  
Ryoko Okahata 130

**S**

Sachiko Yamasaki 47  
Safira Adzani Rahman 65  
Sakarot Na Lampang 77  
Sakiko Kume 72  
Salceanu Mihaela 34, 105, 127  
Samed Satir 38, 40  
Sam-Sun Lee 3, 48, 79, 85, 87, 97, 99, 109, 113, 129, 133, 135  
Sang-Heon Lim 53  
Sang Jun Lee 55  
Sangsom Prapayasatok 77  
Sang-Sun Han 3, 9, 23, 48, 85, 121, 126  
Sanjay M Mallya 71  
Saori Yoshida 62  
Sari Kemaladini 65  
Sawrawit Chairat 77  
Sazkia Febradhany Tania 120  
S Chiemboonsri 46  
Seiki Tomita 103  
Seiko Ichinose 94  
Selale Ozel 38  
Şelale Özel 80

- Seok-Jun Hwang 103  
 Seo-Young An 4, 38, 48, 136  
 Septia Anggreini Wilujeng 75  
 Sergio González P. 104  
 Seung Ho Park 81  
 Sheng-Yao Lai 92  
 Shin-Hyun Kang 133  
 Shin Nakamura 62, 63, 72  
 Shotaro Fuchibe 67, 94  
 Shu-Han Lin 134  
 Shumei Murakami 15, 67, 71, 94, 100, 101, 103, 130  
 Shun Miwa 39, 124  
 Shunsuke Okada 62  
 Sinpitaksakul P 52  
 Sirirat Chawanratikun 132  
 Siska Putri Utami 107  
 Sitthichok Chaichulee 77  
 Sonali Parvatkar 34  
 Soon-Chul Choi 3, 48, 87  
 Soranun Chantarangsu 132  
 S Oruc 138  
 Souichi Yanamoto 47, 128  
 S Pimkow 100  
 Srisermphoak N 52  
 Sri Wigati Mardi Mulyani 66, 82, 83  
 Stephanie Lee Phei Wei 44  
 Suguru Hirota 128  
 Sujeong Kim 54  
 Suk-Ja Yoon 3, 72  
 Sukkarn Themkumkwun 96  
 Sultan Uzun 40, 77  
 Sunali Khanna 16  
 Sungho Oh 91  
 Sung-min Hwang 38  
 Sunjidmaa Zolzaya 61  
 Sunpatch Benjavongkulchai 90, 100  
 Supaluck Deeduai 132  
 Supasith Yomtako 72  
 Sushmita Wayadande 34  
 Su Yang 55, 133  
 Suzuka Yoshida 62  
 Sven Kreiborg 71  
 Syifa Nur Izzati Ainayah 67  
 Syurri Innaddinna Syahraini 122

**T**

- 
- Tadashi Sasai 67, 71, 101  
 Tae Yeon Lee 127  
 Taha Emre Kose 38  
 Taha Zirek 70  
 Taichi Kobayashi 42, 117  
 Taisuke Kawai 39, 124  
 Takafumi Hayashi 42, 117  
 Takashi Kamio 39, 124  
 Takashi Nakamoto 47, 128  
 Takeaki Sudo 76  
 Tati Siti Patimah 115  
 Theerachai Kosanwat 96  
 Ting Teck Jong 44  
 T Jindanil 42  
 T Kondo 86  
 Tomomi Tsujimoto 100, 101  
 Tomoyo Nomura 107  
 Tomoyuki Kondo 91  
 Topoliceanu Claudiu 105, 127  
 Toshikazu Nagasaki 47, 128  
 Toshinori Ando 128  
 Toshiyuki Kawazu 62  
 Tsabitah Azzahra 66, 83  
 T Sawangpanyangkura 52  
 Turgut Felek 40

**U**

Uce Ayuandyka M 93

Ülkem Aydin 58

U Seki 138

U Yessarapat 52

**V**

Varisa Assapattarapun 67, 71, 101

Vera Julia 114, 115, 119, 124, 129

Vicky Eka Firmansyah 66

Vinesh Raj Savumthararaj 45

Virdha Dwi Mulya 121

Vorapat Trachoo 131

**W**

Wan Lee 4, 55, 61, 112

Wariya Panprasit 33, 73

Wen-Chen Wang 17, 134

Wikan Tajali Rosojati 65

William Rachmat Fatah 122

Witsarut Upalananda 77

Won-Jeong Han 3, 97

Won-Jin Yi 3, 51, 53, 54, 55, 79, 85, 87, 91, 97, 99, 109, 113, 116, 117, 118, 123, 127, 129, 133, 135

Woojun Kim 112

W. Suttapak 52

**Y**

Yafangzhou Xu 76

Yeonhee Kim 87

Yeung, Wai Kan Andy 14

Yohei Takeshita 62

Y Oku 86

Yong Chan Park 55

Yoon Joo Choi 48, 85, 121, 126

Yo-Seob Seo 4, 86

Yoshihide Nakamura 62

Yoshihiro Tagami 91

Yoshikazu Nomura 72

Yoshikazu Suei 47, 128

Yoshinobu Yanagi 62

Yoshinori Arai 13, 107

Young-Eun Kwon 4, 38, 136

Y Raruenrom 80

Yuan-Tsun Wang 70

Yuichiro Kadonaga 94

Yuka Uchimoto 71, 103, 130

Yuka Uchiyama 67, 101

Yukina Kobayashi 128

Yuki Shimizu 67, 103, 130

Yun-Hoa Jung 3, 50, 57, 76

Yunita Savitri 64, 66, 68

Yuntrisnawaty Sartika Kasim 89

Yu Ri Kim 61

Yu-Ri Kim 88

Yuri Namba 62

Yuri Nishikawa 100

Yusmiadil Putera Mohd Yusof 45

Yusuke Shimada 37

Yutaka Nikkuni 42, 117

Yuuri Oku 91

**Z**

Zainul Ahmad Rajion 11

Ze Jin 76



Supported by



### Secretariat of ACOMFR 2026

The 15th Asian Congress of Oral and Maxillo-Facial Radiology  
in conjunction with The 58th Annual Scientific Meeting of KAOMFR  
Email: [info@acomfr2026seoul.org](mailto:info@acomfr2026seoul.org) | Tel: 02-6328-0303